HIGH RESOLUTION NMR IN SOLIDS

by

Alexander Pines

B.Sc., Hebrew University

(1967)

SUBMITTED IN PARTIAL FULFILLMENT OF THE

REQUIREMENTS FOR THE DEGREE OF

DOCTOR OF PHILOSOPHY

at the

MASSACHUSETTS INSTITUTE OF TECHNOLOGY

September, 1972

Signature of the Author _____
Department of Chemistry, September 6, 1972

Certified by _____
Thesis Supervisor

Accepted by _____
Chairman, Departmental Committee on Graduate Students

HIGH RESOLUTION NMR IN SOLIDS

by

Alexander Pines

Submitted to the Department of Chemistry in September, 1972 in partial fulfillment of the requirements for the degree of Doctor of Philosophy

ABSTRACT

Two approaches to the problem of high resolution NMR in solids are described. The first involves modulation of the nuclear magnetic dipole-dipole interaction by resonance offset fields in multiple-pulse NMR. A simple treatment of zero order effects is presented which shows that if the resonance offset frequency is smaller than the inverse multiple-pulse cycle time, but larger than the linewidth, then the average dipolar Hamiltonian is just the dipolar Hamiltonian truncated along some average axis in the rotating frame. This is shown to have potential applications to line-narrowing, time-reversal, spin-locking and nuclear double resonance.

The second approach involves the observation of dilute spins (S) in a reservoir of abundant "unlike" spins (I). The problem of dipolar broadening by the I spins is overcome by spin-decoupling and the reduced sensitivity is enhanced by employing a double-resonance procedure due to Hartmann and Hahn. The approach involves "cross-polarization" of the S spins by the I reservoir and observation of the S free induction decay while decoupling the I spins. This is repeated $\sim N_I/N_S$ times until the I polarization is depleted and the S signals are co-added to yield a markedly enhanced sensitivity over conventional Fourier techniques. Some illustrative results on chemical shielding and relaxation of ^{13}C in solids are presented and references are given to results of other experiments both published and in progress. Alternative versions of the experiment employing both direct and indirect detection are discussed briefly.

An important requirement for these experiments is timing flexibility. A description of the computer interface which provides this is given together with circuit and software details.

Finally, a discussion of solid state spin echoes is presented in the form of a paper reprint entitled "Time-Reversal Experiments in Dipolar-Coupled Spin Systems", by W-K. Rhim, A. Pines and J.S. Waugh. It is demonstrated that the spin-temperature hypothesis (which actually forms the basis for a large part of this thesis) must be employed with caution. The effects of cycle symmetry and applications to high resolution NMR in solids are discussed briefly.

Thesis Supervisor: John S. Waugh
Title: Professor of Chemistry

This doctoral thesis has been examined by a Committee of the Department of Chemistry as follows:

Chairman

Thesis Supervisor

ACKNOWLEDGMENTS

I have had the good fortune of being able to work in the laboratory of Professor J. S. Waugh. I am grateful to him for this opportunity and for his expert supervision of my research. I am particularly indebted to him for his encouragement during the difficult times, and for the stimulation and critical evaluation which he provided during the better periods of my years as a graduate student; and finally, for the privilege of his friendship, and for the tolerant attitude which he has shown towards my perhaps overly ambitious and temperamental nature.

I have benefited from my association with many people in this laboratory. I am singularly grateful to Dr. Won-Kyu Rhim for a rewarding collaboration and to Dr. Rhim and Dr. David Ellett for stimulating the ideas and providing the impetus for many of the problems which I have tackled. Collaboration and valuable discussions with Dr. M. G. Gibby, Dr. R. G. Griffin, Dr. M. Mehring and Dr. H. Resing, and the assistance of Mr. S. Kaplan, Mr. S. Pausak and Dr. H. N. Yeung are also gratefully acknowledged. I should like, in addition, to express my appreciation to Professor John M. Deutch for many helpful discussions and to Dr. Maurice Goldman for two memorable meetings and for introducing me so enthusiastically to the concepts of spin-temperature and double-resonance.

Finally, I thank Mrs. S. Toomey and Miss B. Blanchard for their assistance in typing, and Dr. R. G. Griffin for reading and critically commenting on the manuscript.

to Ayala

LIST OF FIGURES

CHAPTER I

CHAPTER II

Chapter II (continued)

CHAPTER III

CHAPTER V

LIST OF TABLES

CHAPTER II

CHAPTER III

TABLE OF CONTENTS

Page

CHAPTER III

Page

Page

CHAPTER I

QUANTITATIVE ASPECTS OF COHERENT AVERAGING. SIMPLE TREATMENT OF RESONANCE OFFSET PROCESSES IN MULTIPLE-PULSE NMR

I. INTRODUCTION

The problem of calculating the response of a coupled spin system to an arbitrary radiofrequency excitation is, in general, an extremely complex one. It is well known, however, that if the excitation fulfills certain conditions of periodicity and duration, an enormous simplification ensues, taking the form of what we have called "coherent averaging" [1]. This theory has formed a powerful tool for the description and design of a variety of effects in pulsed nmr, including spin locking[2-4], line narrowing and high resolution nmr in solids[5-7], spin echoes[8], steady-state behavior[9], and scaling of inhomogeneous shifts[10].

It was noticed in several of these experiments that when pulse trains were applied with the r.f. carrier frequency substantially displaced from the Larmor frequency of the spin system, i.e., with a "resonance offset", a new phenomenon manifested itself in the form of additional averaging, for example enhanced line-narrowing. This phenomenon has recently been explained and, in fact, has been shown to possess a number of useful properties[11].

Basically, what happens, in qualitative terms, is the following: in the presence of r.f. excitation, the coupling between the spins becomes modulated with a period equal to that of the excitation itself, in an appropriate reference frame[1,12]. In the limit of strong modulation we perform

a time average of this time-dependent coupling and obtain an average coupling which effectively governs the response of the spin system. The process of "truncation" of the dipolar interaction in the presence of a large static external field[13-16], for example, is a particular case of this approach[11]. Now consider what happens if there is a large resonance offset. In the rotating frame, this appears as a static magnetic field and, as in the case of truncation just mentioned, this field will provide an additional modulation of the coupling, which may be averaged in the appropriate limit[1]. Thus, the behavior of pulsed nmr experiments near and far from resonance should be distinctly different, as has indeed been observed[11].

In this communication, we wish to present a simple treatment of this phenomenon in a form more amenable to an intuitive understanding and quantitative application to a variety of nmr experiments than that of our previous work. This presentation is warranted by the fact that these multiple-pulse techniques are becoming increasingly useful in studies of chemical problems, and resonance offset effects form an integral component in their usefulness and in their understanding.

The approach here is simple in the sense that only zero order[1] averaging effects are considered, and insofar as is possible the notation and tools used should be quite familiar. Higher order effects are more conveniently treated in terms

of irreducible tensor operators, since we are interested in the transformations of such operators under the rotations induced by the r.f. excitation. This will be deferred to a later detailed exposition of these experiments.

In section II a brief review of pertinent theory is presented and a general description of averaging due to resonance offset fields is derived. In section III this is applied to some simple multiple-pulse sequences and some of its uses and limitations are discussed. Details on the exact steps involved in the calculations of average Hamiltonians in various representations are not given, since this has been presented several times. The procedure is simply mentioned and the results written down directly.

II. GENERAL THEORY

A. HAMILTONIAN AND FRAME OF REFERENCE

We begin by writing down a Hamiltonian for the system. We select as an example of a spin coupling the dipolar interaction, since this is the most important and widely encountered for solids of interest to chemists. The results are easily generalized, as we shall see. We write the Hamiltonian in the laboratory frame in frequency units:

$$H_L(t) = H_0 + H_1(t) + H_d \tag{1}$$

H_0 is the Zeeman interaction with applied static field along the z axis

$$H_0 = -\omega_0 I_z \tag{2}$$

$H_1(t)$ the applied r.f. excitation

$$H_1(t) = -2\omega_1(t)\ I_x \cos(\omega t + \phi(t)) \tag{3}$$

where $\omega_1(t)$ and $\phi(t)$ describe the amplitude and phase modulation of the r.f. excitation applied at freqnency ω, and

$$H_d = -\sum_{i<j} \frac{\gamma^2\hbar}{r_{ij}^3} \left\{ \frac{3(\underset{\sim}{I}_i \cdot \underset{\sim}{r}_{ij})(\underset{\sim}{I}_j \cdot \underset{\sim}{r}_{ij})}{r_{ij}^2} - \underset{\sim}{I}_i \cdot \underset{\sim}{I}_j \right\} \tag{4}$$

is the dipolar interaction.

We now perform the customary transformation to a coordinate system rotating at frequency ω about the z axis. An average is then performed over a time period of $2\pi/\omega$ and this removes the time dependent terms in $H_1(t)$ and H_d in this frame. All this is well known -- it corresponds to discarding the counter-rotating component of the r.f. field and the "nonsecular terms" of the dipolar interaction (or truncation) and is just a special case of coherent averaging. It is clearly legitimate whenever H_0 is much larger than H_1 and H_d. Our Hamiltonian in the rotating frame thus assumes the form

$$H_R^0(t) = H_\Delta + H_1(t) + H_d^0 \tag{5}$$

where R indicates the rotating frame.

H_Δ is the resonance offset

$$H_\Delta = -\Delta\omega I_z; \quad \Delta\omega = (\omega_0 - \omega); \tag{6}$$

$$H_1(t) = -\underset{\sim}{\omega}_1(t)\cdot\underset{\sim}{I}, \tag{7}$$

$$H_d^0 = \sum_{i<j} b_{ij}(3\, I_{iz}I_{jz} - \underset{\sim}{I}_i\cdot\underset{\sim}{I}_j); \quad b_{ij} = \frac{-\gamma^2\hbar}{r^3_{ij}} P_2(\cos\theta_{ij}). \tag{8}$$

The form $\underset{\sim}{\omega}_1(t)$ depends on the particular experiment at hand. Note that for brevity we sometimes use the same

notation for terms of H in different frames to conform with accepted practice - the frame will always be specified if this is done. The ^{0} superscript indicates a truncation or zero order average of the particular term.

If the spin system is initially described in the rotating frame by the density matrix $\rho_R(0) = \rho_L(0)$, then at a time t it has evolved to a state described by

$$\rho_R(t) = U_R^0(t,0)\ \rho_R(0) U_R^{0+}(t,0) \tag{9}$$

here $U_R^0(t,0)$ is the effective time development operator in the rotating frame, given by

$$U_R^0(t,0) = T\exp(-i \int_0^t H_R^0(t')dt') \tag{10}$$

and T is a time ordering operator. It is an expansion of U in which we shall be interested.

B. COHERENT AVERAGING EFFECTS

We now prepare to take account of the modulation that the first two terms in (5) produce in the third. To this end we assume (i) $H_1(t)$ is cyclic and periodic with period t_c, and t is restricted to integer values of t_c, $t = Nt_c$

$$\text{(ii)}\ t_c << t_\Delta, T_2; \ t_\Delta = 2\pi/\Delta\omega\ , \tag{11}$$

(i) has been discussed in detail[1] and (ii) will allow us to perform a factorization of (10) in two steps. Employing the conditions above we obtain to a good approximation, factoring out $H_1(t)$ in a straightforward application of the theory:

$$U_R^0(t,0) = \bar{U}_{TR}^0(t,0) = \exp(-it\bar{H}_{TR}^0), \qquad (12)$$

where

$$\bar{H}_{TR}^0 = \frac{1}{t_c} \int_0^{t_c} U_1^+(t,0)[H_d + H_\Delta]U_1(t,0)dt =$$

$$= \bar{H}_d^0 + \bar{H}_\Delta = \bar{H}_d^0 - \overline{\Delta\omega}\, I_\mu;\ U_1(t,0) = \mathcal{T}\exp(-i\int_0^t H_1(t')dt'). \qquad (13).$$

Note that restriction [11(i)] applies to calculations involving time evolution as Eq. (12) and not, of course, to calculations of expansion terms as in Eq. (13). $\bar{H}_{TR}^0$ is the average Hamiltonian; T stands for "toggling" (12) since $\bar{H}_{TR}^0$ is precisely the average Hamiltonian in an interaction (toggling) frame defined by $H_1(t)$, (due to restriction 11(i), U_{TR}^0 is thus the effective evolution operator in the rotating frame). $\bar{\mu}$ refers symbolically to the average direction $\underset{\sim}{\bar{\mu}}$ in the rotating frame along which the spins are quantized (12). This is easily visualized by taking a unit spin vector $\underset{\sim}{\mu}$ along the z axis and applying $H_1(t)$ in the rotating frame. Then we define

$$\underset{\sim}{\bar{\mu}} = \frac{\int_0^{tc} U_1^+(t,0)\underset{\sim}{\mu}U_1(t,0)dt}{\left|\int_0^{tc} U_1^+(t,0)\underset{\sim}{\mu}\, U_1(t,0)dt\right|}\ . \qquad (14)$$

Figure 1

Pictorial description of resonance offset averaging under the pulse sequence of figure 2(a). The pulses are imagined to be δ-pulses ($t_w = 0$) and are depicted by arrows along x and -x which nutate the unit magnetization vector $\underset{\sim}{\mu}$ alternately by angles θ^0 and $-\theta^0$. Thus $\underset{\sim}{\mu}(t)$ switches between positions 1 and 2 and its average direction is given by the unit vector $\overline{\underset{\sim}{\mu}}$. The average offset field $\overline{\Delta\omega} = \cos(\theta/2)\Delta\omega$ points along $\overline{\underset{\sim}{\mu}}$ and thus any magnetization M will precess on the average about this axis with frequency $\overline{\Delta\omega}$. This gives rise to the scaling of chemical and inhomogeneous shifts. The factor $\overline{P}_2(\overline{\underset{\sim}{\mu}}\cdot\underset{\sim}{\mu}(t))$ in equations (23), (24) is simply evaluated for this sequence as $P_2(\cos\theta/2)$, so the average dipolar interaction is scaled by $\overline{P}_2(\overline{\underset{\sim}{\mu}}\cdot\underset{\sim}{\mu}(t)) = P_2(\cos\theta/2)$.

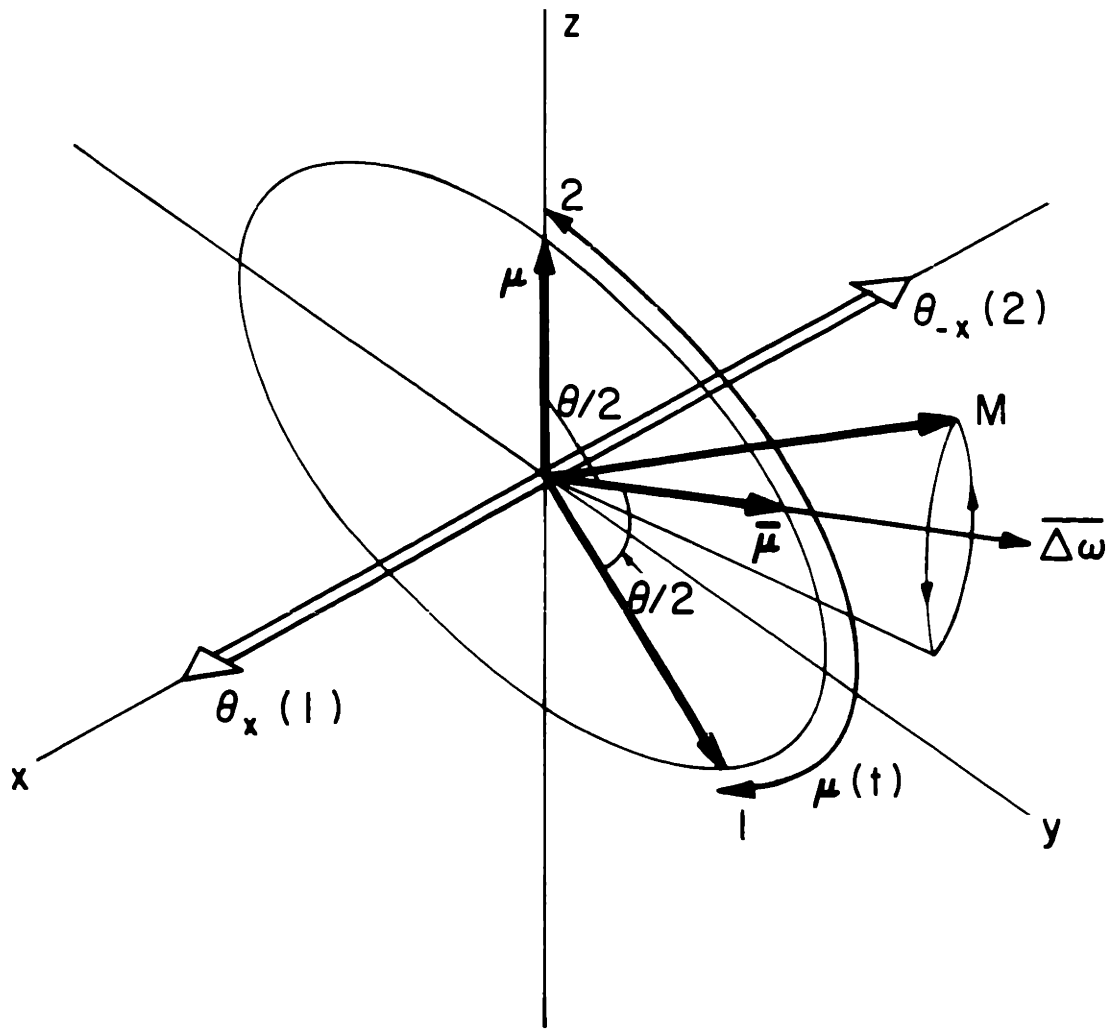
z
2
μ
θ/2
θ_x (2)
M
μ̄
Δω
θ/2
θ_x (1)
x
μ (t)
1
y

For example if $\underset{\sim}{\omega}_1(t)$ consists of 90° phase alternated δ-pulses along the x axis then $\underset{\sim}{\bar{\mu}} = \frac{1}{\sqrt{2}}(\underset{\sim}{j} + \underset{\sim}{k})$. This is illustrated in Figure 1. $\overline{\Delta\omega}$ is analogously the average resonance offset over this cycle:

$$\overline{\Delta\omega} = \frac{\Delta\omega}{t_c} \left| \int_0^{t_c} \underset{\sim}{c}_{\mu}(t)dt \right| . \tag{15}$$

We now add to (11) the further restriction

$$\text{(iii)}\quad t_{\bar{\Delta}} << T_2;\ t_{\bar{\Delta}} = 2\pi\overline{\Delta\omega}^{-1} . \tag{11}$$

This allows us, exactly as above, to factor the operator in (12) and then take an average over one cycle of the interaction with the static field $-\overline{\Delta\omega}\underset{\sim}{I}_{\bar{\mu}}$. What we are doing is in fact a truncation of the average dipolar interaction $\bar{H}_d^0$ due to the presence of a large static field along the $\bar{\mu}$ axis. To a good approximation then

$$\bar{U}_{TR}(t,0) = \bar{U}_{\Delta}(t,0)\bar{U}_{DTR}(t,0) \tag{16}$$

where

$$\bar{U}_{\Delta}(t,0) = \exp(-it\,\bar{H}_{\Delta}) \tag{17}$$

$$\bar{U}_{DTR}(t,0) = \exp(-it\,\bar{H}_{DTR}^{00}) \tag{18}$$

$$\bar{H}_{DTR}^{00} = \bar{H}_d^{00} = \frac{1}{t_{\bar{\Delta}}} \int_0^{t_{\bar{\Delta}}} \bar{U}_{\Delta}^{+}(t,0)\bar{H}_d\bar{U}_{\Delta}(t,0)dt. \tag{19}$$

Here the additional D subscript stands for "doubly rotating" - $\bar{H}^{0\,0}_{DTR}$ is precisely the average Hamiltonian in a frame which now rotates about the $\bar{\mu}$ axis at frequency $\overline{\Delta\omega}$ (12). Superscript $^{0\,0}$ indicates the double averaging or truncation.

Now using equations (13) and (19) and changing the order of integration over t_c and $t_{\bar{\Delta}}$ we have

$$\bar{H}^{0\,0}_{DTR} = \frac{1}{t_c t_{\bar{\Delta}}} \int_0^{tc} dt'' \int_0^{t\bar{\Delta}} dt' \bar{U}^{+}_{\Delta}(t',0) U^{+}_{I}(t'',0) H^{0}_{d} U_{I}(t'',0) \cdot \bar{U}_{\Delta}(t',0), \qquad (20)$$

but using (13) and (17) it is easily found that

$$\frac{1}{t_{\bar{\Delta}}} \int_0^{t\bar{\Delta}} dt' \; \bar{U}^{+}_{\Delta}(t',0) U^{+}_{I}(t'',0) H^{0}_{d} U_{I}(t'',0) \bar{U}_{\Delta}(t',0) = H^{0}_{d\bar{\mu}} P_2(\bar{\mu}\cdot\mu(t'')) \qquad (21)$$

where

$$H^{0}_{d\bar{\mu}} = \sum_{i<j} b_{ij}(3 I_{i\bar{\mu}} I_{j\bar{\mu}} - \underset{\sim}{I}_i \cdot \underset{\sim}{I}_j). \qquad (22)$$

$H^{0}_{d\bar{\mu}}$ is of course just the "secular" part of H^{0}_{d}, the part that commutes with $\bar{H}_{\Delta}$. With this notation, for example, $H^{0}_{d} \equiv H^{0}_{dz}$. Thus we obtain finally for the average Hamiltonian (excluding $\bar{H}_{\Delta}$) putting (21) into (20):

$$\bar{H}^{0\,0}_{DTR} = \bar{H}^{0\,0}_{d} = \bar{H}^{0}_{d\bar{\mu}} \cdot P_2(\bar{\underset{\sim}{\mu}} \cdot \underset{\sim}{\mu}(t)). \qquad (23)$$

As usual the bar denotes an average over the r.f. cycle:

$$\bar{P}_2(\bar{\underset{\sim}{\mu}} \cdot \underset{\sim}{\mu}(t)) = \frac{1}{t_c} \int_0^{t_c} P_2(\bar{\underset{\sim}{\mu}} \cdot \underset{\sim}{\mu}(t))dt \qquad (24)$$

where $\bar{\underset{\sim}{\mu}}$ is defined as (14) and $\underset{\sim}{\mu}(t)$ is the integrand. We prefer to leave (23) in the rotating frame since normal detection methods[17] correspond to measurements in this frame and not in the more suitable tilted frame along $\bar{\underset{\sim}{\mu}}$[14].

C. DISCUSSION

Equation (23) expresses a simple yet remarkable result. It says that no matter how complicated the cycle of r.f. excitation, if it is applied with a resonance offset fulfilling conditions 11(i) - (iii) then the average dipolar Hamiltonian is just the truncated Hamiltonian itself along an average axis in the rotating frame. This is depicted pictorially in Figure 1. Obviously in a frame tilted[14] with its z axis along $\bar{\underset{\sim}{\mu}}$, $\bar{H}^{0\,0}_{d}$ is exactly proportional to (8). In order to calculate this average Hamiltonian it is thus not necessary to calculate $\bar{H}^{0}_{TR}$ in the intermediate step - we need only (i) find $\bar{\underset{\sim}{\mu}}$ and write down $H^{0}_{d\bar{\mu}}$ immediately, (ii) calculate $\bar{P}_2$ as in (24), so no manip-

ulations are necessary on the spin variables. This fact, although rather obvious with a little reflection, is obscured in the original work[11] and with complicated cycles the manipulation of spin operators becomes unwieldy. The form of (23) allows a simple understanding of these experiments and permits us to draw more general conclusions (as we shall see for example in the discussion of spin locking). Of course in the event that we wish to enquire about the behavior at resonance ($\Delta\omega = 0$) this treatment is not valid and $\bar{H}^0_{TR}$ must be calculated separately.

These results are easily generalized. If our interaction is not dipolar but is given, say, by a Hamiltonian H^0_n whose effective spin part transforms like an n'th rank irreducible tensor in the rotating frame, then under the same conditions

$$\bar{H}^{0\,0}_n = H^0_{n\underset{\sim}{\mu}} \bar{P}_n(\underset{\sim}{\bar{\mu}} \cdot \underset{\sim}{\mu}(t)). \qquad (25).$$

For example, the isotropic chemical shift treated by Ellett and Waugh[10] has a spin part which transforms like a first rank irreducible tensor, and indeed their average Hamiltonian is a special case of our results. There, however, $\bar{H}^0_{TR}$ commutes with $\bar{H}_\Delta$ (since $\underset{\sim}{I}$ transforms like $\underset{\sim}{\mu}$) and thus the result is independent of resonance offset.

One nice feature of (23) is that it allows a quantitative comparison with experiment as, for example, in the work of Lee and Goldberg[15]. In the case of irradiation at resonance, $\bar{H}^0_d$ usually has some form different from $\bar{H}^0_d$ and line-

shape comparisons are difficult to reconcile with theory. Thus we have to date mostly satisfied ourselves with qualitative or semiquantitative conclusions, except in special cases. In the present case, however, arguments can be made more precise and quantitative.

Note that this treatment is not applicable to resonance offset experiments such as those of Lee and Goldberg[15] and Barnaal and Lowe[16], since there, requirement 11(ii) is violated ($t_c \sim t_\Delta$). In these cases the first transformation must be made not by $U_1(t,0)$ as in our case, but by the full effective field[14].

$$U_e(t,0) = \exp(-it(H_1 + H_\Delta))$$

In the present case the fact that H_1 is not exactly perpendicular to H_0 would be accounted for by correction terms in the expansion of $\bar{U}_R^0$, which are not considered here.

III. REPRESENTATIVE PULSE SEQUENCES

It now remains for us to specify the form of $\underset{\sim}{\omega}_1(t)$ in (7) and to write down some representative results. We select only simple examples to illustrate the general approach to application of the theory. Other examples will undoubtedly be investigated for fun by the interested reader.

A. TWO-PULSE CYCLE

Figure 2(a) shows the form of $\omega_1(t)$ for a phase alternated two-pulse sequence. By inspection (see Figure 1) we find immediately that $\underset{\sim}{\bar{\mu}}$ is in the y-z plane and makes an angle $\theta/2$ with the z axis. Defining the duty cycle δ by

$$\delta = 2t_w/t_c \tag{26}$$

and using equation (23) we find trivially for a pure dipolar interaction

$$H_d^{00} = H_{d\bar{\mu}}^0 \frac{3p_\delta(\theta) + 1}{4}$$

$$p_\delta(\theta) = (1-\delta)\cos\theta + \delta \frac{\sin\theta}{\theta} \quad . \tag{27}$$

If there is an inhomogeneous or chemical shift term in the rotating frame Hamiltonian

$$H_c^0 = \sum_i \sigma_{izz} I_{iz} \tag{28}$$

Figure 2

Pulse sequences discussed in the text. Although not carried out here, these sequences may be symmetrized by a redefinition of the cycle to eliminate some correction terms to the average Hamiltonian.

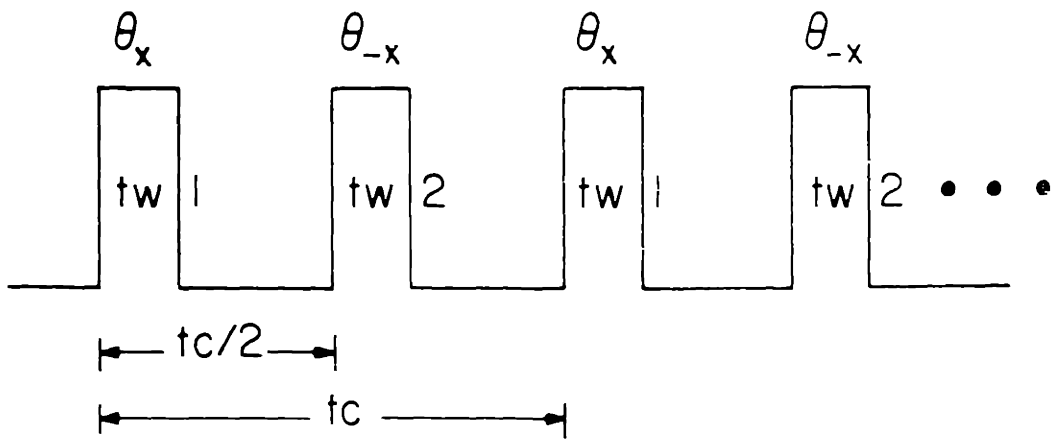
θx
θ-x
θx
θ-x
tw 1
tw 2
tw 1
tw 2 • • •
tc/2
tc

(a)

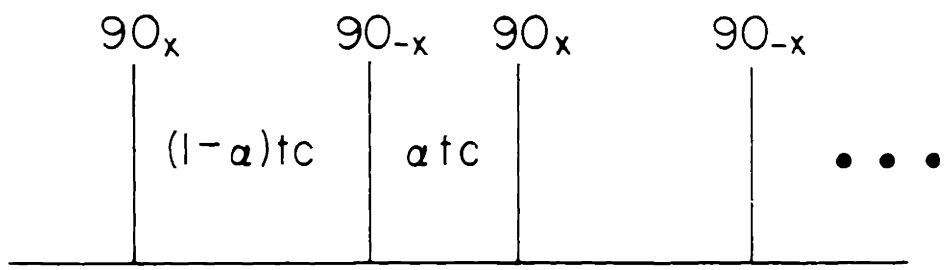
90x
90-x
90x
90-x
(1−α)tc
α tc
• • •

(b)

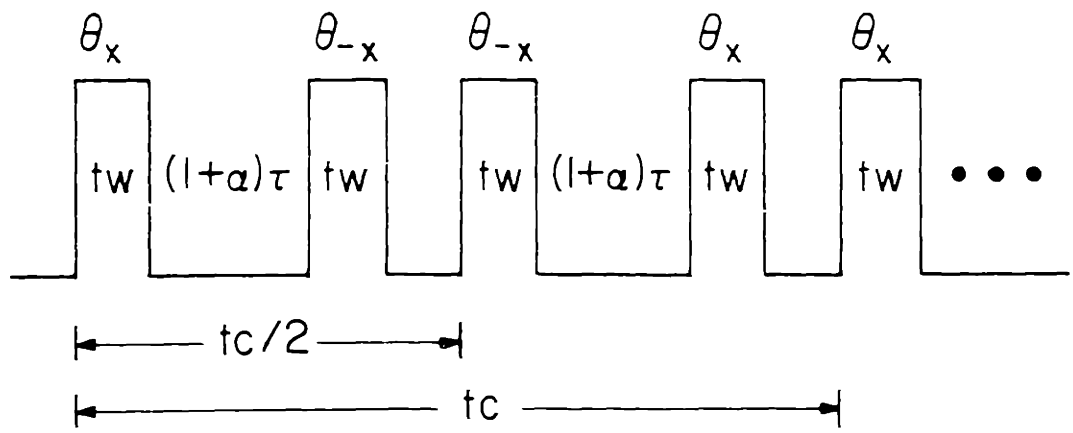
θx
θ-x
θ-x
θx
θx
tw
(1+α)τ
tw
tw
(1+α)τ
tw
tw
• • •
tc/2
tc

(c)

where H_c^0 is again a truncated form of the full chemical shift H_c, then $\bar{H}_{DTR}^{00}$ will contain another term given by

$$\bar{H}_c^{00} = H_{c\bar{\mu}}^0 \, p_\delta(\theta/2) \qquad (29)$$

with p_δ defined in (27); this is in agreement with previous results[10].

B. LINE NARROWING

Figure 3 shows a calculated plot of $\frac{3p_\delta(\theta) + 1}{4}$ as a function of θ for several values of the duty factor δ. For $\delta < 0.75$ we see that $\bar{H}_d^{00}$ can be made to vanish by an appropriate selection of θ and thus leads to a simple technique for line narrowing. For $\delta = 0$, i.e. δ-pulses we need $\theta = \theta_t$ where θ_t is the tetrahedral angle (109°28'); this is just the previously described PAT sequence[11]. However, the present analysis shows that even for $\delta > 0$ the coupling can be made to vanish with $\theta > \theta_t$, thus eliminating the term in equation (21) of reference (11).

The fact that $\theta = \theta_t$ explains the limited line narrowing in Figure 2 of the above work. With careful adjustment of $\theta > \theta_t$ decay times exceeding 1 msec for the ^{19}F nuclei in CaF_2 have actually been attained for this experiment[18]. Interestingly, it appears from Figure 2 that employing $\delta \sim 0.75$ should be superior to the PAT experiment, since the region of line narrowing is then markedly less sensitive

Figure 3

Plot of the dipolar scale factor $\bar{P}_2(\underset{\sim}{\bar{\mu}} \cdot \underset{\sim}{\mu}(t)) = 1/4(3p_\delta(\theta) + 1)$ vs. θ for several values of the duty factor δ in the phase alternated pulse sequence (figure 2(a)). The sequence produces line narrowing and is applicable for high resolution nmr in solids when $\bar{P}_2 = 0$, e.g. at 109.5° for $\delta = 0$ (the phase alternated tetrahedral experiment). For $\bar{P}_2 < 0$ the Hamiltonian becomes "negative" yielding the conditions for time-reversal.

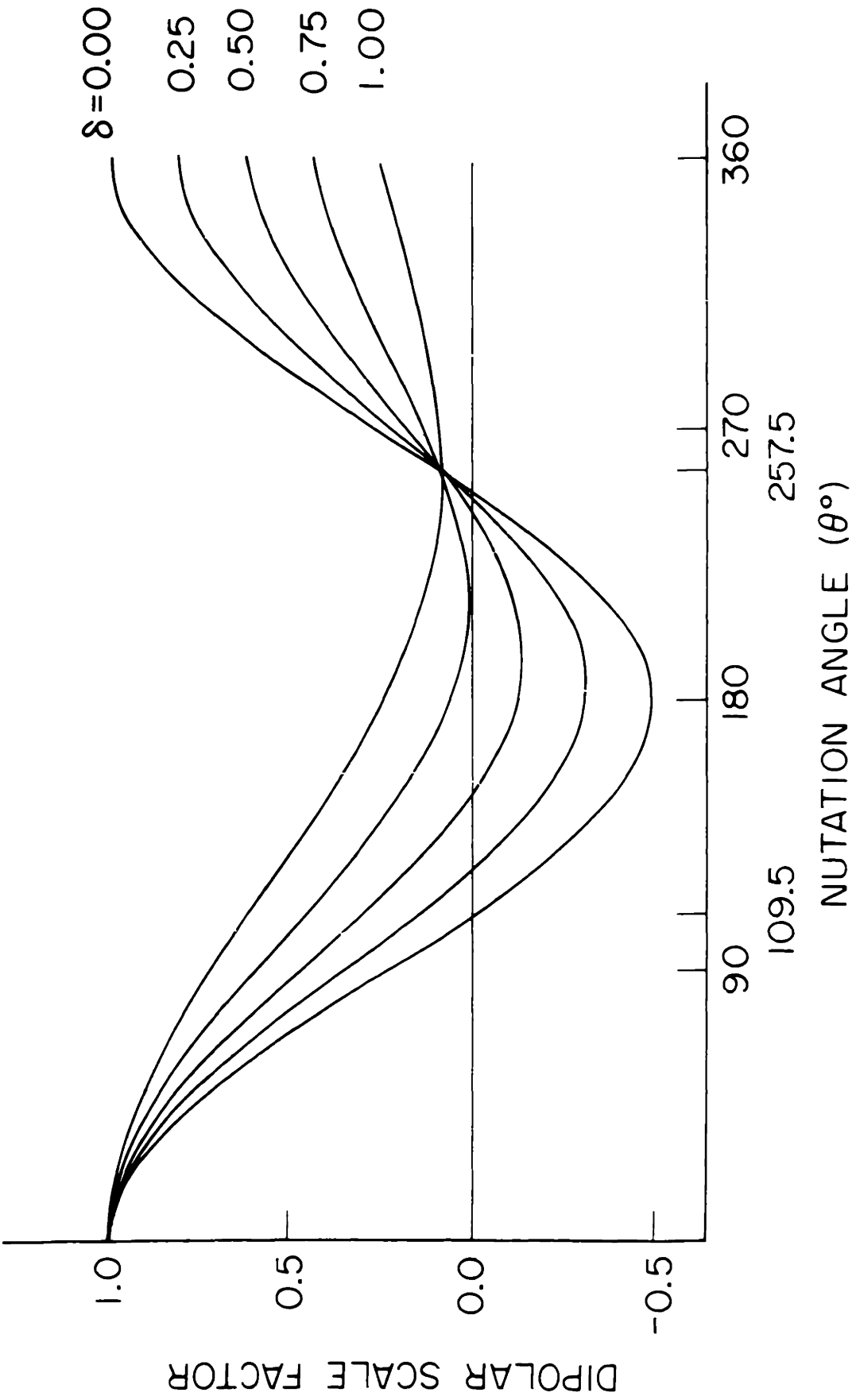
δ=0.00
0.25
0.50
0.75
1.00
1.0
0.5
0.0
-0.5
DIPOLAR SCALE FACTOR
90
109.5
180
257.5
270
360
NUTATION ANGLE (θ°)

to any inhomogeneities in the r.f. field. However, in this range $\overline{\Delta\omega}$ is also reduced so there is no large gain in cycle time. An experimental check of the full curves in Figure 2 will be interesting and should provide an additional verification of this simple thoery. Note that for any solution of $\tan\theta = \theta$, e.g. $\theta = 257.5°$, the line narrowing is predicted to be independent of the duty factor δ.

C. MAGIC ECHOES

Magic echoes, which appear after homogeneous free induction decay in solids, were first reported by Rhim, Pines and Waugh[8]. To remind the reader, magic echoes are produced in the following way: following the decay of magnetization due to H_d^0, a strong r.f. perturbation is applied under which the effective Hamiltonian is given by kH_d^0 with $k < 0$. This induces a negative time development which recalls the previous history of the spin system and produces an echo. See Chapter V for details.

Looking at Figure 2, we see that for small δ, we can make $3\rho_\delta(\theta) + 1 < 0$, i.e. $\overline{H}_d^{0\,0}$ "negative", thus yielding the necessary conditions for time reversal . The observation of magic echoes should provide verification for this aspect of the theory. These could be produced simply by applying a train of phase alternated pulses "sandwiched" between a pair of phase shifted ξ and $-\xi$ pulses as in the analogous on resonance experiments[8].

Note that this is another manifestation of the simple form taken by the average Hamiltonian $\bar{H}^{0\,0}_{DTR}$. In a general pulse experiment, say an on resonance phase alternated sequence, the effective Hamiltonian has some other form except for special cases like 90° pulses[3] (vide infra) and time reversal becomes much more restricted.

D. SPIN LOCKING

The form of $\bar{H}^{0\,0}_{DTR}$ allows another general conclusion. Since

$$[I_{\bar{\mu}}, \bar{H}^{0\,0}_{DTR}] = 0 \qquad (30)$$

we have all the prerequisites for spin locking of the $\bar{\mu}$ component of magnetization. We point out that (30) is the correct criterion to employ for spin locking -- the presence of an average or mean H_1 field is neither sufficient nor a necessary condition as is still sometimes erroneously assumed.

We see then that the observation of $T_{\|}$ and $T_{\perp}$ (20) should be a general phenomena in any resonance offset multiple-pulse experiment. If we start with the magnetization along an arbitrary axis in the rotating frame we may separate it into components perpendicular to and parallel to $\bar{\mu}$. The perpendicular component will then precess about $\bar{\mu}$ and decay by spin-spin processes with a time constant $T_{\perp} = \bar{P}_2^{-1} T_2$; when $\bar{P}_2 \to 0$ the decay will of course be dominated by correction terms. The parallel component will be spin locked

and will change only by spin-lattice relaxation in the rotating frame[12,14,21-24]. The effects of spin-lattice relaxation are very interesting in these experiments and will be treated in detail elsewhere.

If the effective field along $\bar{\mu}$, i.e. in $\bar{H}_\Delta$, is inhomogeneous (for example from an inhomogeneous H_0 or from inhomogeneous shifts as in a polycrystalline solid) then T_1 may be dominated by this inhomogeneity if $\bar{P}_2$ is small. This effect can be demonstrated quite dramatically by production of inhomogeneous rotary spin echoes[25] when $\bar{\mu}$ is at the magic angle (i.e. $\bar{P}_2 = 0$) as in the experiments of Rhim and Kessemeier[26] and Pines, Rhim and Waugh[27]. In the latter experiment, the nature of the two components of magnetization is shown quite clearly using the off resonance four-pulse technique[5].

The simple behavior we have outlined above is a peculiar characteristic of the resonance offset experiment. If we enquire into the behavior of the spin system under the pulse sequence of figure 2(a) at resonance ($\Delta\omega = 0$) we find from (13)

$$\bar{H}_d^0 = -\frac{1}{2}H_{dx}^0 + \frac{3}{2}p_\delta(\theta)\sum_{i<j} b_{ij}\{\cos\theta(I_{iz}I_{jz} - I_{iy}I_{jy}) - \sin\theta\,(I_{iz}I_{jy} + I_{iy}I_{jz})\}. \qquad (31)$$

In this case an analysis of the spin system response is difficult and comparison with the normal unperturbed behavior can be made only on the basis of moments of the decays. For example, the second moments defined by[28]

$$\langle\omega^2\rangle_\mu = \frac{\mathrm{Tr}[H_d^0,\ I_\mu]^2}{\mathrm{Tr}I_\mu^2} \tag{32}$$

are given for (31) by:

$$\langle\omega^2\rangle_x = p_\delta^2(\theta)\ \langle\omega^2\rangle_0 \tag{33}$$

$$\langle\omega^2\rangle_y = \tfrac{1}{4}(p_\delta^2(\theta) + 2\cos\theta\ p_\delta(\theta) + 1)\langle\omega^2\rangle_0 \tag{34}$$

$$\langle\omega^2\rangle_z = \tfrac{1}{4}(p_\delta^2(\theta) - 2\cos\theta\ p_\delta(\theta) + 1)\langle\omega^2\rangle_0 \tag{35}$$

where $\langle\omega^2\rangle_0$ is the normal high field truncated second moment

$$\langle\omega^2\rangle_0 = \frac{\mathrm{Tr}[H_d^0,\ I_x]^2}{\mathrm{Tr}I_x^2}\ . \tag{36}$$

For $\theta = 90°$, $\delta \sim 0$ we have the experiment of Waugh and Huber[29] which produces a prolonged decay only along the x axis as expected from (33). As we have seen though, this picture changes drastically as we go off resonance.

We take this opportunity to note that (33) also gives the second moment of spin echo decays (with constant δ) produced by a 90_x pulse followed by a θ_y pulse since this

is one cycle of the appropriate pulse sequence. This important problem will be dealt with in the near future[9].

E. IDEAL 90° PULSES

Since the simple properties of 90° δ-pulses have a special appeal and in fact most proponents of multiple-pulse nmr have been primarily obsessed with such pulses, we enquire here into the possibility of using them for experiments similar to those mentioned above. A general two-pulse sequence composed of such pulses is shown in figure 2(b) with α variable from 0 through 1. It is trivial to show that if this sequence is applied with the appropriate resonance offset then from (23)

$$\bar{H}_d^{00} = H_{d\bar{\mu}}^{0} \left(1 - \frac{3}{2} \frac{\alpha(1-\alpha)}{\alpha^2+(1-\alpha)^2}\right) \tag{37}$$

where $\bar{\mu}$ is in the yz plane and

$$\underset{\sim}{\mu}\cdot\bar{\underset{\sim}{\mu}} = \frac{\alpha}{\sqrt{(\alpha^2+(1-\alpha)^2)}} \tag{38}$$

and therefore $\bar{H}_d^{00}$ cannot be made to vanish for any real α. Thus using only 90° δ-pulses we conclude that we must resort to a cycle containing more than two pulses to achieve line-narrowing. It is interesting that the maximal line narrowing of 0.25 occurs at α = 1/2 which gives just the pulse sequence of Waugh and Huber[29].

F. FOUR-PULSE CYCLE

There are many possible four-pulse cycles. The most well known to pulsed NMR spectroscopists is the four-pulsed four-phase WAHUHA cycle[5]. Here we treat a four-pulse cycle employing only <u>two</u> phases shown in figure 2(c). Defining δ as in (26) we find again using (23),

$$\bar{H}_d^{00} = H_d^0 \{\tfrac{1}{2}(1-\alpha)(1-\delta) + \tfrac{1}{4}(1+\alpha)(1-\delta)(3\cdot\cos^2\theta - 1) + \frac{\delta}{4}(1 + \frac{3\sin\theta\cos\theta}{\theta})\} \qquad (39)$$

which reduces for $\theta = \pi/2$ to

$$\bar{H}_d^{00} = H_d^0 \frac{1 - 3\alpha(1-\delta)}{4} . \qquad (40)$$

For ideal δ-pulses, $\delta = 0$, we see that we can achieve an effective line narrowing, $\bar{H}_d^{00} = 0$, for $\alpha = 1/3$; this yields precisely the same timing as that of the WHH cycle and has been verified experimentally yielding decay times of 2 msec on the ^{19}F spins of CaF_2. Just as in this latter cycle the effects of finite pulse width can be compensated for. If we wish to retain 90° pulses then this is easily done by varying α (as long as $\delta < 2/3$) using (40). The change in effective decay time going off resonance is quite marked for this pulse sequence. Magic echoes may be produced just as in the two pulse cycle by making $\bar{H}_d^{00}$ "negative".

IV. SUMMARY

We have attempted to present a clear picture of the additional averaging effects produced by resonance offset fields in multiple-pulse nmr, and have illustrated this with some simple examples. In particular, the theory shows that behavior at, and far from resonance may be distinctly different, and that calculations made disregarding the resonance offset field, lead to erroneous results[30]. In addition, several uses of this phenomenon including line narrowing, spin locking, and magic echoes have emerged. We conclude by pointing out two other possible applications of this phenomenon in the future.

(i) Design of more efficient pulse sequences for line narrowing and magic echoes. The discussion in this paper has centered on zero order effects, but there are equally profound higher order effects which can be accounted for by the theory. These effects may in some cases outweigh the conclusions drawn from symmetry considerations alone in designing multiple-pulse experiments[7,8,27,31,32].

(ii) This type of experiment provides a simple means of producing effective static fields in the rotating frame with arbitrary directions and magnitudes, and with modified dipolar interactions, while being able

to observe the magnetization between pulses. These facts give it an appealing potential for application to double-resonance experiments[33,34] which have stirred up some interest among chemists since their recent adaptations to high resolution nmr of dilute spins in solids[35-37].

ACKNOWLEDGMENTS

We are grateful to J. D. Ellett, Jr. for many helpful conversations and for his aid with some aspects of the theory and experiments.

REFERENCES AND FOOTNOTES

1. U. Haeberlen and J. S. Waugh, Phys. Rev., 175, 453 (1968).
2. E. D. Ostroff and J. S. Waugh, Phys. Rev. Lett., 16, 1097 (1966).
3. J. S. Waugh, C. H. Wang, L. M. Huber and R. L. Vold, J. Chem. Phys., 48, 662 (1968).
4. P. Mansfield and D. Ware, Phys. Lett., 22, 133 (1966).
5. J. S. Waugh, L. Huber and U. Haeberlen, Phys. Rev. Lett., 20, 180 (1968).
6. M. Mehring, A. Pines, W.-K. Rhim and J. S. Waugh, J. Chem. Phys., 54, 3239 (1971).
7. M. Mehring and J. S. Waugh, Phys. Rev., (in press).
8. (a) W.-K. Rhim, A. Pines and J. S. Waugh, Phys. Rev., 3, 684 (1971). (b) A. Pines, W.-K. Rhim and J. S. Waugh (unpublished results).
9. A. Pines and J. S. Waugh, (to be published).
10. J. D. Ellett, Jr. and J. S. Waugh, J. Chem. Phys., 51, (2851 (1969).
11. U. Haeberlen, J. D. Ellett, Jr. and J. S. Waugh, J. Chem. Phys., 55, 53 (1971).
12. U. Haeberlen and J. S. Waugh, Phys. Rev., 185, 420 (1969).
13. J. H. Van Vleck, Phys. Rev., 74, 1168 (1948).
14. A. G. Redfield, Phys. Rev., 98, 1787 (1955).
15. (a) W. I. Goldburg and M. Lee, Phys. Rev.Lett., 11, 255 (1963); (b) M. Lee and W. I. Goldburg, Phys. Rev., 140, A1261 (1965).

16. D. Barnaal and I. J. Lowe, Phys. Rev. Lett., 11, 258 (1963).

17. J. D. Ellett, Jr., M. G. Gibby, U. Haeberlen, L. Huber, M. Mehring, A. Pines, and J. S. Waugh, Advances in Magnetic Resonance, Vol. 5,(Academic Press, N. Y., 1971).

18. A. Pines, J. D. Ellet, Jr. and J. S. Waugh, (unpublished).

19. (a) I. Solomon, Compt. Rend., 248, 92 (1950).

20. (b) S. R. Hartmann and E. L. Hahn, Bull. Amer. Phys. Soc., 5, 498 (1960).

20. $T_{\parallel}$ and $T_{\perp}$ refer to the two components of magnetization respectively parallel and perpendicular to the effective field in the rotating frame.

21. I. Solomon and J. Ezratty, Phys. Rev., 127, 78 (1962).

22. B. N. Provotorov, Z. Eks. Teor. Fiz., 41, 1582 (1961).

23. M. Goldman, Spin Temperature and Nuclear Magnetic Resonance in Solids,(Oxford Univ. Press, London, 1970).

24. H. Betsuyaku, J. Phys. Soc., Japan, 30, 641 (1971).

25. I. Solomon, Phys. Rev. Lett., 2, 301 (1959).

26. W -K. Rhim and H. Kessemeier, Phys. Rev., 3, 3655 (1971).

27. A. Pines, W -K. Rhim and J. S. Waugh, J. Mag. Res., 6, 457 (1972).

28. A. Abragam, The Principles of Nuclear Magnetism,(Clarendon, London, 1961).

29. J. S. Waugh and L. M. Huber, J. Chem. Phys., 47, 1862 (1967).

30. This is similar to the trouble encountered when there are microscopic inhomogeneities stronger than the spin-spin interactions. The effects of the inhomogeneities on the spins cannot be accounted for independently, but modulate the spin-spin interactions, making additional truncation or averaging of these interaction terms a necessity: D. Hone, V. Jaccarino, T. Ngwe and P. Pincus, Phys. Rev., 186, 291 (1969).

31. P. Mansfield, J. Phys. C, 4, 1444 (1971).

32. This fact probably explains the observation by us that there is no increase in line narrowing efficiency going from the four-pulse cycle of Ref. 5 to the symmetrical four-pulse cycle of Ref. 8b.

33. S. R. Hartmann and E. L. Hahn, Phys. Rev., 128, 2042 (1962).

34. F. M. Lurie and C. P. Slichter, Phys. Rev., 133, A1108 (1964).

35. H. E. Bleich and A. G. Redfield, J. Chem. Phys., 55, 5405 (1971).

36. P. Mansfield and P. K. Grannell, J. Phys. C, L197 (1971).

37. (a) A. Pines, M. G. Gibby and J. S. Waugh, Bull. Amer. Phys. Soc., 16, 1403 (1971); (b) A. Pines, M. G. Gibby and J. S. Waugh, J. Chem. Phys., 56, 1776 (1972); (c) A. Pines, M. G. Gibby, J. S. Waugh, Chem. Phys. Lett., (in press).

CHAPTER II

HIGH RESOLUTION NUCLEAR DOUBLE RESONANCE OF DILUTE SPINS IN SOLIDS

I. INTRODUCTION

Although high resolution NMR in liquids is established as a powerful tool for structural and dynamical studies of chemical systems,[1] analogous experiments on solids have enjoyed a more limited prosperity. The reason is readily traceable: whereas the direct nuclear magnetic dipole-dipole interaction is averaged to zero in liquids due to rapid rotational and translational diffusion, no such motion prevails in rigid solids, leaving the above interaction as an annoying source of spectral broadening. If we consider that spectral structure due to chemical shifts and spin-spin couplings requires resolution of ~ several Hz, while dipolar broadening is normally of ~ several kHz, it is clear that we are faced with an awesome problem if we wish to bring solids into the realm of conventional high resolution NMR.

In many instances, it is precisely the dipolar interaction in a solid which is at the center of attention (or its presence is a crucial factor). Such is the case, for example, in studies of lineshapes,[2] spin-diffusion,[3] spin-temperature,[4] etc. In addition, it can be used to good advantage in both structural and dynamical studies, as exemplified by wideline dipolar structure[5] and by second moment and spin-lattice relaxation studies of motion.[6] It is clear, however, that a considerable increase

in information could be attained if it were possible to suppress the dipolar broadening and extract details on other interactions such as chemical shifts and indirect nuclear spin-spin couplings. The type of information from solids should be valuable, since the restriction of molecular reorientation preserves any anisotropy (e.g. chemical chielding anisotropy) which is averaged to zero in liquid systems and may show up only indirectly through spin relaxation effects.

Several approaches have been made to this important problem. They may be discussed in terms of the Hamiltonian for a "truncated" dipolar interaction[7] between like spins which we write as:

$$\mathcal{H}_d^0 = -\gamma^2\hbar^2 \sum_{i<j} \frac{1}{r_{ij}^3} P_2(\cos\theta_{ij})(3\, I_{iz}I_{jz} - \underset{\sim}{I}_i \cdot \underset{\sim}{I}_j) \qquad (1)$$

The techniques differ in which part of (1) they choose to affect. In the magic-angle sample-spinning experiment[8-10] it is θ_{ij} which is modulated rapidly giving $\langle P_2(\cos\theta_{ij}(t))\rangle = 0$. In multiple-pulse NMR,[11-14] in an appropriate reference frame, it is $\underset{\sim}{I}$ that is modulated, giving $\langle 3I_{iz}(t)\, I_{jz}(t) - \underset{\sim}{I}_i \cdot \underset{\sim}{I}_j\rangle = 0$. These have met with considerable success. The sample-spinning, however, requires high rotation speeds ($\gtrsim$ 10 kHz) making it difficult for rigid solids. In addition it removes any anisotropy in the chemical shift. The multiple-pulse techniques, on the other hand, require high r.f. phase and amplitude stability, and despite the promise of enhanced resolution through the use of symmetry,[15-19]

resonance-offset effects[20,21] and computer-aided adjustments,[22] they are difficult to perform routinely.

In the present paper we discuss a different approach which we find to be rather simple and widely applicable, and which has produced a significant flux of preliminary experimental results since its recent institution.[23] The basic premise is remarkably simple. Looking at (1), we see that the "size" of $\mathcal{H}_d^0$ could be reduced by simply increasing the magnitude of the r_{ij}. How can we do this? At least one solution presents itself immediately: if the nuclear spins of interest are of an isotope having a low natural abundance, or if they are chemically dilute, then of course the average r_{ij} is increased. Precisely this thinking motivated the experiment of Lauterbur[24] on $Ca^{13}CO_3$ and those of Pines, Rhim and Waugh[25] on $Ca^{13}CO_3$ and $^{13}CS_2$. ^{13}C and ^{15}N constitute ideal nuclei for such studies since they have both low magnetogyric ratios and low isotopic abundance. Their importance in chemical and biological systems goes without saying.

The alert reader will no doubt take issue with the above remarks which appear to be somewhat näive on two counts:

(a) dipolar broadening by abundant unlike spins

(b) low sensitivity.

Both objections are clearly legitimate. Note that in $CaCO_3$ and CS_2, ^{13}C is the only significantly active nucleus. In the general, more interesting case, other "unlike" nuclei (for example ^1H)

will be present in high abundance and cause a severe dipolar broadening of the rare spins under study. The problem would thus appear to revert to that encountered normally in abundant spin systems.

The problem raised in (b) is no less critical. An obvious price which we must pay for the attenuation of dipolar interaction between the spins is a reduction of the number of resonant spins in the sample and a consequent reduction in the sensitivity of NMR detection. The problem of sensitivity is a well known one in liquid studies of rare isotopes, and Fourier-transform and signal averaging techniques are employed to their full extent.[26] In solids, where resolution is lower and spin-lattice relaxation times may be very long, the problem becomes much more acute, making conventional techniques essentially useless.

Lest the reader despair and turn to simpler experiments such as molecular beam studies of radical reactions,[27] we remark that both problems mentioned above can be solved with surprising facility. Dipolar broadening by unlike spins is removed by strong irradiation of these spins at their resonance frequency.[28,29] As in the case of J-coupling in liquids, this induces a "spin-decoupling".[30] The power requirements in the solid case are much greater due to the strength of the dipolar interaction relative to J-coupling. It might appear that this spin-decoupling should be as difficult as the removal of dipolar interactions between like spins making it similar to multiple-pulse experiments.

However, it is actually much simpler due to the simpler transformation properties of the resonant spin operators, and the stability requirements on r.f. phase and amplitude are considerably less stringent.

The sensitivity problem is similarly approached using an idea established by Hartmann and Hahn.[31] In the Hartmann-Hahn experiment, a system of rare spins (S) is detected by observing its accumulative effects on an abundant spin system. The language of spin thermodynamics[4,32] is ideally suited to a discussion of these phenomena (see Figure 1). Basically, the experiment works as follows: the I spin system is brought into equilibrium with the lattice at a temperature T^L. Normally, a large magnetization $\gamma\hbar \langle I \rangle \sim 1/T^L$ could now be observed. Instead, the I spins are now brought into contact with the S spins which are imagined to have no spin order, i.e. an infinite spin-temperature. The contact can be established in many ways some of which will be discussed later in this paper. The simplest to visualize is the application of two strong r.f. fields, H_{1I} and H_{1S}, at the I and S resonance frequencies. The former is arranged by one of several methods to spin-lock[20,21,33,34] the I magnetization.

If the Hartmann-Hahn condition is satisfied, i.e.:

$$\gamma_I H_{1I} = \gamma_S H_{1S} \tag{2}$$

then mutual I and S spin flips via the I-S dipolar interaction become energy conserving and cause the system to proceed rapidly

Figure 1

Simple thermodynamical picture for double-resonance. T_{1S} and T_{1T} are nuclear spin lattice relaxation times which are imagined to be very long, and T_{IS} is a cross-relaxation time. The two energy reservoirs of I and S spins are at spin-temperatures T^I and T^S. In the classical indirect detection method, the I spins are cooled by allowing them to equilibrate for $\sim T_{1I}$ with the lattice. The S spins are detected by bringing them into contact with the I spin reservoir and keeping them hot by one of several techniques. Energy flows at a rate of $\sim\varepsilon/T_{IS}$ from the S to the I spin reservoir (where ε is the ratio of S to I heat capacities) causing a cumulative heating and destruction of the I spin order. Subsequent observation of a reduced I signal indicates the S resonance. The sensitivity demands that I spin order be maintained for long times $\sim T_{IS}/\varepsilon$.

In the direct detection method, the I spin reservoir is used only as a source of polarization and is not observed. Following an I-S contact (the S spins are not kept hot here), the S spins are observed directly, and the signals coadded $\sim 1/\varepsilon$ times to yield a markedly enhanced S spectrum within one T_{1I}.

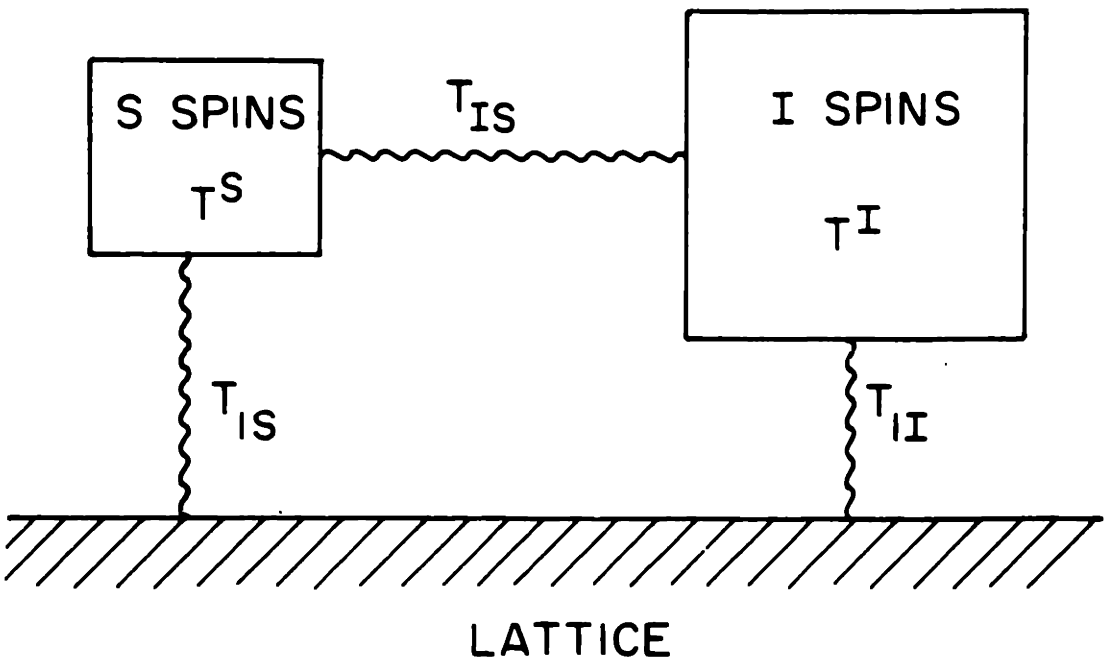
S SPINS
T^S
T_{IS}
I SPINS
T^I
T_{IS}
T_{II}
LATTICE

to internal equilibrium. The result is a cooling of the S spin system by the establishment of an S spin order (in the form of a magnetization along H_{1S}) and a small heating of the I spin reservoir (a small decrease in the I magnetization). The effect on the I spins is very small since the S spins are rare. The process may be repeated by destroying the S spin order and again bringing them into contact with the I spins. The destruction can be performed in several ways--in the Lurie-Slichter[35] experiment it is done by simply removing the H_{1S} field and allowing $\langle S \rangle$ to decay to zero.

If the cycle is repeated many times, the net effect is a substantial heating of the I spin reservoir; subsequent observation of the I magnetization yields a considerably reduced signal, leading to a greatly enhanced sensitivity in the detection of the S spin resonance.

For application to our problem, this experiment suffers from poor resolution. The I and S spins cannot be decoupled as described before since it is precisely their mutual interaction which constitutes the thermal link between their reservoirs and is necessary for the sensitive detection. We therefore make use of the I spin reservoir only as a source of polarization, and instead of detecting the S spins indirectly via the I spins, we observe them directly. The experiment is then exactly the same as the Lurie-Slichter version[35] (of the Hartmann-Hahn experiment[31])

described above, except that the S, and not the I magnetization is observed. Following the I-S contact (in the direct detection method we call this "cross-polarization"), the S spin decay is observed. Spin-decoupling, and thus high resolution, is achieved by the I spin irradiation used for the spin-locking. The cycle is repeated and the S signals accumulated until the I magnetization is depleted. This yields of course a large sensitivity enhancement over a conventional S free induction decay; we have therefore made some recognizable progress in our attack on problem (b), making the present approach an attractive one for high resolution NMR in solids.

The indirect detection methods can also be modified to yield better resolution. Two approaches have been proposed and used in preliminary experiments. We shall see later that depending on circumstances, these may or may not have advantages over our direct detection.

The next section describes our direct detection method, "proton-enhanced nuclear induction spectroscopy", in more detail, with reference to one typical version. Section III gives relevant experimental details and Section IV some exemplary results. In section V we discuss briefly alternative versions of our experiment and finally, compare them with the indirect detection methods.

II. DESCRIPTION OF TECHNIQUE

In this section we present a more detailed account of our direct detection method. Since both the spin-decoupling and double-resonance procedures are not new, only the aspects relevant to the present experiments are discussed. Excellent quantitative details on the double-resonance phenomena can be found in several papers.[31,35,36] We indicate only how they are employed in a novel way for our purposes.

As mentioned in the introduction there are many variants to the experiment since the spin-decoupling and cross-polarization can be done in several ways. These will be discussed in Section V. For the present we have chosen to illustrate one simple version in order to make our presentation concrete for the reader inexperienced in these matters. We shall see later that this may not be the best solution from the view of technical efficiency. Since the purpose of the experiment is to provide an enhanced sensitivity and resolution, we wish to compare with conventional techniques; this is done next, following a brief theoretical digression.

A. BASIC THEORY

We consider the following system in a large external magnetic field: an abundant I spin system with a resonance frequency ω_{0I} is dipolar coupled to a rare S spin system with resonance

frequency ω_{0S}. Two strong r.f. fields with rotating components H_{1I} and H_{1S} are applied at frequencies of ω_{0I} and ω_{0S}, respectively. This is illustrated in Figure 2a. The full Hamiltonian has the form:

$$\mathcal{H} = \mathcal{H}_0 + \mathcal{H}_{dII} + \mathcal{H}_{dIS} + \mathcal{H}_{dSS} + \mathcal{H}_{1I}(t) + \mathcal{H}_{1S}(t) \tag{3}$$

where $\mathcal{H}_0$ is the Zeeman interaction of I and S spins with the external field, $\mathcal{H}_d$ is the dipolar interaction and $\mathcal{H}_{1I}(t)$ and $\mathcal{H}_{1S}(t)$ describe the coupling of the I and S spins to the r.f. excitation. As shown by Redfield,[32b] it is convenient to transform to a rotating frame in which the r.f. fields are stationary. In this case we need a double rotating frame induced by the transformation:[31]

$$R = \exp\left[-it(\omega_I I_z + \omega_S S_z)\right] \tag{4}$$

In this frame, the Hamiltonian has transformed to:

$$\mathcal{H}_R = \mathcal{H}^0_{dII} + \mathcal{H}^0_{dIS} + \mathcal{H}^0_{dSS} + \mathcal{H}_{1I} + \mathcal{H}_{1S} \tag{5}$$

$$+ \text{time-dependent terms}$$

where $\mathcal{H}^0_{dII}$ and $\mathcal{H}^0_{dSS}$ have the form of equation (1), and

$$\mathcal{H}^0_{dIS} = \sum_i S_{iz} \sum_j b_j I_{jz}$$

$$b_i = \frac{-2\gamma_I\gamma_S\hbar^2 P_2(\cos\theta i)}{r_i^3} \tag{6}$$

Figure 2

Double rotating frame transformation. In the laboratory frame (a) the rotating components of the I and S rf have amplitudes H_{1I}, H_{1S}, and angular frequencies ω_I, ω_S. A rotating frame transformation, equation (4) is performed which rotates the I spins at ω_I and the S spins at ω_S about z. In this frame (b) we can effectively view the I spins in their rotating frame experiencing a static field H_{1I} along z and the S spins in their rotating frame experiencing H_{1S} along X. The effects of H_{1S} on I spins and H_{1I} on S spins can be neglected if $\omega_I - \omega_S$ is much larger than the S and I spectral widths, as is normally the case.

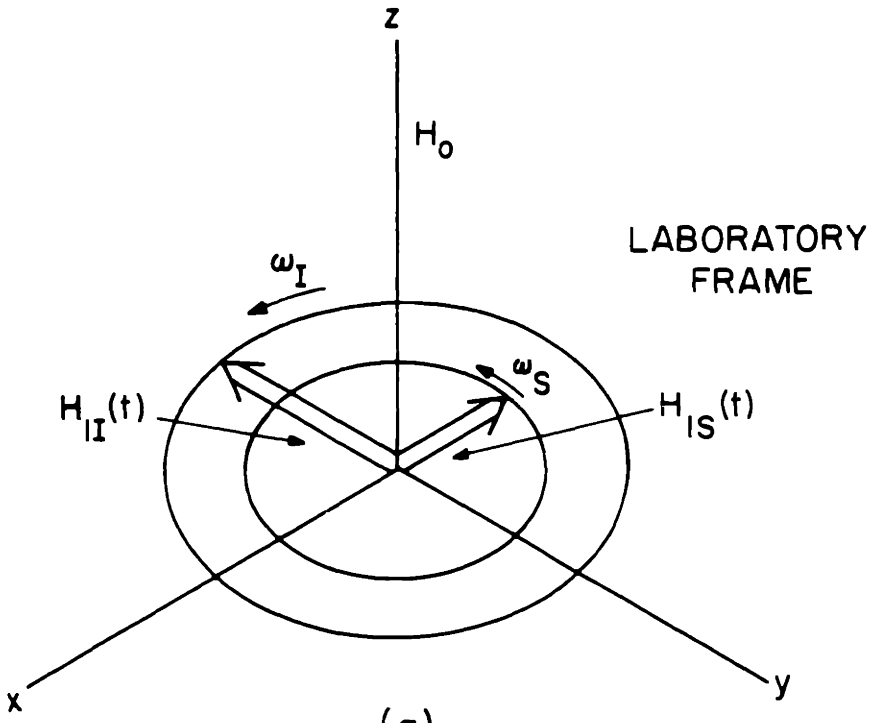
z
H_o
LABORATORY
FRAME
ω_I
ω_S
$H_{II}(t)$
$H_{IS}(t)$
x
y

(a)

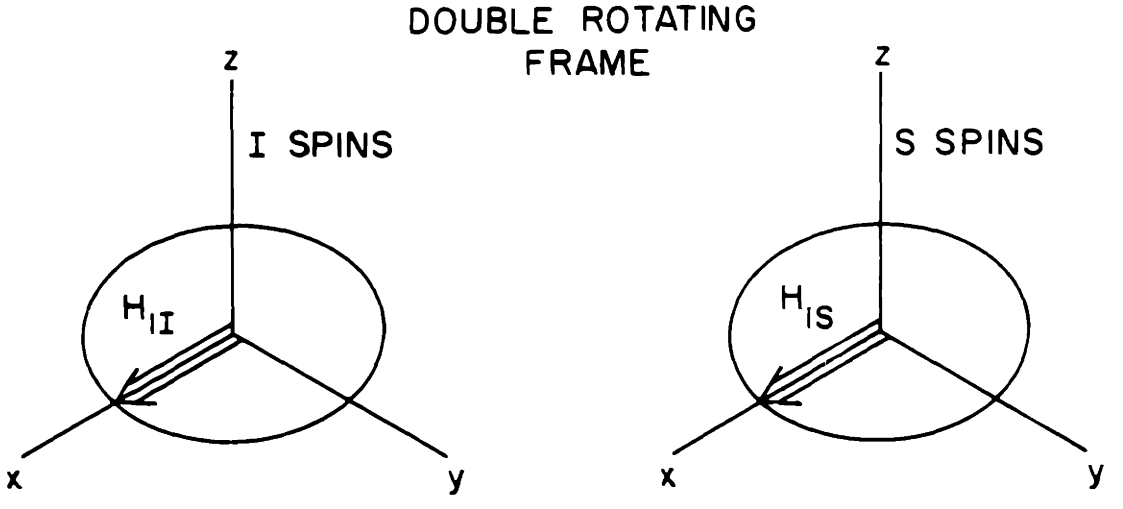
DOUBLE ROTATING
FRAME
z
I SPINS
H_{II}
x
y
z
S SPINS
H_{IS}
x
y

(b)

$$\mathcal{H}_{1I} = -\gamma_I \hbar H_{1I} \sum_i I_{ix} \tag{7}$$

$$\mathcal{H}_{1S} = -\gamma_S \hbar H_{1S} \sum_i S_{ix} \tag{8}$$

The phase of the rotation is chosen to put H_{1I} and H_{1S} along the x axes in the I and S rotating frames as in Figure 2b. Since we are not interested in calculating spin-lattice effects, we may discard the time dependent terms; all this is well known.

Thermodynamics can now be applied in the rotating frame since the Hamiltonian is effectively time-independent.[32b] The two terms $\mathcal{H}_{1I}$ and $\mathcal{H}_{1S}$ are considered as reservoirs of Zeeman energy which exchange energy via the dipolar coupling with which they do not commute. The dipolar reservoir should also be included in the thermodynamics but we shall neglect it for the present since we assume that H_{1I} is very large compared to internal local fields. Following Redfield, we assume that the system ultimately approaches a state of full internal equilibrium in the rotating frame described by the density matrix:

$$\rho_R^{eq} = \frac{\exp(-\mathcal{H}_R/kT)}{\mathrm{Tr}\{\exp(-\mathcal{H}_R/kT)\}} \tag{9}$$

which for high temperatures and large fields is given to a good enough approximation for our purposes by:

$$\rho_R^{eq} = \frac{1}{Z}\left[1 + \frac{1}{kT}(\mathcal{H}_{1I} + \mathcal{H}_{1S})\right] \tag{10}$$

where $Z = \mathrm{Tr}\{1\}$

As pointed out by Hartmann and Hahn,[31] the rate at which this single spin temperature is approached depends strongly on the magnitudes of H_{1I} and H_{1S}. In general, each reservoir can be in internal equilibrium with a different spin temperature:[4]

$$\rho_R = \frac{1}{Z}\left[1 + \frac{\mathcal{H}_{1I}}{kT^I} + \frac{\mathcal{H}_{1S}}{kT^S}\right] \tag{11}$$

and the two subsystems come to equilibrium in a time T_{IS} (Figure 1) which depends on $\gamma_I H_{1I} - \gamma_S H_{1S}$. When condition (2) is fulfilled, the rate is maximal as we shall see.

The quantities of interest to us are the energy, entropy and magnetization. The Zeeman energy of the system in a state described by (11) is given by:

$$E = -\mathrm{Tr}\{\rho_R \mathcal{H}_R\} = E_I + E_S = -\frac{C_I H_{1I}^2}{T^I} - \frac{C_S H_{1S}^2}{T^S} \tag{12}$$

where C_I and C_S are Zeeman spin heat capacities given by:

$$C_I = \frac{\gamma_I^2 \hbar^2 I(I+1) N_I}{3k} \tag{13}$$

and similarly for C_S. N_I and N_S are the numbers of I and S spins.

The x component of the magnetization in the rotating frame (i.e. along the H_1 field) is given by:

$$M_I = \gamma_I \hbar \langle I_x \rangle = \gamma_I \hbar \,\mathrm{Tr}\{\rho_R I_x\} = \frac{C_I H_{1I}}{T^I} \tag{14}$$

and similarly for $\gamma_S \hbar \langle S_x \rangle = M_S$.

Finally, the entropy is given by:[40]

$$S = -k\ \mathrm{Tr}\{\rho_R \log \rho_R\} = \text{const} - \frac{C_I H_{1I}^2}{2T^{I2}} - \frac{C_S H_{1S}^2}{2T^{S2}} \qquad (15)$$

We now turn to an analysis of the experiments using these equations.

B. FREE INDUCTION DECAY

Figure 3 shows how we would obtain a high resolution S spectrum by conventional techniques. The rare S system is allowed to equilibrate with the lattice in the external field H_0 for $\sim T_{1S}$ at temperature T^L, yielding, from (14), a magnetization:

$$M_S^{(0)} = \frac{C_S H_0}{T^L} \qquad (16)$$

This is observed in a free induction decay following a 90° pulse on the S spins.[37,38] The r.f. field on the I spins serves to decouple them, and Fourier transformation of the S decay yields a high resolution NMR spectrum. Before this can be repeated we must wait $\sim T_{1S}$ again; in solids T_1's can be extremely long and thus sensitivity enhancement by signal-averaging is rather painful. Since the S spins are rare, the signals are small; for $S \equiv {}^{13}C$ at low temperatures we might on occasion obtain tolerable signals, but if there are many lines, or if we are dealing with a less favorable isotope such as ${}^{15}N$, then this approach becomes prohibitively difficult.

Figure 3

Conventional high resolution S free induction decay with I spin-decoupling. θ_μ indicates a $\theta°$ pulse about the μ axis of the appropriate rotating frame and $H_{1\mu}$ continuous irradiation along μ. The S spins are polarized every $\sim T_{1S}$ and then observed following a 90° pulse while continuously irradiating the I spins. For the purposes of the analysis in the text it is imagined that $T_{1S} >> T_{2S}^*$. $S(t)$ is the normalized free induction decay.

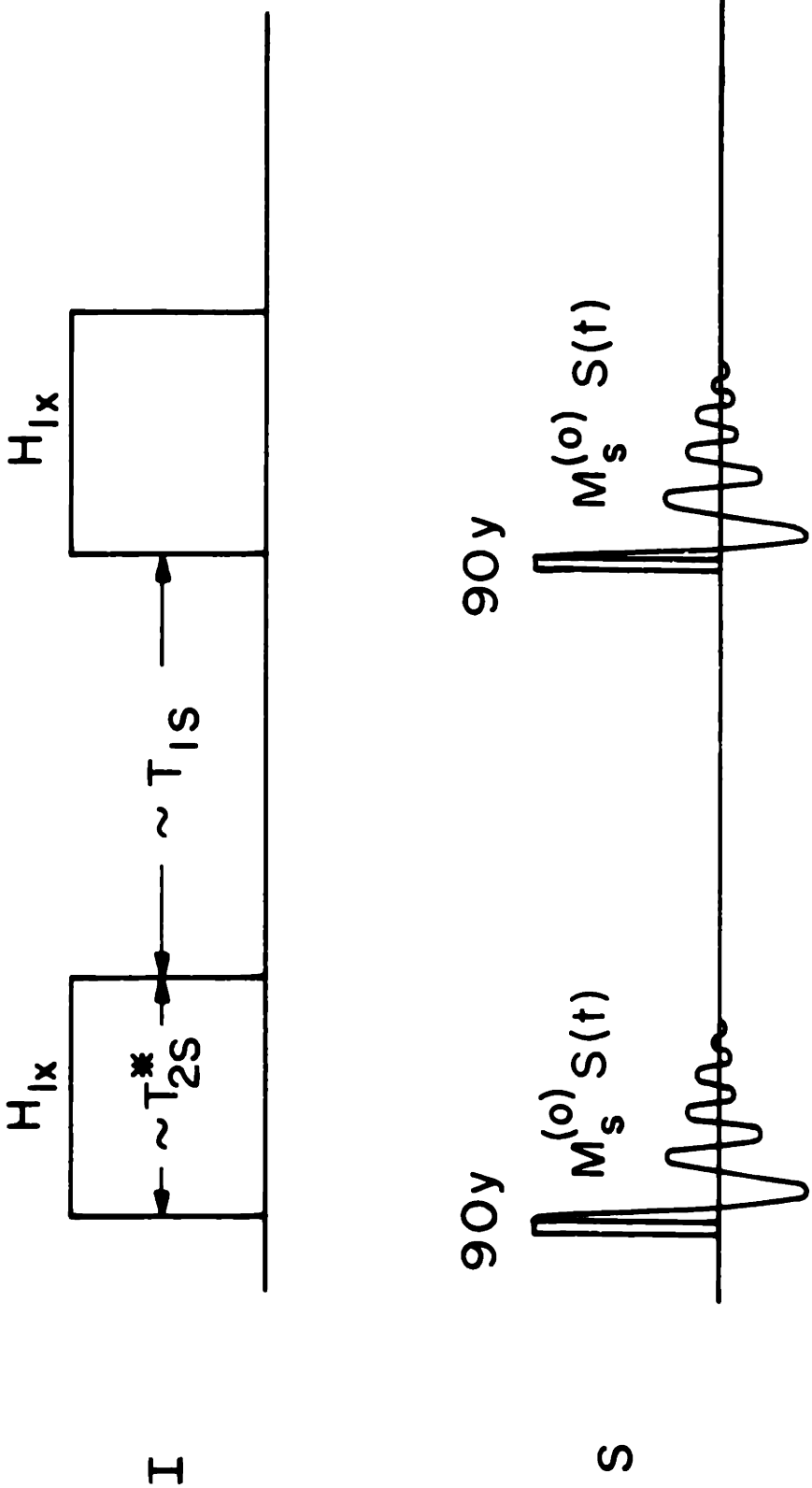
I
S
H_{1x}
H_{1x}
$\sim T_{2S}^{*}$
$\sim T_{1S}$
90y
90y
$M_s^{(o)}$ S(t)
$M_s^{(o)}$ S(t)

Figure 4

One particularly simple version of proton-enhanced nuclear induction spectroscopy, using I-S cross-polarization. After polarization of the I spins in $\sim T_{1I}$, the I magnetization is spin-locked at resonance along H_{1I} in the I rotating frame (see Figure 5). The S spins are brought into contact with the I reservoir by applying a resonant H_{1S} such that the Hartmann-Hahn condition, equation (2), is satisfied. The spin systems comes rapidly to equilibrium causing a small decrease in M_I and a growth of M_S along their H_1 fields. This is indicated schematically in the figure by the curves inside the H_1 irradiation blocks. The H_{1S} field is then removed and the S free induction decay observed while continuing the I irradiation for spin decoupling. This is repeated N times and the S signals coadded until M_I is reduced to ~0. For the purposes of analysis in the text it is imagined that $T_{1\rho I}$, $T_{1I} >> N(T_{2S}^* + T_{IS})$.

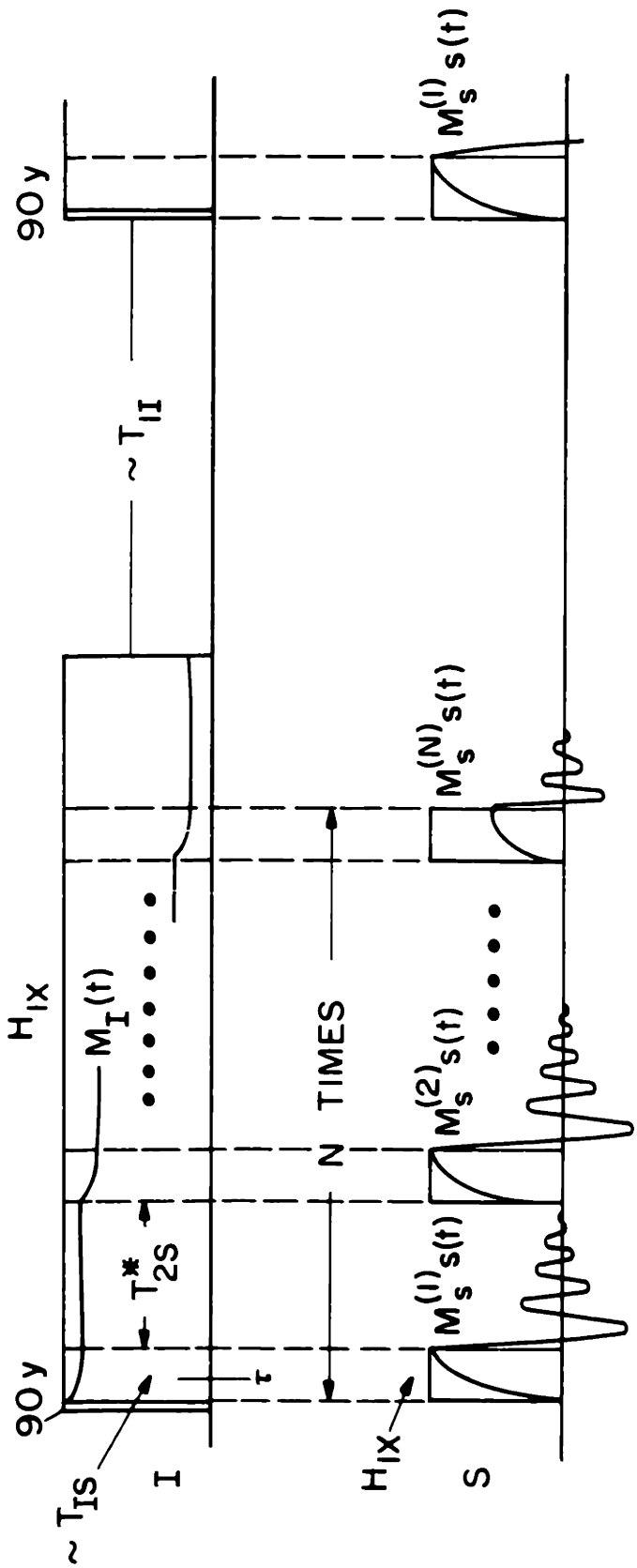
90 y
$M_s^{(1)}s(t)$
$\sim T_{II}$
$M_s^{(N)}s(t)$
H_{IX}
$M_I(t)$
N TIMES
$M_s^{(2)}s(t)$
T_{2S}^*
$M_s^{(1)}s(t)$
90 y
τ
$\sim T_{IS}$
I
H_{IX}
S

Figure 5

One version of spin-locking. Following a 90_y pulse (a) bringing $M_I^{(0)}$ along x, the rf is phase shifted to come along $M_I^{(0)}$ and kept on continuously (b). The magnetization $M_I^{(0)}$ which would normally decay by spin-spin processes is spin-locked and decays by spin-lattice relaxation in a time $T_{1\rho}$.

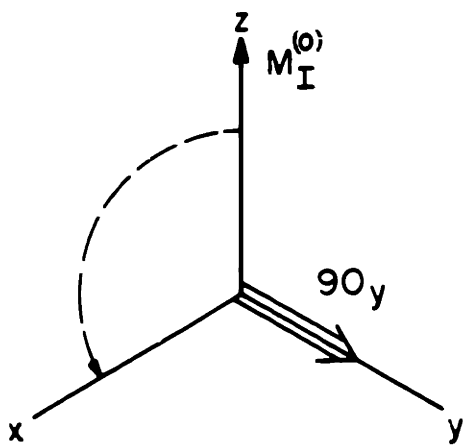

(a)

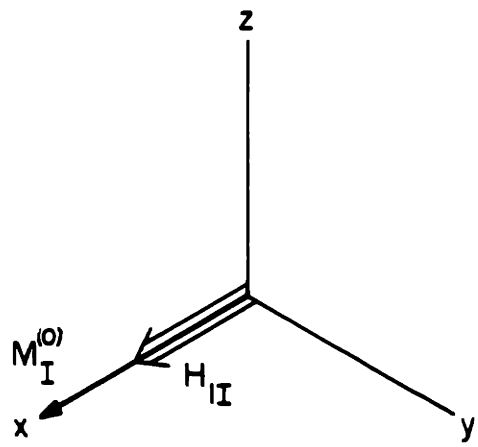

(b)

C. CROSS-POLARIZATION

As we mentioned in the introduction, the S spin signal can be enhanced by using the abundant I spin reservoir. The analysis follows exactly that due to Lurie and Slichter[35] except that we shall be enquiring into the accumulated S signal.

The experiment is illustrated in Figure 4. In this case, the I spins are allowed to equilibrate with the lattice, yielding a magnetization:

$$M_I^{(0)} = \frac{C_I H_0}{T^L} \tag{17}$$

This is now spin-locked along the x axis in the I rotating frame by application of a 90y pulse followed by a long phase-shifted pulse of amplitude H_{1I}. This is one of several ways of producing a spin-locked state and is illustrated in Figure 5. Since the I and S systems are mutually isolated we have:

$$\rho_R^{(0)} = \frac{1}{Z}\left(1 + \frac{\mathcal{H}_{1I}}{kT^{(0)}}\right) \tag{18}$$

and from (14): $$M_I^{(0)} = \frac{C_I H_{1I}}{T^{(0)}} \tag{19}$$

which is an operational definition of $T^{(0)}$, the I Zeeman spin-temperature in the rotating frame. From (17) and (18):

$$T^{(0)} = T^L \frac{H_{1I}}{H_0} \tag{20}$$

so this corresponds to a cooling of the I spin system. The S

spins are now coupled to the I by turning on an r.f. field of amplitude H_{1S} along the x axis in the S rotating frame (see Figure 2b). The magnitude of H_{1S} is arranged to fulfill the Hartmann-Hahn condition (2) so that the I and S systems come rapidly ($\sim T_{IS}$) to equilibrium at a common spin-temperature $T^{(1)}$, i.e.:

$$\rho_R^{(1)} = \frac{1}{Z}\left[1 + \frac{1}{kT^{(1)}}\left(\mathcal{H}_{1I} + \mathcal{H}_{1S}\right)\right] \tag{21}$$

Since energy must be conserved in the equilibration process (spin-lattice relaxation times are long), we have using (12), (18) and (21):

$$\frac{C_I H_{1I}^2}{T^{(1)}} + \frac{C_S H_{1S}^2}{T^{(1)}} = \frac{C_I H_{1I}^2}{T^{(0)}} \tag{22}$$

Putting (2) into (22) and rearranging we find:

$$\frac{1}{T^{(1)}} = \frac{1}{T^{(0)}} \quad \frac{1}{1+\varepsilon} \tag{23}$$

where $$\varepsilon = \frac{\gamma_I^2 C_S}{\gamma_S^2 C_I} = \frac{S(S+1)N_S}{I(I+1)N_I} \tag{24}$$

and from (14), the S magnetization following this first thermal contact is:

$$M_S^{(1)} = \frac{C_S H_{1S}}{T^{(1)}} = \frac{C_S \gamma_I H_{1I}}{\gamma_S T^{(1)}} \tag{25}$$

Using equations (20) and (23) we find from (25):

$$M_S^{(1)} = \frac{\gamma_I}{\gamma_S} \frac{1}{1+\epsilon} \frac{C_S H_0}{T^L}$$

or since $\epsilon << 1$, to an excellent approximation

$$M_S^{(1)} = \frac{\gamma_I}{\gamma_S} (1-\epsilon) \frac{C_S H_0}{T^L} \tag{26}$$

Recall from B that if we had allowed the S spins to equilibrate directly with the lattice then from (16) we would have $M_S^{(0)} = C_S H_0/T^L$; so looking at (26), we see that even in a single cross-polarization we have gained a factor of $\frac{\gamma_I}{\gamma_S}(1-\epsilon)$. This is ~4 for I ≡ ^{1}H, S ≡ ^{13}C and ~10 for I ≡ ^{1}H, S ≡ ^{15}N.

The H_{1S} field is now removed and the decay of $M_S^{(1)}$ is observed. Then contact is established again, and going through the same procedure, we find after N such steps:

$$M_S^{(N)} = \frac{\gamma_I}{\gamma_S} (1-\epsilon)^n M_S^{(0)}$$

or again to a good approximation:

$$M_S^{(N)} = \frac{\gamma_I}{\gamma_S} e^{-N\epsilon} M_S^{(0)} \tag{27}$$

If the signals are added then the total cross-polarization signal after depletion of the I magnetization is:

$$M_S^{(CP)} = \frac{\gamma_I}{\gamma_S} M_S^{(0)} \sum_{n=1}^{\infty} e^{-n\epsilon}$$

which is to a good approximation:

$$M_S^{(CP)} = \frac{\gamma_I}{\gamma_S} \frac{1}{\epsilon} M_S^{(0)} \tag{28}$$

or $\frac{\gamma_I}{\gamma_S} \frac{1}{\epsilon}$ times the single shot normal equilibrium signal.

D. SIGNAL TO NOISE CONSIDERATIONS

The calculation leading to (28) is naive in that we have neglected one important fact: the signal is necessarily measured in the presence of noise. It is the signal/noise or more precisely the data rate (S/N per unit time) in which we should be interested; obviously when N gets large enough we shall be accumulating mostly noise and degrading the signal/noise.

We assume that the noise voltage in our detector bandwidth for a given point S(t) on the S free induction decay is given by V_{ns}, and that the signal voltage is given by $K_S M_S$ when the initial magnetization is M_S. The accumulated power signal to noise for this point after N steps of the cross-polarization is then

$$\left(\frac{S}{N}\right)_{CP} = \left(\frac{\gamma_I}{\gamma_S} \frac{K_S}{\sqrt{N}} \frac{M_S^{(0)}}{V_{ns}} \sum_{n=1}^{N} e^{-n\epsilon} \right)^2 \tag{29}$$

since the signals add coherently and the noise adds incoherently. The optimal value of N is that which maximizes (29) and is found to be given by:

$$N\epsilon \sim 1.3 \tag{30}$$

Inserting this into (29) then gives us to a good approximation for optimal power signal/noise in $\sim T_{1I}$:

$$\left(\frac{S}{N}\right)_{CP} = 0.41 \left(\frac{\gamma_I}{\gamma_S}\right)^2 \frac{1}{\epsilon} \left(\frac{K_S M_S^{(0)}}{V_{nS}}\right)^2 \tag{31}$$

It is convenient to express the efficiency of an experiment in terms of a data rate, Q, the extracted signal/noise per unit time. For the cross-polarization procedure this is given by:

$$Q_{CP} = \frac{1}{T_{1I}} \left(\frac{S}{N}\right)_{CP} \tag{32}$$

An analogous calculation for the same point S(t) on the conventional free induction decay in Section B gives us in $\sim T_{1S}$:

$$\left(\frac{S}{N}\right)_{FID} = \left(\frac{K_S M_S^{(0)}}{V_{nS}}\right)^2 \tag{33}$$

and a data rate:

$$Q_{FID} = \frac{1}{T_{1S}} \left(\frac{S}{N}\right)_{FID} \tag{34}$$

Finally, combining (31) to (34) we summarize the sensitivity enhancement as:

$$Q_{CP} = \mathcal{G}_{CP} Q_{FID} \tag{35}$$

where

$$\mathcal{G}_{CP} = \frac{0.41}{\epsilon} \left(\frac{\gamma_I}{\gamma_S}\right)^2 \frac{T_{1S}}{T_{1I}} \tag{36}$$

We remark that the whole analysis is based on T_1 and $T_{1\rho}$ for the I spins being long enough for the duration of the full cross-polarization. If this is not so, the enhancement expressed by (36) is reduced.

For I ≡ ^{1}H S ≡ ^{13}C in typical organic compounds, $\mathcal{G}_{CP} \sim 10^3$ if $T_{1S} \sim T_{1I}$; for I ≡ ^{1}H S ≡ ^{15}N, $\mathcal{G}_{CP} \sim 10^5 - 10^6$. These get larger if $T_{1S} > T_{1I}$ which is generally the case. In fact at low temperature, paramagnetic or chemical doping would shorten T_{1I} much more than T_{1S} due to the more efficient spin diffusion amongst the I spins.

E. ADIABATIC TRANSFER

Here we compare (36) with the most efficient process possible, namely an adiabatic one. We assume as in Figure 6 that we can somehow transfer adiabatically (and thus reversibly) all the polarization from the I to the S spin reservoir. How this can be done does not interest us at present since we wish only to calculate a figure of merit for the above experiment. Suffice it to say that the process is indeed feasible[39] and will be discussed in detail elsewhere.

Before the transfer, all the polarization is in the I system and we assume the density matrix is given by (18). At

Figure 6

Schematic representation of a complete adiabatic transfer of I spin order into S spin order and observation of the S signal. This is the most effecient process possible; magnetization can be calculated by imposing conservation of entropy. For the purposes of analysis it is assumed that $T_{1I} >> T_{AD}$.

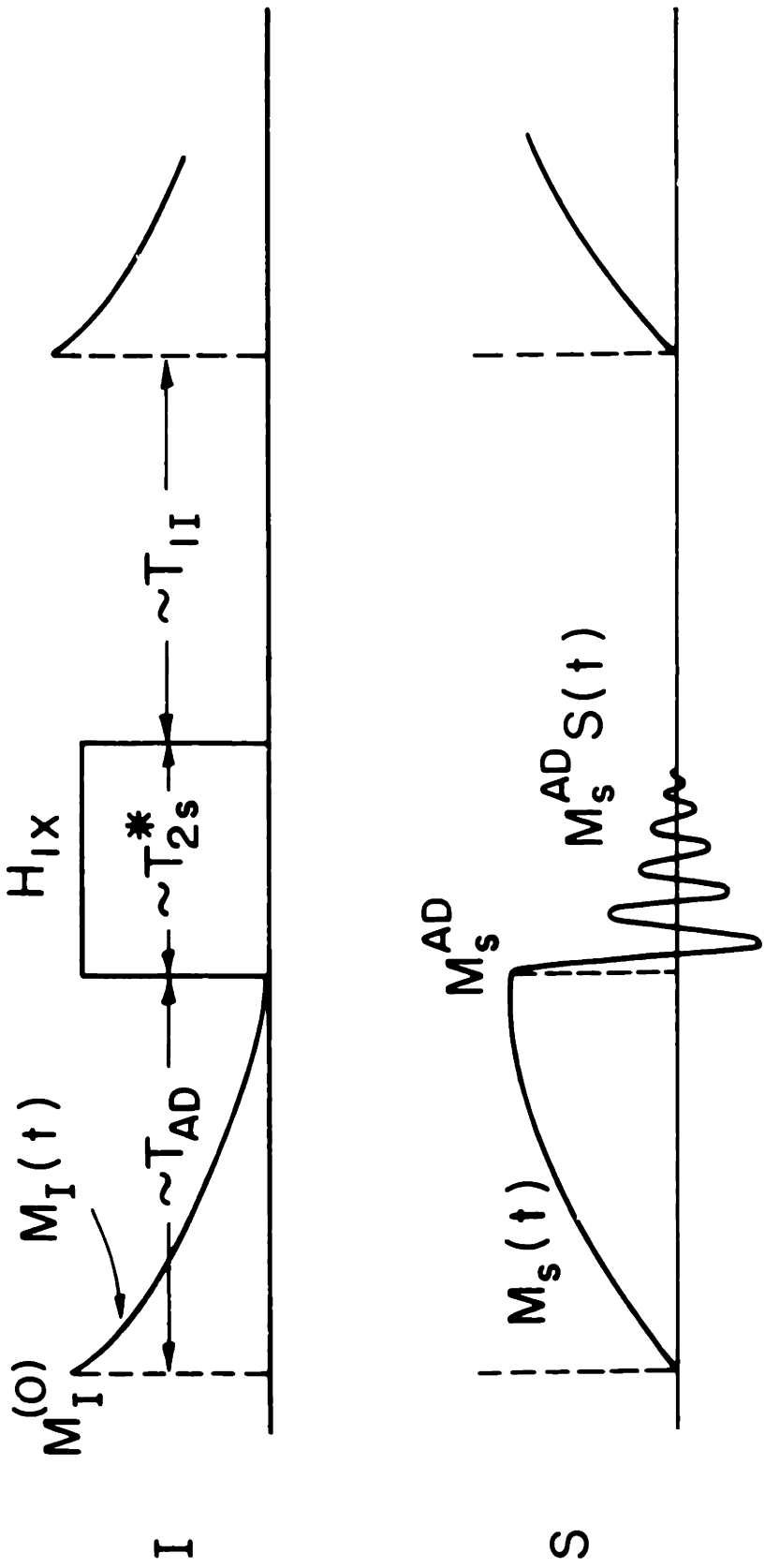
I
S
$M_I^{(0)}$
$M_I(t)$
H_{1x}
$\sim T_{AD}$
$\sim T_{2s}^*$
$\sim T_{11}$
M_s^{AD}
$M_s(t)$
$M_s^{AD}S(t)$

the end of the transfer, the S spins only are polarized and thus:

$$\rho_R^{AD} = \frac{1}{Z}\left(1 + \frac{\mathcal{H}_{1S}}{kT^{AD}}\right) \tag{37}$$

Since we postulate that the process is adiabatic we invoke conservation of entropy. Using equation (15) this tells us:

$$\frac{C_I H_{1I}^2}{T(0)^2} = \frac{C_S H_{1S}^2}{T^{AD2}} \tag{38}$$

Plugging equations (16), (17) and (24) into (38) and rearranging, we find for the final S magnetization:

$$M_S^{AD} = \frac{\gamma_I}{\gamma_S}\,\frac{1}{\sqrt{\epsilon}}\,M_S^{(0)} \tag{39}$$

which gives us for the data rate of our fixed point in exactly the same way as before:

$$Q_{AD} = \mathcal{G}_{AD}\, Q_{FID} \tag{40}$$

where:

$$\mathcal{G}_{AD} = \frac{1}{\epsilon}\left(\frac{\gamma_I}{\gamma_S}\right)^2 \frac{T_{1S}}{T_{1I}} \tag{41}$$

Thus, looking at (36), we have lost only a factor of 0.41 in the cross-polarization technique. Considering the simplicity of our approach, this is certainly not a great price to pay.

III. EXPERIMENTAL

The basic features of the pulsed NMR spectrometer used in these experiments have been described in detail elsewhere.[40-42] Changes were made to accommodate the double-resonance facilities, and these, together with the relevant experimental details are described in this section. We also make some comparisons between spectrometer requirements for these experiments and those for multiple-pulse experiments.

A. SPECTROMETER

A schematic diagram of the spectrometer is shown in Figure 7. The external magnetic field for our experiments was 22.8 KG provided by an Oxford Instruments superconducting solenoid. The configuration shown is for ^{1}H (97.2 MHz) and ^{13}C (22.4 MHz). Two synthesizers provide the basic rf for the two frequencies. Operation is superheterodyne; the intermediate frequency of 30 MHz is split into four channels by a quadripole network.[43] Three of these, with relative phases of 0^{o}, 90^{o} and 180^{o} are gated by the ^{1}H gating network, controlled by the pulse programmer, to produce the ^{1}H pulse sequence. Transmission of 97.2 MHz is from an amplified signal from the single sideband (lower) generator. This is necessary since the ^{1}H transmitter is a wideband device[44] and power considerations are crucial.

Figure 7

Block diagram of double-resonance spectrometer shown in configuration for ^{13}C-^{1}H operation with ^{13}C detection.

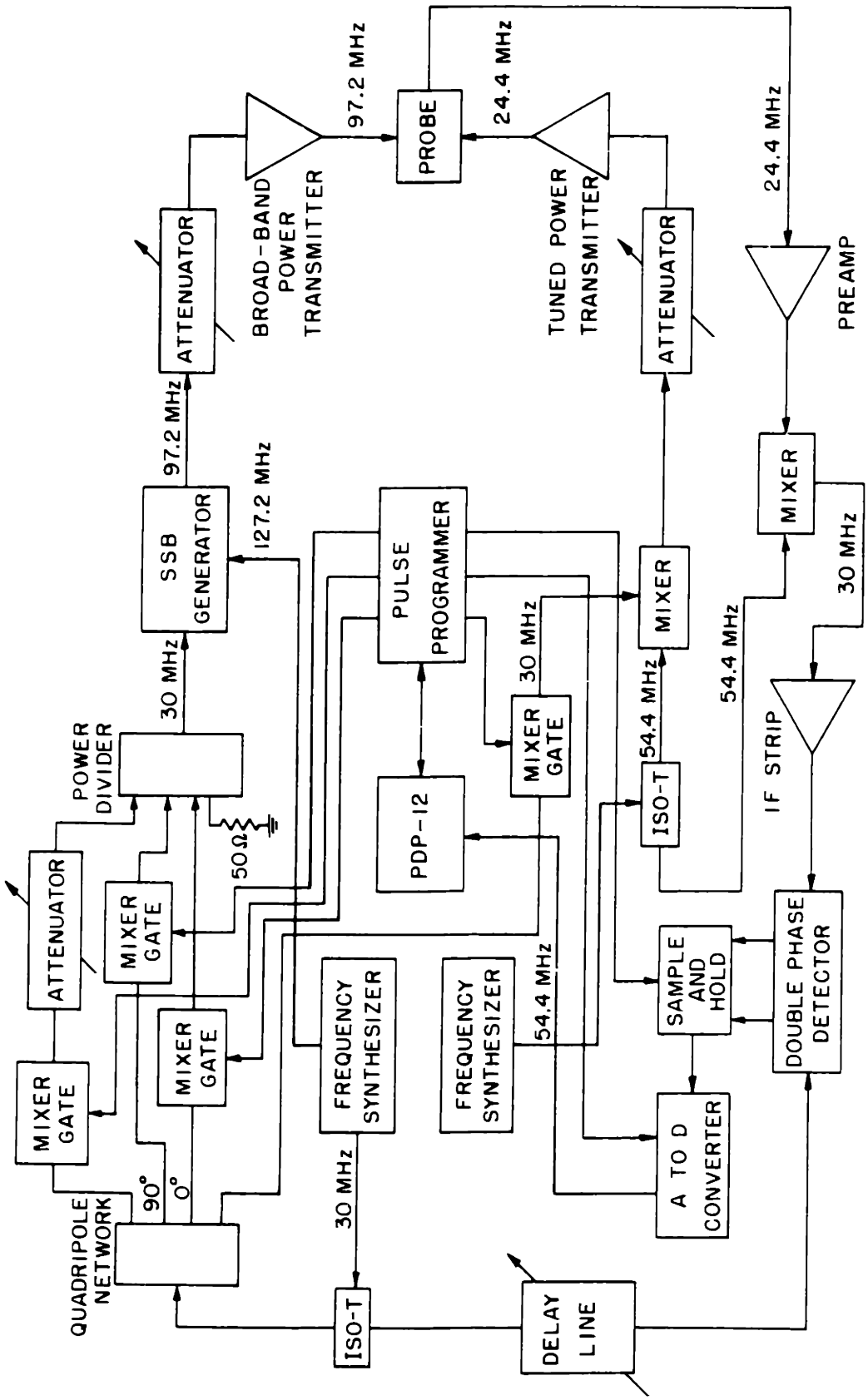
97.2 MHz
PROBE
24.4 MHz
24.4 MHz
BROAD-BAND POWER TRANSMITTER
TUNED POWER TRANSMITTER
PREAMP
ATTENUATOR
ATTENUATOR
97.2 MHz
SSB GENERATOR
127.2 MHz
PULSE PROGRAMMER
MIXER
MIXER
30 MHz
30 MHz
54.4 MHz
54.4 MHz
IF STRIP
POWER DIVIDER
30 MHz
MIXER GATE
ISO-T
50 Ω
PDP-12
ATTENUATOR
MIXER GATE
MIXER GATE
FREQUENCY SYNTHESIZER
FREQUENCY SYNTHESIZER
54.4 MHz
SAMPLE AND HOLD
DOUBLE PHASE DETECTOR
MIXER GATE
90°
0°
30 MHz
A TO D CONVERTER
QUADRIPOLE NETWORK
ISO-T
DELAY LINE

Figure 8

Low temperature double-resonance probe adapted to geometry of superconducting solenoid. The crossed coil geometry is shown in more detail in Figure 9.

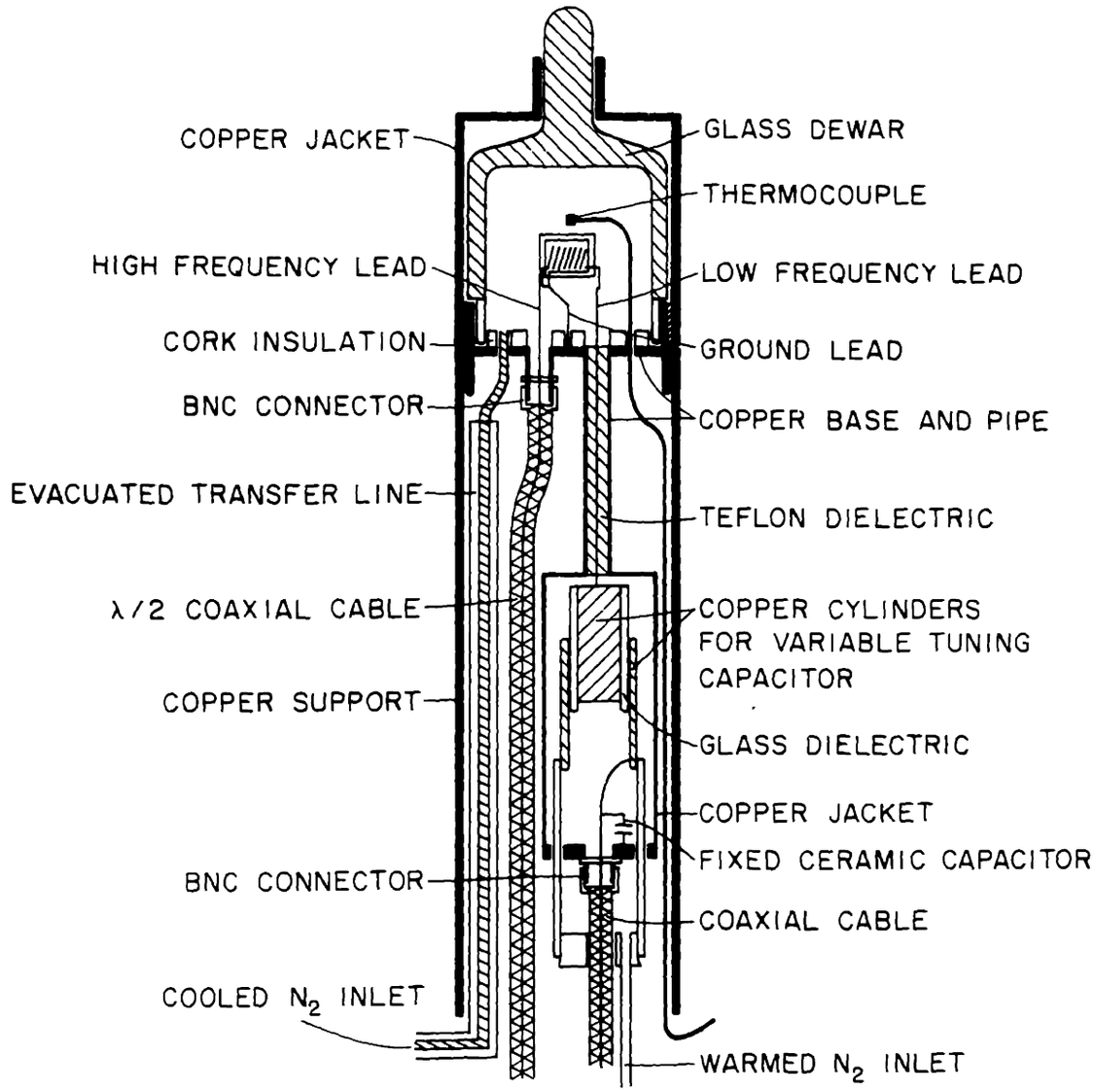
COPPER JACKET
GLASS DEWAR
THERMOCOUPLE
HIGH FREQUENCY LEAD
LOW FREQUENCY LEAD
CORK INSULATION
GROUND LEAD
BNC CONNECTOR
COPPER BASE AND PIPE
EVACUATED TRANSFER LINE
TEFLON DIELECTRIC
λ/2 COAXIAL CABLE
COPPER CYLINDERS FOR VARIABLE TUNING CAPACITOR
COPPER SUPPORT
GLASS DIELECTRIC
COPPER JACKET
FIXED CERAMIC CAPACITOR
BNC CONNECTOR
COAXIAL CABLE
COOLED N_2 INLET
WARMED N_2 INLET

Figure 9

Crossed coil geometry for double-resonance experiments. Diameter of the inner coil is ~0.6 cm and length ~1.5 cm. Support is provided by a ~1 mm pyrex tube between the two coil systems. Care is taken to mount the coils orthogonally to reduce mutual coupling and leakage into the low frequency detection system.

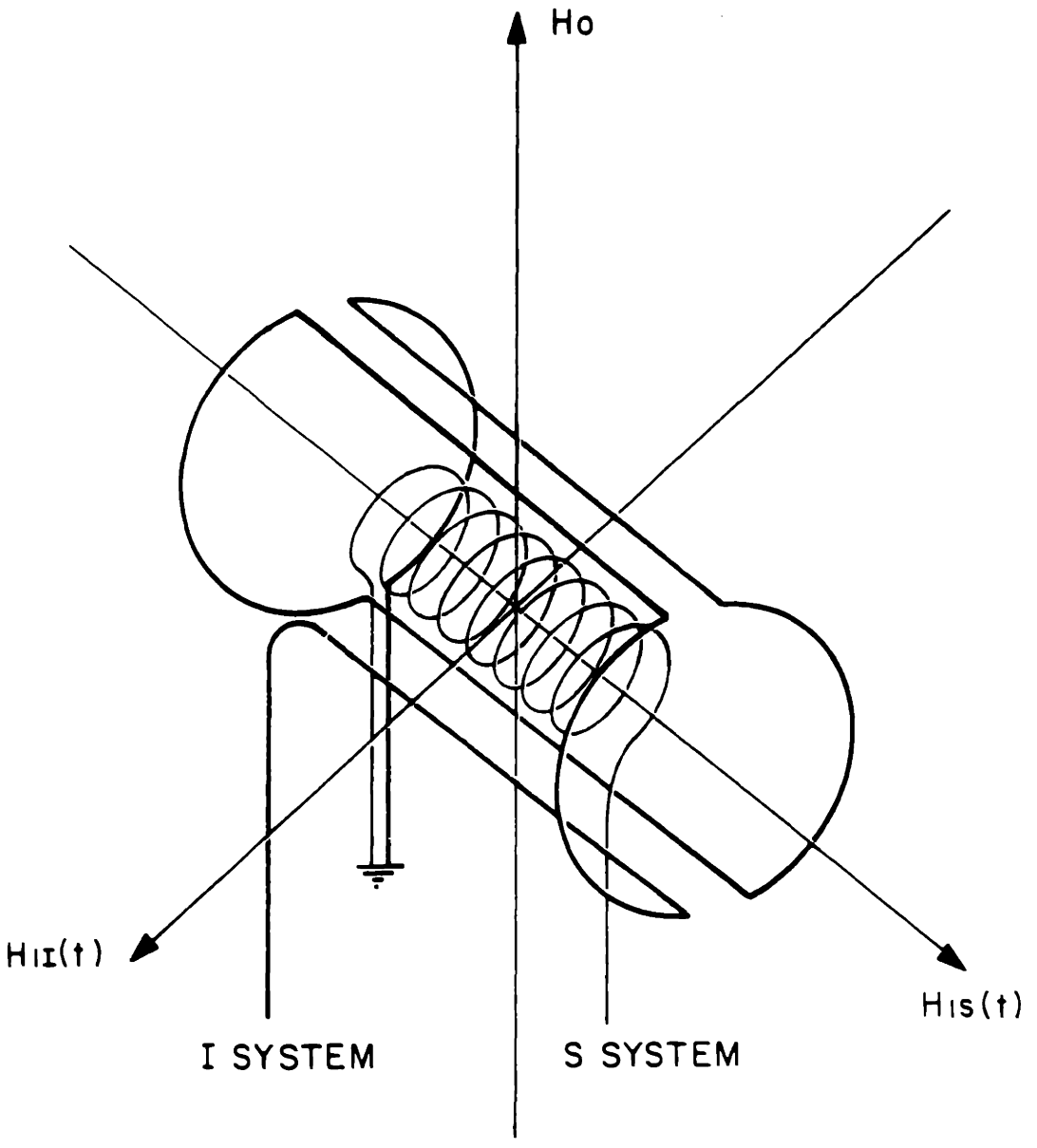
Ho
HiI(t)
HiS(t)
I SYSTEM
S SYSTEM

Since the final ^{13}C stage is tuned, SSB operation is not required for the 24.4 MHz and this is obtained directly from 54.4 MHz and the fourth 30 MHz channel. We do not go into a detailed discussion of power requirement, since these vary greatly from experiment to experiment. As an example, for the high Q, 5 mm sample coils used in most of our ^{13}C work, ~200 watts of rf power has been found to suffice for both final stages.

Reception of the 24.4 MHz signal is made with a tuned preamplifier (several have been used) and dual phase detection produces quadrature free induction decay signals for processing by complex Fourier transformation.[40,45] One problem in reception for these experiments is that of isolating the high-power ^{1}H frequency which leaks into the ^{13}C receiving system and produces large (bias) voltages at the preamplifier input. This is solved in several stages:

(a) orthogonal sample coils

(b) 97.2 MHz trap filter in the ^{13}C receiver line.

Without these precautions, detecting the small ^{13}C signals while irradiating the ^{1}H spins (decoupling) with high power rf is exceedingly difficult.

B. PROBE

The low temperature double-resonance probe, depicted in Figure 8, is designed for operation in the superconducting solenoid geometry. A double coil is used; the inner one is a

horizontal solenoid of diameter ~0.6 cm and length ~ 1.5 cm wound around the sample tube and used for the low frequency transmission and reception. The outer is of Helmholtz geometry, insulated from the inner one by ~1 mm of pyrex dielectric, and provides the high power 'H fields. Figure 9 shows in more detail the double coil geometry.

Matching and tuning of these coils is accomplished by standard techniques; the ^{13}C system can be tuned in situu by means of the variable capacitor which consists of two concentric copper tubes with a glass dielectric. The 'H coil is connected via a $\lambda/2$ coaxial cable and tuning and impedance matching are done remotely. The coaxial cables depicted contain high temperature resistant teflon dielectric, since conventional materials are prone to melting on extended application of high power rf.[46]

Temperature control is achieved in a standard way by passing dry nitrogen gas through a cooled copper coil and then into the sample chamber through evacuated transfer lines.

Samples were prepared in cylindrical pyrex ampules with o.d. 0.5 cm and sealed under vacuum.

C. TIMING AND SIGNAL PROCESSING

An important consideration for the initial period of experimentation for the double resonance was timing flexibility. Several versions of the experiment are possible and each has advantages and disadvantages which are strong functions of the

circumstances. In the present spectrometer, timing is provided by a homelbuilt pulse programmer[41] under control of an on-line minicomputer (PDP 12). This provides variable pulse widths and delays for the four rf channels, and extremely flexible counting facilities. Pulse programs are entered through the computer from magnetic tape storage. This leads to very convenient interchangeability of programs and makes the experimentation with new revisions and sequences a simple matter.

In addition to supervising the timing, the computer is also responsible for signal processing. After each cross-polarization, the free induction decay is digitized and stored directly in computer core. Subsequent processing includes signal averaging, Fourier transformation, apodization and digital smoothing, plotting, mass storage, etc. The spectrometer operates with a dual phase detector and advantage can be taken of this by using complex Fourier transformation which extends the effective spectral bandwidth by a factor of two.

Timing requirements vary from experiment to experiment. Cross-polarization times vary in the range $\sim$ 0.1 - 1 msec when condition (2) is satisfied. The decoupling time ($\sim T_{2S}^{*}$) depends of course on the resolution achievable or desirable in the experiment. Ideally, this should approach the pure S-S dipolar broadening which for ^{13}C is expected to be of the order of $\sim$ 10 Hz.[47] In practice, other limitations are inherent in

our experiments, including magnetic field inhomogeneities and incomplete spin-decoupling. Routinely we have operated with ~ 60 Hz linewidths (as evidenced from rigid single crystal studies) but have on occasion reduced linewidths to ~ 20 Hz in favorable cases. For ^{15}N, there is considerable broadening by the abundant ^{14}N isotope (~ 200 Hz) and data collection requires only ~ 10 msec per contact. Of course these requirements may change as auxiliary techniques such as sample-spinning are implemented.

In favorable cases, where T_{1I} is not too long a single cross-polarization can be useful. One then obtains a single free induction decay per T_{1I} with γ_I/γ_S enhancement. Many of our ^{13}C experiments were done in this way since the sensitivity is sufficient and sample heating by prolonged irradiation is avoided. For the less abundant isotopes, like ^{15}N, multiple contact was found to be essential.

D. ADDITIONAL COMMENTS

We make some final remarks concerning the stability requirements for these experiments as compared to the multiple-pulse techniques.[11-14] In multiple-pulse experiments, phase and amplitude stability are of crucial importance since the process requires long term coherent excitation of the spins. Any instabilities will cause accumulative precessional phase lags between the spins and a subsequent rapid destruction of the magnetization.

In addition, phase transients occur with the turn-on and turn-off of the rf pulses and these must either be minimized by using low Q probe circuits or a tedious amount of tuning must be performed to eliminate their effects. Since we are dealing in the dilute spin case, with heteronuclear decoupling the requirements are considerably less stringent on several counts:

(i) power: both experiments require sufficient rf field strengths to decouple spins interacting with strong dipolar couplings. However, in the double-resonance experiment decoupling is continuous (since observation is at a different frequency); this means that multiple-pulse experiments require $\frac{1}{\delta}$ times the power to produce the same average H_1 field (where δ is the duty cycle), since power is proportional to H_1^2. An additional advantage is indicated in consideration (iii) below.

(ii) stability: neither the spin-locking nor the spin-decoupling require extraordinary stability of phase or amplitude of the rf. Only if quantitative cross-relaxation studies are the purpose of the research do stability requirements assume any importance, since T_{IS} is sensitive to the H_1's.

(iii) probe Q: it is advantageous for the purposes of producing large H_1 fields and enhancing the sensitivity of signal detection to use high Q probe circuits. In multiple-pulse work this cannot be done indiscriminately since the magnetization must be sampled between closely spaced pulses, and receiver

dead-time due to probe ringing becomes an important consideration. In the double-resonance experiments, of course, there is no such problem and high Q circuits like those used in liquid studies, can be implemented. In fact our initial experiments have utilized circuits with Q ~ 100 at 24 MHz which is far greater than one is accustomed to in solid state multiple-pulse NMR.

Finally we remark that the above considerations are not intended to imply that double-resonance always constitutes a wiser selection than multiple-pulse NMR, since both are relevant to different conditions. For abundant spins such as ^{1}H, ^{19}F, the double-resonance procedure is irrelevant and one must resort to the more challenging technical requirements of multiple-pulse NMR. We think that the two techniques will probably find their ultimate usefulness working in concert on the same systems--the multiple pulse approach on the abundant spins (^{1}H, ^{19}F) and the cross-polarization on the dilute spins (^{13}C, ^{15}N).

IV. RESULTS

In this section we present a discussion and some exemplary results to illustrate the utility and scope of the technique. We do not present a detailed and quantitative account of the experiments and results--these have been dealt with elsewhere and detailed references to them will be made where appropriate.

A. POLYCRYSTALLINE SAMPLES

Our main interest in the preliminary experiments has been the measurement of chemical shielding anisotropies[48] which are not available from liquid measurements. This information should be extremely valuable since it is related to molecular structure and is a much more severe test of chemical shielding theories than is the isotropic shift alone.

To remind the reader, the chemical shift is a second rank tensor ($\underset{\approx}{\sigma}$) which transforms under a rotation from (x,y,z) to (x',y',z') as:

$$\sigma'_{ik} = \sum_{j,\ell} R_{ij} R_{k\ell} \sigma_{j\ell} \qquad (42)$$

In high field, only σ_{zz} in the laboratory system of coordinates is of interest;[49] if $R(\varphi,\theta,\psi)$ is the transformation from the principal axes (1,2,3) of $\underset{\sim}{\sigma}$ to the laboratory system (x,y,z) in terms of the Euler angles φ,θ,ψ then the observed shift $\sigma \equiv \sigma_{zz}$ is given by:

$$\sigma = \sin^2\theta \cos^2\phi\ \sigma_{11} + \sin^2\theta \sin^2\phi\ \sigma_{22} + \cos^2\theta\ \sigma_{33} \qquad (43)$$

where σ_{11}, σ_{22}, σ_{33} are eigenvalues of $\underset{\approx}{\sigma}$ and we adopt the convention:

$$\sigma_{11} \leq \sigma_{22} \leq \sigma_{33} \qquad (44)$$

In a polycrystalline sample, the effective chemical shift σ_{zz} must be weighted according to the probability of (θ,ϕ), yielding the following absorption lineshape derived by Bloembergen and Rowland:[50]

$$I(\sigma)\ \alpha \begin{cases} \left(\dfrac{\sigma_{33}-\sigma_{11}}{\sigma-\sigma_{11}}\right)^{\frac{1}{2}} K(\sin\alpha) & \text{for } \sigma_{22} < \sigma < \sigma_{33} \\ \left[\dfrac{(\sigma_{33}-\sigma_{11})(\sigma_{33}-\sigma_{22})}{(\sigma_{33}-\sigma)(\sigma_{22}-\sigma_{11})}\right]^{\frac{1}{2}} K\left(\dfrac{1}{\sin\alpha}\right) & \text{for } \sigma_{11} < \sigma < \sigma_{22} \\ 0 & \text{elsewhere} \end{cases} \qquad (45)$$

where: $$\sin^2\alpha = \frac{(\sigma_{22}-\sigma_{11})(\sigma_{33}-\sigma)}{(\sigma_{33}-\sigma_{22})(\sigma-\sigma_{11})} \qquad (46)$$

and K(k) is the complete eliptic integral of the first kind:

$$K(k) = \int_0^{\pi/2} (1 - k^2 \sin^2\gamma)^{-\frac{1}{2}}\, d\gamma \qquad (47)$$

This lineshape is depicted in Figure 10(a). σ_{11}, σ_{22} and σ_{33} may be read off directly from the lineshape. For a tensor

Figure 10

Absorption lineshapes for polycrystalline samples with (a) axially asymmetric, and (b) axially symmetric chemical shielding tensor $\underset{\sim}{\sigma}$. The lineshapes are given by equations (45) and (48). The principal values σ_{11}, σ_{22}, σ_{33} ($\sigma_{11} = \sigma_{22} = \sigma_{\perp}$, $\sigma_{33} = \sigma_{\parallel}$ in (b)) can be read off directly.

(a)

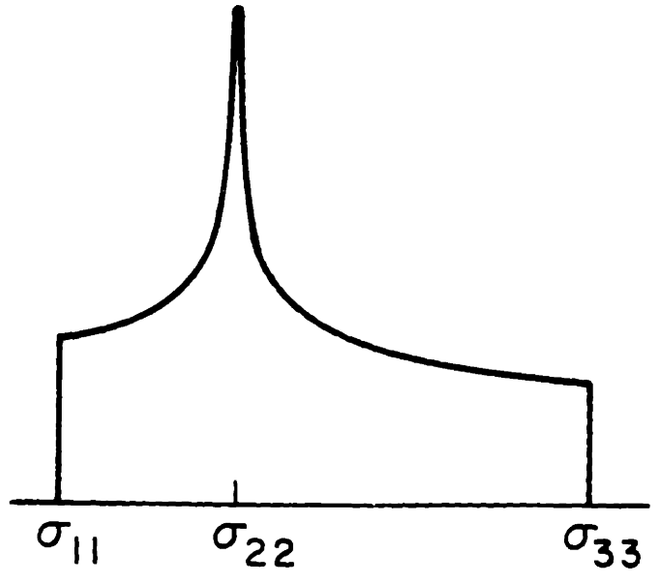

(b)

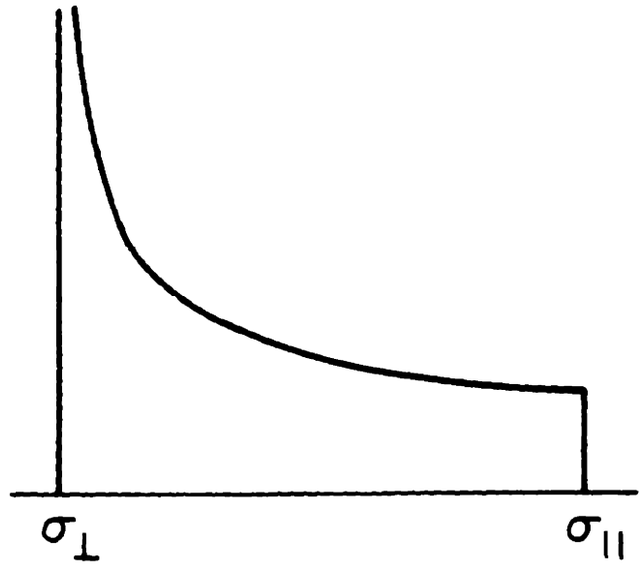

Figure 11

Proton-enhanced ^{13}C spectra of polycrystalline compounds containing carbonyl groups. The low field peaks are from the C=0 and the high field ones from CH_3. The spectra were obtained using the sequence in Figure 4 with various values of N, typically in minutes. Temperatures were all close to liquid nitrogen. Note the sensitivity of σ_{22} to substituents. The horizontal axis is calibrated in ppm relative to an external reference of liquid benzene (23°C).

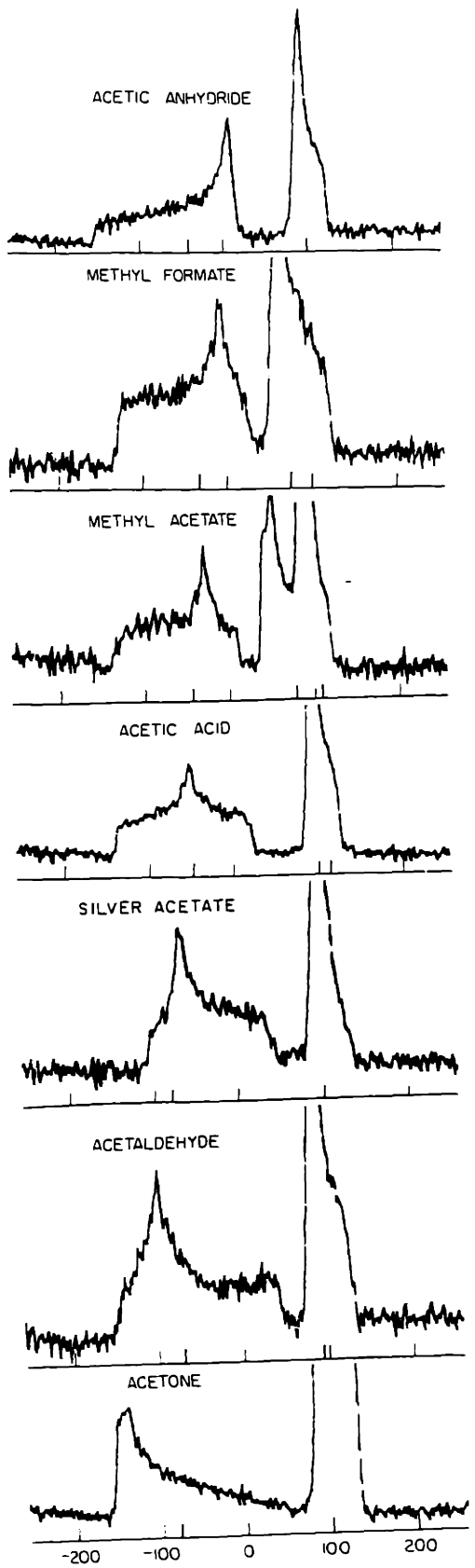
ACETIC ANHYDRIDE
METHYL FORMATE
METHYL ACETATE
ACETIC ACID
SILVER ACETATE
ACETALDEHYDE
ACETONE
-200
-100
0
100
200

Figure 12

Proton-enhanced ^{13}C spectra of polycrystalline methanol and dimethyl disulfide. Note how σ_{11} and σ_{22} change when we go from $O-CH_3$ to $S-CH_3$ whereas σ_{33} remains relatively unperturbed. The horizontal axis is in ppm relative to external liquid benzene (23°C).

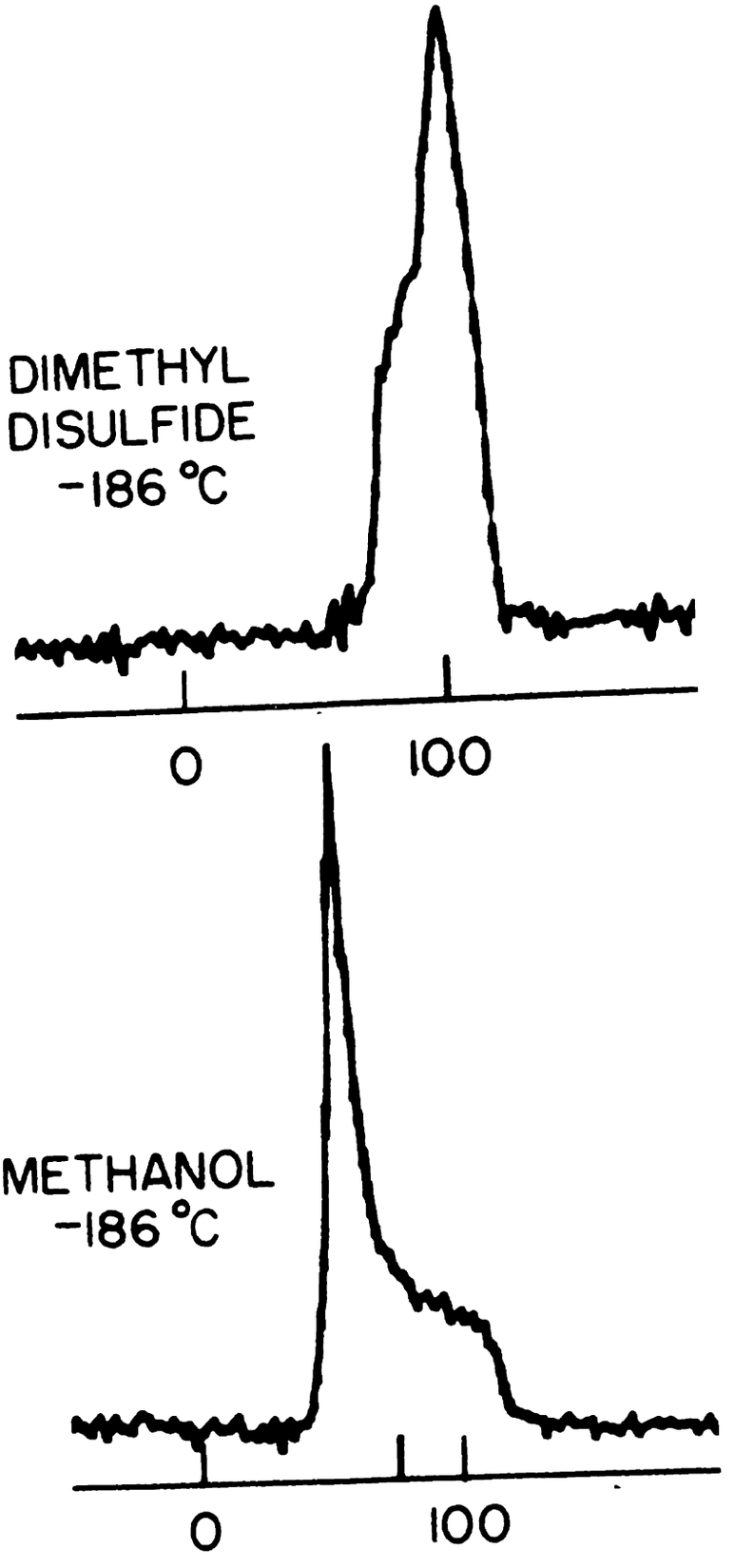
DIMETHYL
DISULFIDE
-186 °C
0
100
METHANOL
-186 °C
0
100

with uniaxial symmetry the lineshape simplifies to:

$$I(\sigma) \alpha \begin{cases} (\sigma - \sigma_{\perp})^{-\frac{1}{2}} & \text{for } \sigma_{\perp} < \sigma < \sigma_{\parallel} \\ 0 & \text{elsewhere} \end{cases} \qquad (48)$$

where we have taken the case:

$$\sigma_{11} = \sigma_{22} = \sigma_{\perp}$$

$$\sigma_{33} = \sigma_{\parallel} \qquad (49)$$

This is shown in Figure 10(b).

Although this is all well known, it is very seldom that such lineshapes have been observed in NMR; except in unusual favorable cases (examples are given in references 51-55)[25,51-55] or where multiple pulse techniques are applicable,[56] they are normally obscured by the strong dipolar broadening.

Figure 11 shows proton-enhanced ^{13}C spectra in some polycrystalline organic compounds at low temperatures. The low field absorption is due to the carbonyl carbon in each compound. The lineshapes conform to those in figure 10 and the elements of $\underset{\approx}{\sigma}$ are read off with facility. Note the extreme sensitivity of σ_{22} to substituents. Methyl group ^{13}C shielding (e.g. the high field absorption figure 11) displayssomewhat smaller anisotropies; an interesting feature in this case is that σ_{33} remains relatively unperturbed while σ_{11} and σ_{22} are very sensitive to

substituent.[57] An example of this is shown in Figure 12 which compares CH_3 bonded to oxygen and CH_3 bonded to sulphur.

In this way we have determined the elements of $\underset{\approx}{\sigma}$ for several low abundance nuclei in a variety of compounds in polycrystalline form. These include:

(a) ^{13}C: An extensive list of chemical shielding parameters illustrating different functional groups and substituents has been reported for organic compounds.[58,59]† More recent measurements include acetonitrile, nitromethane, oxalates, glycine, ethylenes and organometallic materials.[60]

(b) ^{29}Si: Chemical Shielding parameters have been reported for a number of organo-silicon compounds.[61]

(c) ^{15}N: Chemical shielding parameters were obtained for $(NH_4)_2\ SO_4$, NH_4NO_3 and glycine;[62] more recently some additional compounds have been studied including acetonitrile, nitromethane, dimethylformamide, etc.[60]

Conditions for these experiments varied. Typically, for the ^{13}C and ^{29}Si work high frequency H_1 was ~ 12 G and low frequency H_1 was ~ 40-50 G. For the ^{15}N work, the corresponding values were ~ 5 G and ~ 40-50 G.

† These are reproduced in Table I which follows.

TABLE I

^{13}C Shielding parameters in some organic compounds

Carbon Type	Compound	Formula	T(°C)	σ_{11}	σ_{22}	σ_{33}	$\bar{\sigma}$	σ_i
Aromatic	Benzene	C_6H_6	-50	-63_1	-63_1	117_1	-3_1	0
	Hexamethylbenzene	$(CCH_3)_6$	23	-61	-61	107_{14}	-5_9	---
			-186	-104	-26	104_{16}	-9_9	---
	Toluene	$C_6H_5CH_3$	-186	-93_7	-6	132	11	3
	Durene	$C_6H_2(CH_3)_4$	+23	-101	-30	114_{16}	-6_9	---
	Hexafluorobenzene	C_6F_6	-40	-42	-42	-2_8	-29_7	-7_7
Carbonyl	Acetaldehyde	CH_3CHO	-186	-147_7	-105	42	-70	-72
	Acetone	$(CH_3)_2CO$	-186	-150	-136	50_7	-79	-78
	Acetic Acid	CH_3COOH	-186	-140	-55	19	-59	-49
	Thioacetic Acid	CH_3COSH	-186	-145	-101	+28	-73	-65
	Silver Acetate	CH_3COOAg	-186	-110	-73	+39	-48	---
	Acetic Anhydride	$(CH_3CO)_2O$	-182	-152	13	13	-42	-38
	Methyl Formate	$HCOOCH_3$	-186	-124	-7_7	22_7	-36_7	-32
	Methyl Acetate	CH_3COOCH_3	-140	-138	-31	9	-53	-43
	Dimethyl Carbonate	$(CH_3O)_2CO$	-186	-102_9	19	19	-21_7	-29
	Dimethyl Oxalate	$(CH_3OCO)_2$	-186	-118	30_{15}	30_{15}	-19_{12}	---
	Silver Trifluoroacetate	CF_3COOAg	23	-116	0_{18}	0_{18}	-39_{14}	---
	Trifluoroacetic Anhydride	$(CF_3CO)_2O$	-164	-131	23_{16}	39_{16}	-23_{17}	-21
Acetylenic	Dimethyl Acetylene	$(CH_3C)_2$	-186	-29	-29	173_{17}	38_{10}	51
$-O-CH_2-$	Methanol	CH_3OH	-186	55	55	118	76	80
	Ethanol	CH_3CH_2OH	-170	56	56	113_{16}	75_9	71
	Diethyl Ether	$(CH_3CH_2)_2O$	-140	31	43	110_{15}	61_9	63
	Methyl Formate	$HCOOCH_3$	-186	53	65	121	80	79
	Methyl Acetate	CH_3COOCH_3	-140	37	53	121	70	77

Carbon Type	Compound	Formula	T(°C)	σ_{11}	σ_{22}	σ_{33}	$\bar{\sigma}$	σ_i
	Dimethyl Carbonate	$(CH_3O)_2CO$	-186	50	56	121	76	79
	Dimethyl Oxalate	$(CH_3OCO)_2$	-186	52_{15}	64_{15}	122	79_{12}	---
	Dimethyl Dimethoxy Silane	$(CH_3)_2(CH_3O)_2Si$	-186	+55	+60	$+132_{18}$	$+82_{10}$	+81
	Tetramethoxy Silane	$(CH_3O)_4Si$	-186	157	+63	+127	+82	+81
S-CH_3	Dimethyl Disulfide	$(CH_3S)_2$	-186	81	111	123	105	109
	Dimethyl Sulfoxide	$(CH_3)_2SO$	-47	63_7	85	111_7	86_7	86
Si-CH_3	Octamethyl Cyclotetra-Siloxane	$[(CH_3)_2SiO]_4$	-186	128	128	128	128	128
	Hexamethyl Disiloxane	$[(CH_3)_3Si]_2O$	-186	124	124	124	124	124
C-CH_3	Ethanol	CH_3CH_2OH	-170	104	113	128	115	110
	Diethyl Ether	$(CH_3CH_2)_2O$	-140	100	110	124	111	113
	Acetaldehyde	CH_3CHO	-186	74	86	126	95	96
	Acetone	$(CH_3)_2CO$	-186	81	81	131	98	98
	Acetic Acid	CH_3COOH	-186	83	83	118	95	108
	Acetic Anhydride	$(CH_3CO)_2O$	-182	90	93	128	103	106
	Methyl Acetate	CH_3COOCH_3	-140	86	89	107	95	107
	Dimethyl Acetylene	$(CH_3C)_2$	-186	113	113	127	118	124
	Toluene	$C_6H_5CH_3$	-186	96	107	124	109	107
	Durene	$C_6H_2(CH_3)_4$	23	104_8	104_8	124	111_7	---
	Hexamethylbenzene	$(CCH_3)_6$	23	107	107	107	107	---
			-186	104	104	104	104	---
	Hexamethyl Dewar Benzene		-186	118	118	118	118	118

Carbon Type	Compound	Formula	T(°C)	σ_{11}	σ_{22}	σ_{33}	$\bar{\sigma}$	σ_i
	Silver Acetate	CH_3COOAg	-186	94	100	136	110	---
	Dimethyl Dimethoxy Silane	$(CH_3)_2(CH_3O)_2Si$	-186	132	132	132	132	132
	Thioacetic Acid	CH_3COSH	-186	73	80	129	94	100
C-CF_3	Silver Trifluoro-acetate	CF_3COOAg	23	0	0	19	6	---
	Trifluoroacetic Anhydride	$(CF_3CO)_2O$	-164	10_{11}	10_{11}	27_{14}	6_{12}	14
Misc.	Carbon Disulfide	CS_2	-200	-205_{10}	-205_{10}	220_{14}	-63_{11}	-65
	Hexamethyl Dewar Benzene	$(C^1CH_3)_4(C^2CH_3)_2$	-186	[1] -115	-20	93_{40}	-14_{19}	-17
				[2] 57	72	86	72	72

TCA

Carbon Type	Compound	Formula	T(°C)		σ_{11}	σ_{22}	σ_{33}	$\bar{\sigma}$	σ_i
	Silver Acetate	CH_3COOAg	-186		94	100	136	110	---
	Dimethyl Dimethoxy Silane	$(CH_3)_2(CH_3O)_2Si$	-186		132	132	132	132	132
	Thioacetic Acid	CH_3COSH	-186		73	80	129	94	100
C-CF_3	Silver Trifluoro-acetate	CF_3COOAg	23		0	0	19	6	---
	Trifluoroacetic Anhydride	$(CF_3CO)_2O$	-164		10_{11}	10_{11}	27_{14}	6_{12}	14
Misc.	Carbon Disulfide	CS_2	-200		-205_{10}	-205_{10}	220_{14}	-63_{11}	-65
	Hexamethyl Dewar Benzene	$(C^1CH_3)_4(C^2CH_3)_2$	-186	[1]	-115	-20	93_{40}	-14_{19}	-17
				[2]	57	72	86	72	72

B. MOTIONAL EFFECTS

The type of spectra we have seen above may be severely modified in the presence of motion. Three types of motion are particularly relevant:

(i) macroscopic sample rotation

(ii) molecular reorientation

(iii) molecular conformational changes

In the case that (i) is performed about an axis inclined at the magic angle (54^{o} 44') to H_0 it is easy to show that the average shift $\bar{\sigma} = \bar{\sigma}_{zz}$ over one cycle of rotation becomes independent of orientation and is given by the isotropic shift σ_i:[10]

$$\sigma_i = \mathrm{Tr}\ \underset{\approx}{\sigma} = \frac{1}{3}(\sigma_{11} + \sigma_{22} + \sigma_{33}) \qquad (50)$$

This means that in a polycrystalline sample only a single sharp line will be observed, for each inequivalent nucleus, at σ_i, if the above rotation is performed rapidly compared to the anisotropy spread $(\sigma_{33} - \sigma_{11})$. This provides a convenient means of retaining the sensitivity of the cross-polarization and eliminating the broadening due to chemical shielding anisotropy where the latter is of no interest or difficult to evaluate due to overlapping peaks. It would certainly be a valuable accessory in the use of these techniques for structural studies in the solid state.[63]

The motion mentioned in (ii) may also manifest itself in

these experiments and indeed may on occasion serve some useful purpose. A trivial case is that of rapid isotropic or nearly isotropic molecular reorientation in the solid. In this case the chemical shielding anisotropy is averaged to zero and we should expect to see a sharp line at σ_i. Since the intramolecular I-S dipole-dipole coupling is also averaged away, the proton-enhancement cross-polarization proceeds entirely through the average intermolecular dipole-dipole coupling. A simple example of this phenomenon was provided by our early spectrum of adamantane using this technique.[23b] As is well known, adamantane undergoes rapid ($t_c \sim 10^{-11}$ sec) molecular rotation at 300 K.[64] and indeed two sharp lines were obtained in the solid ^{13}C spectrum.

An additional example is afforded by another "roundish" molecule, camphor, whose solid state ^{13}C spectrum is shown in Figure 13. Eight lines are resolved and the spectrum compares well with the high resolution spectrum in solution.[65]

Other molecules have been found to behave similarly including TMS, neopentane, cyclohexane, etc. In all these cases the requirements for proton H_1 fields are much less stringent in decoupling since the average dipolar interactions are reduced by the motion. Fields of ~ 3G were found to produce acceptable resolution.

A more interesting case is that of very anisotropic molecular

Figure 13

Proton-enhanced ^{13}C spectrum of solid polycrystalline camphor. In this case, no anisotropy of the ^{13}C chemical shift is observed since the molecules undergo rapid reorientation more or less isotropically. The spectrum is similar to that obtained in solution; the resolution is worse, but the sensitivity of detection substantially greater. Spectra such as these can be obtained in seconds. The reference is again external liquid benzene.

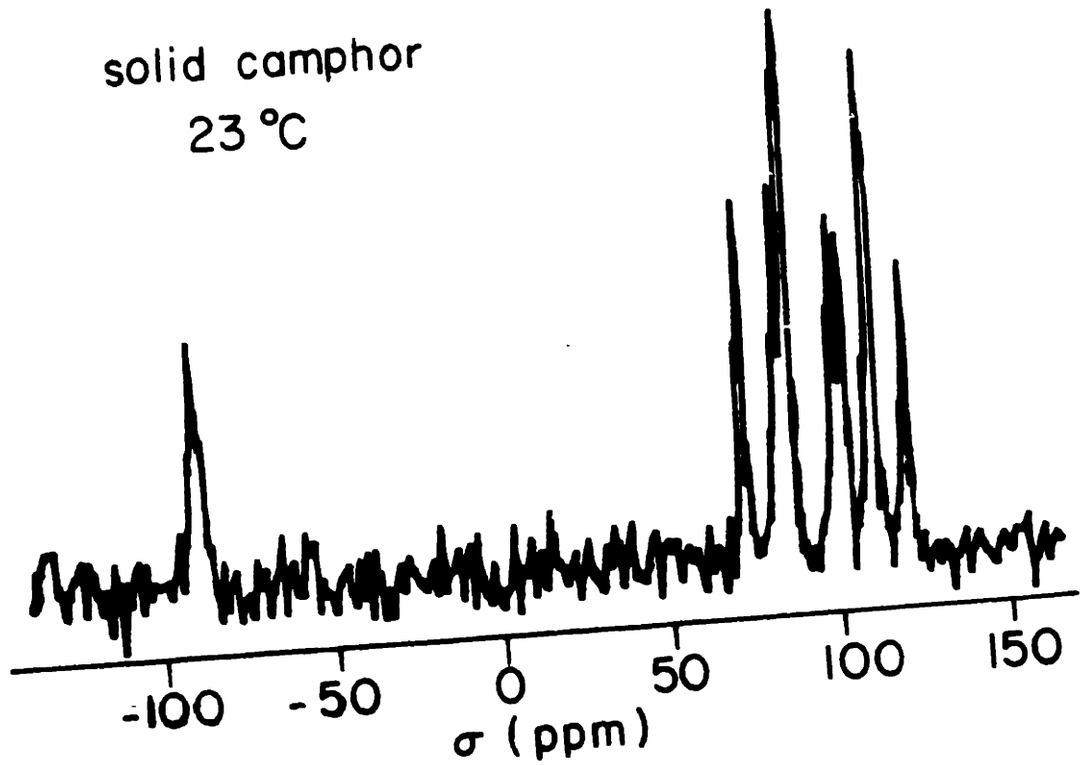
solid camphor
23 °C
-100
-50
0
50
100
150
σ (ppm)

motion, for example restricted rotation about one axis in the molecule. When this is rapid a partial averaging of shielding tensor ensues.[56a] Again, the rotation may be described by the operator $R(\alpha,\beta,\gamma(t))$ in terms of the Euler angles α, β, $\gamma(t)$ in the principal axes system; this is illustrated in Figure 14. If an average is performed over $\gamma(t)$ we find for the effective shielding tensor $\bar{\underset{\approx}{\sigma}}$ the principal values:

$$\bar{\sigma}_{33} = \bar{\sigma}_{\parallel} = \mathrm{Sin}^2\beta\ \cos^2\alpha\ \sigma_{11} + \mathrm{Sin}^2\beta\ \mathrm{Sin}^2\alpha\ \sigma_{22} + \cos^2\beta\ \sigma_{33}$$

$$\bar{\sigma}_{11} = \bar{\sigma}_{22} = \bar{\sigma}_{\perp} = \frac{1}{2}(3\ \sigma_i - \bar{\sigma}_{33}) \qquad (51)$$

So the average shielding tensor displays (as expected) axial symmetry about the rotation axis. This may be very helpful in polycrystalline samples for assigning σ_{ii} to the molecular frame if something is known or assumed about the motion. On the other hand, where the orientation information is available from other sources (see below) this may be used to learn a great deal about the nature of the motion.

We have reported a striking example of such behavior in polycrystalline hexamethylbenzene.[58] The low temperature aromatic region of the ^{13}C spectrum exhibits an axial asymmetry and at high temperatures, with the onset of molecular motion the spectrum displays pseudoaxial symmetry, with

Figure 14

Coordinate systems describing anisotropic molecular reorientation about one axis in the molecule. (1,2,3) are the principal axes of $\underset{\sim}{\sigma}$, $(\bar{1},\bar{2},\bar{3})$ are the rotating system about $\bar{3}$. When rotation is rapid, an average over $\gamma(t)$ is taken and one finds the average shielding tensor $\underset{\sim}{\bar{\sigma}}$ to be axially stmmetric about $\bar{3}$. In the text is is shown how this may be used to learn about the orientation of (1,2,3) in the molecule.

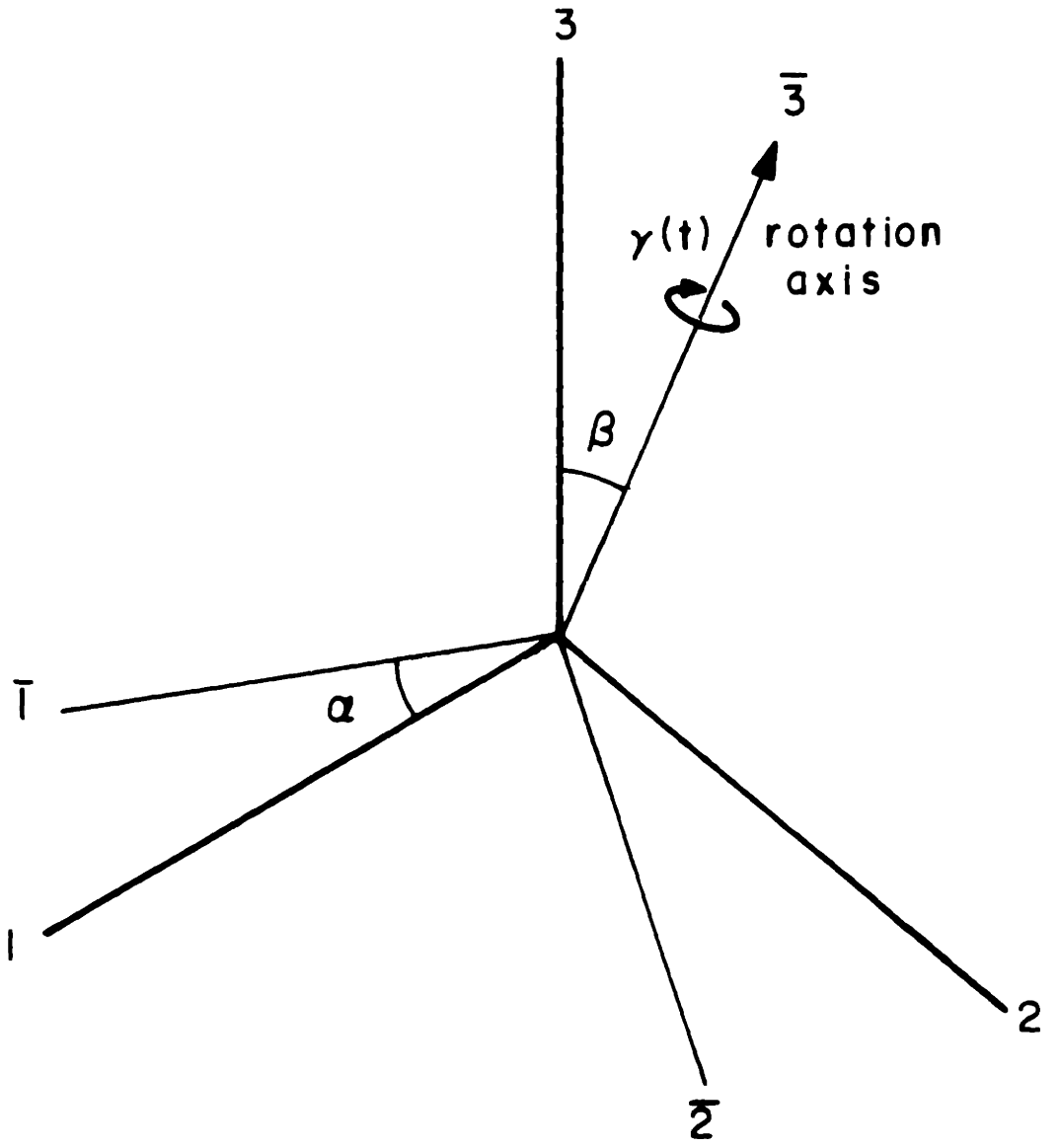
3
$\bar{3}$
$\gamma(t)$ rotation axis
β
α
$\bar{1}$
1
2
$\bar{2}$

$$\bar{\sigma}_{\parallel} = \sigma_{33}$$
$$\bar{\sigma}_{\perp} = \frac{1}{2}(\sigma_{11} + \sigma_{22}) \qquad (52)$$

This shows that $\beta = 0$ in (51); i.e. rotation is about the molecular axis 3 corresponding to σ_{33}. Since it is known that the motion in hexamethyebenzene,[66] like that in benzene,[67] consists of reorientation about the C_6 axis, this immediately assigns σ_{33}, the most shielded component, to the C_6 axis. The enhanced shielding of the ring carbons perpendicular to the aromatic plane has subsequently been verified in single crystal experiments.[68]

Finally, we mention that the motion indicated in (iii), molecular conformational change, may also be studied using these techniques. Solid state ^{13}C NMR should provide a powerful means of treating conformational processes in solids,[69] just as conventional NMR has served a vital role in studying these processes in liquids.[70] The information content in solid state spectral changes should be greater due to the orientational information contained in the chemical shielding anisotropy.

C. SINGLE CRYSTAL STUDIES

Although the principal values of $\underset{\approx}{\sigma}$ are of great interest, valuable additional information could be obtained from the orientation of the principal axes in the molecular frame, thus specifying the full shielding tensor. In polycrystalline spectra this

information is generally, but not always, lost. There are several ways to approach this problem the most direct and clear cut of which is by working with single crystals, where these are are available.

If we denote, as before, the laboratory coordinate system as (x,y,z), the principal axis system of $\underset{\approx}{\sigma}$ as (1,2,3) and some axes fixed in the crystal as (X,Y,Z), then the elements of $\underset{\approx}{\sigma}$ in the (XYZ) system can be obtained by rotating the crystal about three independent axes and recording the chemical shift σ (= σ_{zz} as mentioned before) vs. rotation angle. Computation is simplified if the rotations are about orthogonal axes, say X Y and Z. For example, a rotation about X perpendicular to H_0 with Z along H_0 (= z) for θ = 0 yields:

$$\sigma(\theta) = \frac{1}{2}(\sigma_{YY} + \sigma_{ZZ}) - \frac{1}{2}(\sigma_{YZ} + \sigma_{ZY}) \text{ Sin}2\theta + \frac{1}{2}(\sigma_{ZZ} - \sigma_{YY}) \cos 2\theta$$

$$= A + B \text{ Sin}2\theta + C \cos 2\theta \qquad (53)$$

and similarly with permutations, for rotations about Y and Z. A, B and C are determined by least-squares fitting of (53) to the experimental rotation plot and from three such plots, nine equations are obtained for the six elements of the (symmetric part of) $\underset{\approx}{\sigma}$ in the crystal frame:

$$\sigma_{XX},\ \sigma_{YY},\ \sigma_{ZZ},\ \frac{1}{2}(\sigma_{XZ} + \sigma_{ZX}),\ \frac{1}{2}(\sigma_{XY} + \sigma_{YX}),\ \frac{1}{2}(\sigma_{YZ} + \sigma_{ZY}) \qquad (54)$$

These are again solved by least-squares fitting. In the more general case that the rotations are not about orthogonal axes, then the rotations in (53) contain all six elements of (54) and a more general least-squares fitting is used. Once the elements of (54) have been obtained, the tensor is diagonalized, yielding the eigenvalues σ_{11}, σ_{22}, σ_{33}, and the corresponding eigenvectors; the eigenvectors give the orientation of (1,2,3) in (X,Y,Z). If the molecular orientation in the crystal is known, say from x-ray studies, then (1,2,3) may be related to the molecular geometry, yielding the fullest possible information on $\underset{\approx}{\sigma}$.

We have undertaken such studies in several crystalline compounds. Two initial systems to be studied, contain aromatic and carbonyl groups. In the former case, a study of ^{13}C in single crystal durene (1,2,4,5--tetramethylbenzene) shows the most shielded element, σ_{33}, for the aromatic carbon to be perpendicular to the plane of the molecule.[68] In addition, the methyl groups present substantial perturbations and the chemical shielding anisotropy is markedly different for ring carbons with and without methyl groups; this was not evident from the powder spectra.[59] In the second case, single crystals of ammonium oxalate and glycine show the ^{13}C σ_{33} to be perpendicular to the COO^- plane. Results on these and other experiments will be presented in detail elsewhere.[71]

We mention briefly, in passing, that even when single crystals are not available, a substantial amount of orientational information may be extracted by auxiliary experiments. One possibility already mentioned is that of molecular motion. Another is to utilize dipolar splitting by a third nucleus (like or unlike S, unlike I). For ^{13}C-^{1}H, the third nucleus could be ^{13}C, ^{2}H, ^{14}N etc. From the lineshape in a polycrystalline sample, information can be obtained on the mutual orientation of the principal axes of $\underset{\approx}{\sigma}$ and the dipolar interaction tensor. Since the latter have a well defined orientation in the molecule this is a useful way of assigning $\underset{\approx}{\sigma}$ to the molecular frame. An additional possibility is the study of cross-polarization times (see below). A study of the differential cross-polarization times for different regions of the S spectrum should yield additional information on $\underset{\approx}{\sigma}$ since these are also related to geometry through the orientation-dependent I-S dipolar interactions. Studies of both these types are in progress for several compounds from which crystals cannot be grown with facility.

D. CROSS-POLARIZATION DYNAMICS

The theoretical discussion in Section II assumed that the cross-polarization step (Figure 4) proceeded to full equilibrium between I and S. It is possible to learn a lot about orientation and motion in solids by interrupting this step after a time τ and observing the high resolution S spectrum as a function of

τ. This would measure the I-S cross relaxation times for different lines or portions of the S spectrum in much the same spirit that high resolution T_1 measurements are made in liquids.[72,73]

We do not go into a detailed discussion of the cross-relaxation since we have performed no quantitative experiments. We point out only the principal aspects of the theory relevant to our experiments and mention the possible potential in structural and dynamical studies.

If we assume that the coupling term $\mathcal{H}^0_{dIS}$ in (5) is a perturbation on the large reservoir terms $\mathcal{H}_{1I}$ and $\mathcal{H}_{1S}$, then we can arrive at an exponential form for the flow of energy between the I and S systems:[74]

$$\frac{d}{dt}\left(\frac{1}{T^I} - \frac{1}{T^S}\right) = -\frac{1}{T_{IS}}\left(\frac{1}{T^I} - \frac{1}{T^S}\right) \tag{55}$$

The cross-relaxation time T_{IS} is calculated by the density matrix perturbation approach used by McArthur, Hahn and Walstedt.[36] For the case of the resonant spin-locking version (Figure 4) which we have discussed, we find:

$$\frac{1}{T_{IS}} = \frac{1}{2}\langle\Delta\omega^2\rangle_{IS}\int_0^\infty f(\tau)\cos\Delta\omega_1\tau\, d\tau \tag{56}$$

where:

$$\Delta\omega_1 = \gamma_I H_{1I} - \gamma_S H_{1S} \tag{57}$$

$\langle\Delta\omega\rangle_{IS}$ is the S second moment due to I-S dipolar interactions

$$\langle\Delta\omega^2\rangle_{IS} = -\frac{\mathrm{Tr}\,[\mathcal{H}^0_{dIS},\ \sum_i S_{ix}]^2}{\mathrm{Tr}\left(\sum_i S_{ix}\right)^2} \tag{58}$$

and $f(\tau)$ is the autocorrelation function of $\mathcal{H}^0_{dIS}$ modulated by $\mathcal{H}^0_{dII}$

$$f(\tau) = \frac{\mathrm{Tr}\left(\sum_i b_i I_{ix}\right)\exp\left(-\frac{i}{2\pi}\mathcal{H}^0_{dII}\tau\right)\left(\sum_i b_i I_{ix}\right)\exp\left(\frac{i}{2\pi}\mathcal{H}^0_{dII}\tau\right)}{\mathrm{Tr}\left(\sum_i b_i I_{ix}\right)^2} \tag{59}$$

$\mathcal{H}^0_{dII}$, $\mathcal{H}^0_{dIS}$ and b_i are given in equations (1) and (6). The form of $f(\tau)$ can be determined experimentally by measuring its Fourier transform $\frac{1}{T_{IS}}$ vs. $\Delta\omega_1$ (since it is practically impossible to calculate $f(\tau)$ exactly) as in the work of McArthur, Hahn and Walstedt.[36] We have not done this but for the present assume that the behavior in our case is also exponential i.e.:

$\frac{1}{T_{IS}} \propto \exp(-\Delta\omega_1\tau)$ so:

$$f(\tau) = \frac{1}{1+\frac{\tau^2}{\tau_c^2}} \tag{60}$$

The exact form of $f(\tau)$ is not crucial for the purposes of our discussion where the Hartmann-Hahn condition[31] (2) is satisfied, $\Delta\omega_1 = 0$. The correlation time τ_c is given, comparing (56) and (60), by:

$$\frac{1}{\tau_c^2} = -\frac{1}{8}\,\frac{\mathrm{Tr}\,[\mathcal{H}^0_{dII},\ \sum_i b_i I_{ix}]^2}{\mathrm{Tr}(\sum_i b_i I_{ix})^2} \tag{61}$$

Plugging this into (56) and taking the case that $\Delta\omega_1 = 0$ we get:

$$\frac{1}{T_{IS}} = C_{IS}\,\langle\Delta\omega^2\rangle_{IS}\,\langle\Delta\omega^2\rangle_{II}^{-\frac{1}{2}} \tag{62}$$

where $\langle\Delta\omega^2\rangle_{II}$ is the normal high field truncated second moment:

$$\langle\Delta\omega^2\rangle_{II} = -\frac{\mathrm{Tr}\,[\mathcal{H}^0_{dII},\ \sum_i I_{ix}]^2}{\mathrm{Tr}(\sum_i I_{ix})^2} \tag{63}$$

C_{IS} is a lumped constant given by:

$$C_{IS} = 3\pi\left(\frac{\sum_{i\neq j} a_{ij}^2 \sum_i b_i^2}{N_I \sum_{i\neq j} a_{ij}^2 [(2b_i+b_j)^2 + (b_i+2b_j)^2]}\right)^{\frac{1}{2}} \tag{64}$$

and a_{ij} is the geometrical factor in (1) for I spins

$$a_{ij} = \frac{-\gamma_I^2\hbar^2\,P_2(\cos\theta_{ij})}{r_{ij}^3} \tag{65}$$

From (62) we see that the dependence of T_{IS} on geometry is contained predominantly in $\langle\Delta\omega^2\rangle_{IS}$ and to a lesser extent in the remaining factors. Typical values of $\langle\Delta\omega^2\rangle_{IS}$, $\langle\Delta\omega^2\rangle_{II}$ and C_{IS} indicate that T_{IS} should range from $\sim$ 0.1-1 msec for ^{13}C-^{1}H as we have indeed observed.

A good example of this behavior is exhibited by the ^{13}C NMR of solid polycrystalline benzene. Figure 15(b) shows the normal proton-enhanced spectrum with full cross-polarization. The spectrum displays an axial symmetry due to rapid reorientation about the C_6 axis, as discussed in Section IV.A. The lineshape is that of equation (48) (Figure 10(b)) with σ given by:

$$\frac{\sigma - \sigma_\perp}{\sigma_{||} - \sigma_\perp} = \cos^2\beta \tag{66}$$

where β is the angle between the C_6 axis and H_0 as shown in Figure 15(a). Figures 15(c), (d), show the effects of cross-relaxation. For ^{13}C, the main contribution to $\langle\Delta\omega^2\rangle_{IS}$ is intramolecular and is given by:

$$\langle\Delta\omega^2\rangle_{IS} = \langle\Delta\omega^2\rangle_0 \left(P_2(\cos\beta)\right)^2 \tag{67}$$

where $\langle\Delta\omega^2\rangle_0$ is the intramolecular second moment for $\beta = 0$, since the dipolar interaction is proportional to $P_2(\cos\beta)$. This predicts that the cross-relaxation should be strongly inhibited at the magic angle ($54^o\ 44'$) where $P_2(\cos\beta) = 0$, i.e.

$$\frac{\sigma - \sigma_\perp}{\sigma_{||} - \sigma_\perp} = \frac{1}{3} \tag{68}$$

This is indeed observed in Figure 15 in agreement with the result obtained using indirect detection by Yannoni and Bleich.[75] Note, however, that the distortion due to cross-relaxation is a

Figure 15

Effects of incomplete cross-relaxation in proton-enhanced ^{13}C NMR of solid polycrystalline benzene at -50°C. The molecule is undergoing rapid reorientation about the C_6 axis which makes an angle β with H_0(a). The spectra are obtained from a single-contact version of Figure 4 (N=1) with variable τ. For long $\tau > T_{IS}$ (b) we see a fully relaxed ^{13}C spectrum. For short τ, we see that ^{13}C in molecules with $P_2(\cos\beta) \sim 0$ (i.e. $\frac{\sigma - \sigma_\perp}{\sigma_\parallel - \sigma_\perp} \sim \frac{1}{3}$) cross-polarize very slowly as expected from theory.

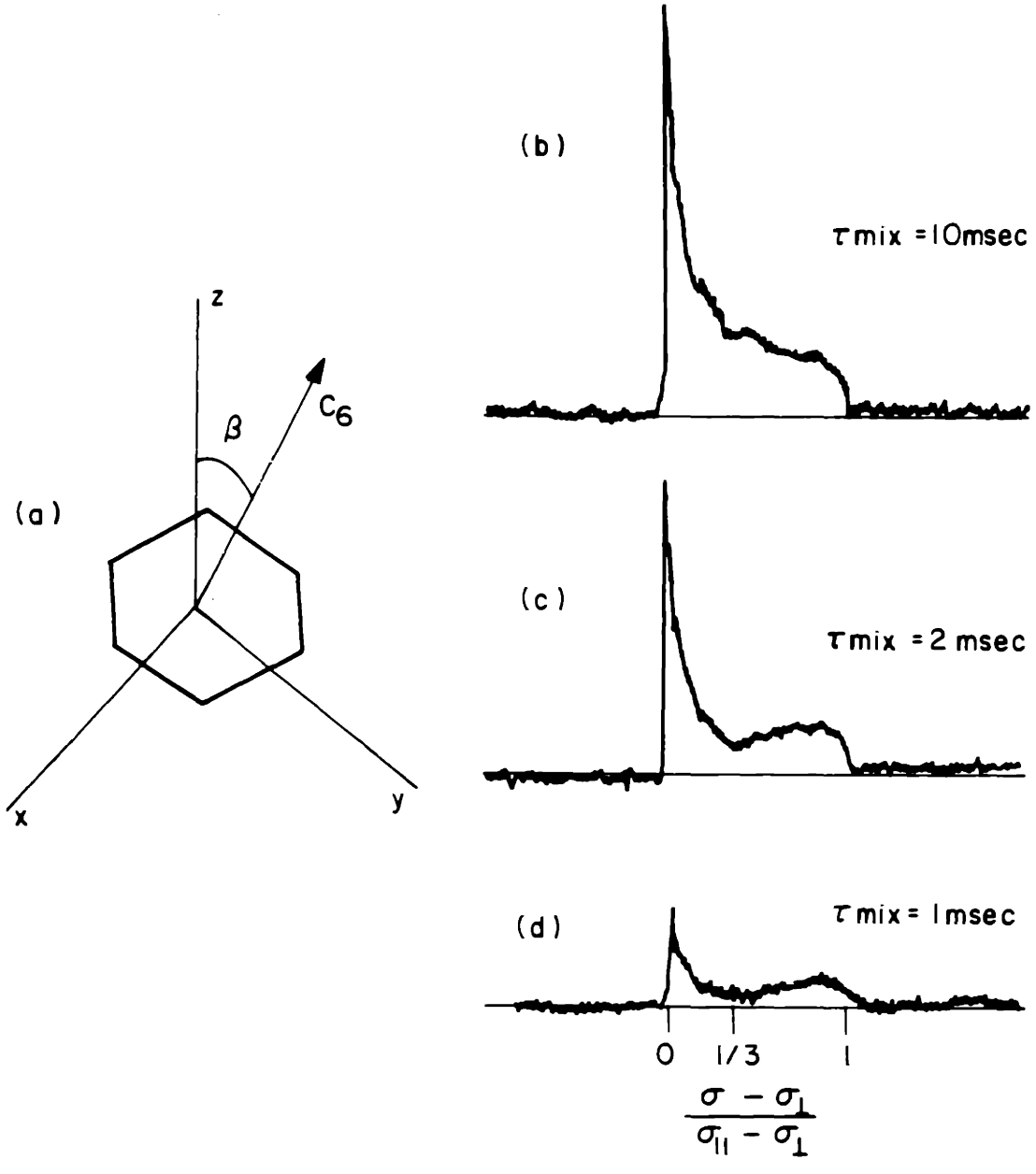
(a)
z
β
C_6
x
y
(b)
τmix = 10msec
(c)
τmix = 2 msec
(d)
τmix = 1msec
0
1/3
1
$\frac{\sigma - \sigma_\perp}{\sigma_{11} - \sigma_\perp}$

necessary consequence of the latter technique, whereas it is an option in our direct detection method.

A quantitative study would necessitate a calculation of the intra- and intermolecular contributions to $\langle\Delta\omega^2\rangle_{IS}$, $\langle\Delta\omega^2\rangle_{II}$ and C_{IS} from the crystal structure. It is known, for example, that in benzene both contributions are about equal for $\langle\Delta\omega^2\rangle_{II}$.(67a) In addition, from the experimental point of view, a calibration of the H_1's would be essential--in our case this was not done due to a rather large instability in the amplitudes of the rf. Thus at present no quantitative discussion is pertinent and only the relative behavior discussed above is meaningfull. A full quantitative study of this system (including the case $\Delta\omega_1 = 0$ to check the form of $f(\tau)$ in (59)) would be very interesting.

Another case which we have studied is solid adamantane at room temperature. There, both sharp ^{13}C lines are found to cross-polarize at the same rate (~ 1 msec for the conditions of our experiment). This is in line with the isotropic motion notion which wipes out the anisotropy in $\langle\Delta\omega^2\rangle$. Cross-relaxation proceeds purely by intermolecular dipolar coupling. If there was no motion, the carbon with two protons bonded would be expected to cross-polarize more rapidly than that with one.

Preliminary results have also been reported for ^{13}C spin-lattice relaxation in solid benzene.(76) This is a useful additional experiment to the cross-relaxation, and also fits in with

accepted model of anisotropic motion.[67] In adamantane, spin-lattice relaxation does distinguish the two carbons, that with two protons relaxing more rapidly (as expected for dipolar relaxation) as in solution.[77] Full details on these experiments will be presented separately.

V. ALTERNATIVE VERSIONS

The discussion so far has centered on one particular version of the double-resonance experiment. This has served, we hope, to illustrate the main features of the technique. In this section we wish to point out that many versions are possible and that each one, or some combinations thereof may be more advantageous in different circumstances. We first talk about alternative direct detection methods and then mention briefly some high resolution modifications of the direct detection.

A. DIRECT DETECTION

For the purposes of this discussion it is convenient to reduce the direct detection methods to four major steps depicted schematically in Figure 16. Step 1, preparation, is usually the polarization of I spins to full magnetization in H_0. The hold period is that during which the I spin order must be maintained. In the version we have discussed, this is done in the I rotating frame by spin-locking. Mix constitutes the transfer of spin order from the I to S spin systems which was done by transfer of polarization from H_{1I} in the I rotating frame to H_{1S} in the S rotating frame. Finally, in the observe step the S signal is observed and recorded--the I spins may be decoupled if we desire high resolution S spectra, or remain undecoupled if we are interested in broad line S spectra.

Figure 16

Schematic general representation of direct detection double-resonance such as proton-enhanced NMR. Examples of options for the various steps are presented in the text.

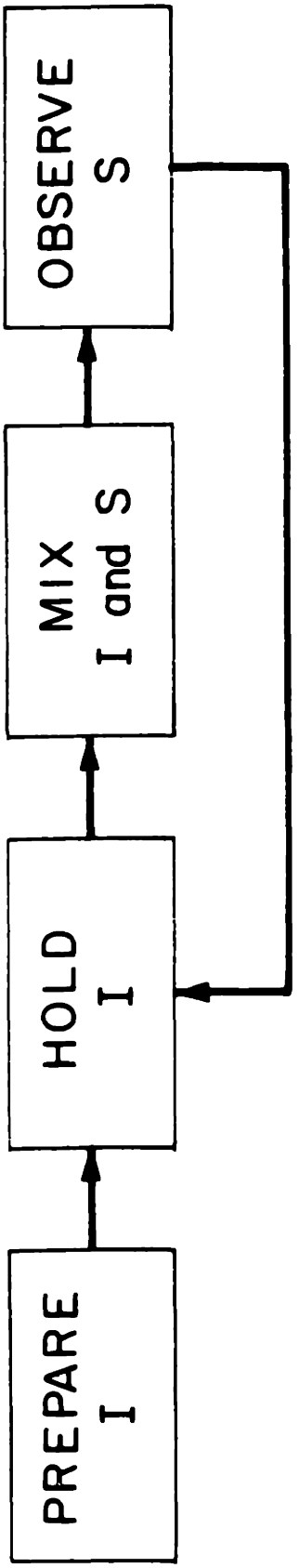
PREPARE
I
HOLD
I
MIX
I and S
OBSERVE
S

In our preceeding version, decoupling was performed continuously by the I spin-locking field.

The following is not intended to be an encyclopaedia of all the methods available as alternatives for the above steps. We wish only to point out illustrative examples. Many others will surely occur to the reader. Which one or which combination is best suited to the particular experiment at hand is largely a matter of the experimenter's discretion and may be the result, in some cases, of trial and error. We shall also indicate a few combinations suited for general application.

1. Prepare.
   (a) polarize I by spin-lattice relaxation in H_0
   (b) dynamically polarize I by optical polarization[78]
   (c) polarize I using polarized quadrupolar nucleus with short spin-lattice relaxation time[79]
2. Hold.
   (a) hold M_I along H_0 in laboratory frame
   (b) spin-lock M_I along H_{1I} in rotating frame
   (c) hold I order in dipolar state in laboratory or rotating frame.[39]
3. Mix.
   (a) Hartmann-Hahn; matched or unmatched
   (b) Solid effect in laboratory or rotating frames[80]

(c) adiabatic crossover[81]

4. Observe. (a) undecoupled I

(b) continuous I spin-decoupling[28]

(c) pulsed I spin-decoupling[29]

The nature of these phenomena has been discussed in detail in the references cited. Matched and unmatched Hartmann-Hahn mixing refer to mixing satisfying, or not satisfying, equation (2) respectively. More generally, H_{1I} would be replaced by $\bar{H}_{1I}$ where $\bar{H}_{1I}$ is either the average H_1 over a pulse train or a local dipolar field.[82,83]

An important consideration in these experiments is sample heating. In the version we talked about in Section II, long continuous irradiation of the I system is required and this may lead to unacceptable average power dissipation in the probe. This is the purpose of the hold period--to allow a cooling of the sample and probe while maintaining the I spin order. A particularly useful option in this respect, mentioned in 2(c) is the dipolar state which we discuss now in a little more detail. This presents a means of storing I order in the rotating frame without the need for strong spin-locking fields.

A low temperature dipolar-ordered state may be obtained by transforming Zeeman order into dipolar order by one of several techniques, e.g.[84]

(i) adiabatic demagnetization in the rotating frame (ADRF)[85] following spin-locking.

(ii) ADRF by adiabatic fast passage with a small H_1 into resonance, and removal of H_1.

(iii) 90y-45x two pulse transfer[86]--this is not adiabatic but is a simple and rapid way to make a ~ 50% efficiency transfer.

Following such a conversion, the high temperature density matrix assumes the form:

$$\rho_{dip} = \frac{1}{Z}\left(1 + \frac{\mathcal{H}^0_{dII}}{kT^{dip}}\right) \tag{69}$$

with T^{dip} depending on the initial spin temperature and the technique used. The thermodynamical discussion in Section II is still valid if H_{lI} is replaced by H'_L, the local dipolar field defined by:

$$\frac{C_I H'^2_L}{T^{dip}} = Tr\left\{\rho_{dip}\ \mathcal{H}^0_{dII}\right\} \tag{70}$$

to make the analogy with the Zeeman field H_{lI} in the expression for the Zeeman energy in (12). H'_L is given by:

$$H'^2_L = \frac{1}{3\gamma_I^2}\ \langle\Delta\omega^2\rangle_{II} \tag{71}$$

where $\langle\Delta\omega^2\rangle_{II}$ appears in (63). This is all well known and will not be enlarged on here. The main point is that this order may still be transferred from the I to the S spins by application

of an S field H_{1S} in the S rotating frame. The dynamics of this process have been treated in detail by McArthur, Hahn and Walstedt[36] for the case of ^{43}Ca-^{19}F double-resonance.

Assume as in Section II.C that we begin again with the I spinspolarized at the lattice temperature, and perform an ADRF. The density matrix is then given to a good approximation, in analogy to (18), by:

$$\rho_R^{(0)} = \frac{1}{Z} \left(1 + \frac{\mathcal{K}_{dII}^0}{kT^{(0)}}\right) \tag{72}$$

where this time it is easily seen:

$$T^{(0)} = T^L \frac{H_L'}{H_0} \tag{73}$$

We now turn on an S field H_{1S} at exact resonance such that:

$$\gamma_S H_{1S} = \alpha \gamma_I H_L' \tag{74}$$

The I and S spins now come to equilibrium with:

$$\rho_R^{(1)} = \frac{1}{Z} \left[1 + \frac{1}{kT^{(1)}} (\mathcal{K}_{dII}^0 + \mathcal{K}_{1S})\right] \tag{75}$$

yielding, using exactly the same considerations as those leading to (23) and (26):

$$M_S^{(1)} = \frac{\gamma_I}{\gamma_S} \frac{\alpha}{1 + \alpha^2 \epsilon} M_S^{(0)} \tag{76}$$

with $M_S^{(0)}$ given by (16). The spin-locking case we treated before corresponds to $H_L' \rightarrow H_{1I}$ and $\alpha = 1$ (Hartmann-Hahn condition). The

cross-relaxation time T_{IS} for this type of experiment calculated by McArthur, Hahn and Walstedt is:[36]

$$\frac{1}{T_{IS}} = \langle \Delta\omega^2 \rangle_{IS} \int_0^\infty a(\tau) \cos\alpha\omega_L'\tau \, d\tau \tag{77}$$

where $\omega_L' = \gamma_I H_L'$ is constant and $a(\tau)$ is the same as $f(\tau)$ in (59) with I_{ix} replaced by I_{iz}. The above authors measured an exponential dependence of T_{IS} on α, i.e. $\frac{1}{T_{IS}} \alpha \exp(-\alpha\omega_L'\tau_c)$. If we assume this to be generally true then we can use equation (17) of their work:

$$\frac{1}{T_{IS}} = \frac{\pi}{2} \langle \Delta\omega^2 \rangle_{IS} \tau_c \exp(-\alpha\omega_L'\tau_c) \tag{78}$$

with τ_c given by (61) and I_{ix} replaced by I_{iz}.

Two interesting cases arise:

(i) $\alpha \sim 1$. In this case T_{IS} can still be short and one obtains after N cycles of transfer a magnetization $M_S^{(N)}$ given by (27) exactly as before. The signals from $M_S^{(K)}$ are again co-added yielding ~ the same sensitivity as before. Several versions of this approach are illustrated in Figure 17 which also shows some permissible combinations of decoupling sequences.

(ii) $\alpha >> 1$. In this case we can obtain, looking at (76), a large S polarization in one shot. The maximal value of $M_S^{(1)}$ occurs for

$$\alpha\sqrt{\epsilon} = 1 \tag{79}$$

whence:

Figure 17

Examples of high resolution cross-polarization experiments using an I dipolar state in the rotating frame. The I dipolar state in each case is produced by an adiabatic demagnetization in the rotating frame (ADRF). The mixing in each case is between the I spins in the dipolar state and the S spins with field H_{1X}. The hold period is to allow the probe and sample to cool. Several mixing steps may be used for each holding one until heating is excessive. (a) The I spins are decoupled while in the dipolar state. The 90° pulses cause a "spin-locking" of the I dipolar state (magic sandwich). Direct irradiation would cause a 75% destruction. (b) An adiabatic remagnetization in the rotating frame (ARRF) brings back the I magnetization along H_{1X} and it is spin-locked and decoupled during S observation. (c) The I spins are maintained in the dipolar state and decoupled with 180° pulses. Since H^0_{dII} is invariant to a 180° rotation this does not affect the spin order. (d) Here the decoupling is done with 90° pulses (to which H^0_{dII} is not invariant), so the system must be spin-locked by 90°_y pulses. This is a pulsed version of (a). Many other versions are possible. (e) S spin irradiation for mixing and observation; $\gamma_S H_{1S}$ may be larger than $\gamma_S H_{1I}$ to provide even mixing of all the S spins.

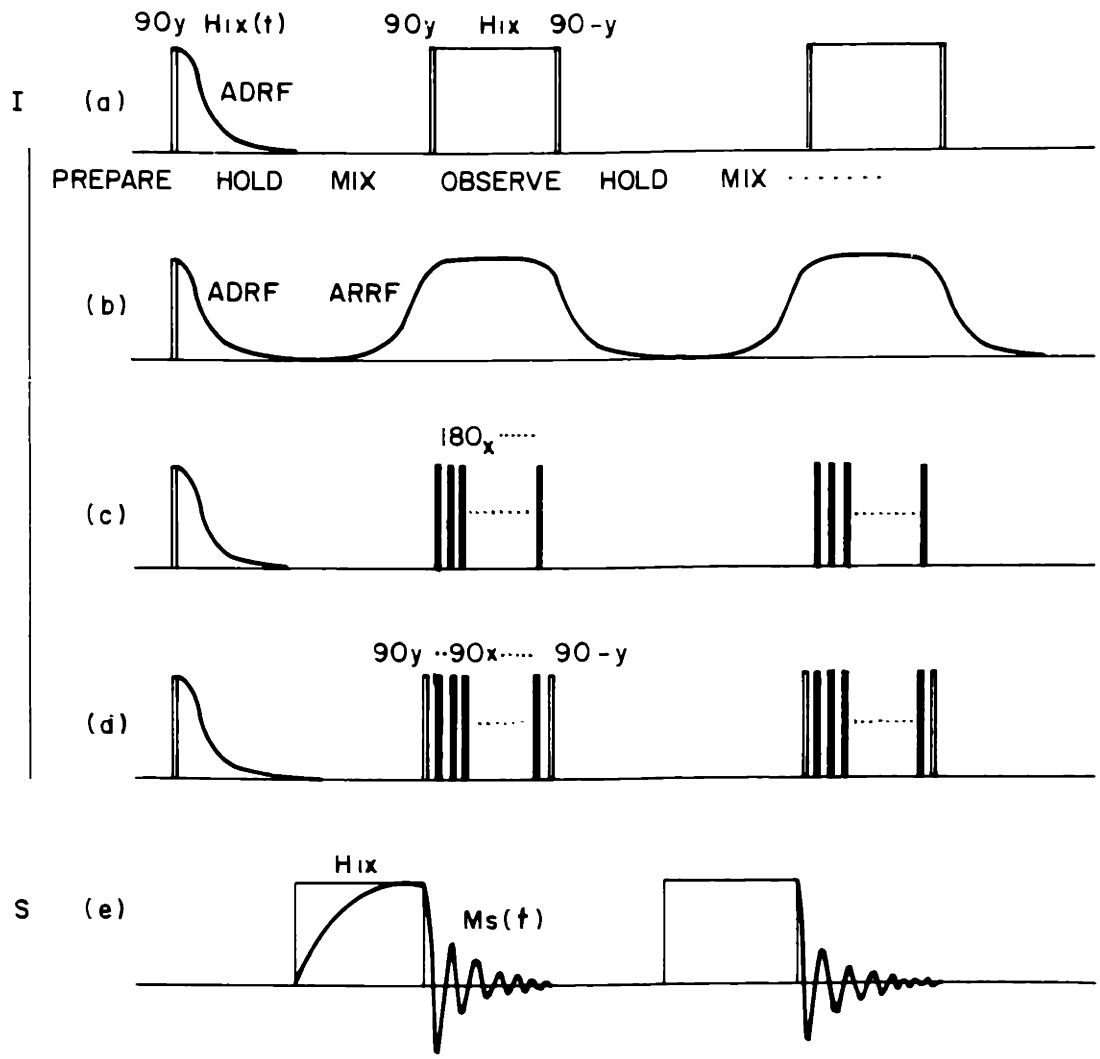
90y Hix(t)
90y Hix 90-y
I (a)
ADRF
PREPARE HOLD MIX OBSERVE HOLD MIX
(b)
ADRF ARRF
180x
(c)
90y 90x 90-y
(d)
S (e)
Hix
Ms(t)

Figure 18

Scheme for high-resolution study of S spin-lattice relaxation. The I spins are prepared in a dipolar state by ADRF. Cross-polarization of the S spins is achieved with $\gamma_S H_{1S} > \gamma_I H_{1I}$ which gives a large S polarization (albeit more slowly, as explained in the text). This is placed along the z axis and allowed to relax for a time τ. Subsequent observation with I spin-decoupling gives a high resolution partially relaxed S spectrum. Again, many other versions are possible.

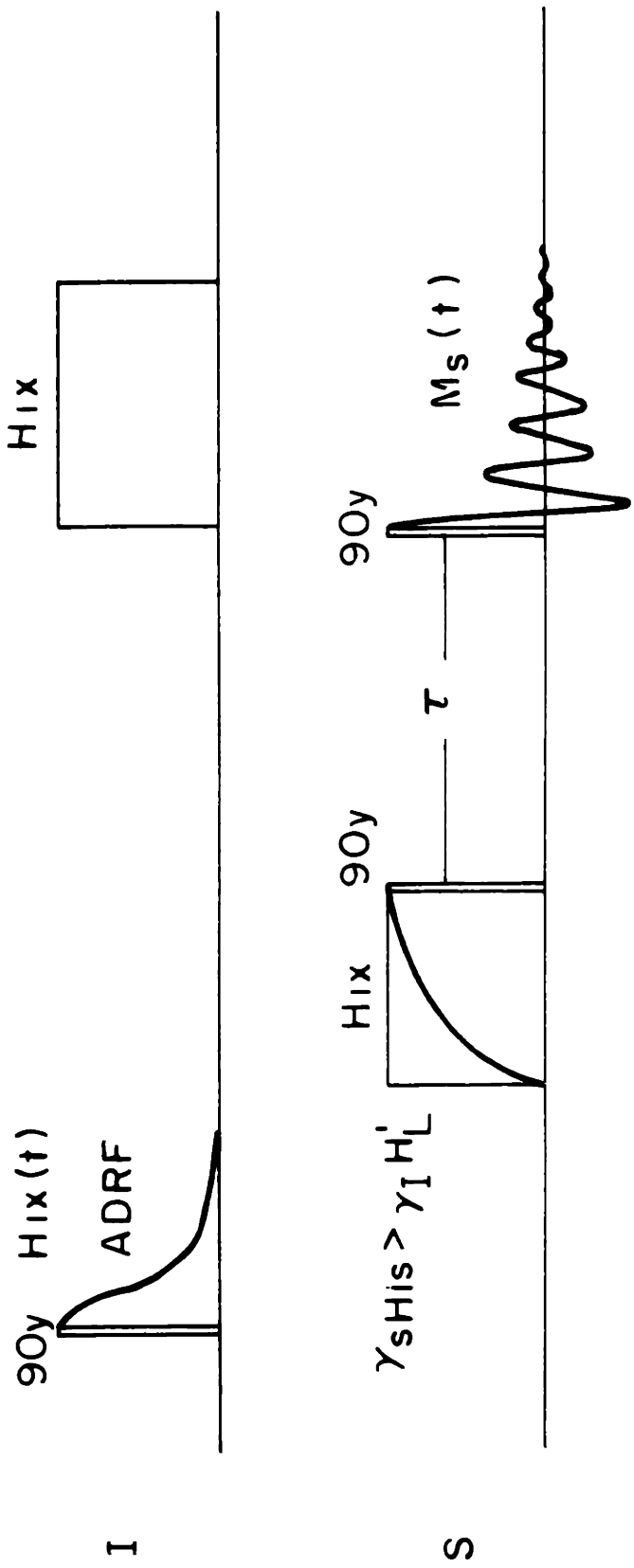
I
S
90y
H1x(t)
ADRF
H1x
90y
H1x
τ
90y
Ms(t)
γsHis > γI H'L

$$M_S^{(1)} = \frac{\gamma_I}{\gamma_S} \frac{1}{2\sqrt{\epsilon}} M_S^{(0)} \tag{80}$$

or one half the polarization from an adiabatic transfer in (39). Adiabatic transfers are also possible as mentioned in Section II.E and will be discussed in detail elsewhere.

The above looks like a very profitable venture since we obtain a massive ($\epsilon << 1$) S polarization in one shot. Note however, from (78) that T_{IS} gets longer as α is increased and may become prohibitively long. This is especially bad since H_{1S} is then large and sample heating may become a problem. The form of $a(\tau)$ also becomes crucial--Gaussian behavior, as some authors have assumed, would make things even worse if $\frac{\omega_L' \tau_c}{\sqrt{\epsilon}} >> 1$ as would usually be the case for small ϵ. In any case, the final sensitivity or data rate is about the same as in the multiple contact version ($\alpha \sim 1$) if T_{1I} is long.

There is at least one case where (ii) above may clearly offer a considerable advantage, namely in T_1 measurements of the S spin system as discussed by McArthur, Hahn and Walstedt.[36] In this case a single-shot large S polarization is very useful since there is no analogy to the co-addition of many S signals from a single I polarization if T_{1S} is long. It is thus worthwhile to put $\alpha >> 1$ and accept the long T_{IS} (the sample heating may be alleviated by periodically putting M_S along H_0). Figure 18 shows how we adapt this approach to high resolution T_1 studies in

our direct detection scheme. This is similar to T_1 studies in liquids[72,73] except for the enhanced sensitivity.

Finally, note that the unmatched Hartmann-Hahn experiment ($\gamma_S H_{1S} = \alpha\, \gamma_I H_{1I}$) may be used to obtain large $M_S^{(1)}$ even in the spin-locking version of Section II. There however the equation (62) for T_{IS} would read:

$$\frac{1}{T_{IS}} = C_{IS} \langle \Delta\omega^2 \rangle_{IS} \langle \Delta\omega^2 \rangle_{II}^{-\frac{1}{2}} \exp\left[-(\alpha-1)\omega_{1I}\tau_c\right] \qquad (81)$$

and we see that since ω_{1I} is large, this becomes much more sensitive to the unmatching.

B. INDIRECT DETECTION

Two modifications of the normal Hartmann-Hahn indirect detection method have been proposed for high resolution.[87,88] An obvious appeal of these techniques is that it is the abundant I spins which are observed making the signals much larger (due to number and frequency) than that of the direct S detection. This is not the whole story, however, since the indirect detection methods, signal strength not withstanding, involve a mapping of the S spectrum point by point and thus require long times to acquire the whole S spectrum. Thus, although the sensitivity may be very good, it may in some cases be <u>too</u> good, requiring long times, and making the rapid S detection, where the whole spectrum is obtained immediately, preferable. In this section

we discuss one of the above two techniques. Both are similar --one involves a direct mapping of the S absorption spectrum; the second involves a mapping of the S free induction decay. We discuss the latter since it is easier to compare to our direct detection scheme. However, the sensitivity is similar in both and thus the conclusions we draw from the comparison should be generally useful.

Figure 19 shows the high resolution modification of the T_2 experiment of McArthur, Hahn and Walstedt[36] used by Mansfield and Grannell.[88] The mixing and decoupling steps are performed through spin-locking in the same way as for our direct detection scheme. Following the mixing step the S spins are allowed to undergo a decoupled (high resolution) free induction decay for a time τ, and the mixing performed again. If the normalized free induction decay is S(t) as in II.D and the above cycle is performed N times then an accumulative destruction of the I magnetization ensues. Considerations similar to those used in Section II yield:

$$M_I^{(N)} = M_I^{(0)} \exp\left(-N\epsilon(1 - S(\tau))\right) \tag{82}$$

where $M_I^{(0)}$ is given by (17).

To prevent distortion of the signal it is necessary that

$$N\epsilon = \lambda << 1 \tag{83}$$

for which:

Figure 19

Adaptation (reference (88)) of indirect detection techniques to high resolution. In this case, the I spins are observed. Following an I-S contact (cross-polarization) the S magnetization is allowed to decay, while decoupling I, for a time τ. This is performed N times with fixed τ, and the final I magnetization recorded. From the dependence of the I magnetization destruction on τ, the S free induction decay $S(\tau)$ may be extracted with very high sensitivity.

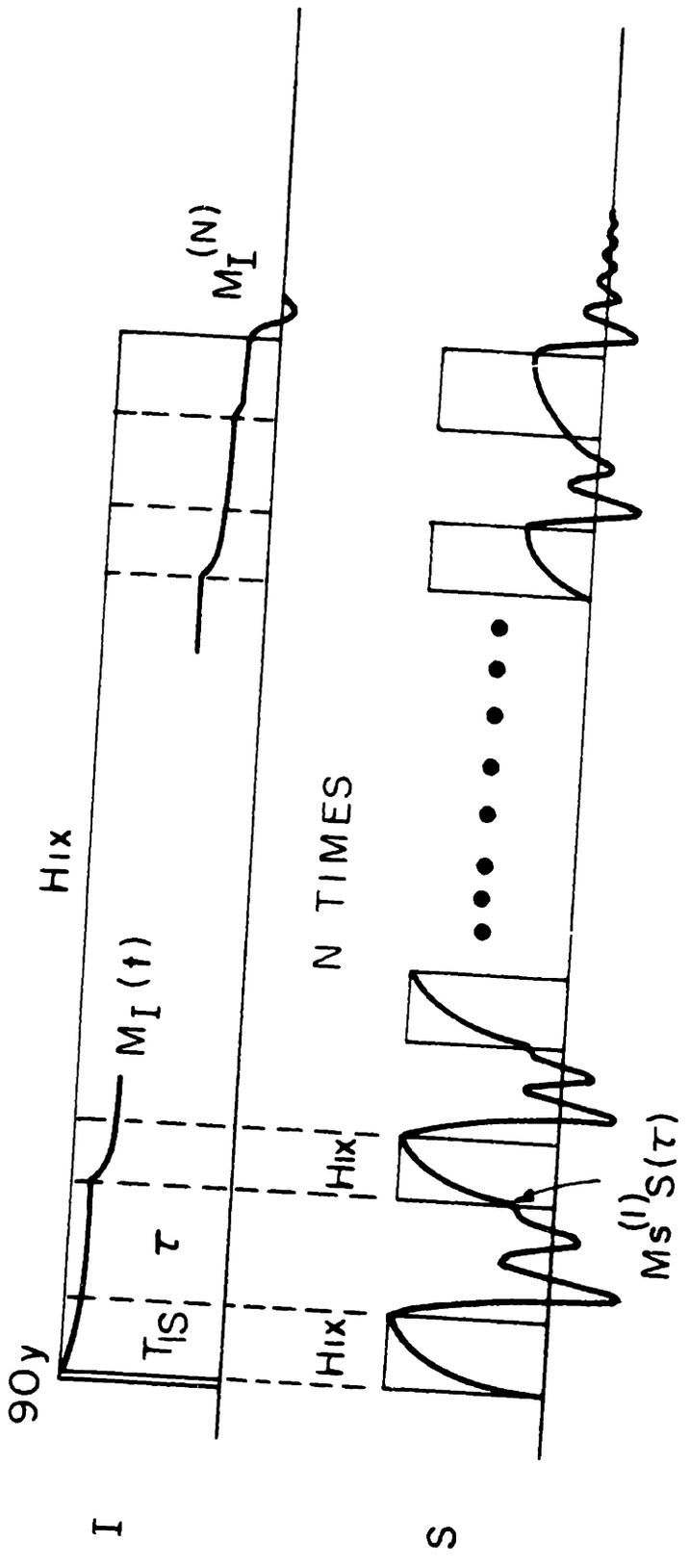
I
S
90y
TIS
τ
H1x
H1x
H1x
MI(t)
N TIMES
MI(N)
MS(1)S(τ)

$$M_I^{(0)} - M_I^{(N)} = \lambda M_I^{(0)} \quad (1 - S(\tau)) \tag{84}$$

So the destruction is proportional to $S(\tau)$. The S free induction decay can therefore be mapped out by plotting the destruction vs. τ. For each point it is necessary to wait $\sim \lambda T_{1I}$ for repolarization of the I spins. If $\lambda \sim 1$ this can still be performed but a correction for distortion must be made.

Assume now that the voltage produced by $M_I^{(0)}$ is $K_I M_I^{(0)}$ and that like in Section II.D the noise voltage in the I detector bandwidth is V_{nI}. The data rate for our fixed point $S(\tau)$ on the S free induction decay by the I detection is then

$$Q_{IND}^{(\tau)} \sim \frac{1}{\lambda T_{1I}} \left(\frac{\lambda K_I M_I^{(0)}}{\sqrt{2} V_{nI}} \right)^2 \tag{85}$$

Since the power (S/N) involves the destruction λ for the I magnetization and the noise voltage involves a difference ($\sqrt{2}$).

We now note one important difference between the direct and indirect detection methods. In the former, within one T_1 it is the full free induction decay, not just the point $S(\tau)$ that is obtained. In the latter only one point is obtained per $\sim \lambda T_1$. Assume then that the number of points required on the free induction decay is given by

$$M = \frac{\Delta_S}{\delta_S} \tag{86}$$

where Δ_S and δ_S are the spectral bandwidth and requisite resolution of the S spectrum. To compare the data rate of (85) with the direct detection for the full free induction decay we must then write:

$$Q_{IND} \sim \frac{\delta_S}{\Delta_S} \frac{1}{\lambda T_{1I}} \left(\frac{\lambda K_I M_I^{(0)}}{\sqrt{2}\, V_{nI}}\right)^2 \tag{87}$$

Since we are interested only in a general semiquantitative comparison of the techniques, we do not take into account details such as sampling widths which depend on factors such as T_{2I} etc. These effects will usually be of order unity if $\Delta_S \sim T_{2I}^{-1}$ which is normally a realistic estimate. For comparison then, (87) can finally be written:

$$Q_{IND} = \mathcal{G}_{IND}\, Q_{FID} \tag{88}$$

where

$$\mathcal{G}_{IND} = \frac{\delta_S\, T_{1S}\, \lambda}{2\, \Delta_S\, T_{1I}} \left(\frac{K_I\, M_I^{(0)}\, V_{nS}}{K_S\, M_S^{(0)}\, V_{nI}}\right)^2 \tag{89}$$

Comparing this with the analogous expression from the direct cross-polarization technique (36) we find:

$$\frac{\mathcal{G}_{CP}}{\mathcal{G}_{IND}} \equiv \mu \sim \frac{1}{\varepsilon} \left(\frac{\gamma_I}{\gamma_S}\right)^2 \frac{\Delta_S}{\lambda\, \delta_S} \left(\frac{K_S\, M_S^{(0)}\, V_{nI}}{K_I\, M_I^{(0)}\, V_{nS}}\right)^2 \tag{90}$$

where μ is a measure of the relative efficiency of the two experiments in terms of long term data rate. It can be shown that the relative power (S/N) for I and S spins due to difference

in γ's and number of spins is given by:

$$\frac{K_S M_S^{(0)} V_{nI}}{K_I M_I^{(0)} V_{nS}} \sim \epsilon^2 \left(\frac{\gamma_S}{\gamma_I}\right)^5 \tag{91}$$

This assumes that both systems operate with the same unloaded Q and that detector noise is similar. Using this ratio, (91) assumes the form:

$$\mu \sim \epsilon \left(\frac{\gamma_S}{\gamma_I}\right)^3 \frac{\Delta_S}{\lambda \delta_S} \tag{92}$$

C. COMPARISON

Although the above analysis is terribly simplistic it does allow some general conclusions:

(a) In terms of long term data rate ($T > n\lambda T_{1I}$) on which the above analysis is based, the indirect detection method appears to gain when ϵ and $\frac{\gamma_S}{\gamma_I}$ get smaller. For ^1H-^{13}C $\frac{\gamma_S}{\gamma_I} = 0.25$ and typical values of ϵ and $\frac{\Delta_S}{\delta_S}$ are $\sim 0.5 \times 10^{-2}$ and $\sim 10^3$ respectively. Taking $\lambda \sim 1$ (which gives good S/N but produces a distortion according to (82)), we see $\mu \sim 10^{-1}$ so the indirect detection approach appears to be superior. For ^{15}N the difference becomes even greater.

(b) By adaptation of steady state techniques[83,87,89] the sensitivity of the indirect detection can be enhanced even further. In this approach, the I magnetization is not allowed

to decay but is spin-locked off resonance with a pulse train and observed between the pulses. Both the frequency and time domain indirect experiments can benefit from this, and yield an enhancement in sensitivity of $\sim T_{1\rho}/T_2$ for the I spins. In the present context we do not feel that a detailed discussion of this is warranted, but mention that the method does produce a gain in sensitivity but suffers from spectral distortion due to cross-relaxation effects.

(c) The conclusions above might superficially lead one to suspect the merit of the direct direction methods that we have so laboriously outlined in this paper, despite their evident success in terms of preliminary experimental showing. That this would be foolish is made transparent by the following observations:

(i) the technique is simple and requires no serious modification of conventional Fourier transform spectrometers. The indirect detection requires rather more elaborate automation and timing and an effort must be expended to eliminate spectral distortion.

(ii) in many cases the cross-polarization, direct detection experiment will yield a sufficient S/N ratio from one polarization of the I spins. In this case, the whole long term analysis above breaks down and, in general, the direct detection

will be vastly superior to the indirect one if T_{1I} is very long. This is because the latter requires ~ T_{1I} per point and even though the final S/N may be tremendous, the time expended in collecting it is unrealistically long. The direct method yields sufficient S/N in a short time. Modifications could be introduced to aid the direct detection approach in this respect but they deduct from the straightforwardness and simplicity of the experiment.

Finally, we mention that similar remarks can be made about the modification of Bleich and Redfield.[87] We feel that both direct and indirect detection will prove valuable; the former should be more useful in routine applications to ^{13}C spectroscopy, whereas the latter should find its potential in applications to very dilute spin such as ^{15}N in biologically interesting systems.

ACKNOWLEDGMENTS

We have benefitted from the advice, assistance and ideas of many people. We are especially grateful in this respect to W-K. Rhim, J. D. Ellett, Jr., R. G. Griffin and S. Kaplan. A.P. is particularly indebted to M. Goldman and J. M. Deutch for delightful and illuminating discussions of several aspects of the theory related to these techniques. We also acknowledge stimulating correspondence and discussions with A. G. Redfield and C. S. Yannoni.

REFERENCES AND FOOTNOTES

1. J. W. Emsley, J. Feeney and L. H. Sutcliffe, High Resolution Nuclear Magnetic Resonance Spectroscopy, (Pergamon, Oxford, 1967).

2. Examples are: (a) B. T. Gravely and J. D. Memory, Phys. Rev. B, 3, 3426 (1971). (b) S. Gade, Phys. Rev., 187, 419 (1969). (c) D. K. Hutchins and S. M. Day, Phys. Rev., 180, 432 (1969).

3. Examples are: (a) I. J. Lowe and S. Gade, Phys. Rev., 156, 817 (1967). (b) G. W. Leppelmeier and J. Jeener, Phys. Rev., 175, 498 (1968). (c) W. E. Blumberg, Phys. Rev., 119, 79 (1960). (d) D. Tse and S. R. Hartmann, Phys. Rev. Lett., 21, 511 (1968). (e) N. Bloembergen, Physica, 15, 386 (1949).

4. (a) J. Jeener, Advances in Magnetic Resonance, (Academic, N.Y., 1968), Vol. III. (b) A. G. Redfield, Science, 164, 1015 (1969). (c) M. Goldman, Spin Temperature and Nuclear Magnetic Resonance in Solids, (Oxford, 1970).

5. (a) A. Abragam, The Principles of Nuclear Magnetism, (Oxford, 1961), Chapters 4 and 7. (b) G. E. Pake, J. Chem. Phys., 16, 317 (1948). (c) R. Bersohn and H. S. Gutowsky, J. Chem. Phys., 22, 651 (1954).

6. Examples are: (a) E. R. Andrew and R. Bersohn, J. Chem. Phys., 18, 159 (1950). (b) H. S. Gutowsky and G. E. Pake, J. Chem. Phys., 18, 162 (1950). (c) E. O. Stejskal and H. S. Gutowsky, J. Chem. Phys., 28, 388 (1958).

(d) T. B. Cobb and C. S. Johnson, Jr., J. Chem. Phys., 52, 6224 (1970). (e) D. C. Look and I. J. Lowe, J. Chem. Phys., 44, 2995 (1966). (f) D. W. McCall, Acc. Chem. Res., 223 (1971).

7. J. H. Van Vleck, Phys. Rev., 74, 1168 (1948).
8. (a) E. R. Andrew, A. Bradbury and R. G. Eades, Arch. Sci., 11, 223 (1958). (b) E. R. Andrew, and V. T. Wynn, Proc. Roy. Soc., A291, 257 (1966).
9. H. Kessemeier and R. E. Norberg, Phys. Rev., 155, 321 (1967).
10. E. R. Andrew, Progress in NMR Spectroscopy, (Pergamon N.Y., 1971). Vol. VIII.
11. J. S. Waugh, C. H. Wang, L. M. Huber and R. L. Vold, J. Chem. Phys., 48, 662 (1968).
12. J. S. Waugh, L. M. Huber and U. Haeberlen, Phys. Rev. Lett., 20, 180 (1968).
13. (a) U. Haeberlen and J. S. Waugh, Phys. Rev., 175, 453 (1968). (b) U. Haeberlen and J. S. Waugh, Phys. Rev., 185, 420 (1969).
14. P. Mansfield, Progress in NMR Spectroscopy, (Pergamon, N. Y., 1971), Vol. VIII.
15. P. Mansfield, J. Phys. C, 4, 1444 (1971).
16. W -K. Rhim, A. Pines and J. S. Waugh, Phys. Rev. B, 3, 684 (1971).
17. A. Pines, W -K. Rhim and J. S. Waugh, J. Mag. Res., 6, 457 (1972).

18. M. Mehring and J. S. Waugh, Phys. Rev. B., 5, 3459 (1972).

19. C. H. Wang and J. D. Ramshaw, Phys. Rev. (in press).

20. U. Haeberlen, J. D. Ellett, Jr., and J. S. Waugh, J. Chem. Phys., 55, 53 (1971).

21. A. Pines and J. S. Waugh, J. Mag. Res., (in press).

22. (a) R. W. Vaughan, D. D. Elleman, L. M. Stacey, W -K. Rhim and J. W. Lee, Rev. Sci. Instr., (in press).

23. (a) A. Pines, M. G. Gibby and J. S. Waugh, Bull. Am. Phys. Soc., 16, 1403 (1971). (b) A. Pines, M. G. Gibby and J. S. Waugh, J. Chem. Phys., 56, 1776 (1972).

24. P. C. Lauterbur, Phys. Rev. Lett., 1, 343 (1958).

25. A. Pines, W -K. Rhim and J. S. Waugh, J. Chem. Phys., 54, 5439 (1971).

26. (a) T. C. Farrar and E. D. Becker, Pulse and Fourier Transform NMR, (Academic, N. Y., 1971).
(b) J. M. Briggs, L. F. Farnell and E. W. Randall, Chem. Commun., 680 (1971).

27. D. L. McFadden, Ph.D. Thesis, M.I.T. (1972).

28. L. R. Sarles and R. M. Cotts, Phys. Rev., 111, 853 (1958).

29. M. Mehring, A. Pines, W -K. Rhim and J. S. Waugh, J. Chem. Phys., 54, 3239 (1971).

30. A. Carrington and A. D. McLachlan, Introduction to Magnetic Resonance, (Harper and Row, London, 1967), Chapt. 13.

31. S. R. Hartmann and E. L. Hahn, Phys. Rev., 128, 2042 (1962).

32. (a) A. Abragam and W. G. Proctor, Phys. Rev., 109, 1441 (1958). (b) A. G. Redfield, Phys. Rev., 98, 1787 (1955).

33. I. Solomon, Comp. Rend., 248, 92 (1950).

34. E. D. Ostroff and J. S. Waugh, Phys. Rev. Lett., 16, 1097 (1966).

35. F. M. Lurie and C. P. Slichter, Phys. Rev., 133, A1108 (1964).

36. D. A. McArthur, E. L. Hahn and R. Walstedt, Phys. Rev., 188, 609 (1969).

37. I. J. Lowe and R. E. Norberg, Phys. Rev., 107, 46 (1957).

38. R. R. Ernst and W. A. Anderson, Rev. Sci. Instr., 37, 93 (1966).

39. A. G. Anderson and S. R. Hartmann, Phys. Rev., 128, 2023 (1962).

40. J. D. Ellett, Jr., M. G. Gibby, U. Haeberlen, L. M. Huber, M. Mehring, A. Pines, and J. S. Waugh, Advances in Magnetic Resonance, (Academic, N. Y., 1971), Vol. V.

41. A. Pines, Ph.D. Thesis, M.I.T. (1972).

42. M. G. Gibby, Ph.D. Thesis, M.I.T. (1972).

43. Merrimac Research and Development, Inc., West Cadwell, N. J., Custom built.

44. Instruments for Industry, Inc., Farmingdale, N.Y., Model M404P.

45. A. G. Redfield and R. K. Gupta, Advances in Magnetic Resonance, (Academic, N.Y., 1971), Vol. V.

46. A. Pines, unpublished results.

47. C. Kittell and E. Abrahams, Phys. Rev., 90, 238 (1953).

48. (a) N. F. Ramsey, Phys. Rev., 78, 699 (1951). (b) N. Bloembergen and T. J. Rowland, Phys. Rev., 97, 1679 (1955). (c) P. Diehl and C. L. Khetrapal, NMR: Basic Principles and Progress, (Springer, Berlin, 1969), Vol. I. (d) A. D. Buckingham and K. A. McLauchlan, Progress in NMR Spectroscopy, (Pergamon, N.Y., 1967), Vol. II. (e) Reference 5(a) Chap. 6.

49. The terms containing other elements are non-secular in high field (oscillate rapidly) and cause only small second order shifts.

50. N. Bloembergen and T. J. Rowland, Act. Metal., 1, 731 (1953).

51. J. L. Ragle, J. Chem. Phys., 35, 753 (1961).

52. D. L. VanderHart, H. S. Gutowsky and T. C. Farrar, J. Chem. Phys., 50, 1058 (1969).

53. N. Bloembergen and T. J. Rowland, Phys. Rev., 97, 1679 (1955).

54. D. K. Hindermann and W. E. Falconer, J. Chem. Phys., 52, 6198 (1970).

55. M. G. Gibby, A. Pines, W.-K. Rhim and J. S. Waugh, J. Chem. Phys., 56, 991 (1972).

56. M. Mehring, R. G. Griffin and J. S. Waugh, J. Chem. Phys., 55, 746 (1971).

57. This is in line with recent theoretical calculations on ^{13}C shielding using gauge increment orbitals: R. Ditchfield, (private communication).

58. A. Pines, M. G. Gibby and J. S. Waugh, Chem. Phys. Lett., (in press).

59. J. S. Waugh, M. G. Gibby, S. Kaplan, and A. Pines, Colloque Ampère, Turku, Finland, 1972 (to be published). References 58 and 59 report measurements on the following compounds: benzene, hexamethylbenzene, toluene, durene, hexafluorobenzene, acetaldehyde, acetone, acetic acid,thioacetic acid, silver acetate, acetic anhydride, methyl formate, methyl acetate, dimethyl carbonate, dimethyl oxalate, silver trifluoroacetate, trifluroacetic anhydride, dimethyl acetylene, methanol, ethanol, diethyl ether, dimethyl dimethoxy silane, tetramethoxy, silane, dimethyl disulfide, dimethylsulfoxide, octamethyl cyclotetrasiloxane, hexamethyl disiloxane, hexamethyl Dewar benzene, carbon disulfide.

60. A. Pines, R. G. Griffin, S. Kaplan and J. S. Waugh, (to be published).

61. M. G. Gibby, A. Pines and J. S. Waugh, J. Am. Chem. Soc., (in press).

62. M. G. Gibby, A. Pines.,R. G. Griffin and J. S. Waugh, Chem. Phys. Lett, (in press).

63. (a) J. Schaeffer, presented at the Thirteenth Experimental NMR Conference, Asilomar, California, 1972. (b) J. Schaeffer, S. H. Chin and S. I. Weissman, (to be published).

64. H. A. Resing, Molecular Crystals and Liquid Crystals, 9, 101 (1969).

65. P. V. Demarco, D. Doddrell and E. Wenkert, Chem. Comm., 1418 (1969).

66. (a) P. S. Allen and A. Cowking, J. Chem. Phys., 47, 4286 (1967). (b) J. E. Anderson and W. P. Slichter, J. Chem. Phys., 44, 1797 (1966).(c) H. W. Bernard, J. E. Tanner and J. G. Aston, J. Chem. Phys., 50, 5016 (1969).

67. (a) E. R. Andrew and R. G. Eades, Proc. Roy. Soc., A218, 537 (1953). (b) J. E. Anderson, J. Chem. Phys., 43, 3575 (1965). (cO R. van Steenwinkel, Z. Nat., 24a, 1526 (1969). (d) U. Haeberlen and G. Maier, Z. Nat., 22a, 1236 (1967). (e) U. Haeberlen, Z. Nat., 25a, 1459 (1970).

68. A. Pines, S. Pausak and J. S. Waugh, (to be published).

69. J. D. Ellett, Jr., U. Haeberlen and J. S. Waugh, J. Am. Chem. Soc., 92, 411 (1970).

70. C. S. Johnson, Jr., Advances in Magnetic Resonance, (Academic, N.Y., 1965), Vol. I.

71. R. G. Griffin, A. Pines, and J. S. Waugh, (to be published).

72. R. L. Vold, J. S. Waugh, M. P. Klein and D. E. Phelps, J. Chem. Phys., 48, 3831 (1968).

73. A. Allerhand, D. Doddrell and R. Komoroski, J. Chem. Phys., 55, 189 (1971).

74. R. T. Schumacher, Phys. Rev., 112, 837 (1958).

75. C. S. Yannoni and H. E. Bleich, J. Chem. Phys., 55, 5406 (1971).

76. M. G. Gibby, A. Pines and J. S. Waugh, Chem. Phys. Lett., (in press).

77. K. F. Kuhlman, D. M. Grant and R. K. Harris, J. Chem. Phys., 52, 3439 (1970).

78. K. H. Hausser and D. Stehlik, (private communication).

79. M. Goldman and A. Landesman, Phys. Rev., 132, 610 (1963). M. Schwab and E. L. Hahn, J. Chem. Phys., 52, 3152 (1970). Y. Hsieh, J. C. Koo and E. L. Hahn, Chem. Phys. Lett., 13, 563 (1972).

80. Reference 4(c), chapter 7.

81. Reference 4(c), chapter 6.

82. P. Mansfield, K. H. B. Richards and D. Ware, Phys. Rev. B, 1, 2048 (1970).

83. (a) E. P. Jones and S. R. Hartmann, Phys. Rev. Lett., 22, 867 (1969). (b) E. P. Jones and S. R. Hartmann, Phys. Rev. B., 6, 757 (1972).

84. An excellent discussion with leading references is given in reference 4(c), chapters 2 and 3.

85. C. P. Slichter and W. C. Holton, Phys. Rev., 122, 1701 (1961).

86. J. Jeener and P. Broekaert, Phys. Rev., 157, 232 (1967).

87. H. E. Bleich and A. G. Redfield, J. Chem. Phys., 55, 5405 (1971).

88. P. Mansfield and P. K. Grannell, J. Phys. C., 4, L197 (1971).

89. I. Solomon and J. Ezratty, Phys. Rev., 127, 78 (1962).

CHAPTER III

HARDWARE

I. PULSE PROGRAMMER OPERATION

A. INTRODUCTION

The complexity of pulse experiments in our laboratory has increased appreciably in recent years. Previously, the implementation of new pulse experiments invariably necessitated the time consuming design and construction of specific logic circuits. To overcome this obstacle we therefore set out to produce a more versatile and generally powerful pulse programmer, and the end result of our endeavor is described in the following sections. The device contains an independent memory unit of its own which carries all the information necessary for the execution of an arbitrary pulse sequence, and is preloaded and otherwise serviced by an on-line computer. The realization of new pulse experiments is thus essentially reduced to a computer software problem--a considerable advance over previous methods--and recent experiments have already utilized this facility with promising efficiency. A schematic diagram of the programmer is shown in Fig. 1. Components include mostly homemade circuits and currently available TTL and DTL logic.

Section B describes the basic operation including the memory, cycling, and addressing. Sections C-G describe the different units involved in the production of a pulse sequence, and Section H elaborates on the points of access and function of the

Figure 1

Functional schematic diagram of computer-controlled pulse programmer. 12 refers to the PDP 12 computer.

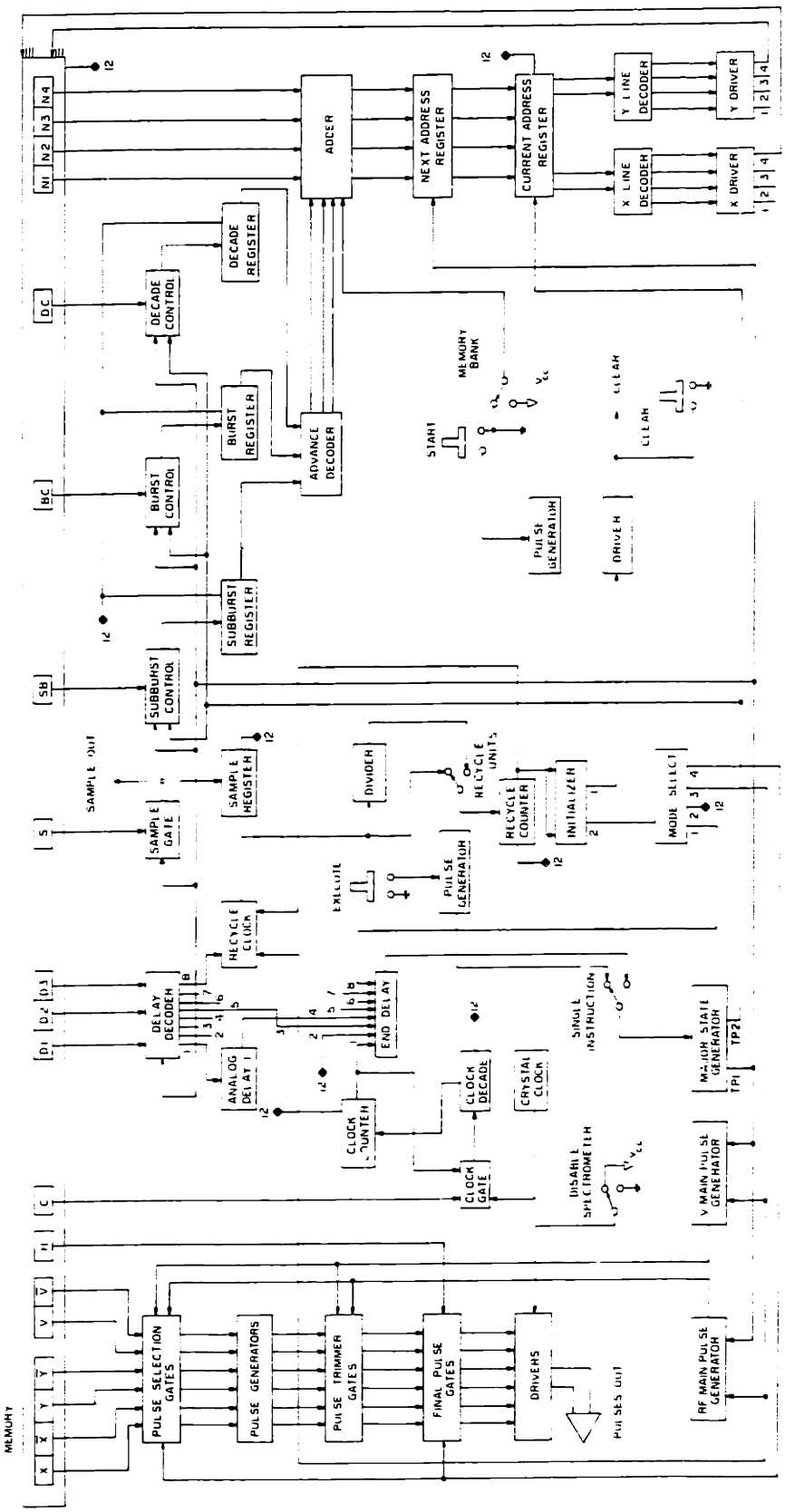
MEMORY
X
X̄
Y
Ȳ
V
V̄
H
C
D1
D2
D3
DC
BC
SB
S
N1
N2
N3
N4
12
PULSE SELECTION GATES
PULSE GENERATORS
PULSE TRIMMER GATES
FINAL PULSE GATES
DRIVERS
PULSES OUT
RF MAIN PULSE GENERATOR
MAIN STATE GENERATOR
TP1
TP2
V MAIN PULSE GENERATOR
DISABLE SPECTROMETER
SINGLE INSTRUCTION
CRYSTAL CLOCK
CLOCK DECADE
CLOCK GATE
CLOCK COUNTER
ANALOG DELAY
DELAY DECODER
END DELAY
RECYCLE CLOCK
EXECUTE
SAMPLE OUT
SAMPLE GATE
SAMPLE REGISTER
DIVIDER
PULSE GENERATION
RECYCLE UNITS
RECYCLE COUNTER
INITIALIZER
MODE SELECT
SUBBURST CONTROL
SUBBURST REGISTER
BURST CONTROL
BURST REGISTER
DECADE CONTROL
DECADE REGISTER
ADDER
ADVANCE DECODER
NEXT ADDRESS REGISTER
CURRENT ADDRESS REGISTER
X LINE DECODER
Y LINE DECODER
X DRIVER
Y DRIVER
START
MEMORY BANK
CLEAR
DRIVER
PULSE GENERATION

computer in servicing the instrument. Section I gives a sample pulse program.

B. BASIC OPERATION

The heart of the programmer is an extendable 384 bit flip-flop memory organized as sixteen words of 24 bits each. Each word is assigned an address in the memory and contains an instruction to be executed by the programmer. The assignment of bits within each word is depicted in the schematic diagram. Here we give a brief description of the function of these bits, the basic cycling of the instrument and addressing of the memory. More specific details on the different units involved are presented in later sections.

The cycling of the instrument is achieved very simply. Each instruction contains several basic pieces of information: (i) the function to be performed (pulse output, sampling, counting, etc.), (ii) address of the next instruction, and (iii) the delay until execution of the next instruction. The main operating unit is the major state generator. This emits 2 pulses called TP1 and TP2 about 0.1 μsec apart. TP1 triggers the execution of the current instruction and the specified delay and TP2 then selects the next word specified by the next address (NA) bits in the memory. The major state generator is then retriggered at the end of the delay through the end-delay gate and the next instruction is executed. In this way cycling is

maintained and we see that the cycle time is redetermined at each instruction and is normally not clock-controlled as in previous devices.

Summarizing, the basic chain of events is: (i) end of previous delay triggers major state generator, (ii) TP1 triggers execution of instruction and next delay, and (iii) TP2 selects next instruction. The function of the memory bits is as follows:

(i) N1 N2 N3 N4--Next address. There are sixteen words coded in binary with addresses 0000-1111. The addressing of a selected word is done in "x-y" fashion. One of four "x" lines and one of four "y" lines specify which one of the sixteen words is to be accessed. This memory location may be written into by the computer in loading or read by the programmer during operation. To understand the addressing more explicitly let us assume that the programmer is just executing the instruction in word 0010 and the NA bits N1-N4 of this word contain 0011 as the next address. (This next address may or may not be modified at the adder as explained later in this section.) In any case, TP1 transfers the number 0011 or the modified address to the NA register whence TP2, after execution of instruction 0010, then transfers it to the current address register where it becomes the new current address. The decoders use the 4 bits from the current address register as two sets of two, each of which is decoded to 1 of 4 lines, the x and y sets mentioned above. These are used, by driving them with current-sinking transistors, to

select the corresponding word 0011 (or modification) in the memory.

(ii) $X,\overline{X},Y,\overline{Y},V,\overline{V}$ and H. These bits specify whether or not a pulse is to be produced in any of the six output channels. For every bit that is set to logic 1 a pulse will be produced in the corresponding output channel. $X,\overline{X},Y,\overline{Y}$ designate the 4 channels used to gate the 4-phase box described in Section C. $\overline{VV}$ are auxiliary outputs which may be used for producing video pulses, double resonance pulses, or for general triggering purposes.

Bit H, the hold bit, extends the capabilities of the pulse output. If H is set to 0 we obtain normal pulsed output. If H is set to 1 the specified output channels are held open for the duration of the present delay, i.e., until the execution of the next instruction where they may be closed or, of course, held open. All this is discussed further in Section F.

(iii) C, D1, D2, D3. These bits specify the delay. D1 D2 D3 specify one of 8 available codes for analog delays (Section D) and a recycle delay (Section D) and C specifies a clocked delay using a crystal clock with computer-controlled timing (Section D).

(iv) S-Sample bit. When set to 1 the sample-and-hold is triggered and the magnetization sampled. (See Section G).

(v) SB, BC, DC. Counter bits: These control three

counters called the subburst, burst, and decade counters. When any of these bits is set to 1 the corresponding counter is incremented until overflow occurs at some specified count (either set manually or under computer control) and the advance decoder then modifies the next address by adding to it some number dependent on which counters have overflowed. This allows us to accomplish skipping and branching in the pulse program after a specific preset number of instructions or groups of instructions. A more complete discussion of this facility appears in Section E.

It is often useful to step through a pulse program one instruction at a time in order to examine the contents of the programmer memory or to check the program's operation. This can be done using the single instruction switch. In normal operation this is set to allow triggering of the major state generator through the end-delay gate. In single-step operation the end of a delay will not trigger the next instruction. Instead each instruction is triggered manually through the execute switch which produces a pulse from the corresponding pulse generator. All pushbutton switches of this sort are equipped with circuits to prevent multiple triggering due to contact bounce.

A little thought, together with the example at the end, will convince the reader that most feasible pulse sequences require very few of the sixteen available memory locations. Thus another switch, the memory bank switch, enables us to store and use two pulse programs each of less than eight words. The switch allows

the programmer to operate in either the lower memory bank, locations 0-7, or in the upper bank, locations 8-15. For longer pulse sequences the whole memory may of course be used as one unit.

C. RECYCLING AND INITIALIZATION

During an experiment one usually wishes to repeat the pulse sequence periodically; for example, in order to make adjustments or perform some averaging. The experiment is thus composed of a major cycle consisting of what we call a "burst" during which the pulses are emitted and the signal observed, and a "recycle delay" during which the spin system returns to full equilibrium before initiation of the next burst. During the recycle delay the data may also be manipulated and the programmer serviced if necessary.

The recycle delay is one of the 8 possible delays selected with each instruction. When its code is encountered by TP1, a 1 KHz astable multivibrator is activated. The output of this is fed into two channels, in one of which the frequency is divided by 1000. One or the other channel, selected by a manual switch is fed to a 12 bit ripple counter. The overflow bit of the counter is selected on the front panel giving us recycle times of $1\text{-}2^{11}$, in powers of 2, with msec or sec units. The end of the recycle delay does not trigger the execution of the next instruction as with other delays. Instead it is sensed by the initializer (consisting of three monostables) which prepares for

initialization and triggering of the next burst. First, a clear pulse is emitted (output 1 of initializer), which after current amplification by a driver clears all the registers in the programmer. This includes the various counter registers, the current address register, the clock counter, and all skip and interrupt flags connected to the computer. Clearing may also be accomplished manually using the clear pushbutton. About 1 μsec later a second pulse "BG" (output 2) is sent to the mode select switch from which it may be directed to one of several places depending on the mode selected. The available modes and subsequent operation are:

(i) Normal Operation. In this mode the retriggering is automatic. The pulse BG (output 1 of mode select) enters the end delay gate which then triggers the first instruction through the major state generator.

(ii) Computer Control. Here the pulse BG (output 2) is channeled to the computer and continuation is thus computer controlled, the triggering of a new burst being initiated through input 2 of the end delay. This is discussed further in Section H.

(iii) Bloch Decay. This mode is used if one wishes at any time to look at a single pulse, or a Bloch decay of the sample, independent of the contents of the programmer memory. There are six positions in this mode, X, $\overline{X}$, ..., $\overline{V}$, and for the one selected a single corresponding output pulse is produced by

hardwiring of the appropriate bit and disabling of the memory (symbolized by output 4). BG (output 3) is channeled to trigger the main pulse generators (see Section F) and retrigger the recycle delay. Thus recycling here is automatic and a single pulse is repeated with a recycle delay period.

(iv) Off. The pulse BG is unused, there is no retriggering of the burst, and programmer operation ceases.

The initial cycling of the computer is activated by the start pushbutton switch, after loading a new pulse program or after cessation of operation for any number of reasons. This activates the pulse generator and simulates the end of a recycle delay, thus performing the necessary initialization and starting operation in the selected mode.

D. DELAYS

The 8 available delay codes are used as follows:

(i) Four Variable Analog Delays. Each analog delay consists of two identical monostable multivibrators (type 9601) with RC time constants controllable manually. The first monostable is triggered by a pulse from the delay decoder when its code is encountered by TP1. The end of the pulse triggers the second monostable and the end of the pulse from this triggers the major state generator through the end-delay gate and the next instruction is then executed. The use of two cascaded monostables is an artifice for insuring that the same delay can be immediately

retriggered if this is called for by the next instruction.

These delays cover different ranges. Two produce delays varying from 0.2 to 8 μsec to 1 msec. These may also be multiplied by one of the counters available (Section E) so that any practically useful delay is accessible.

(ii) One Fixed Analog Delay. This is the same as above except not controllable on the front panel. Normally it is set at about 1 μsec and is useful when one wishes to generate an instruction immediately on termination of a 90^{o} pulse without using one of the variable delays.

(iii) Recycle Delay. This was described in detail in Section C.

(iv) Two are unused. One is available for extension and one remains open to be used when the crystal clock is requested and we want no extra delay triggered simultaneously.

In addition to these delays we have available a crystal clock. When bit C is set to 1 a gate is opened and a 1 MHz crystal clock counts into a series of 6 decade counters providing us with 7 selectable channels with counting units of 1 μsec to 1 sec. The desired channel is selected manually or by the computer and the clock register then fills at the corresponding frequency. The latter is a 12 bit ripple counter which can be preloaded and read by the computer. This opens up two modes of operation for the clock: (i) To produce a clocked delay the

clock counter is preloaded by the computer with the complement of the desired delay. This is useful for experiments where computer-controlled timing of pulses is necessary; for example, in T_1 measurements. (ii) In order to measure the length of a burst the clock counter is preloaded with 0 by the computer. The clock gate is then opened at the beginning of the burst and is automatically shut when a recycle delay is requested. The real time of the burst may then be read by the computer.

E. COUNTERS

Clearly, for most conceivable pulse experiments it is necessary to be able to count--we may need to produce a certain number of pulses or cycles of pulses, or to sample a fixed number of times, and so on. Three counters in the programmer provide this facility; called the subburst counter, burst counter, and decade counter they count respectively from 1 to 2^7 in powers of 2, from 2^5 to 2^{11} in powers of 2, and from 1 to 1000 continuously, and all have either manual or computer-controlled selection.

When a counter memory bit is encountered by TP1 the corresponding counter control looks at the counter register to see if it has overflowed at the preselected bit. If not, the register will then be incremented by TP2. If it has overflowed, i.e., the count is over, the register will be cleared by TP2 in preparation for recounting. When overflow has occurred at some

instruction, the next instruction is modified and branching of the pulse program can occur. Modification of the address is simple--the next address (see Section B) enters a 4 bit binary adder as one addend. The other addend is a decoded 4 bit binary number with 3 bits from a decoder and 1 from the memory bank switch (Section B). The decoder will present a number different from 0 in the selected memory bank only if an overflow has occurred in one or more of the counter registers. The number there presented will add to the next address 1 for a subburst overflow, 2 for a burst overflow, and 4 for a decade overflow, thus permitting separate branching for each of these counters inside the selected memory bank. Obviously, the counters may also be used as multipliers, specifically to create long pulses or delays and provide a convenient extension of their ranges.

The sample pulse program in Section I demonstrates some uses of these counters.

F. PULSE OUTPUT

A major feature of most pulse experiments is the necessity for very sensitive pulse width adjustments. There are six pulse output channels in the programmer and these are divided into 2 groups labeled X $\overline{X}$ Y $\overline{Y}$ and V $\overline{V}$. The first four provide gating for the 4 phase box described later. The other two provide separate gating, for example, for a second frequency in double resonance experiments or video current pulses in tilted coil

experiments. The pulse output is produced quite simply. TP1 triggers two pulse generators--the rf and V main pulse generators. These are monostable multivibrators with RC time constants selectable manually, from 0 to 4 μsec. They are fed respectively into 4 and 2 channels which are then gated by 6 pulse selection gates. We now differentiate again between the modes of operation described in Section C.

(i) Normal Operation or Computer Control. The gates are controlled by the 6 appropriate bits in the memory.

(ii) Bloch Decay. The gates are controlled by bits set from the mode select switch and the memory is disabled totally.

For every bit that is 1 the corresponding gate is open and the main pulse passes through to the pulse generators and triggers a pulse from one of 6 monostables with RC constants again determined manually and with sensitive continuous selection of 0-4 μsec. The output from the pulse generators is thus a pulse for each pulse bit set to 1 either by the memory or the mode select switch, with each pulse separately controllable. Now we introduce the possibility for an overall pulse width control--this is done separately for the two groups of pulses at the pulse trimmer gates as described for pulse programmer **A**.†

The last manipulation that the pulses undergo occurs at the final pulse gates. These provide another useful facility described in Section B, namely, the possibility of holding open a

† J. D. Ellett, Jr., Ph.D. Thesis, M.I.T. (1971)

pulse gate until the next instruction occurs. This is necessary when the desired output is not short pulses but long ones or continuous rf bursts with or without phase switching as employed in some recent experiments. This is determined by bit H in the memory. If set to 0, the trimmed pulses pass straight through the final gates and form the final output. If set to 1, the selected pulse channels are not closed at the end of the trimmed pulse and are kept open until the end of the current delay or more if necessary (by keeping H and the pulse bit set to 1). Clearly this also extends the range of accessible pulse widths by having them set with the delays. If the mode of operation is Bloch decay then the hold function is suspended and only pulsed output is possible.

A switch which opens the final driver gates (disable spectrometer switch) enables us to disconnect the logic from the rf circuitry, thus avoiding burning out the transmitter with excessive duty cycles when new pulse sequences are being tested.

G. SAMPLING

At any instruction where we wish to sample the magnetization the S bit is set to 1, opening the sample gate. TP1 then triggers the integrate and hold described elsewhere and the magnetization is sampled a manually variable time later. In addition to this a sample register is incremented. The output of this 10 bit ripple counter is connected to the computer direct

address lines and one higher order bit is provided from the sample and hold unit. The latter bit selects one of two buffers in computer core for the deposit of real and imaginary digitized data from the dual phase detector. The sample register increments the address within each buffer thus providing sequential storage of digitized data in computer core whence it may be displayed and otherwise manipulated by the computer.

H. COMPUTER ACCESS

The great versatility in programming experiments and in signal processing is provided by the computer and this has several points of access to the programmer, all provided by standard interface techniques. The more important of these access points are symbolized in the schematic diagram by a "12" (for PDP 12). The computer has two main functions, namely, servicing the pulse programmer, and storing and processing data. Here we describe the more important aspects of these two functions.

(i) Servicing the Pulse Programmer. This includes loading in pulse programs, setting the counter registers for preset counts, selecting the clock decade, preloading and reading the clock counter, triggering and controlling the operation of some auxiliary external devices, and triggering the bursts when in computer control mode. All of these are carried out either when the programmer is at a standstill or just at the end of a recycle delay during operation.

Loading is carried out simply: Assuming the program is in computer core, either from the teletype or from tape, the computer steps through the programmer memory by incrementing the current address register and reads in the pulse program through the I/O bus. Programs may be read in and changed at any time during operation--this is entirely determined by the available computer software. Our library of pulse programs currently contains about 150 entries.

Servicing is initiated when the computer is interrupted by the BG pulse at the end of a recycle delay (Section C). The service functions mentioned above are then performed and the computer then triggers a new burst through input 2 of the end-delay gate.

(ii) During the burst data are stored in computer core. The end of the burst interrupts the computer through the recycle delay request. During the recycle delay, processing of the data occurs. This may include, for example, displaying and plotting, storing on tape, averaging, fourier transformation, counter and clock time readout, etc. The end of the recycle delay is sensed by the computer which then enters a service routine as in (i). If signal processing has not been completed the computer may choose, under software control, to lengthen the recycle delay. All in all, operation is extremely flexible and a variety of service and signal processing routines have been used for different experiments. The last section shows an example of one such simple experiment.

I. EXAMPLE

Pulse programs are written in a format closely related to the organization of the pulse programmer memory described previously. Table I shows

TABLE I

CA	X	$\overline{X}$	Y	$\overline{Y}$	V	$\overline{V}$	H	C	D1	D2	D3	S	SB	B	DC	N1	N2	N3	N4
0000	1	0	0	0	0	0	0	0	0	0	1	1	0	0	0	0	1	0	0
0001	1	0	0	0	0	0	0	0	0	0	1	0	0	0	0	0	1	0	0
0010	1	0	0	0	0	0	0	0	0	0	1	1	0	0	0	0	1	0	0
0011	0	0	0	0	0	0	0	0	1	1	1	0	0	0	0	0	0	0	0
0100	0	1	0	0	0	0	0	0	0	1	0	0	0	0	0	0	1	0	1
0101	0	0	1	0	0	0	0	0	0	0	1	0	0	0	0	0	1	1	0
0110	0	0	0	1	0	0	0	0	0	1	0	0	1	1	0	0	0	0	1

the pulse program used for the present four-pulse experiment. N1-DC represent the instruction bits described in detail in Section A and CA depitcs the location of this instruction in the pulse programmer's memory. The program is entered in octal form into the computer (see Fig. 2) whence it may be stored on magnetic tape for future use or loaded into the pulse programmer. Operation can then begin under control of the computer. It may easily be verified that this pulse program will produce the following pulse sequence:

Figure 2

PPMOD computer program display for making new pulse programs. These are typed in octal format as explained in the text and may then be stored on tape or read into the pulse programmer. In the latter case they may be retrieved by an updated version of GOLEM.

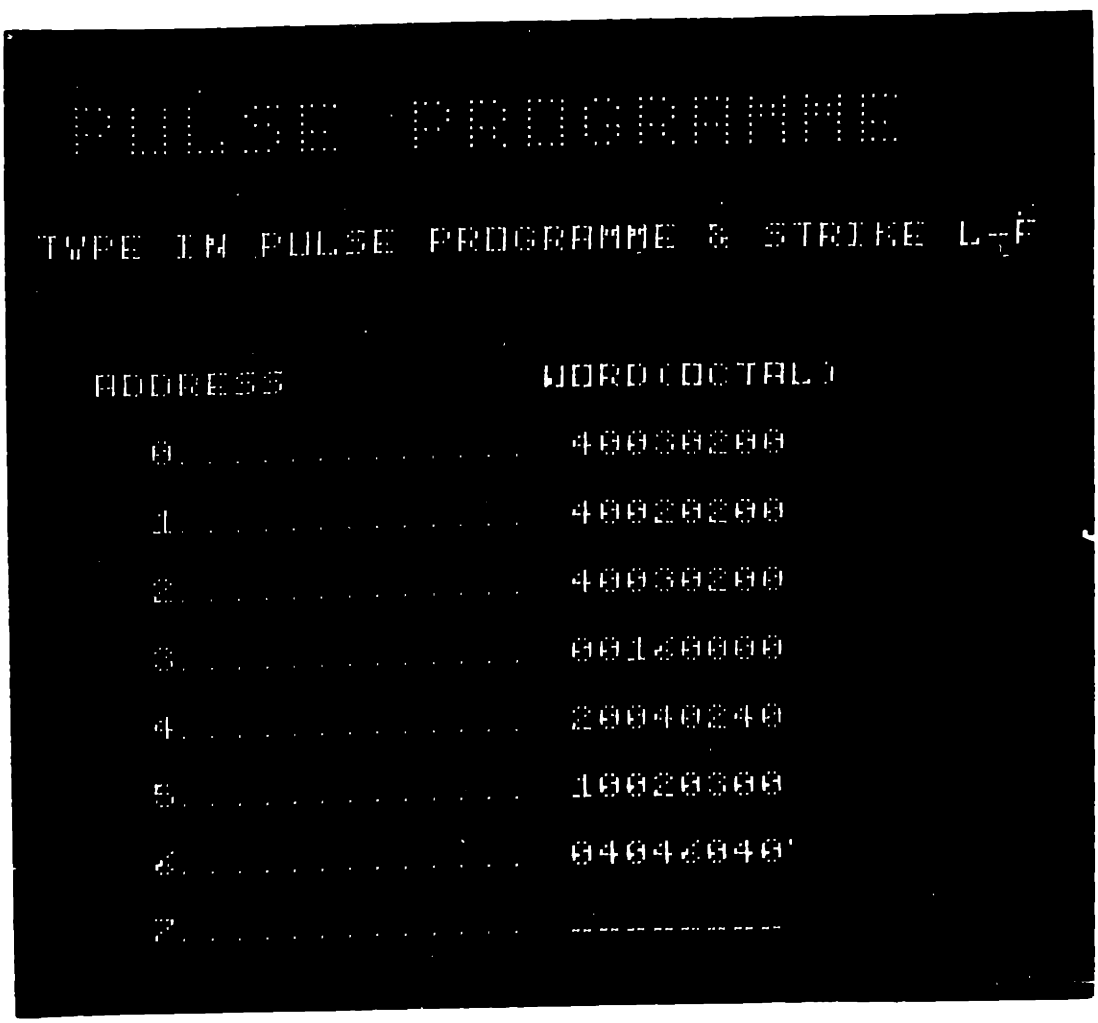
PULSE PROGRAMME
TYPE IN PULSE PROGRAMME & STROKE L-F
ADDRESS
WORD(OCTAL)
0 4000002000
1 4000002000
2 4000002000
3 0001000000
4 2000402400
5 1000200000
6 0400400400
7

$$(x,\tau_1, -x,\tau_2,y,\tau_1, -y,\tau_2)_n, \text{ RD}$$

where $\underline{x}$ denotes an $\underline{x}$ pulse, etc. and $\underline{\tau}_1$ and $\underline{\tau}_2$ are the analog delays called for by the delay codes (001) and (010). RD denotes a recycle delay called for by code (111). Sampling is initiated through the S bit between the $\underline{x}$ and $-\underline{x}$ pulses, and $\underline{n}$, the number of four-pulse cycles, is determined by the burst counter. The sampling frequency is decided by the subburst counter; when the latter is set to $\underline{m}$, the magnetization is sampled every $\underline{m}$ cycles. At the end of the recycle delay the pulse train is automatically reinitialized at address (0000) by the computer. During this delay, data sampled in the pulse train is displayed and Chapter IV demonstrateshow it may be accumulated and averaged, transformed, plotted, or stored on tape.

II. HARDWARE AND SCHEMATICS

A. PULSE PROGRAMMER CARD LAYOUT

The functional blocks described in the previous section are handwired on Digital Equipment Corporation (DEC) cards and housed in H803 blocks mounted in an H925 module drawer. The accessories are all described in DEC's logic handbook (1969 version was used). Table II shows the card layout in the available slots. Detailed schematics of the cards are shown in Section III and detailed wiring lists for block pin connections in Section IV.E.

B. SELECTED MNEMONICS

MP - master pulse

MPA - master pulse allowed

XMP - MPA $\oplus$ specific pulse (X, $\overline{X}$ ...)

CCL - crystal clock

AD - analog delay

S - sample

H - hold

ESB - enable sub-burst counter

SSB - skip on sub-burst overflow

EBC - enable burst counter

SBL - skip on burst overflow

CA - current address register

LDM - load memory

ED - end of delay

MS - major state

BD - block decay

NO - normal operation

CC - computer control

ND - no delay

PC - pulse codes

EPC - enable pulse codes

PS - pulse select

ESP - enable spectrometer

TABLE II

Pulse Programmer Card Layout

Cards such as M624, M103, M111, K681, M908 and M903 refer to standard DEC modules. The card schematics appear in Section III and are referenced by the slot numbers in this table.

	A	B	C	D
1	PDP12 M9032 N15	PDP12 M903 1 N14	PDP12 M903 5 N18	BIOMATION
2				M624-6
3	PDP12 M903 6 N13	PDP12 M903 3 N16	PDP12 M903 4 N17	M624 3
4				M624 1
5	ADC 1	ADC 2	SAMPLE	M624 2
6		GATE	ADC DATA	M624 4
7	ADC 3	ADC 4	P.I.	M624 5
8			V P GATES	M111 1
9	SKIP	B C		M103 6
10			Y P GATES	M103 5
11	SBC ——	SBC		M103 4
12			X P GATES	M103 3
13	ADDRESS ADV. ——	ADDRESS ADV.		M103 1
14	MO 19,20		DRIVERS	M103 2
15	MO 17,18	MO 1,2,3,4	DRIVERS	M111 2
16	MO 15,16	MO 5,6	COMPUTER Light	M103-7
17	MO 13,14	MO 7,8	DELAY DECODE	M103-8
18	MO 11,12	MO 9,10		BIOMATION
19	CLOCK DECADE ——	CLOCK DECADE	CLOCK COUNTER	CRYSTAL CLOCK
20			V M P GEN	
21	MODE ——	MODE	Y M P GEN	K 681 6
22			X M P GEN	K681 5

	A	B	C	D
23	MAJOR STATE GEN ——	MAJOR STATE GEN	END DELAY	K681 4
24				K681 3
25	RECYCLE DELAY ——	RECYCLE DELAY	MPA GEN	K681 2
26				K681 1
27	M908 4	M908 7	M908 1	M908 8
28	M908 2	M908 3	M908 5	M908 6

FRONT

SBC	- sub-burst counter	PI	- program interrupt
BC	- burst counter	WE	- write enable
RD	- recycle delay	SC	- sampling counter
SIPB	- single instruction pushbutton	MS	- major state
PB	- pushbutton	CCBG	- computer controlled begin
CL	- clear	AC	- accumulator
BG	- begin	INL	- initialize
NA	- next address register	SI	- single instruction
PLT	- plot	NC	- not connected
GND	- ground	MEM	- memory
EX	- execute	ERD	- end recycle delay
BCO	- burst counter overflow	SBO	- sub-burst overflow
EADα	- end analog delay α	VDMP	- video main pulse
RFMP	- RF main pulse	MOα	- memory cell α

C. DEVICE SELECTOR ASSIGNMENTS

M1031 (30IOP - load memory)

30IOP1 - WE1 to pulse programmer memory

30IOP2 - WE2 to pulse programmer memory

$\overline{30IOP4}$ - address advance clock pulse

M103 2 (30IOP - initialize)

$\overline{31IOP1}$ - SBC selection strobe

BC selection strobe

clock decade selection strobe

$\overline{31IOP2}$ - clear SC register

$\overline{31IOP4}$ - $\overline{CCBG}$ (computer controlled begin) to MS generator

M103 3 (32IOP - clock and SC)

$\overline{32IOP1}$ - strobe SC into AC

$\overline{32IOP2}$ - strobe final time from clock register to AC

$\overline{32IOP4}$ - strobe initial time into clock register from AC

M103 4 (33IOP - plotter and RD)

$\overline{33IOP1}$ - enable plotter (flip-flop → 0

$\overline{33IOP2}$ - check RD PI-flag

$\overline{33IOP4}$ - disable plotter (FF → 1)

M103 5 (34IOP - check flags)

$\overline{34IOP1}$ - check LDM PI flag

$\overline{34IOP2}$ - check INL PI flag

$\overline{34IOP4}$ - check PLT PI flag

M103 6 (35IOP - clear flags)

$\overline{35IOP1}$ - clear LDM PI flag

$\overline{35IOP2}$ - clear PLT PI flag

$\overline{35IOP4}$ - clear INL PI flag

D. XY PLOTTER INTERFACE

PLOTTER SIDE - Hewlett Packard 7004A X-Y Recorder with 17173A Null Detector

1. Null Detector

Pin No.	Signal	Connection*
1	- polarity seek pulse	NC
2	+ polarity seek pulse	C7U1 (EPLT) on pulse programmer
3	high current ground	blue and gray
4	complete plot pulse	pulse programmer
5-9	———	NC

2. Plotter

Pin No.	Signal	Connection
1	+Y	NC
2	-Y	white
6	ground	black
14	+X	yellow
15	-X	violet

* colors correspond to connections on following page.

PDP 12 SIDE - via Blue 26-B96 Female Connector on Front Panel

Pin No.	Signal	Wire Color
1	Channel Select	yellow
2	NC	
3	Shield chassis ground	
4	Intensify pulse	green--to C7D2 (PI)on pulse programmer
5	NC	
6	Shield chassis ground	
7	X high Q ground	blue
8	X deflection	violet
9	Shield chassis ground	
10	Y high Q ground	gray
11	Y deflection	white
12	Shield chassis ground	
13-18	NC	
19	503 intensify	
20-24	NC	

E. CRYSTAL CLOCK DECADE CODE

000	µsec	100	10 µsec
001	100 msec	101	sec
010	100 µsec	110	not used
011	10 msec	111	msec

III. SCHEMATIC DIAGRAMS

A. WIRING CONVENTION

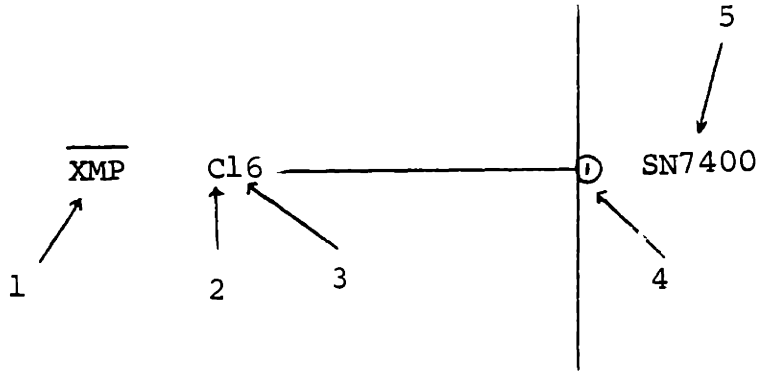

1. signal mnemonic
2. C indicates pin number on card according to my convention. See the correspondence with DEC convention on next page.
3. pin number
4. pin number connected on integrated circuit
5. device number.

B. CARD PIN NUMBER INTERCONVERSION

CONVENTION		CONVENTION	
Mine	DEC	Mine	DEC
1	A2	19	V1
2	B2	20	U1
3	C2	21	T1
4	D2	22	S1
5	E2	23	R1

CONVENTION		CONVENTION	
Mine	DEC	Mine	DEC
6	F2	24	P1
7	H2	25	N1
8	J2	26	M1
9	K2	27	L1
10	L2	28	K1
11	M2	29	J1
12	N2	30	H1
13	P2	31	F1
14	R2	32	E1
15	S2	33	D1
16	T2	34	C1
17	U2	35	B1
18	V2	36	A1

Figures 3-36 show the schematics for the pulse programmer cards. The detailed pin wiring can be found in the next section (IV).

Figure 3-Figure 36

Schematic diagrams of the main computer interface and pulse programmer cards. The signal names are for cross-referencing. Detailed pin connections are given in the wiring lists (next section). Schematics of the standard DEC modules (e.g. M103) are not presented--they may be found in DEC's logic handbook, and connections are in the wiring lists. The names for the cards are related to their function as described in the operation section. A convenient index for locating them is in the layout--Section II.A of this chapter.

Figure 3: Memory Cells A15-18
B16-18

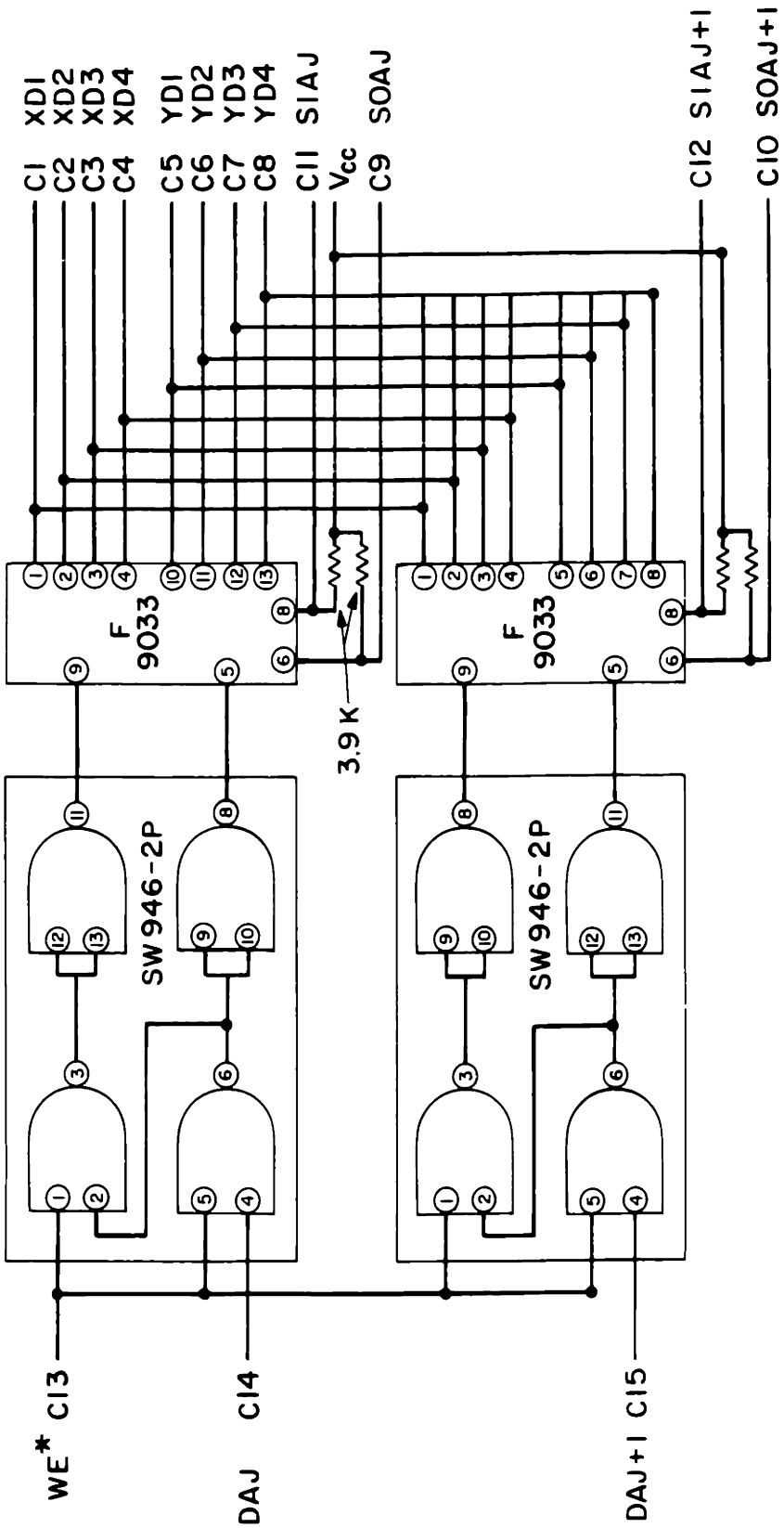

*WE1 OR WE2 IN WIRING LIST. SEE LOADING INSTRUCTIONS.

Figure 4: Memory Address B15

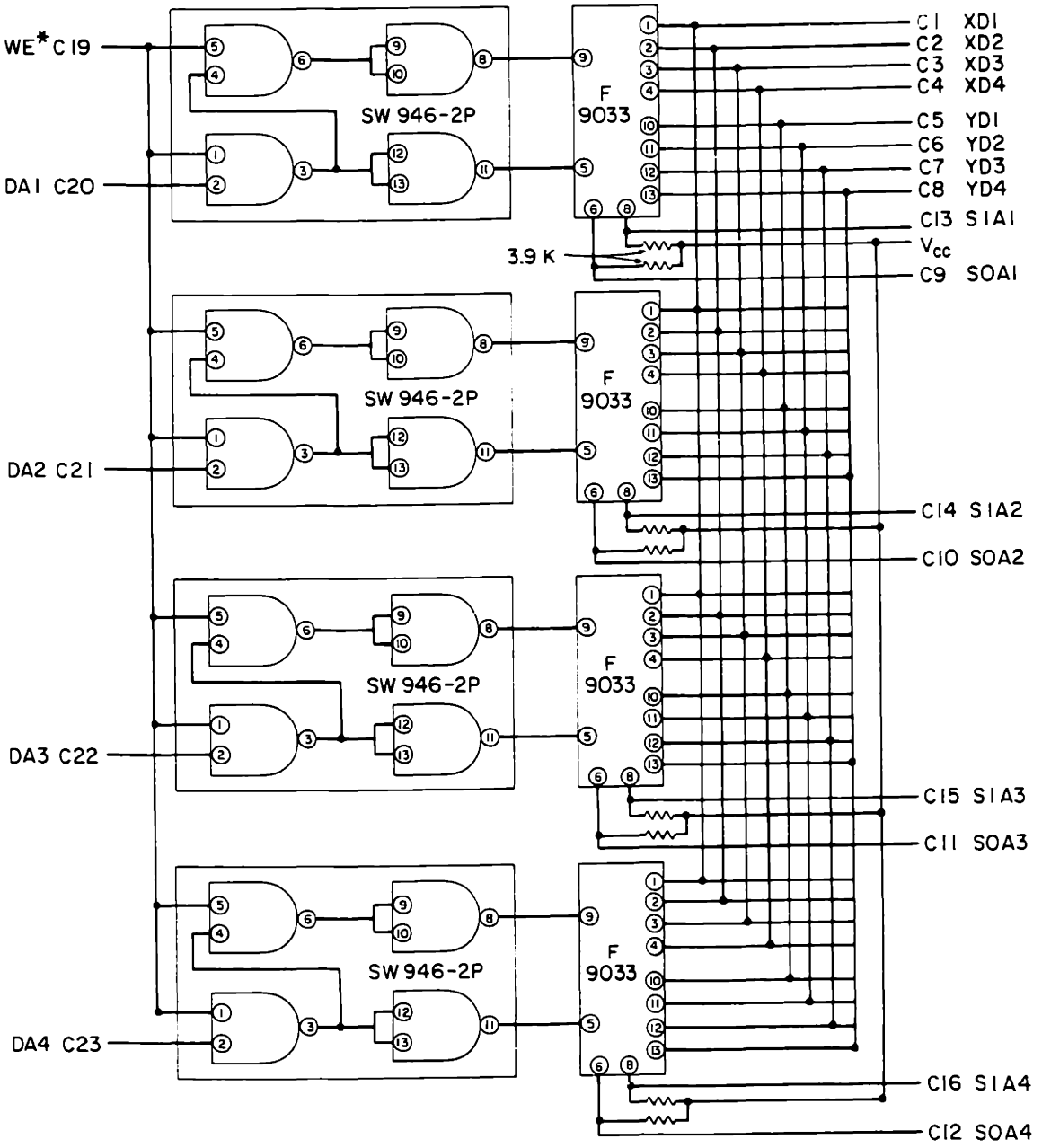

* WE1 OR WE2 IN WIRING LIST - SEE LOADING INSTRUCTIONS

Figure 5: Address Advance AB13

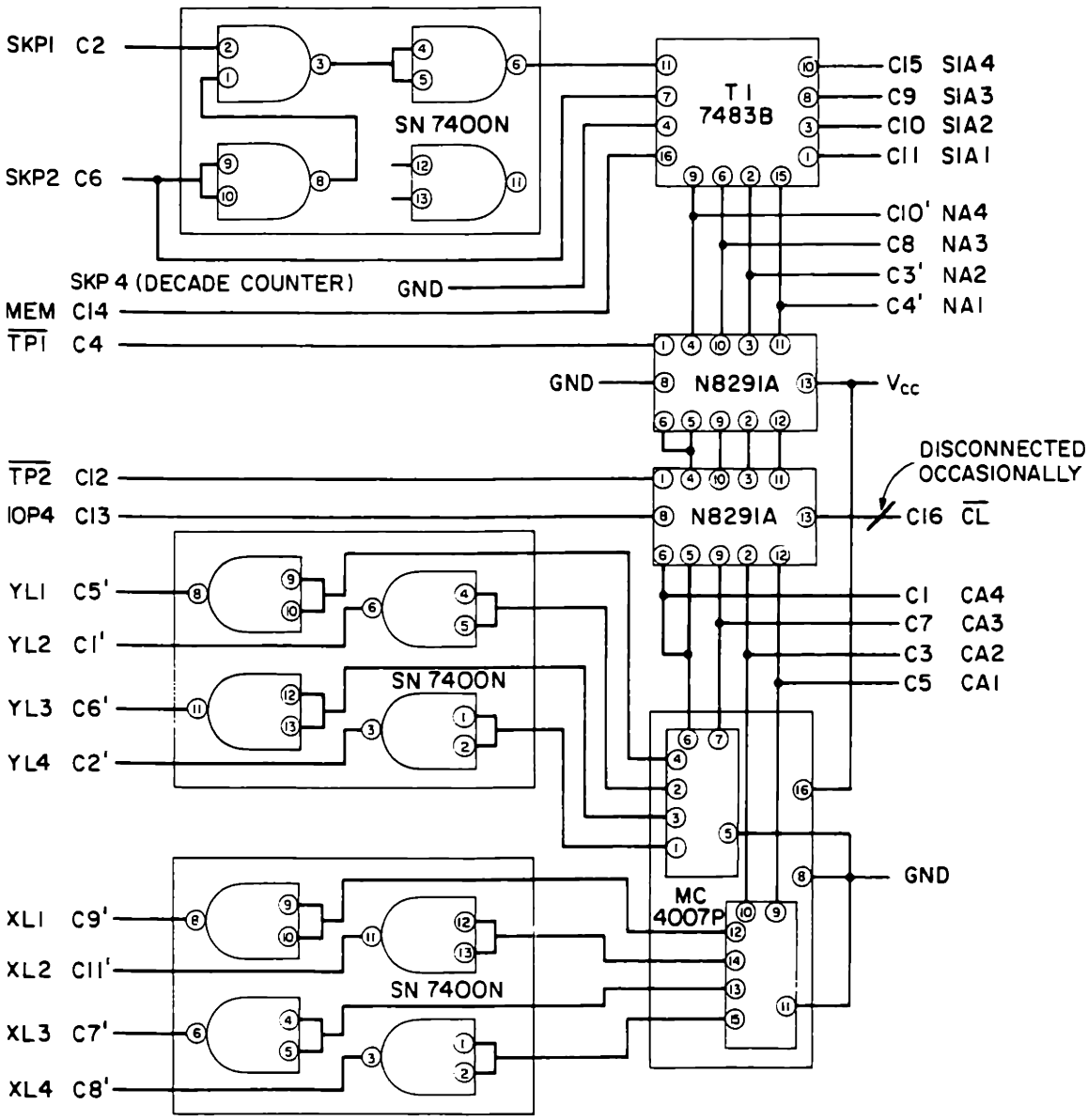

Figure 6: Line Drivers C14, C15

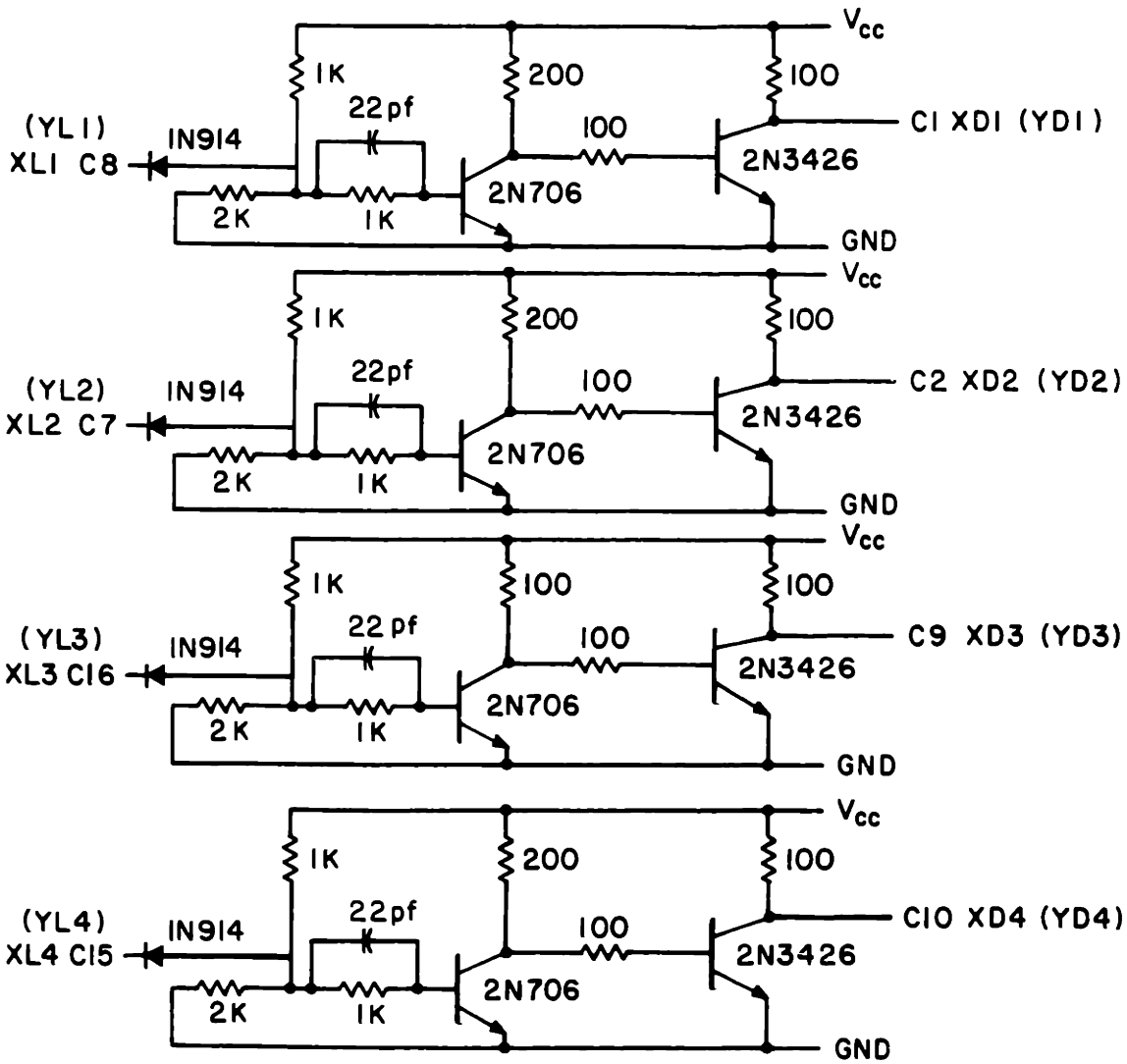

Figure 7: MPA Generators C25

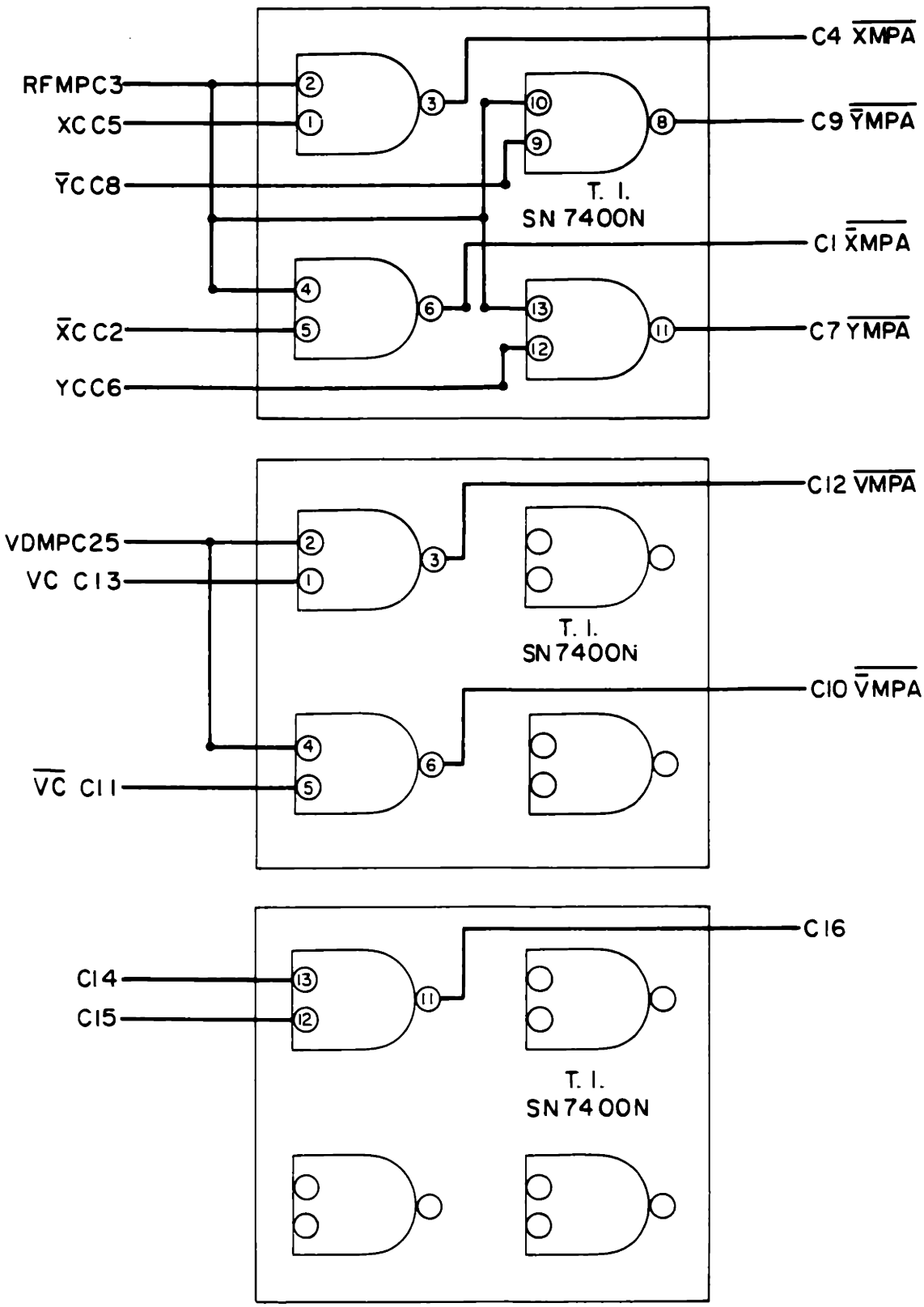

Figure 8: XMP Generators C20-22

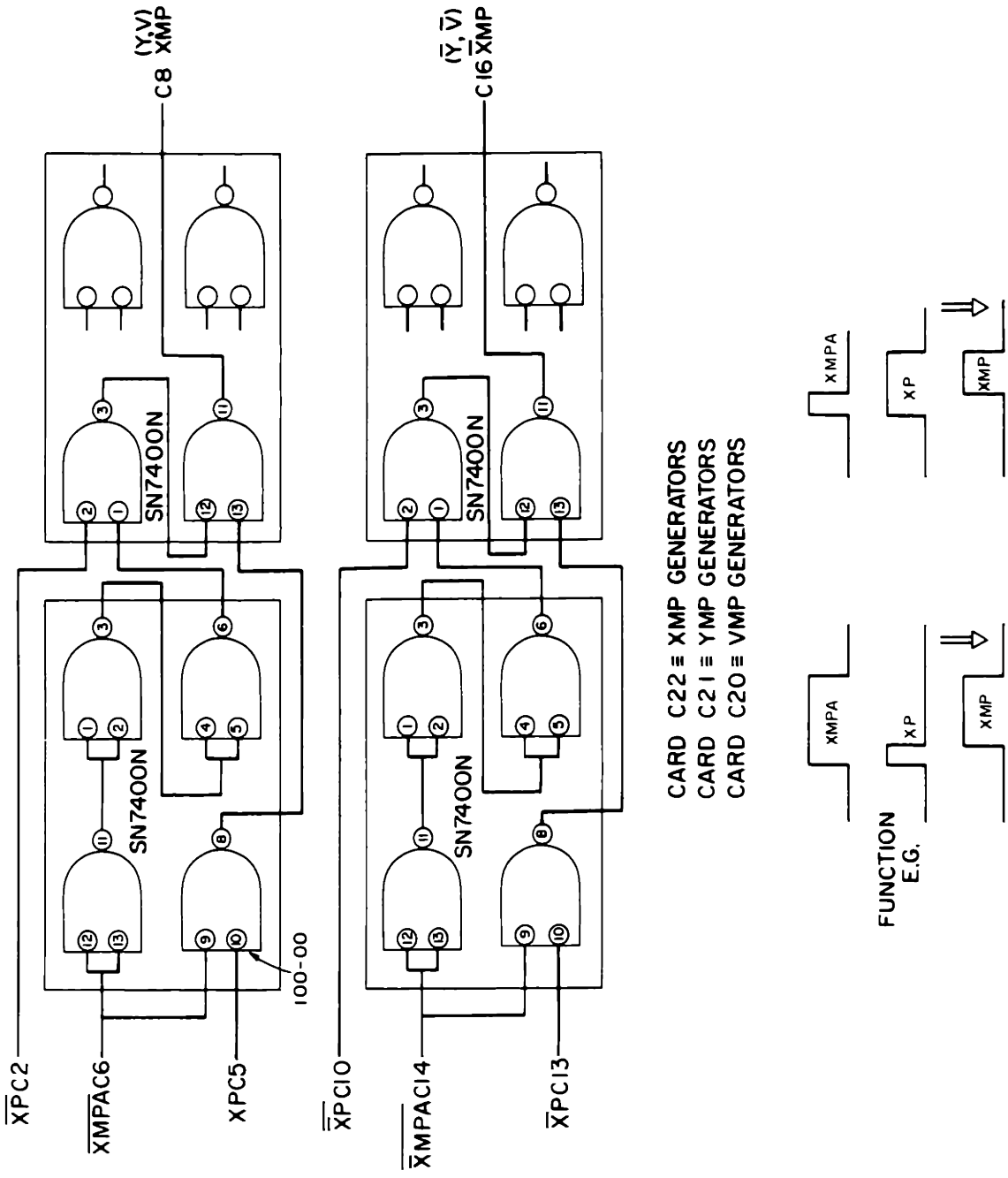

Figure 9: X Pulse Gates C8, C10, C12

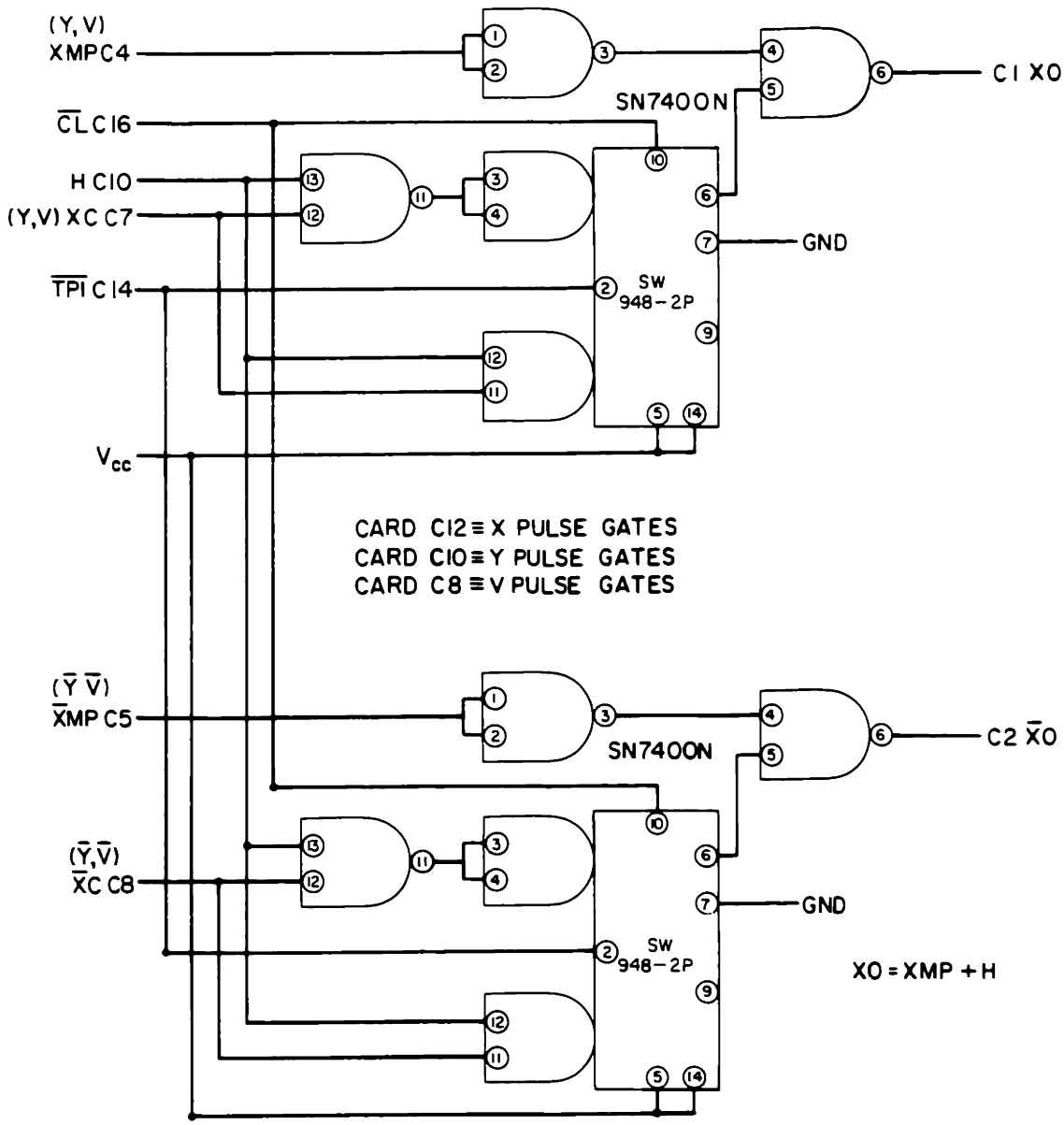

Figure 10: MS Generator AB23

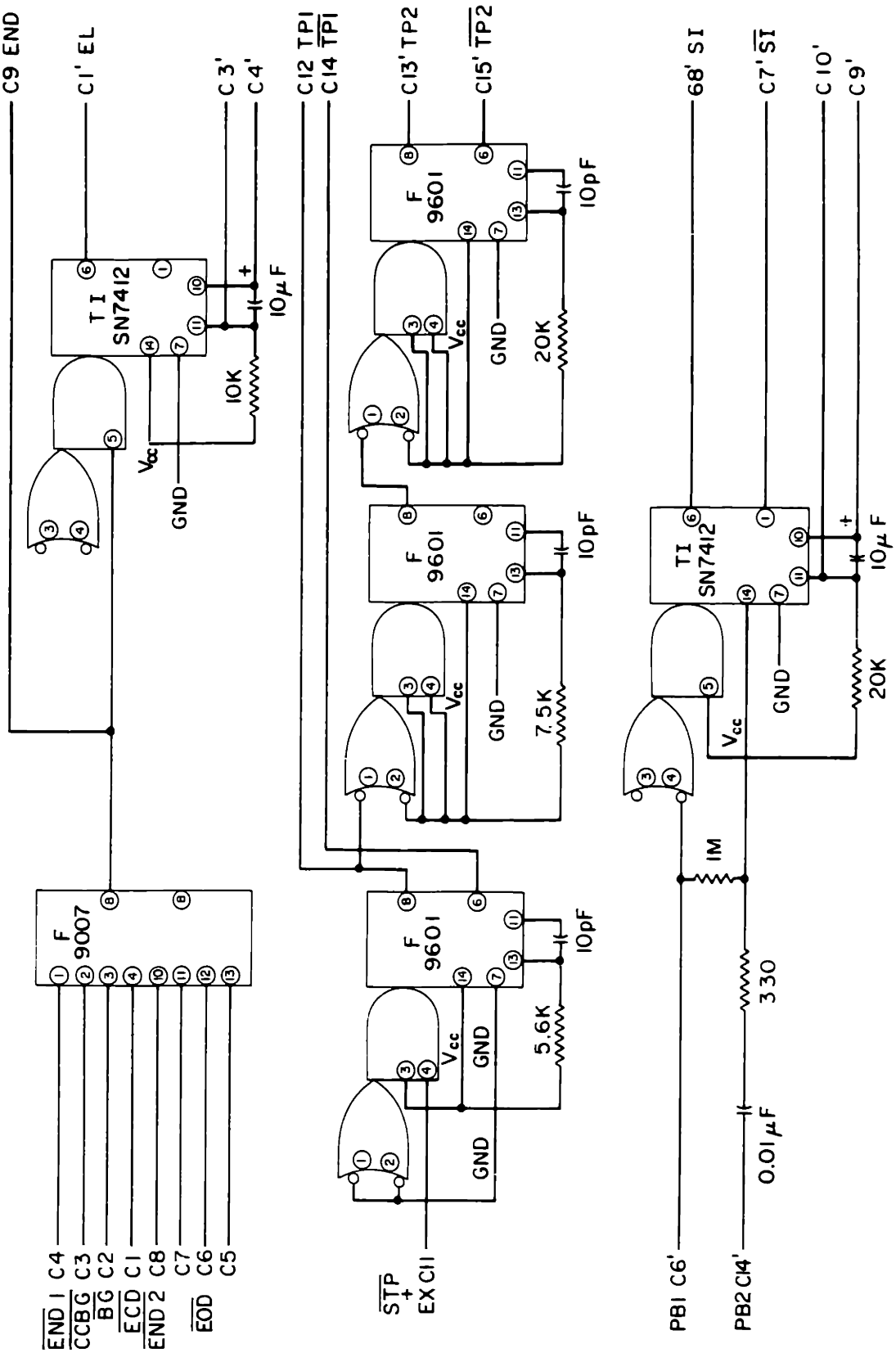

Figure 11 Subburst Counter AB11

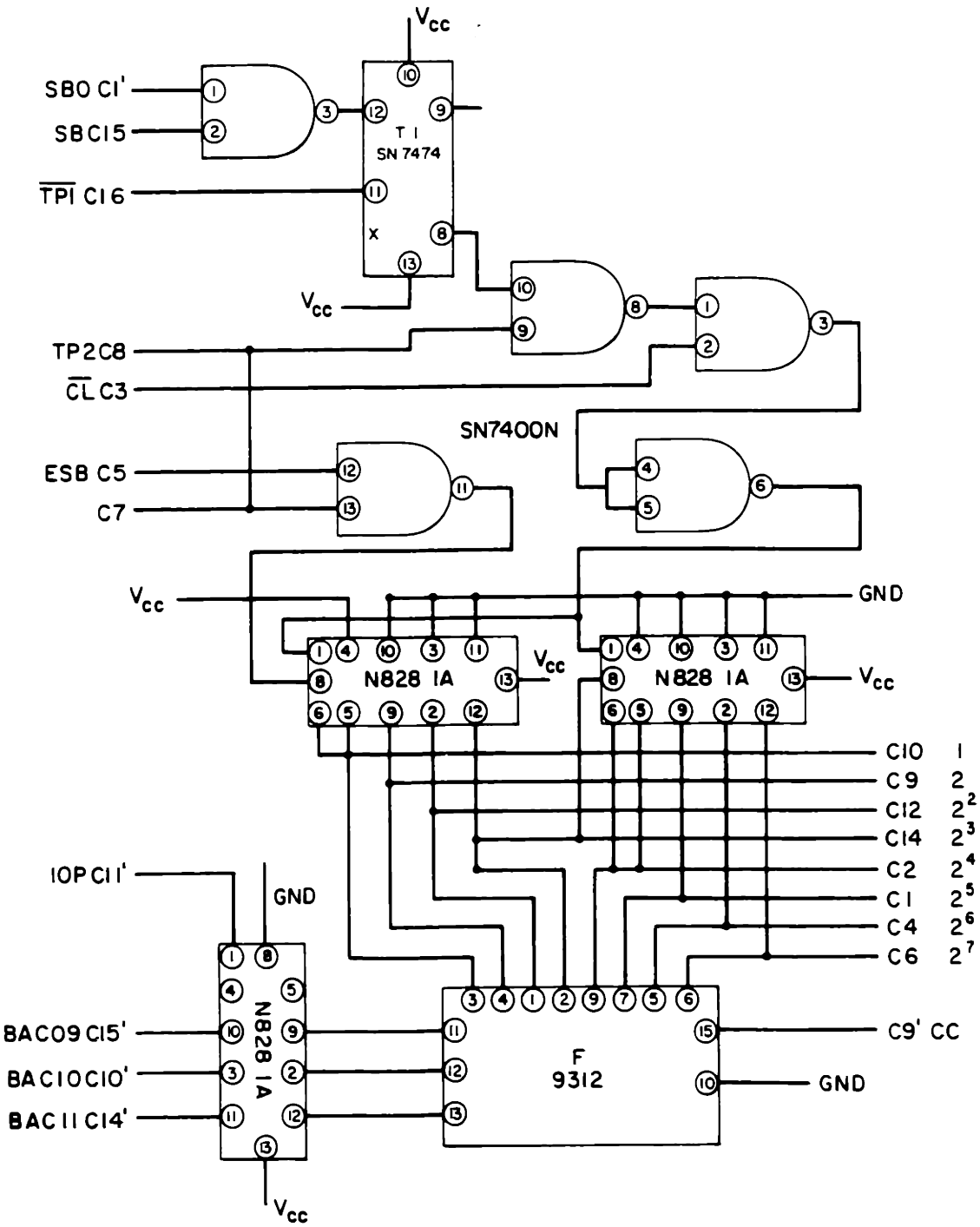

Figure 12: Burst Counter B9

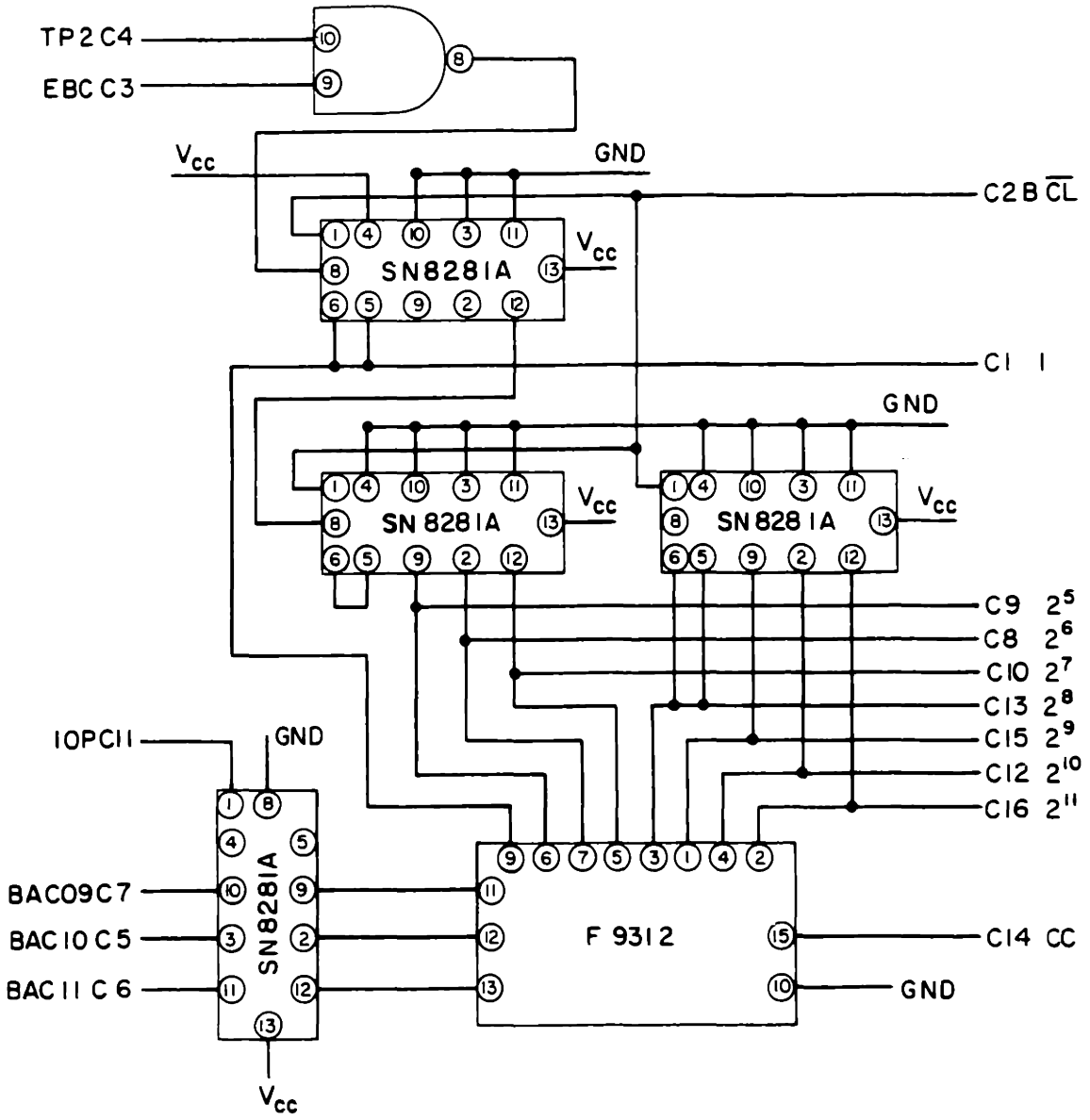

Figure 13: Skip A9

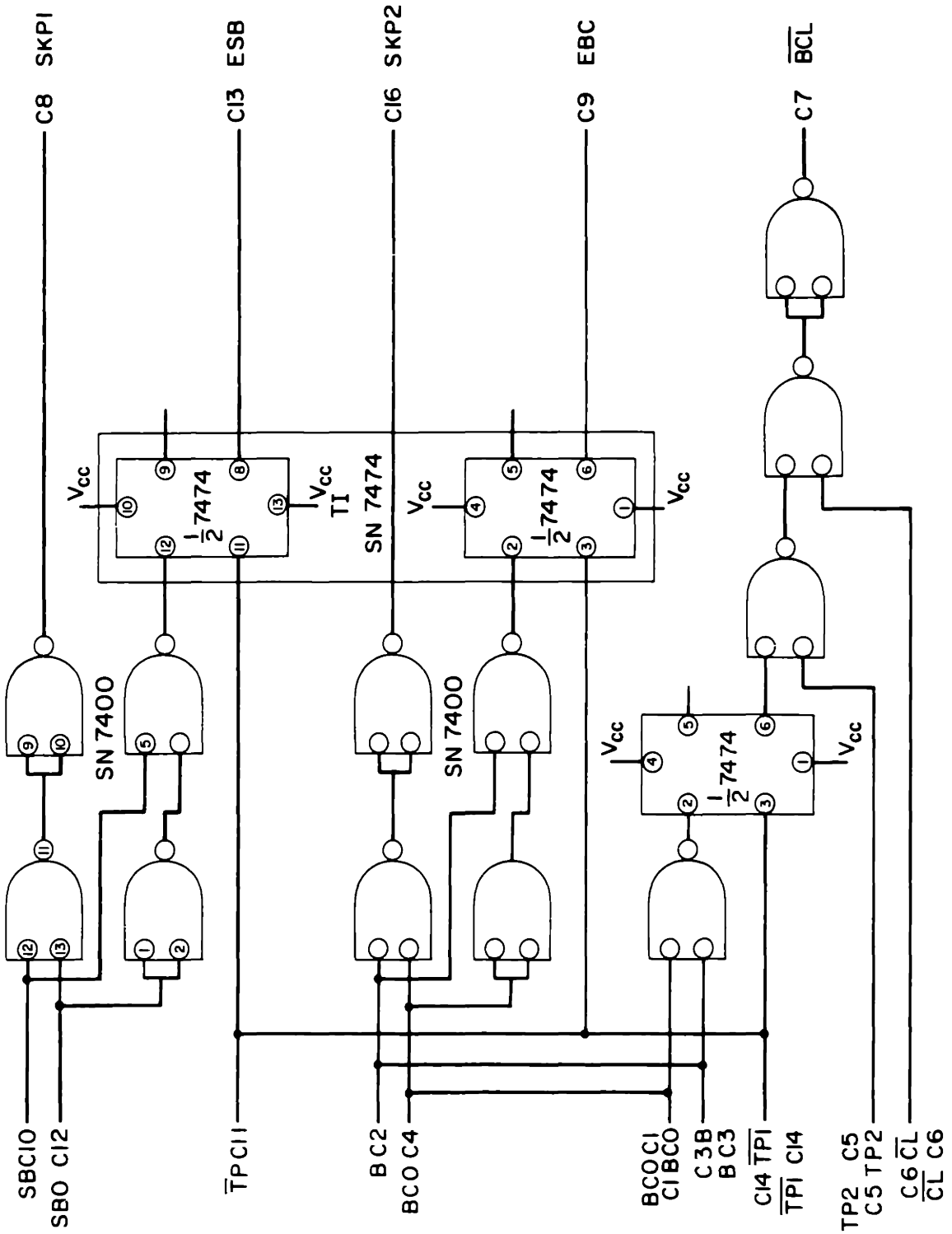

Figure 14: Clock decade AB19

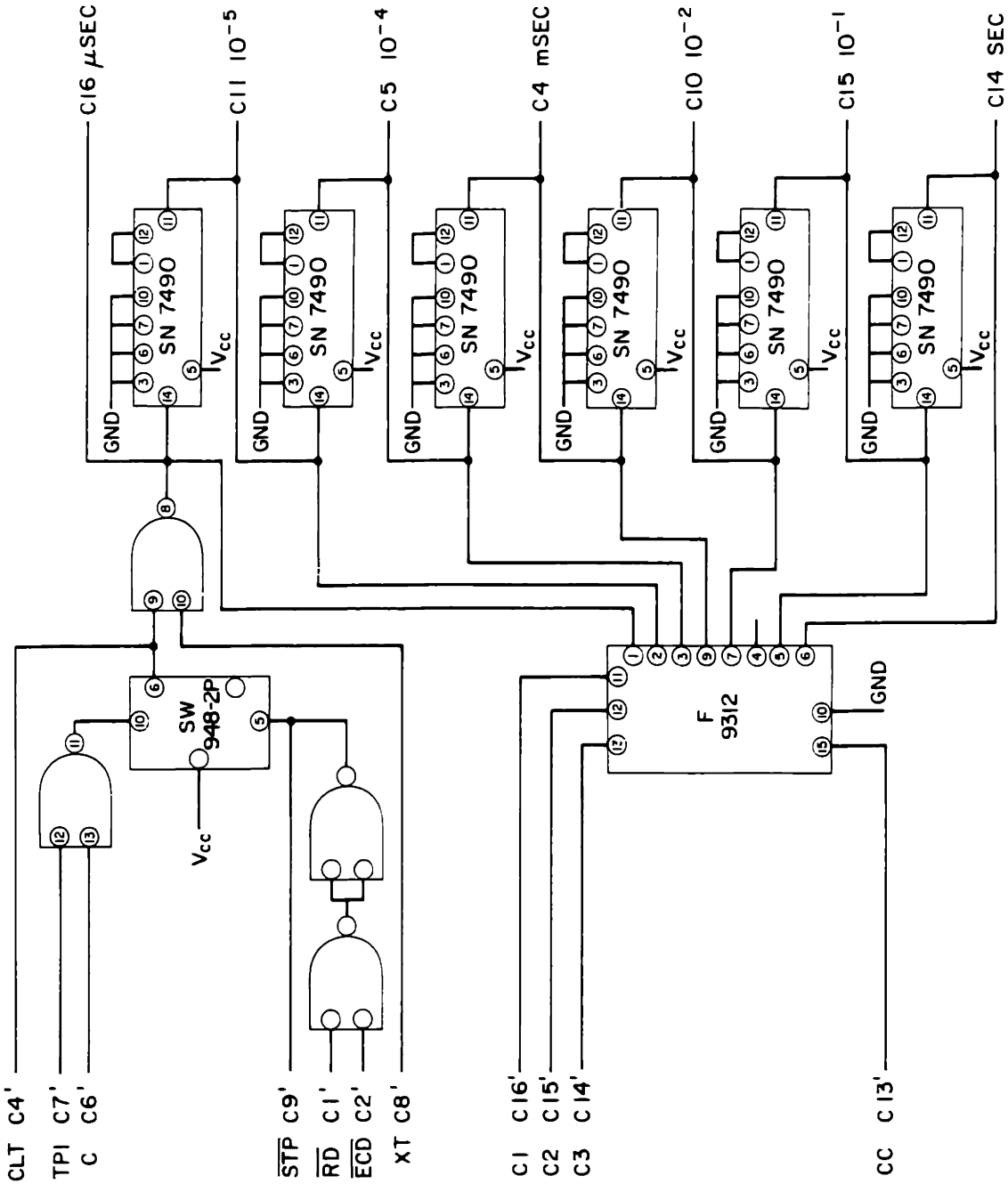

Figure 15: Clock Counter C19

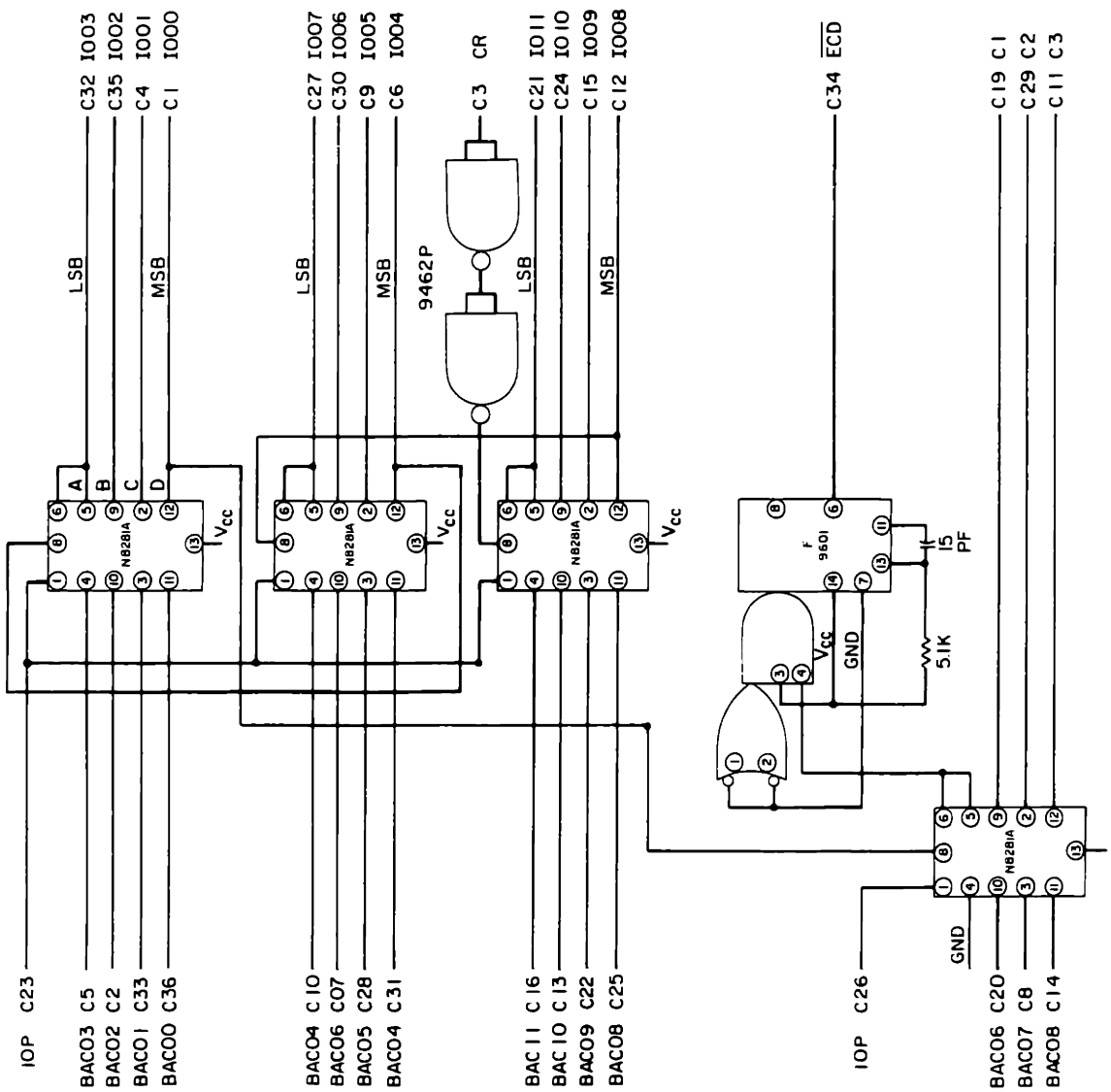

Figure 16: Delay Decoder C17

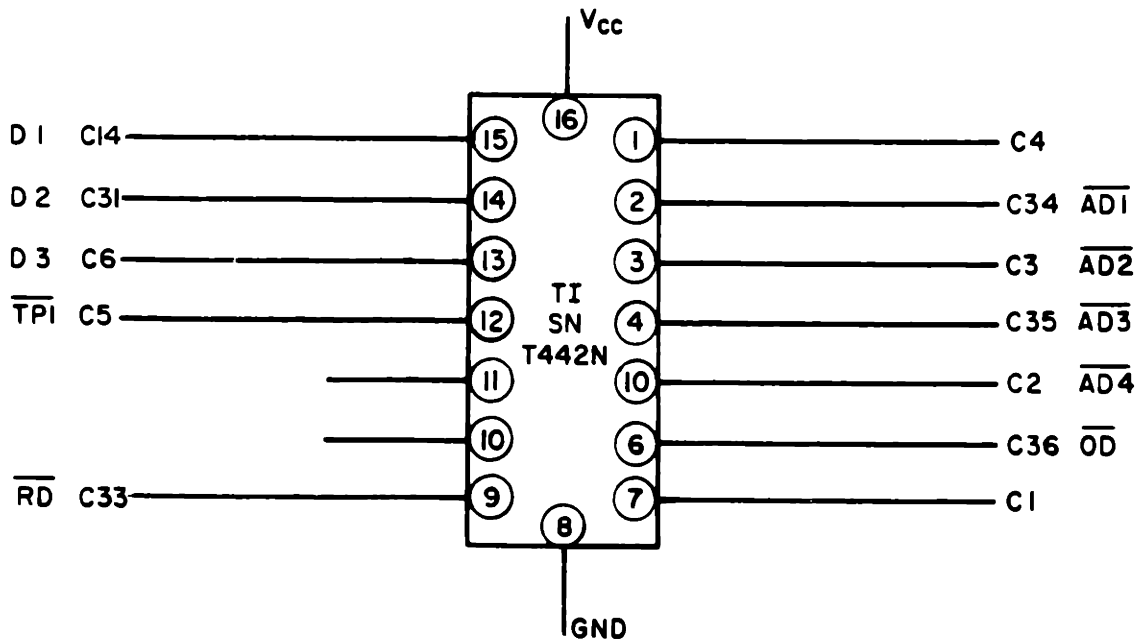

Figure 17: End Delay C23

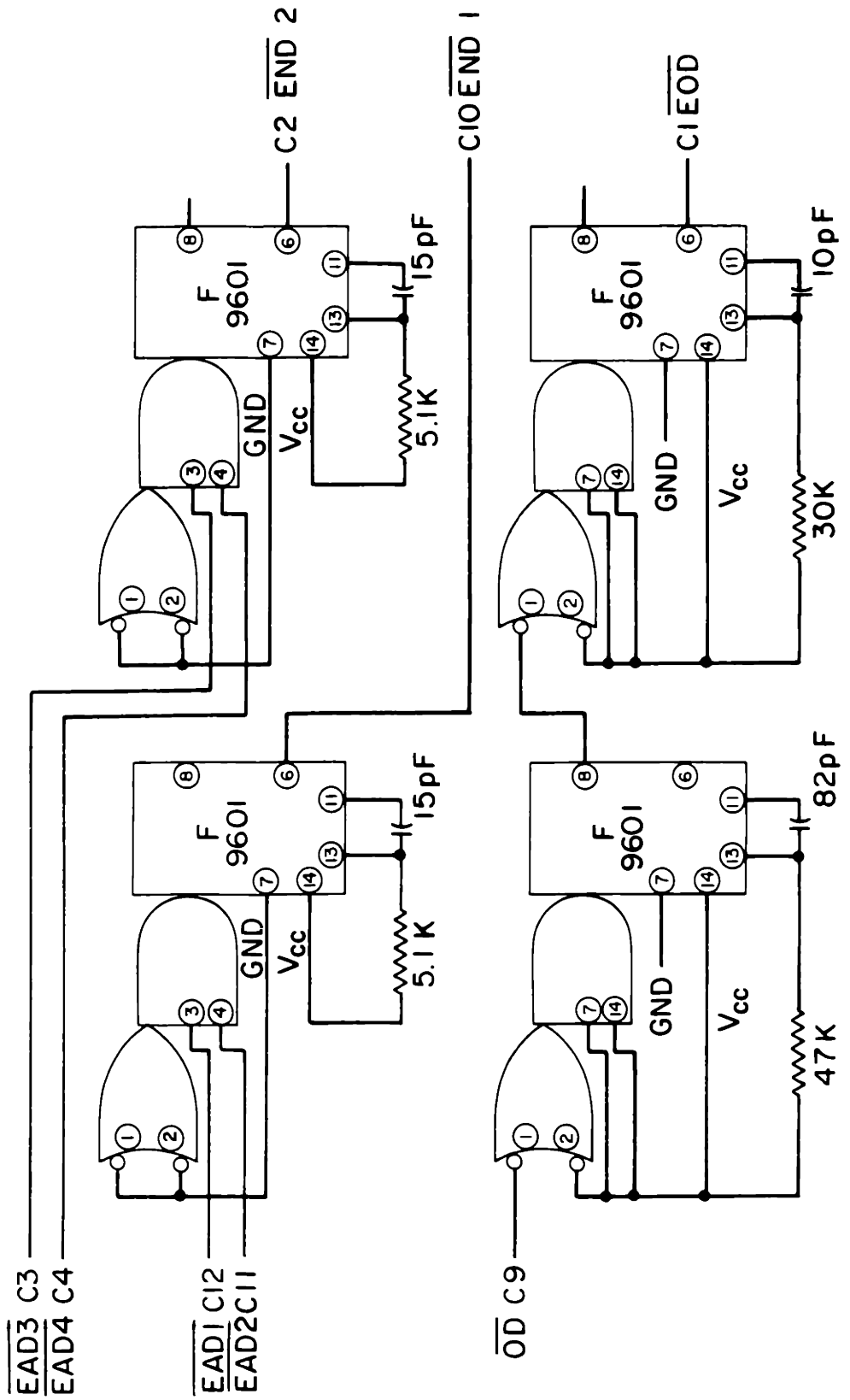

Figure 18: Recycle Delay AB25

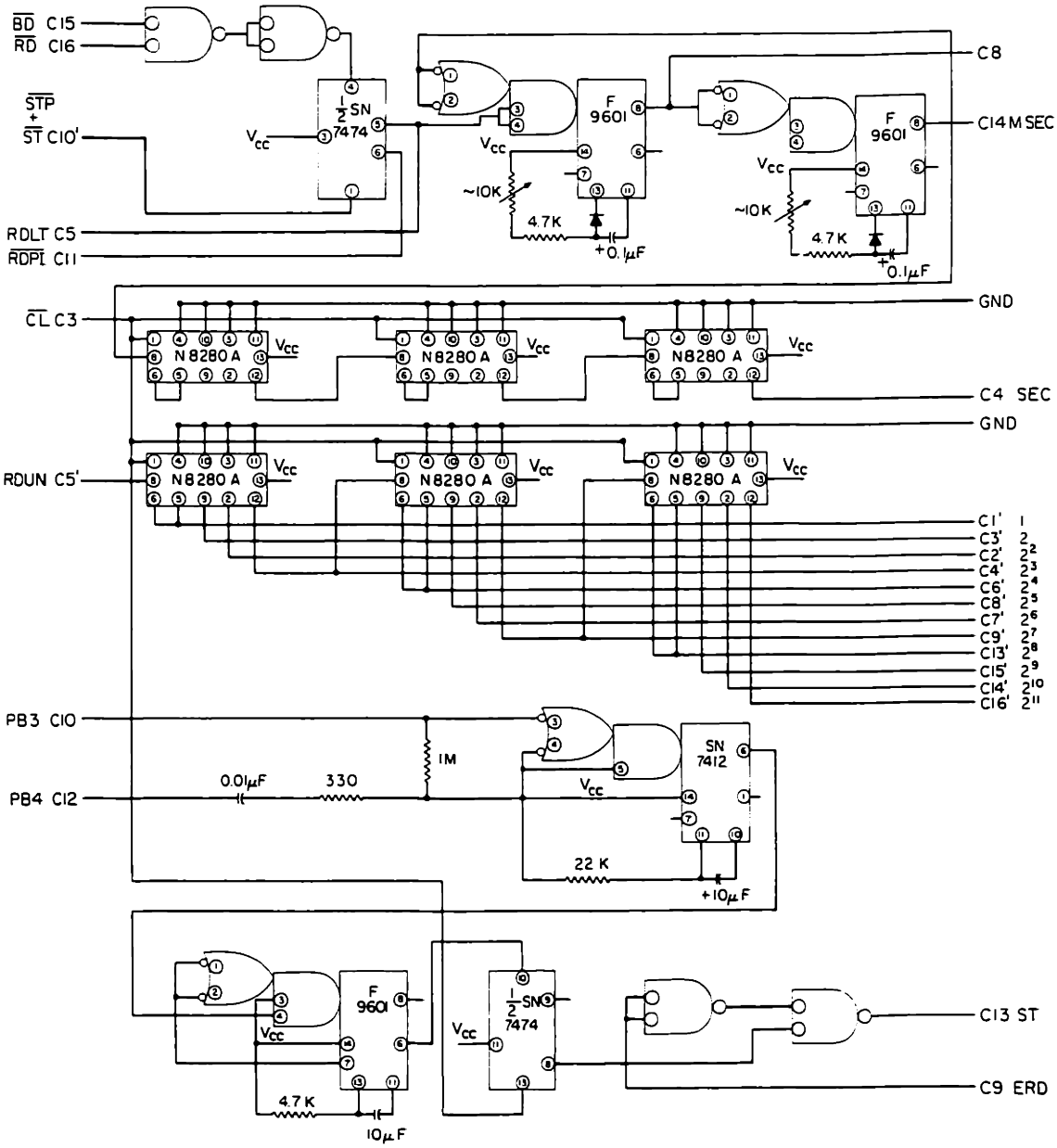

Figure 19: Mode AB21

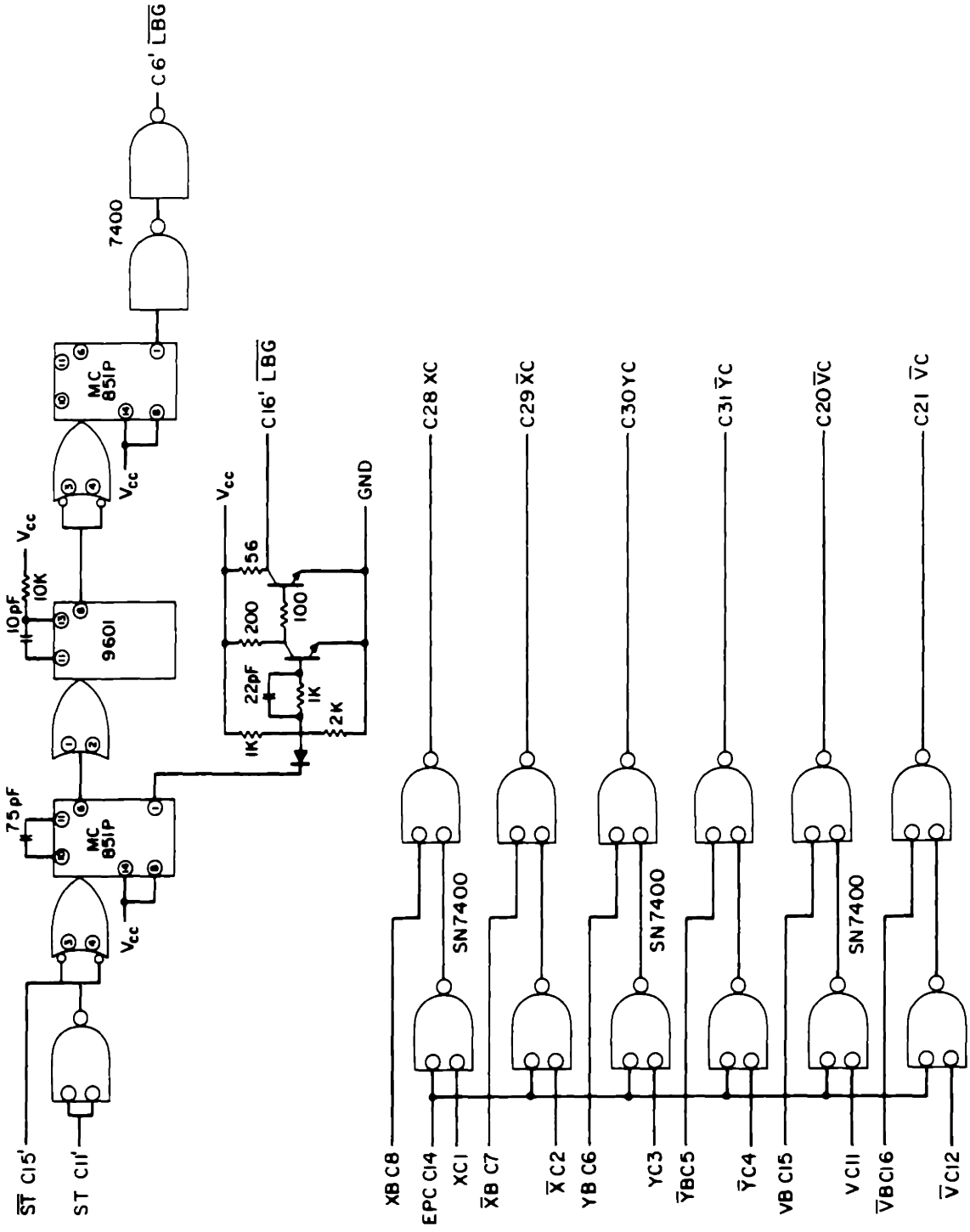

Figure 20: Sample C5

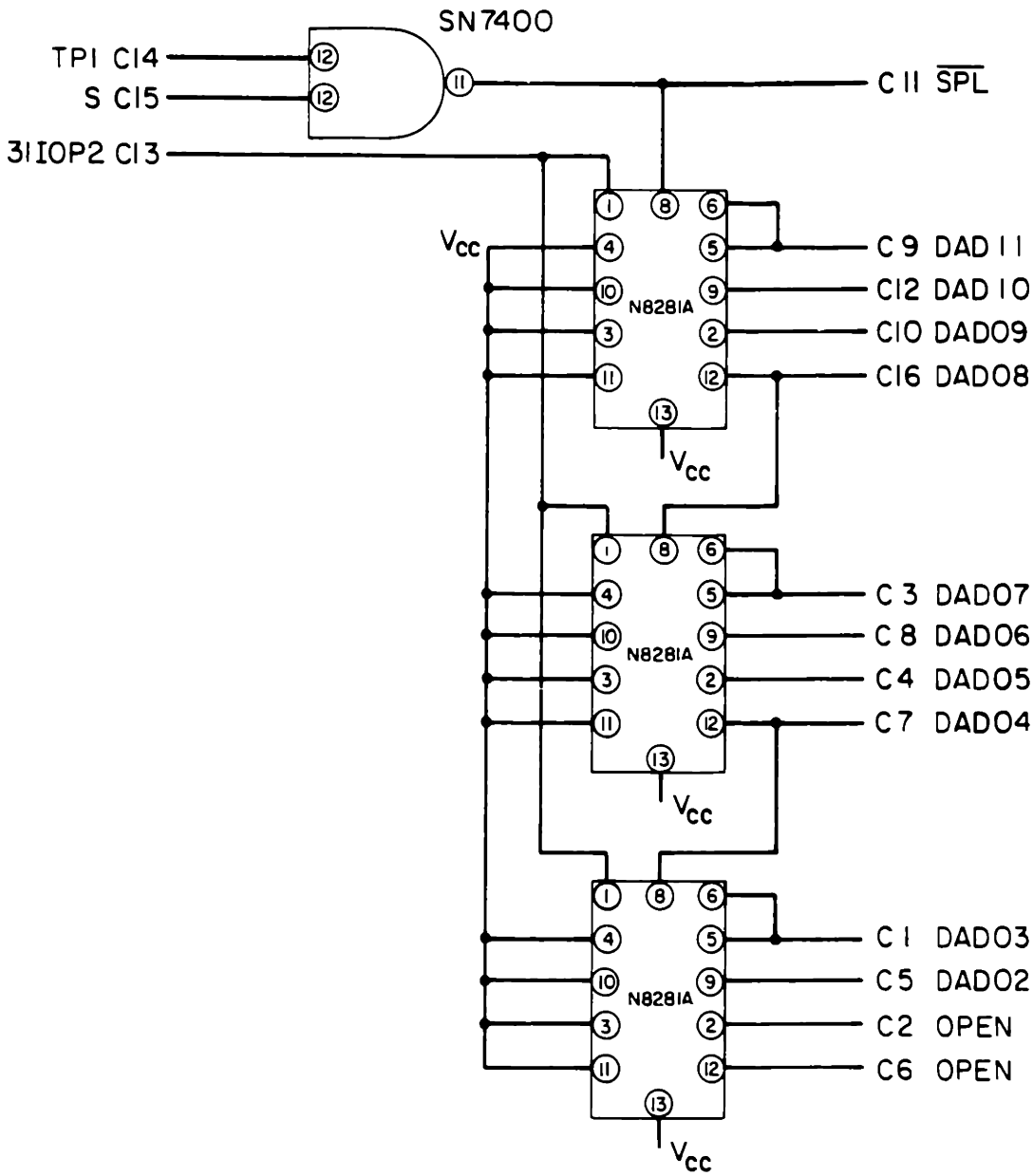

Figure 21: Program Interrupt C7

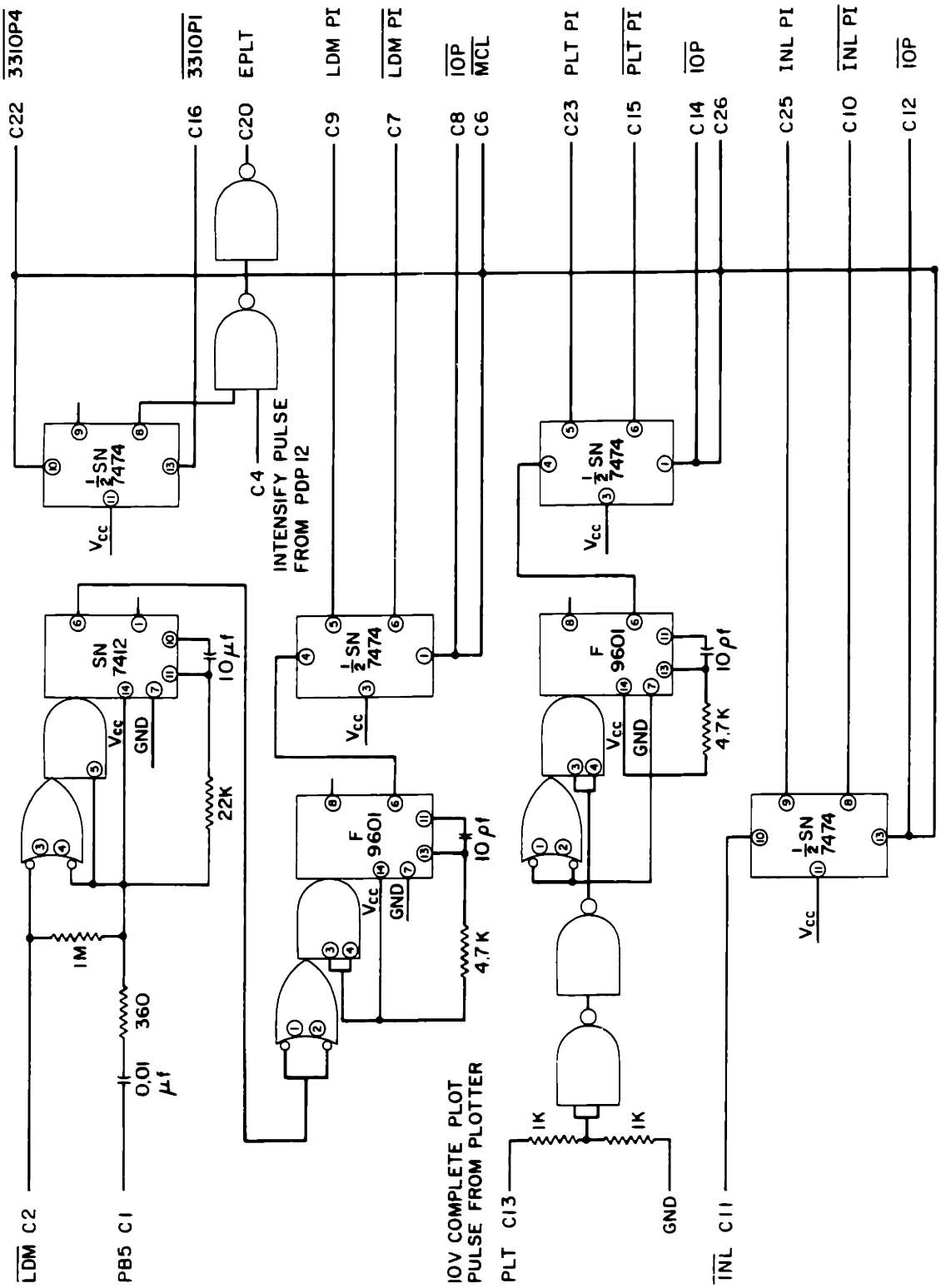

Figure 22: Computer Light C16

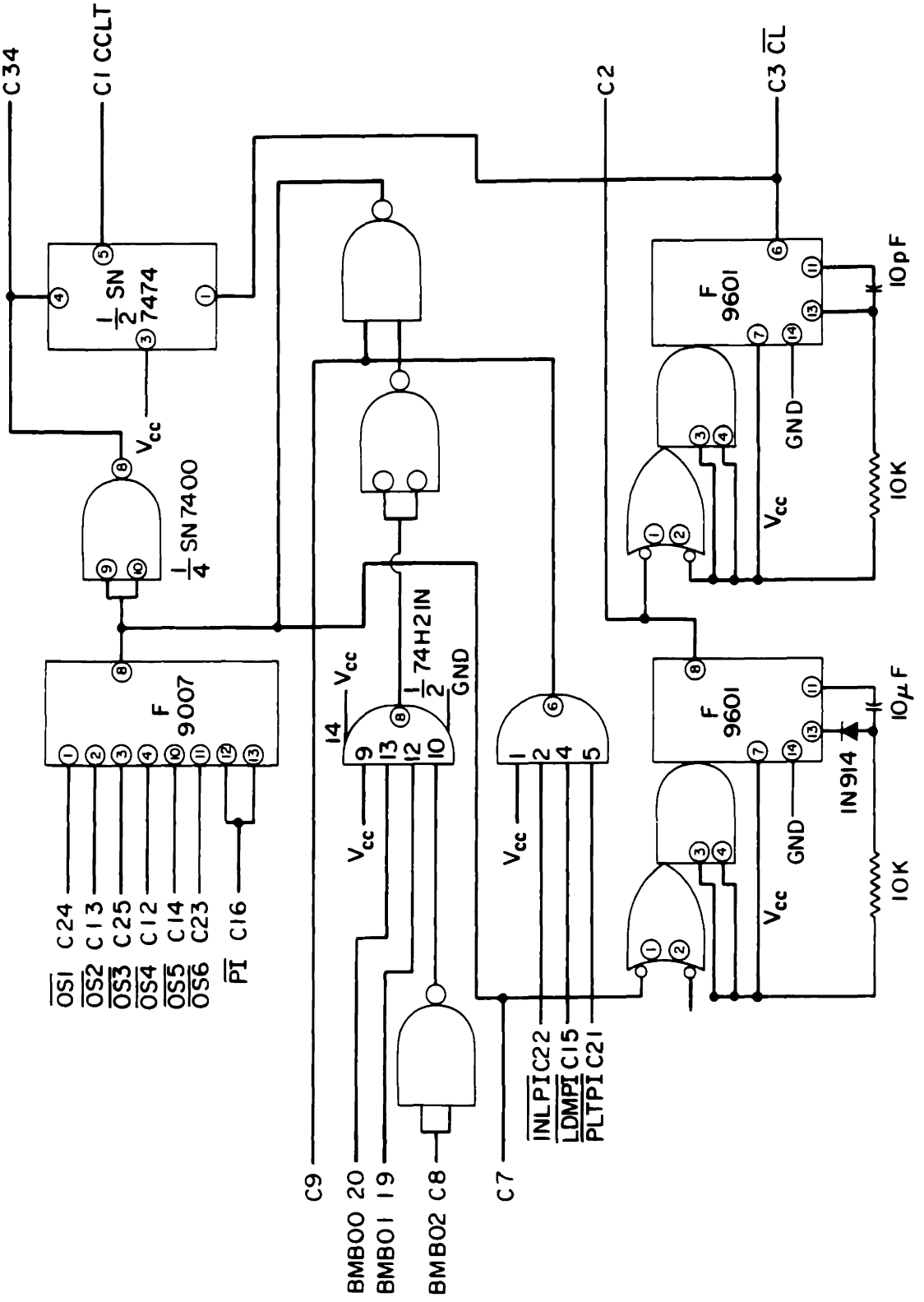

Figure 23: RFMP and VDMP Generator Switches

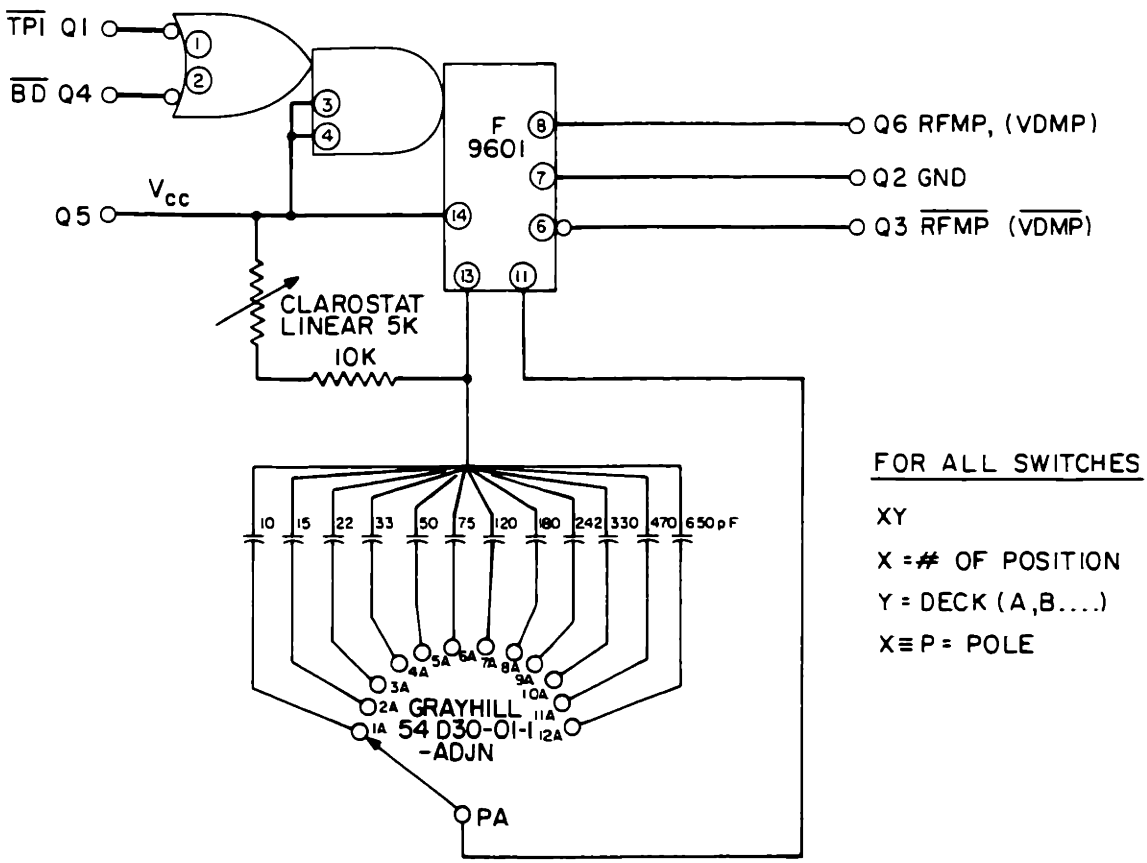

Figure 24: AD1., AD2 Switches

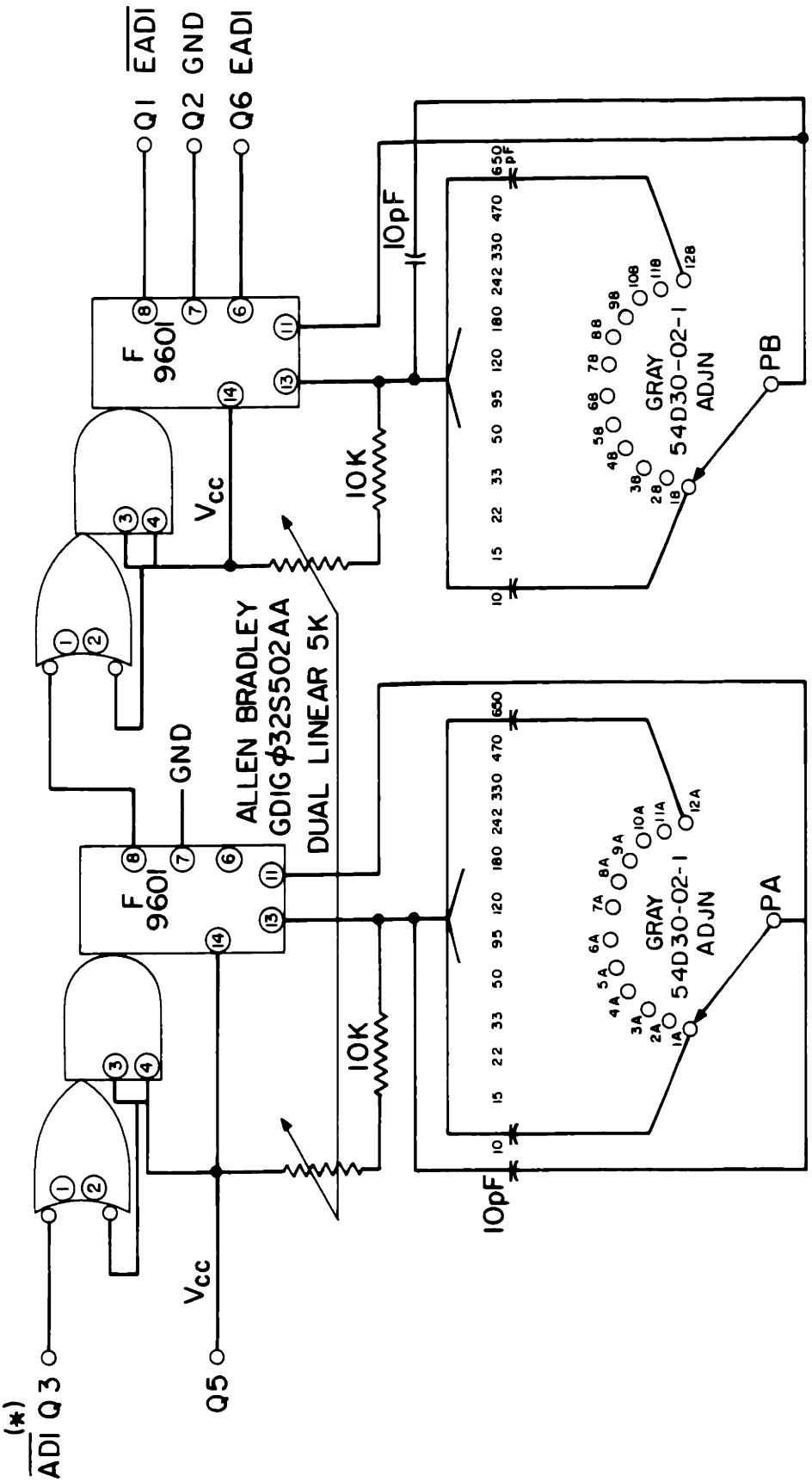

Figure 25: Mode Switch

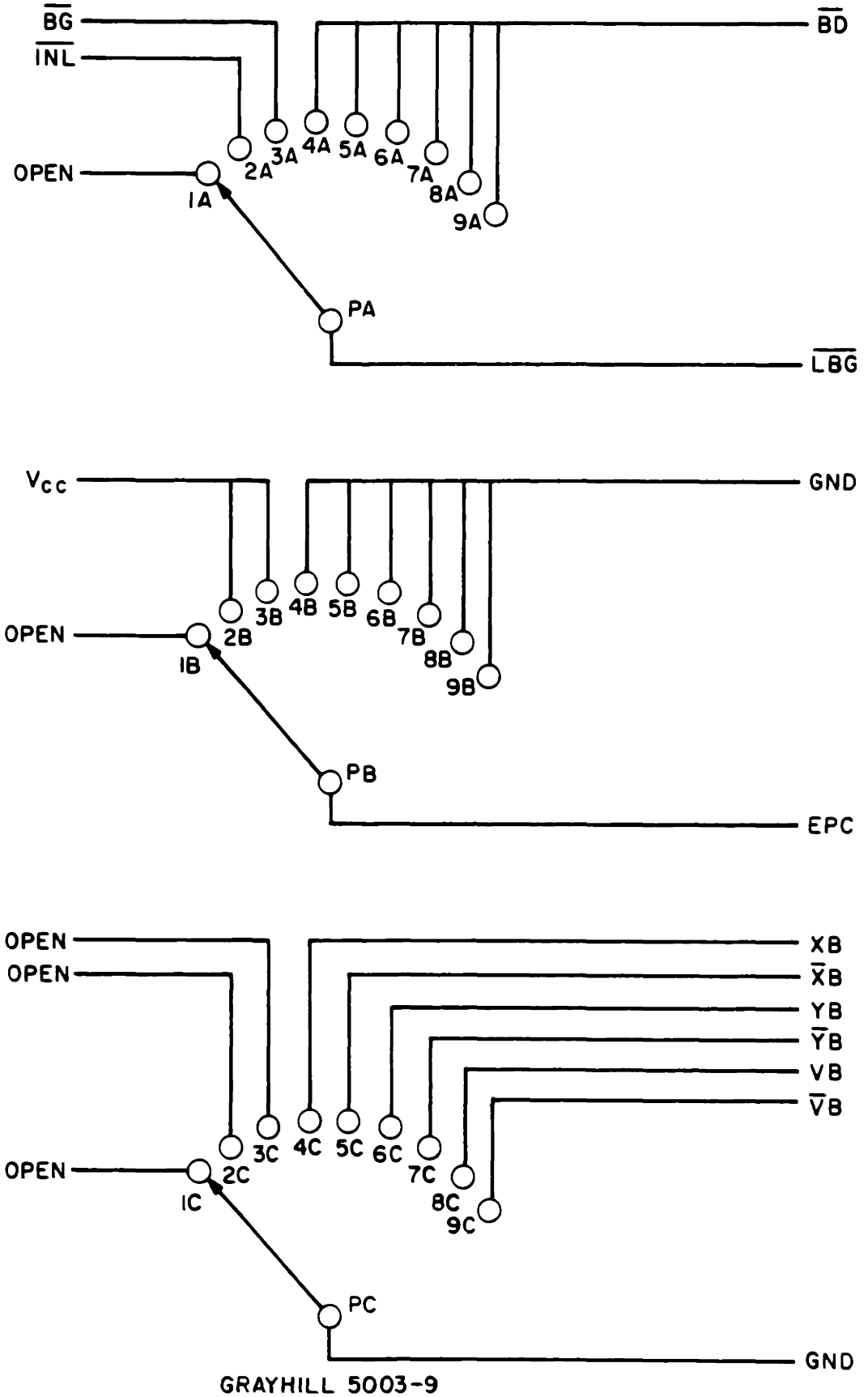

GRAYHILL 5003-9

Figure 26: (a) Clock Switch, (b) Recycle Delay Switch

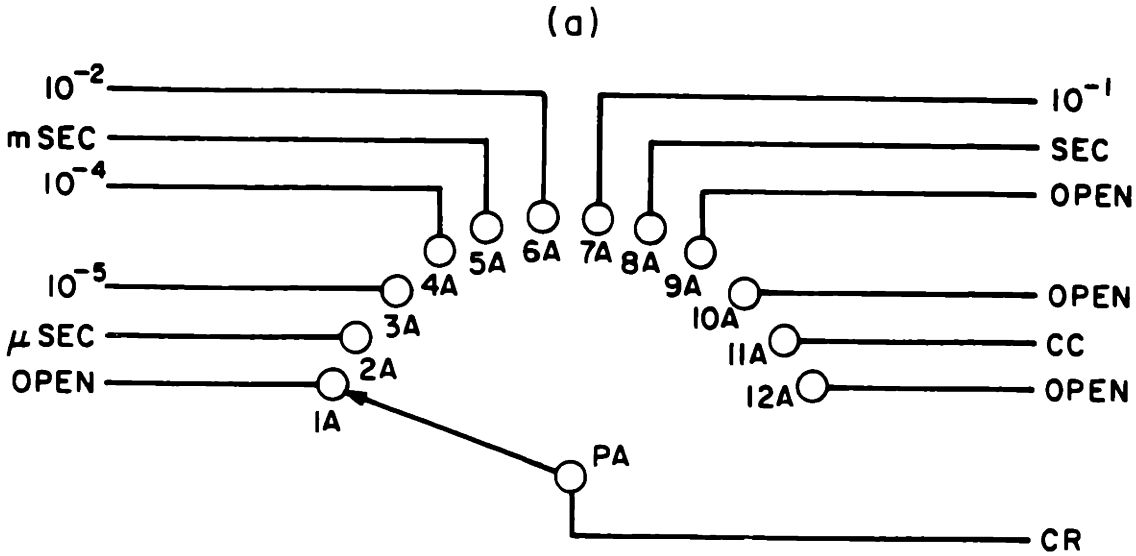

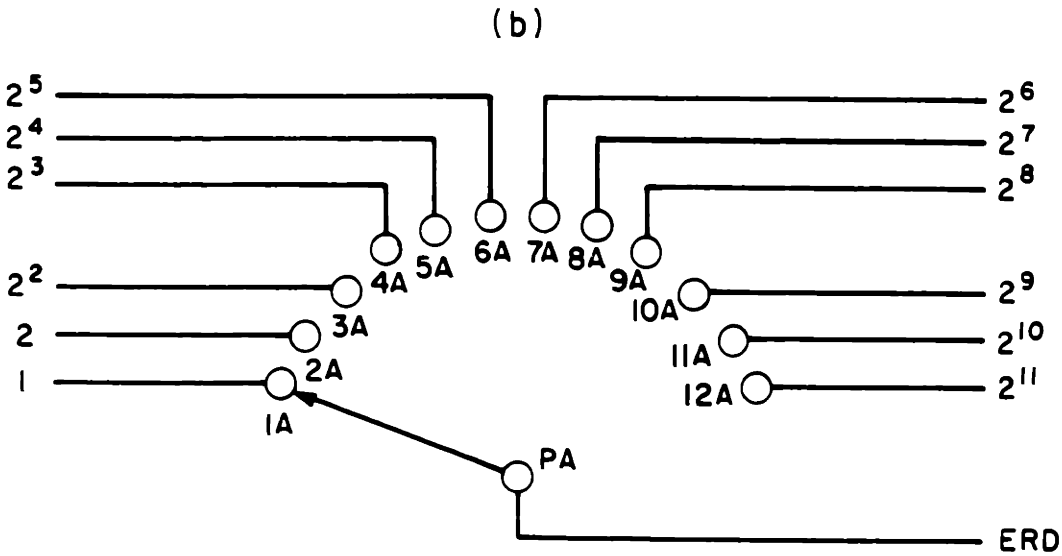

Figure 27: (a) Subburst Switch, (b) Burst Switch

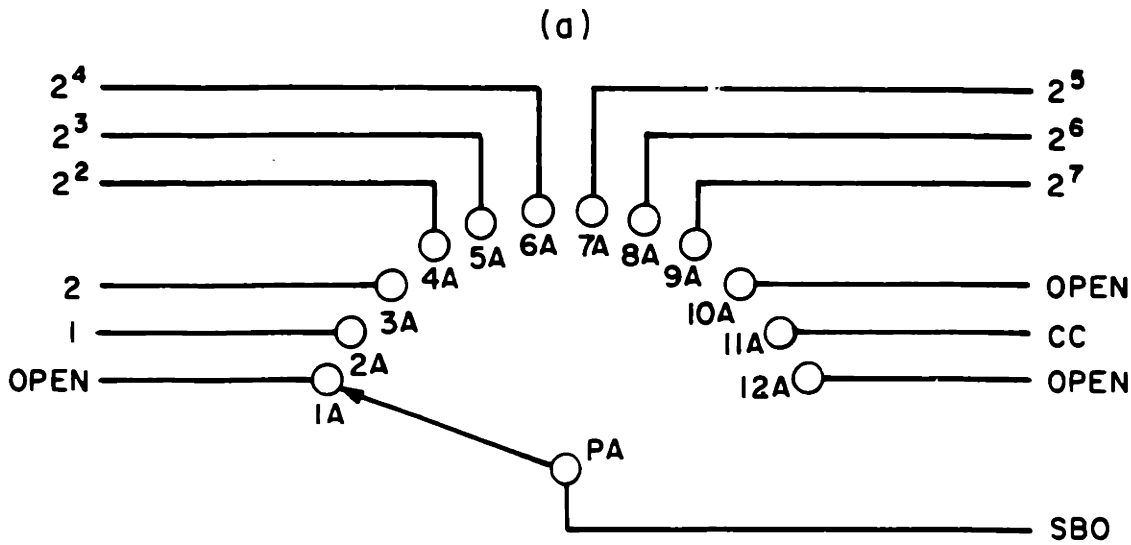

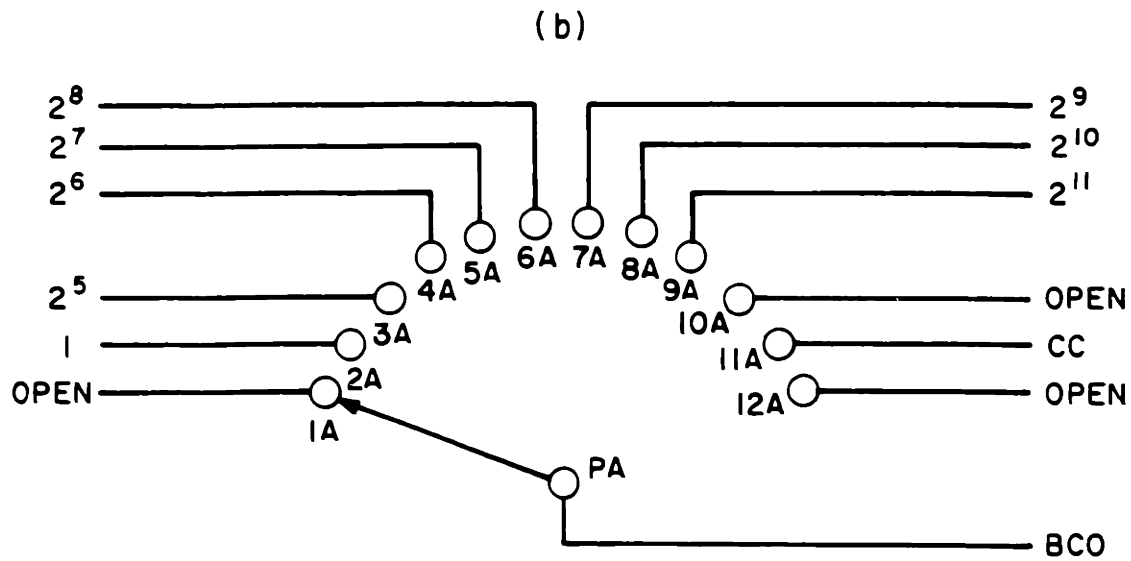

Figure 28: (a) SI Switch, (b) Execute Switch

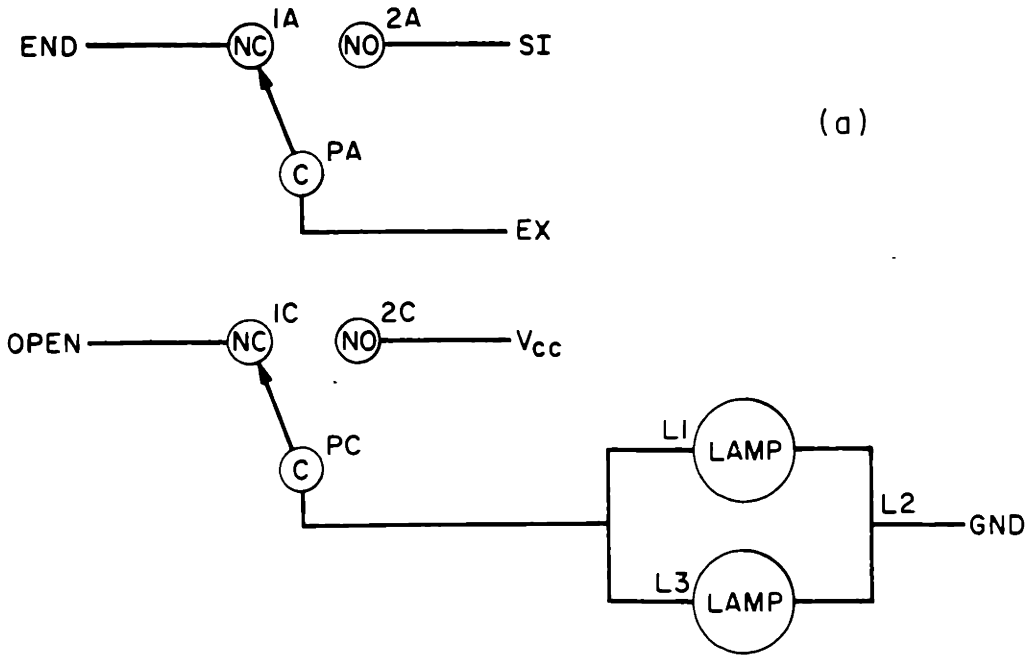

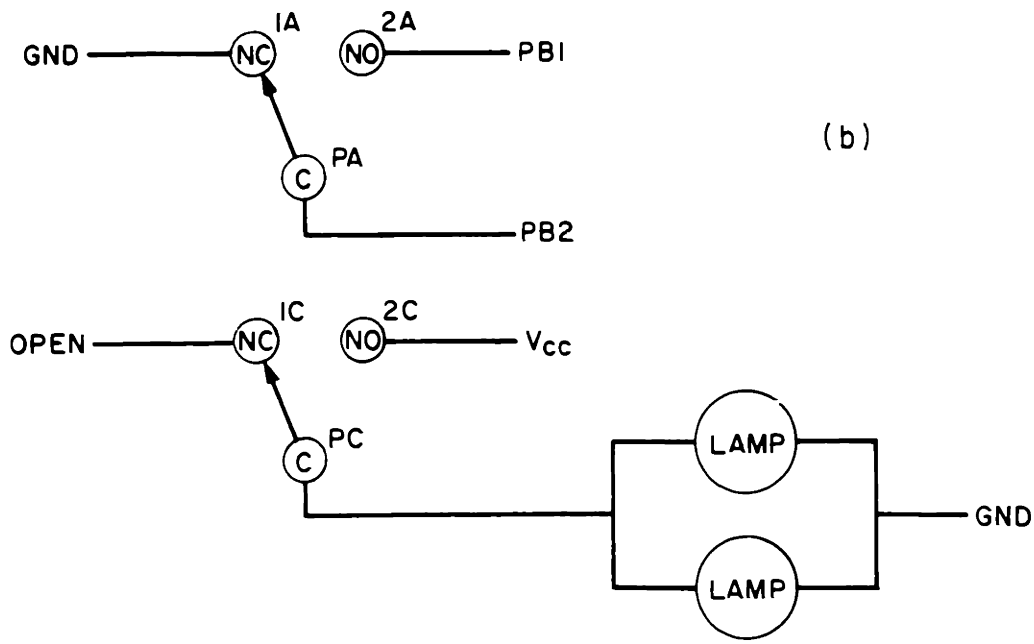

Figure 29: (a) RD Units Switch, (b) DIS PDP12 Switch

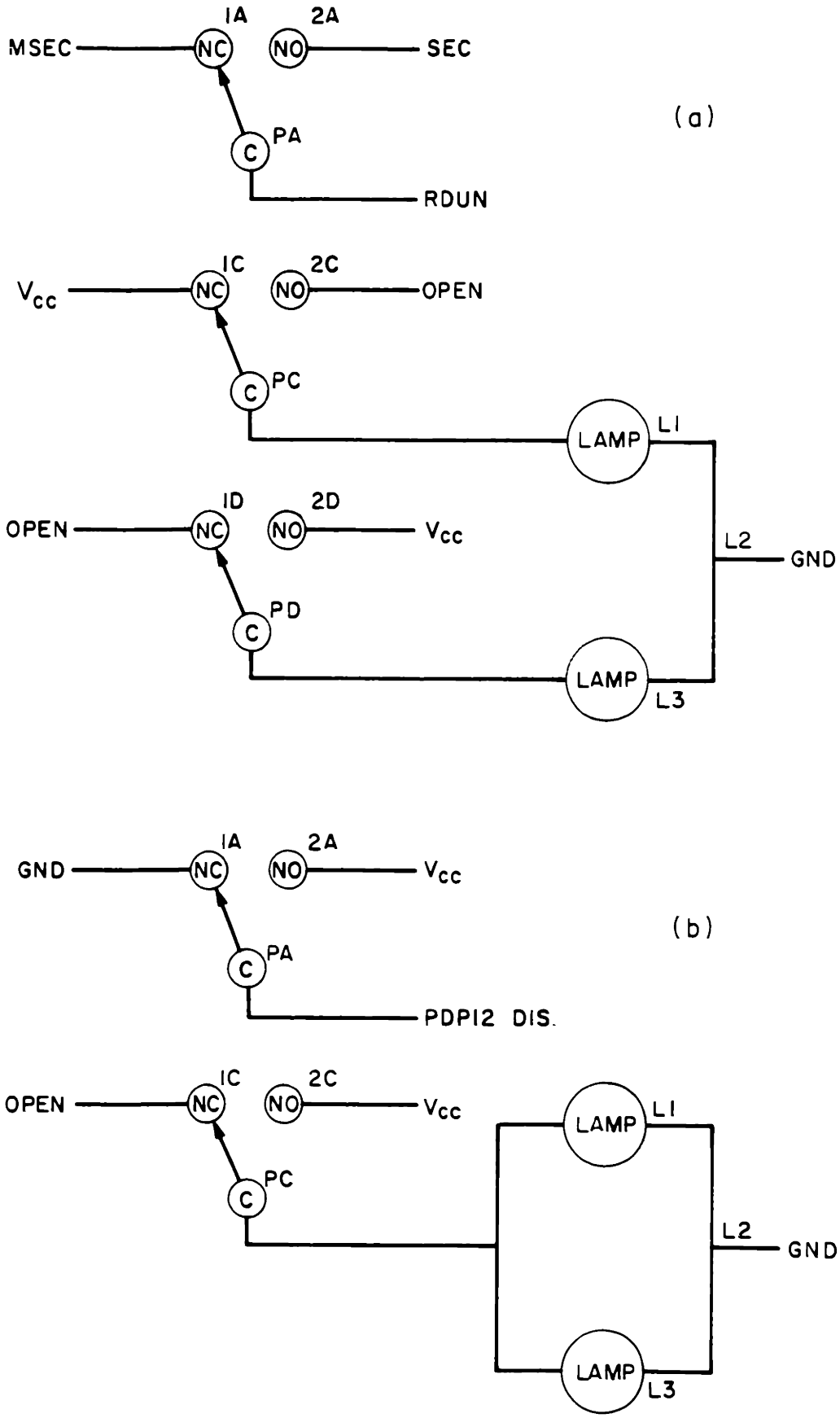

Figure 30: (a) Top/Bot. Mem. Switch
(b) Dis. Spectr. Switch

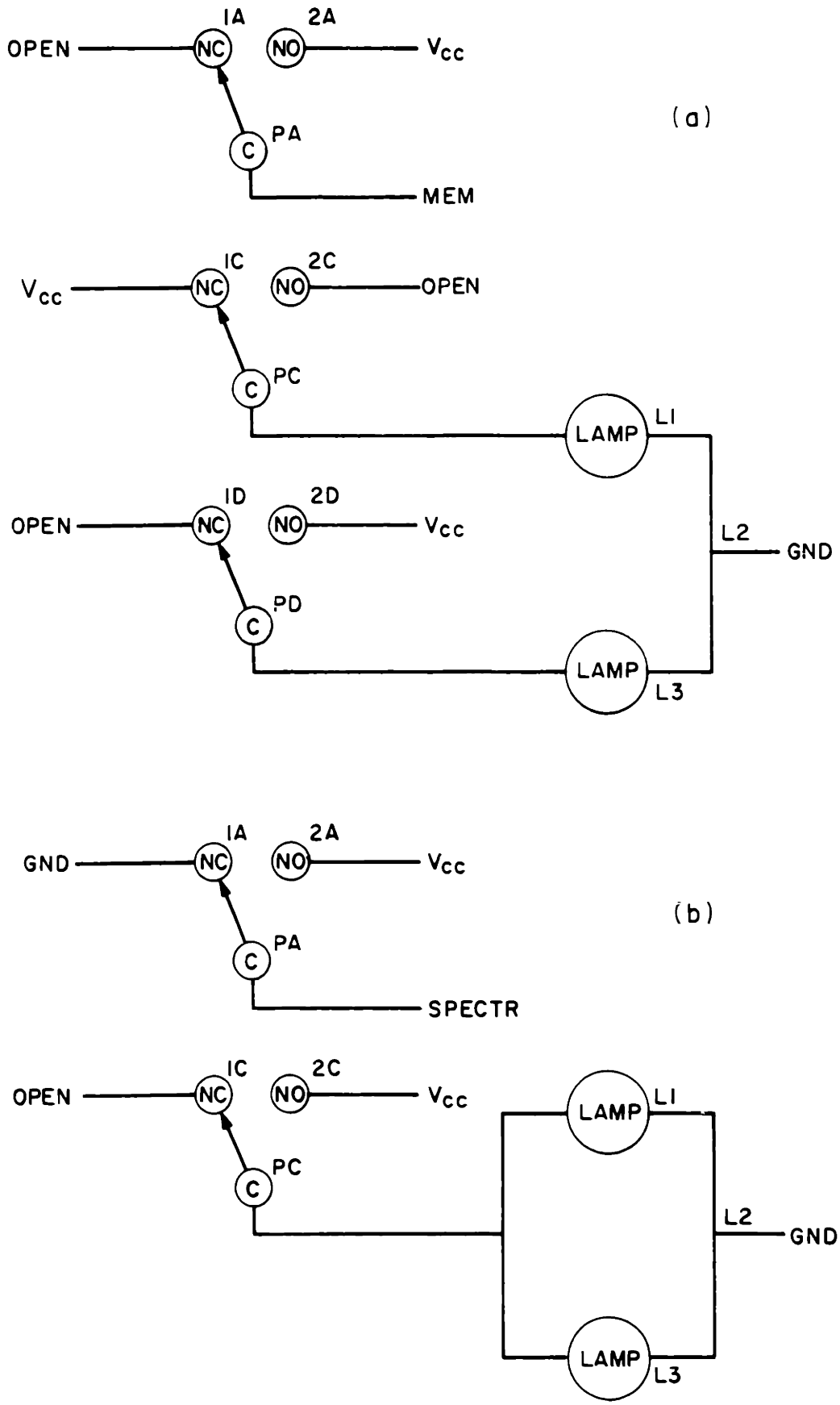

Figure 31: Start Switch, (b) Stop Switch

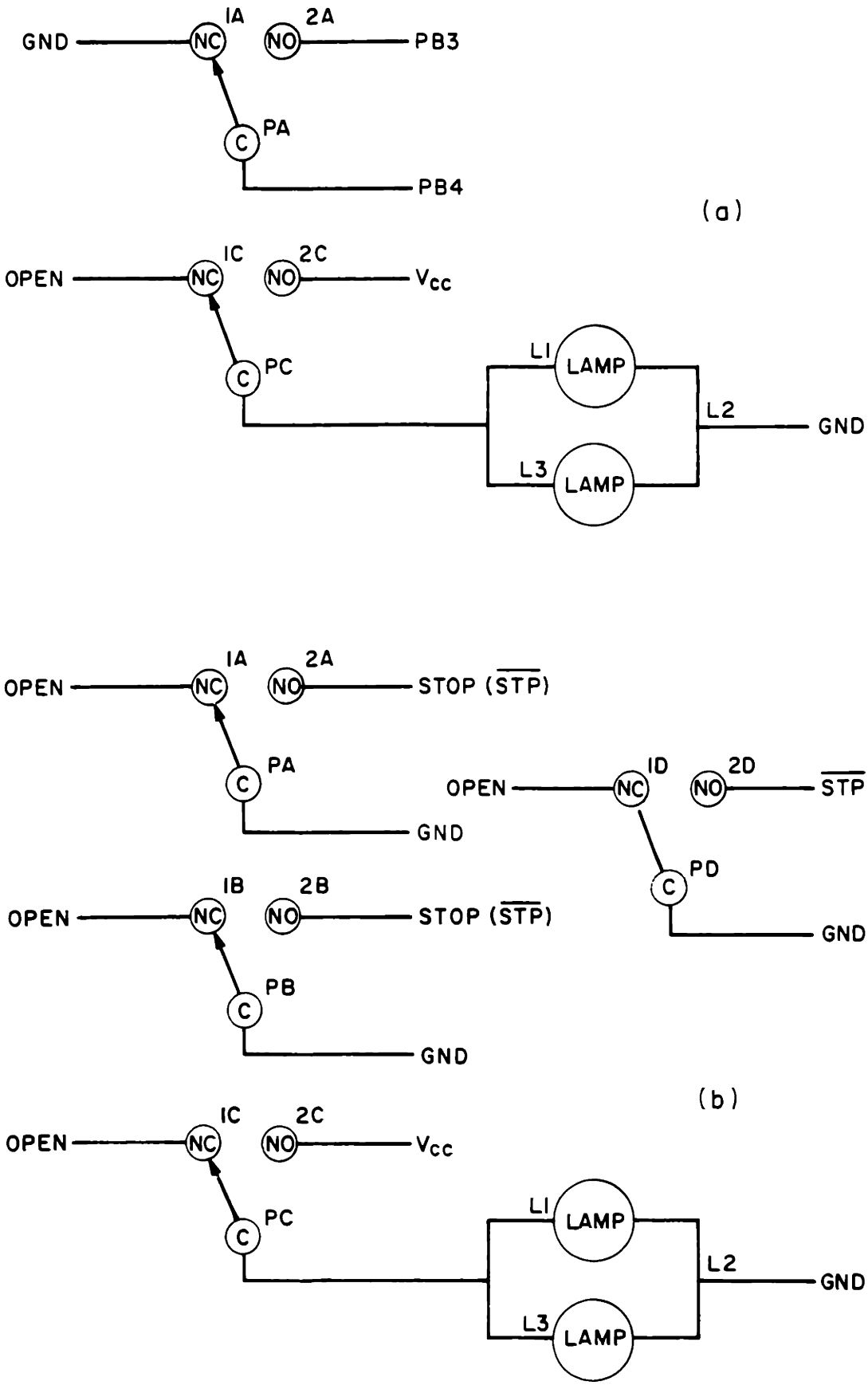

Figure 32: (a) Clear Switch, (b) Load Switch

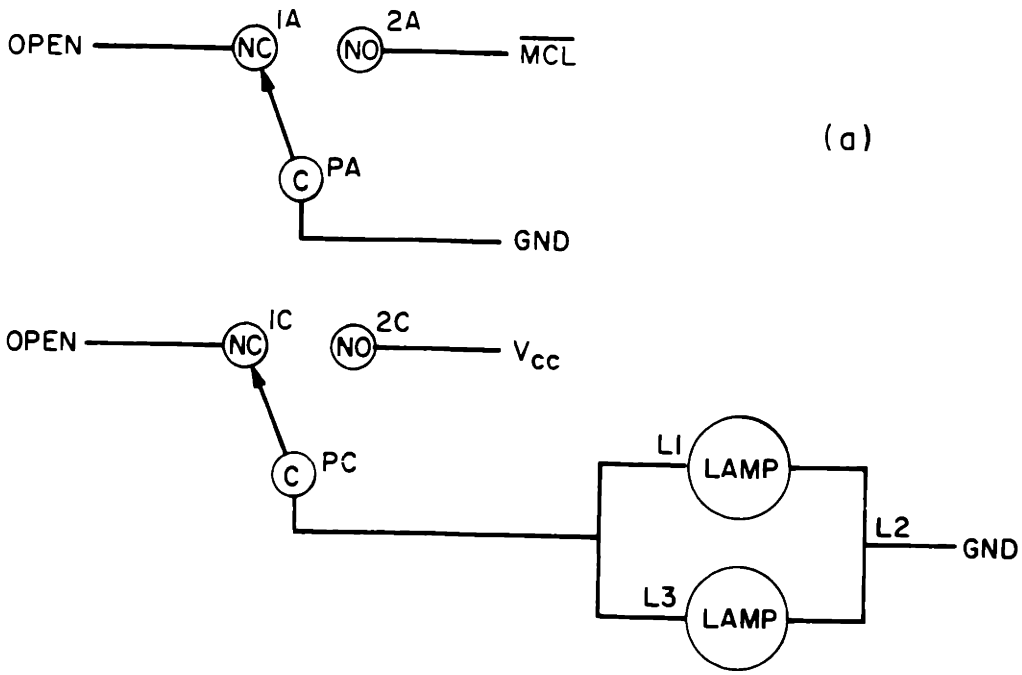

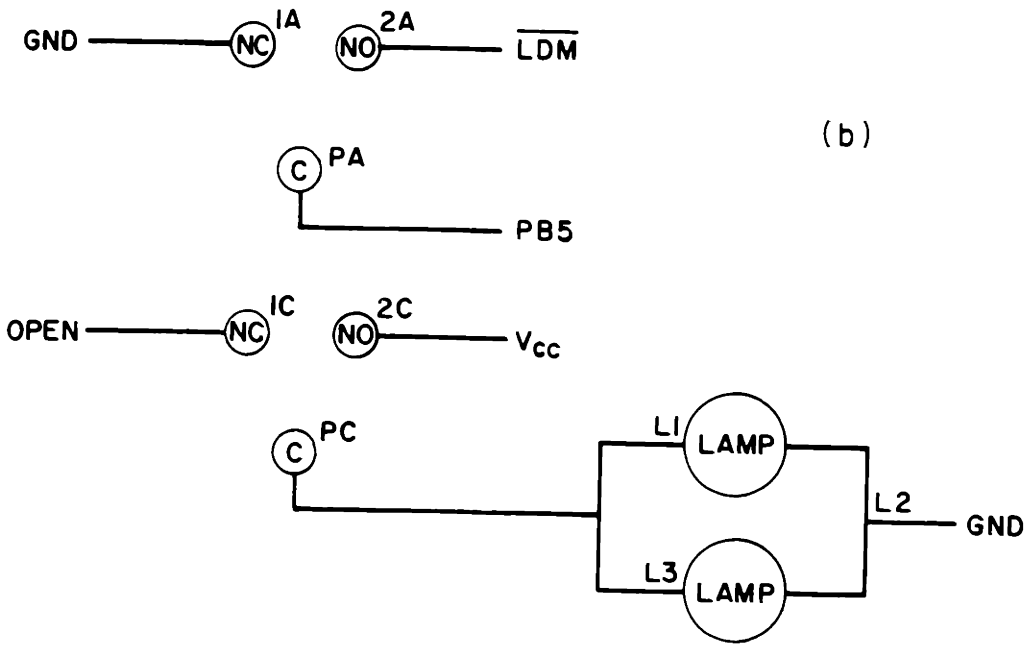

Figure 33: Gate B6

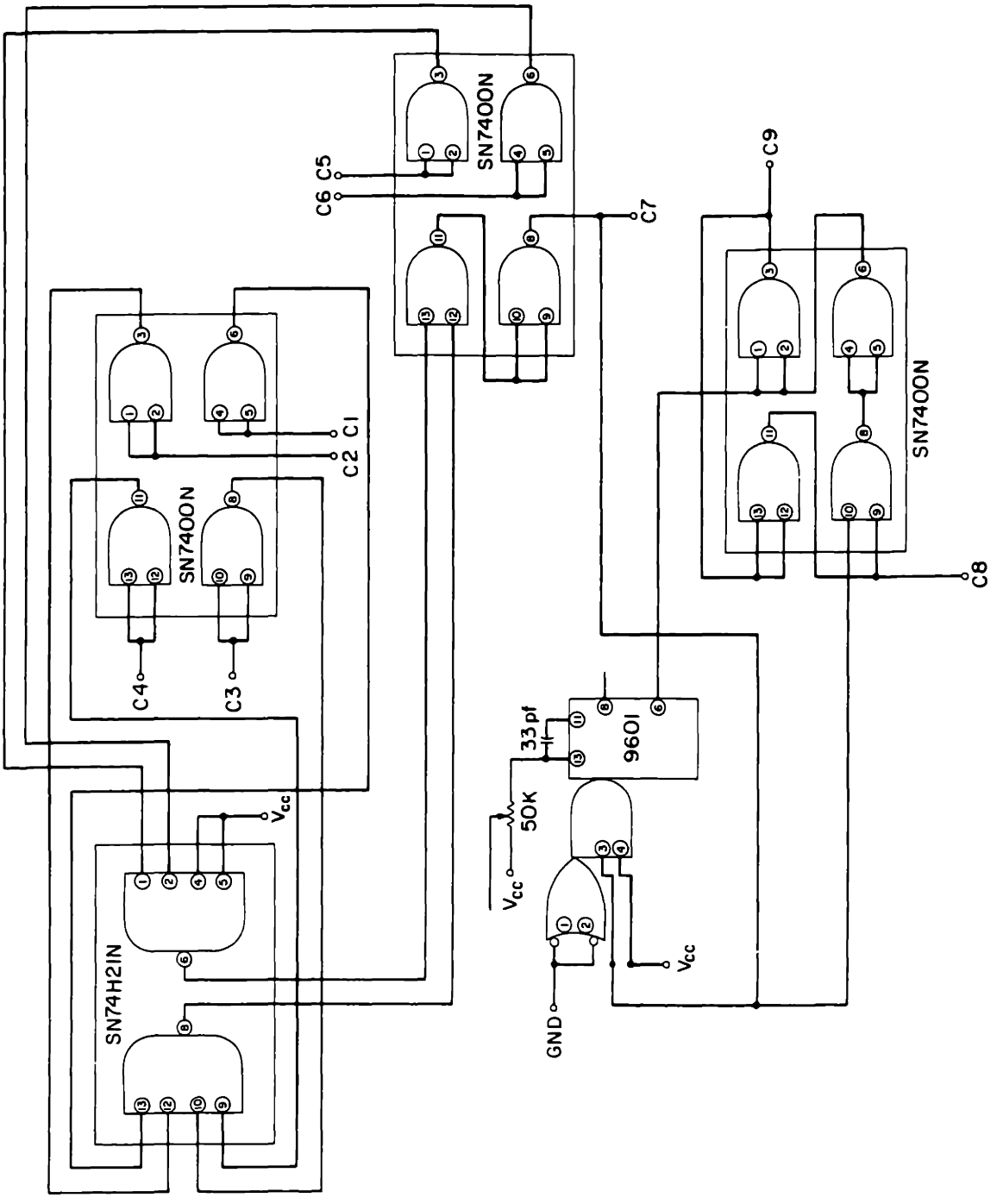

Figure 34: ADC4: Data Multiplexer and Break Request B7

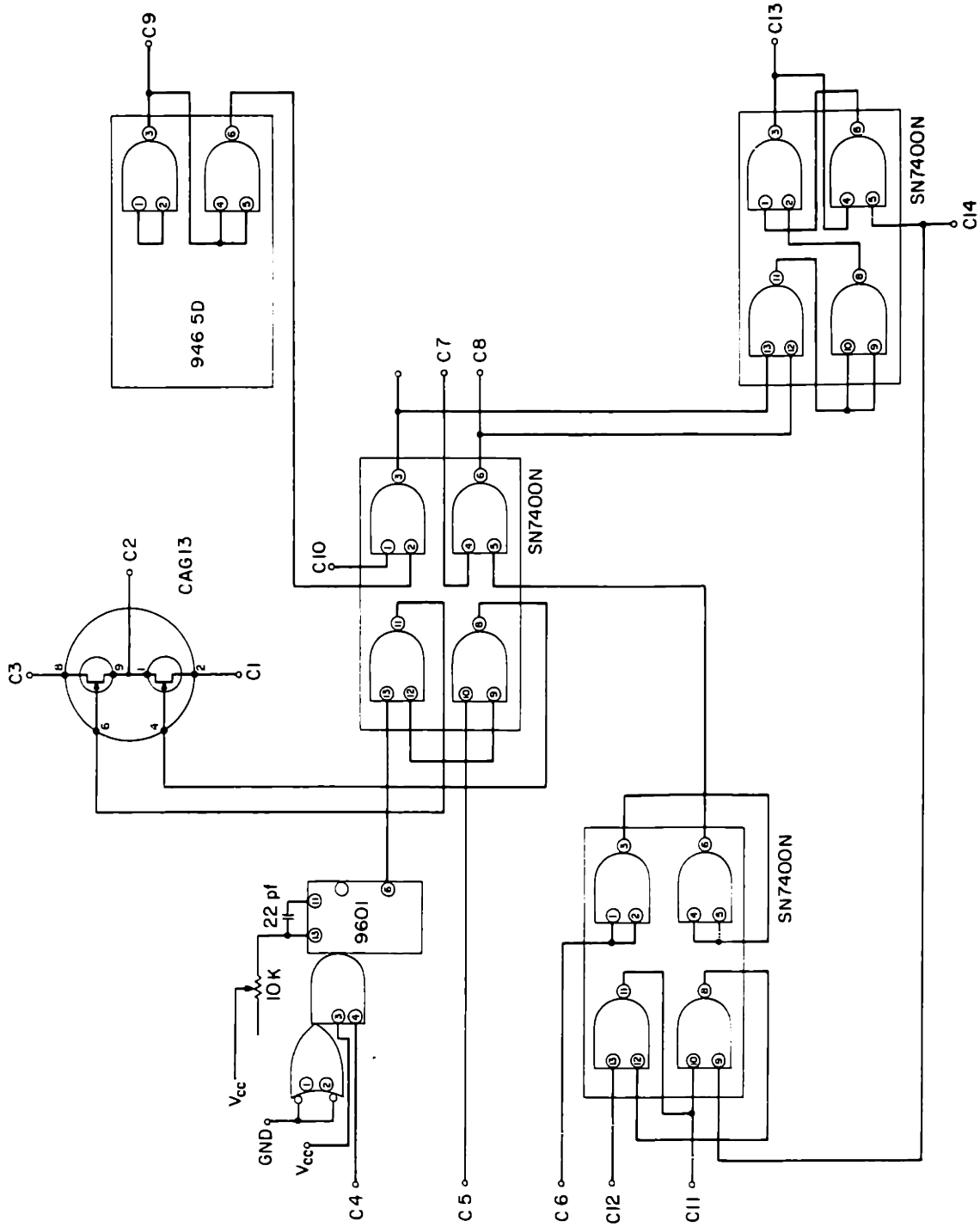

Figure 35: ADC3: data timing circuit A7

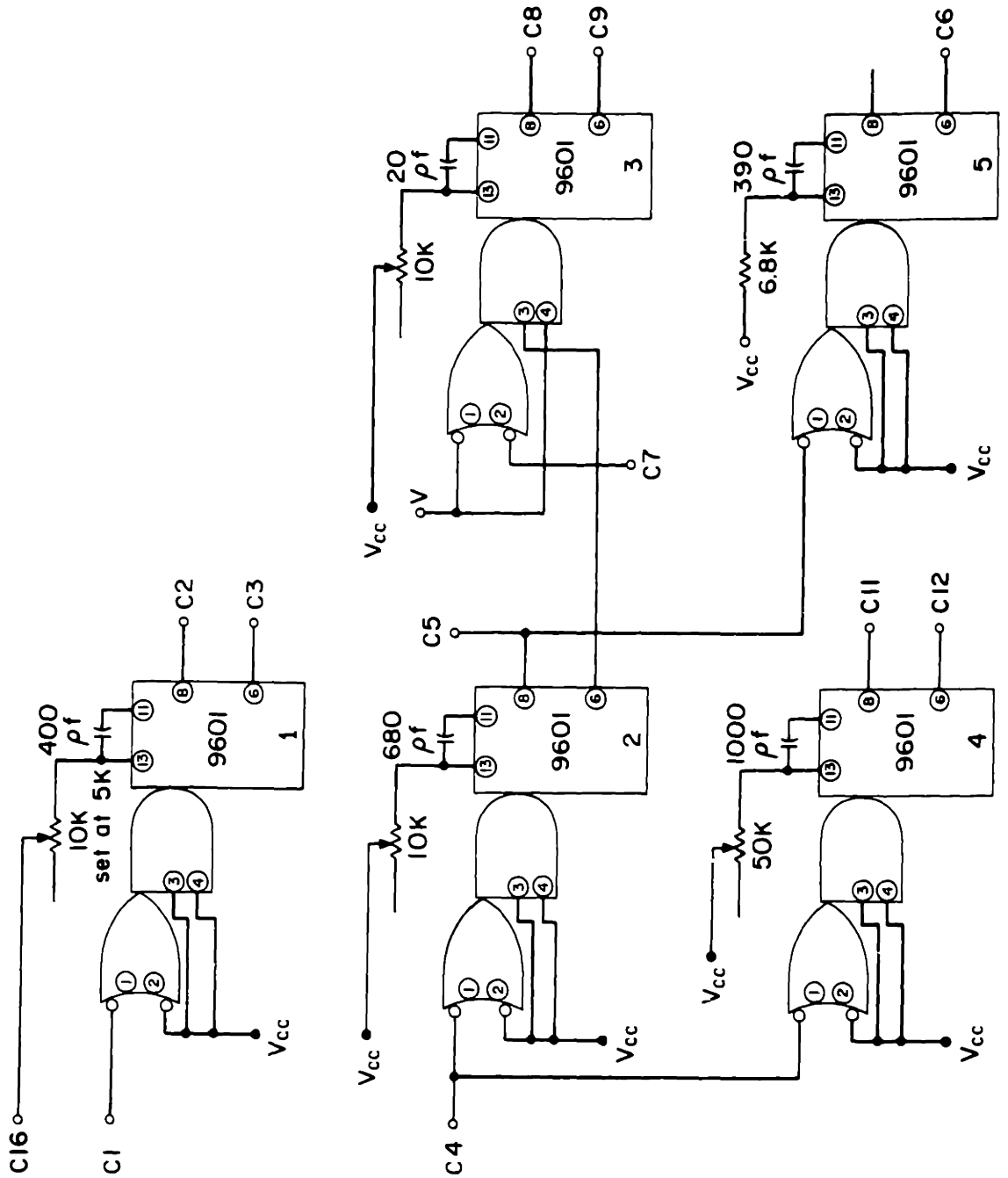

Figure 36: ADC Data: Gray/Binary Converter C6

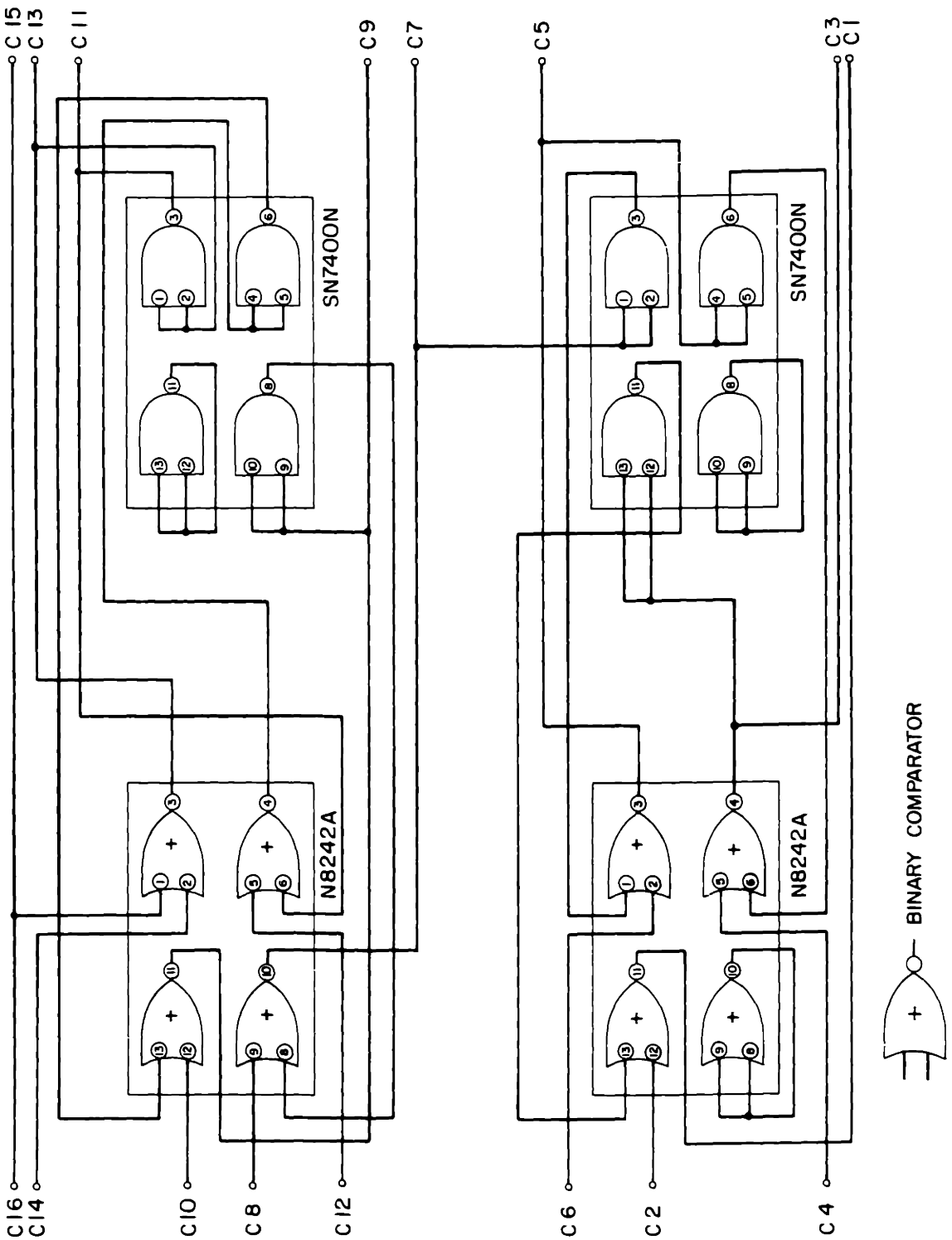

IV. WIRING

A. GENERAL PIN CARDS

Wire list convention is the following:

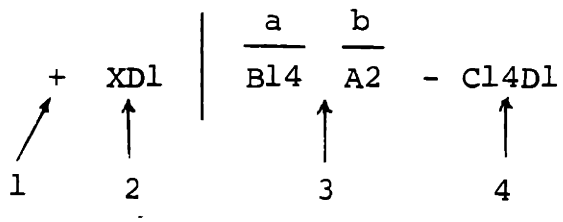

1. + incoming signal name

   - outgoing signal name

   ǂ bussed or multiply-connected incoming signal

   = bussed or multiply-connected outgoing signal

   a bar on the signal indicates active LOW.

2. Signal mnemonic

3. (a) card slot number for this card in the pulse programmer

   (b) pin number (DEC convention)

4. Same as 3--pin 3 is connected to pin 4.

B. PANEL CONNECTOR CARDS

Same as above but with wire connection to panel indicated. Wire numbering corresponds to the panel connector pin number.

C. ROTARY SWITCHES

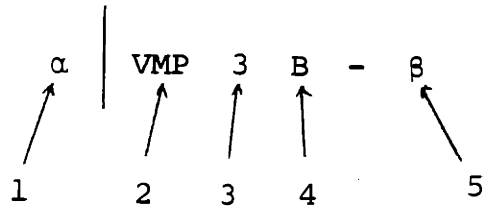

1. Same as 1 and 2 of A.

2. Switch name (usually mnemonic for function).

3. Number of switch position. P stands for pole.

4. Switch deck number. For the rotary switches corresponding to pulses (x y etc) and analog delays 3 and 4 are replaced by something like

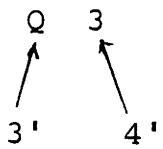

3' indicates switch connection (my labelling)

4' connection number

5. Connector card wire or pin number connected.

D. PUSHBUTTON SWITCHES

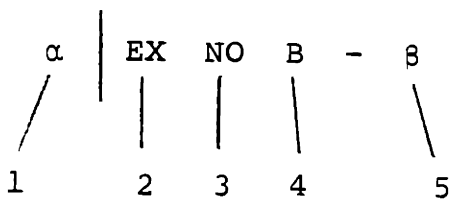

1. Same as 1 and 2 of A

2. Switch name

3. Position of single-pole double-throw switch

C : pole

NC : normally connected

NO : normally off

4. deck of switch 5. connection

For pushbutton switches L1, L2, L3 indicate light connections on the switch:

L1 - top lamp

L2 - common (connected to ground)

L3 - bottom lamp

E. WIRING LISTS

Detailed wiring lists follow in this section. The pins are named according to the conventions in Sections A-D. The lists are labelled in alphabetical order for easy access and may be cross-referenced to the schematic diagrams and card layout diagram in Section II of this chapter.

A1

	A1	A2 - NC	-GND	A1	A2 - GND
	"	B2 - NC	(1)BMB00	"	B1 - C16U1
-GND	"	C2 - GND	-GND	"	C1 - GND
(0)BMB06	"	D2 - D13H2, D14H2, D12H2 D11H2	(1)BMB01	"	S1 - C16V1
(1) BMB06	"	E2 - D10H2, D9H2	(1)BMB02	"	E1 - C16J2
# GND	"	F2 - NC	-GND	"	F1 - GND
(0)BMB07	"	H2 - D13J2,D14J2,D10J2 D9J2	(0)BMB03	"	H1-D14D2,D13D2, D12D2,D11D2, D10D2,D9D2
#GND	"	J2 - NC	(1)BMB03	"	J1 - NC
(1)BMB07	"	K2 - D12J2, D11J2	-GND	"	K1 - GND
#GND	"	L2 - NC	(0)BMB04	"	L1 - NC
(0)BMB08	"	M2 - D13K2, D12K2,D10K2	(1)BMB04	"	M1 - D14L2, D13L2, D12E2,D11E2, D10E2,D9E2
#GND	"	N2 - NC	-GND	"	N1 - NC
(1)BMB08	"	P2 - D14K2,D11K2, D9K2	(0)BMB05	"	P1 - NC
#GND	"	R2 - NC	-GND	"	R1 - GND
(1)BMB09	"	S2 -	(1)BMB05	"	S1 -D14F2,D13F2 D12F2,D11F2, D10F2,D9F2
(1)BMB10	"	T2 -	-GND	"	T1 - GND
-GND	"	U2 - GND		"	U1 - NC
(1)BMB11	"	V2 -		"	V1 - NC

A7

C1	$\overline{SPL}$	A7	A2 - C5M2
C2	DLY	"	B2 - C28N1
C3	$\overline{DLY}$	"	C2 - NC
C4	INTG	"	D2 - C28R1
C5	DDLY	"	E2 - NC
C6	$\overline{DDLY}$	"	F2 - B7R2
C7	ADD.ACP.T.	"	H2 - D15F2
C8	INTRPG.	"	J2 - pin 1 of ADC
C9	$\overline{INTROG.}$	"	K2 - B7D2
C10		"	L2 - NC
C11	SCP	"	M2 - back panel
C12	$\overline{SCP}$	"	N2 - B7H2
C13		"	P2 - NC
C14		"	R2 - NC
C15		"	S2 - NC
C16	DPOT	"	T2 - C28T1
C17	Vcc	"	U2 - Vcc
C18	GND	"	V2 - GND

A9

BCO	A9	A2 - NC	
+B	"	B2 - A16 N2	
B	"	C2 - NC	
-BCO	"	D2 - C27 Y2	
TP2	"	E2 - B23 P2	
$\overline{CL}$	"	F2 - B21 P1	
$\overline{SCL}$	"	H2 - B9 B2	
-SKP1	"	J2 - A13 B2	
-EBC	"	K2 - B9 C2	
-SB	"	L2 - A15 M2	
$\overline{TP1}$	"	M2 - A23 P2	
-SBO	"	N2 - C27 Y1	
-ESB	"	P2 - A11 E2	
$\overline{TP1}$	"	R2 - NC	
	"	S2 - NC	
-SKP2	"	T2 - A13 F2	
#Vcc	"	U2 - NC	
-GND	"	V2 - NC	

AB11

-2^5	A11	A2 - C27 F1	SBO	B11	A2 - C27 Y1
-2^4	"	B2 - C27 J1		"	B2 - NC
#$\overline{CL}$	"	C2 - B21 P1		"	C2 - NC
-2^6	"	D2 - C27 D1		"	D2 - NC
-ESB	"	E2 - A9 P2		"	E2 - NC
-2^7	"	F2 - C27 B1		"	F2 - NC
- TP2	"	H2 - NC		"	H2 - NC
-TP2	"	J2 - B23 P2		"	J2 - NC
-2	"	K2 - C27 R1	-CC	"	K2 - C27 A1
-1	"	L2 - C27 T1	-BAC10	"	L2 - B1 E2
-J1$\overline{IOP1}$	"	M2 - D14 B1		"	M2 - Nc
-2^2	"	N2 - C27 N1		"	N2 - NC
	"	P2 - NC		"	P2 - NC
-2^3	"	R2 - C27 L1	-BAC11	"	R2 - B1 H2
SB	"	S2 - A15 M2	-BAC09	"	S2 - B1 D2
#$\overline{TP1}$	"	T2 - A23 R2		"	T2 - NC
#Vcc	"	T2 - NC	#Vcc	"	T2 - NC
#GND	"	V2 - NC	#GND	"	V2 - NC

AB13

- CA4	A13	A2 - D22 N2	-CL2	B13	A2 - C15 H2
- SKP1	"	B2 - A9 J2	-CL4	"	B2 - C15 S2
- CA2	"	C2 - D22 T2	+MA2	"	C2 - D22 J2
# $\overline{TP1}$	"	D2 - A23 R2	+MA1	"	D2 - D22 L2
- CA1	"	E2 - D22 Y2	-CL1	"	E2 - C15 J2
- SKP2	"	F2 - A9 T2	-CL3	"	F2 - C15 T2
- CA3	"	H2 - D22 R2	-CL3	"	H2 - C14 T2
- MA3	"	J2 - D22 F2	-CL4	"	J2 - C14 S2
- SLA3	"	K2 - B15 S2	-CL1	"	K2 - C14 J2
- SLA2	"	L2 - B15 R2	+MA4	"	L2 - D22 D2
- SLA1	"	M2 - B15 P2	-CL2	"	M2 - C14 H2
- $\overline{TP2}$	"	N2 - B23 S2	+SKP4	"	N2 - from DC
- J0 $\overline{IOP4}$	"	P2 - D13 F1		"	P2 - NC
- MEM	"	R2 - C28 S2		"	R2 - NC
- SLA4	"	S2 - B15 T2		"	S2 - NC
- $\overline{CC}$	"	T2 - B21 T2		"	T2 - NC
# Vcc	"	T2 - NC	# Vcc	"	T2 - NC
# GND	"	T2 - NC	# GND	"	T2 - NC

A14

# XD1	A15 A2	C14 A2
# XD2	" B2	C14 B2
# XD3	" C2	C14 K2
# XD4	" D2	C14 L2
# YD1	" E2	C15 A2
# YD2	" F2	C15 B2
# YD3	" H2	C15 K2
# YD4	" J2	C15 L2
-SOA14	" K2	NC
-SOA 15	" L2	NC
- DC	" M2	D24F2, [illegible]
	" N2	NC
# WE2	" P2	D13 C1
- DA5	" R2	B1 M1
- DA6	" S2	B1 P1
	" T2	NC
# Vcc	" U2	NC
# GND	" V2	NC

A15

# XD1	A15 A2	C14 A2
# XD2	" B2	C14 B2
# XD3	" C2	C15 K2
# YD4	" D2	C14 L2
# YD1	" E2	C15 A2
# YD2	" F2	C15 B2
# YD3	" H2	C15 K2
# YD4	" J2	C15 L2
-SOA17	" K2	NC
-SOA18	" L2	NC
- SB	" M2	D24L2, A11S2, A9L2
- S	" N2	C5S2, D24J2
# WE2	" P2	D13 C1
- DA5	" R2	B1 J1
- DA6	" S2	B1 L1
	" T2	NC
# Vcc	" U2	NC
# GND	" V2	NC

A16

# XD1	A16 A2	C14 A2
# XD2	" B2	C14 B2
# XD3	" C2	C14 K2
# XD4	" D2	C14 L2
# YD1	" E2	C15 A2
# YD2	" F2	C15 B2
# YD3	" H2	C15 K2
# YD4	" J2	C15 L2
-SOA15	" F2	NC
-SOA16	" L2	NC
- DJ	" M2	C17F2, D24R2
- B	" N2	A9B2, D24N2
# WE2	" P2	D13 C1
- DA3	" R2	B1 E1
- DA4	" S2	B1 H1
	" T2	NC
# Vcc	" U2	NC
# GND	" V2	NC

A17

# XD1	A17 A2	C14 A2
# XD2	" B2	C14 B2
# XD3	" C2	C14 K2
# XD4	" D2	C14 L2
# YD1	" E2	C15 A2
# YD2	" F2	C15 B2
# YD3	" H2	C15 K2
# YD4	" J2	C15 L2
-SOA13	" K2	NC
-SOA14	" L2	NC
- DI	" M2	C17R2, D24T2
- DZ	" N2	C17F1, D24T2
# WE2	" P2	D13 C1
- DA1	" R2	B1 B1
- DA2	" S2	B1 D1
	" T2	NC
# Vcc	" U2	NC
# GND	" V2	NC

A18

# XD1	A18 A2	C14 A2
# XD2	" B2	C14 B2
# XD3	" C2	C14 K2
# XD4	" D2	C14 L2
# YD1	" E2	C15 A2
# YD2	" F2	C15 B2
# YD3	" H2	C15 K2
# YD4	" J2	C15 L2
-SOA11	" K2	NC
-SOA12	" L2	NC
-H	" M2	D25F2, C8,10,12,L2
-J	" N2	B19F2, D25D2
# WE1	" P2	D13 A1
- DA11	" R2	B1 E2
- DA12	" S2	B1 M2
	" T2	NC
# Vcc	" U2	NC
# GND	" V2	NC

A19

	A19 A2	NC
	" B2	NC
	" C2	NC
nSec	" D2	A27 M2
10^{-4}	" E2	A27 K2
	" F2	NC
	" H2	NC
	" J2	NC
	" K2	NC
10^{-2}	" L2	A27 E2
10^{-3}	" M2	A27 M2
	" N2	NC
	" P2	NC
Sec	" R2	A27 A2
10^{-1}	" S2	A27 C2
1Sec	" T2	A27 P2
Vcc	" U2	NC
GND	" V2	NC

A20

-$\overline{AD}$	B19 A2	C17 D1
-$\overline{DCD}$	" B2	C19 C1
	" C2	NC
DIR	" D2	D23 J2
	" E2	NC
C	" F2	A18 N2
TP1	" H2	A23 N2
CT	" J2	D19 D2
	" K2	A27 C1
	" L2	NC
	" M2	NC
	" N2	NC
CC	" P2	A27 U2
C3	" R2	C19 M2
C2	" S2	C19 J1
C1	" T2	C19 V1
GND	" U2	NC
Vcc	" V2	NC

A821

-X	A21 A2	B16 M2
-$\overline{X}$	" B2	B16 N2
-Y	" C2	B17 M2
-$\overline{Y}$	" D2	B17 N2
-$\overline{YB}$	" E2	B27 E2
-YB	" F2	B27 H2
-$\overline{XB}$	" H2	B27 K2
-$\overline{XB}$	" J2	B27 M2
	" L2	NC
-V	" M2	B18 M2
-$\overline{V}$	" N2	B18 N2
	" P2	NC
-EPC	" R2	A28 A1
-VB	" S2	B27 C2
-$\overline{VB}$	" T2	B27 A2
#Vcc	" U2	NC
#GND	" V2	NC

	A21 A1	NC
	" B1	NC
	" C1	NC
	" D1	NC
	" E1	NC
-$\overline{YC}$	" F1	C25J2,C10J2
-YC	" H1	C25F2,C10H2
-$\overline{XC}$	" J1	C25B2, C12J2
-XC	" K1	C25E2, C12H2
	" M1	NC
	" N1	NC
	" P1	NC
	" R1	NC
	" S1	NC
-$\overline{VC}$	" T1	C25M2, C8J2
-VC	" U1	C25P2, C8 H2
	" V1	NC

AB21

	B21 A2 - NC		B21 A1 - NC
	" B2 - NC		" B1 - NC
	" C2 - NC		" C1 - NC
	" D2 - NC		" D1 - NC
	" E2 - NC		" E1 - NC
-$\overline{LBG}$	" F2 - B27 U2, BACK COAX		" F1 - NC
	" H2 - NC		" H1 - NC
	" J2 - NC		" J1 - NC
	" K2 - NC		" K1 - NC
	" L2 - NC		" L1 - NC
-ST	" M2 - A25 P2		" M1 -NC
	" N2 - Nc	+$\overline{CL}$	" N1 - C10T2,C8T2, to DC
	" P2 - NC	+$\overline{CL}$	" P1 - A11C2, A9F2
	" R2 - NC	+$\overline{CL}$	" R1 - A25 C2, C16C2
-$\overline{ST}$	" S2 - B25 L2	+$\overline{MCL}$	" S1 - A27 A1
+$\overline{CL}$	" T2 - A13 T2, C12 T2		" T1 - NC
#Vcc	" U2 - NC		" U1 - NC
#GND	" V2 - NC		" V1 - NC

AB23

- $\overline{ECD}$	A23 A2 - C19 C1	-EL	B23 A2 - D23 D2
- $\overline{BG}$	" B2 - B27 P2		" B2 - NC
$\overline{CCBG}$	" C2 - D14 F1		" C2 - NC
- $\overline{ENDI}$	" D2 - C23 L2		" D2 - NC
	" E2 - A23 H2		" E2 - NC
- $\overline{EOD}$	" F2 - C23 A2	-PB1	" F2 - A27 M1
- Vcc	" H2 - A23 U2	-$\overline{SI}$	" H2 - NC
- $\overline{END2}$	" J2 - C23 B2	-SI	" J2 - A27 U1
-END	" K2 - A27 S1		" K2 - NC
	" L2 - NC		" L2 - NC
- Ex	" M2 - A27 P1		" M2 - NC
+ TPI	" N2 - C19 H1, C5 R2 COAX		" N2 - NC
+ $\overline{TPI}$	" P2 - C10 R2, C8 R2 A2 M2	-TP2	" P2-A11J2,A9E2 to DC,B4 D2
+ $\overline{TPI}$	" R2 - A13 D2, C12 R2 A11 T2	-PB2	" R2 - A27 K1
+ $\overline{TPI}$	" S2 - C17 E2, D28 H2 D28 P2	-$\overline{TP2}$	" S2 - A13 N2
+ $\overline{TPI}$	" T2 - to DC		" T2 - NC
+ Vcc	" U2 - A23 H2	+ Vcc	" U2 - NC
+ GND	" V2 - NC	+ Gnd	" V2 - NC

* Wire 1st 8 inputs along different paths from corresponding M908's to MS generator.

AB25

	A25 A2 - NC	-1	B25 A2 - A28 P1
	" B2 - NC	-2^1	" B2 - A28 U1
+$\overline{CL}$	" C2 - B21 R1	-2	" C2 - A28 S1
-SEC	" D2 - A28 K1	-2^3	" D2 - A28 U2
-RDLT	" E2 - C23 F2	-RDUN	" E2 - A28 E1
	" F2 - NC	-2^4	" F2 - A28 S2
	" H2 - NC	-2^6	" H2 - A28 M2
	" J2 - NC	-2^5	" J2 - A28 P2
-ERD	" K2 - A28 M1	-2^7	" K2 - A28 K2
+PB3	" L2 - A27 H1	$\overline{STP}$ - $\overline{ST}$	" L2 - B21 S2, C28U2
	" M2 - NC	$\overline{RDPI}$	" M2 - D7 D2
-PB4	" N2 - A27 E1		" N2 - NC
-ST	" P2 - B21 M2	-2^8	" P2 - A28 H2
+SEC	" R2 - A28 H1	-2^{10}	" R2 - A28 C2
-$\overline{BD}$	" S2 - A28 C1	-2^9	" S2 - A28 E2
-$\overline{RD}$	" T2 - C17 D1	-2^{11}	" T2 - A28 A2
#Vcc	" U2 - NC	#Vcc	" U2 - NC
#GND	" V2 - NC	#GND	" V2 - NC

A27

-SEC	A 27 A2 - A19 R2	: 8A
#GND	" B2 - NC	GND BUS
-10^{-1}	" C2 - A19 S2	: 7A
#GND	" D2 - NC	GND BUS
-10^{-2}	" E2 - A19L2	: 6A
#GND	" F2 - NC	GND - BUS
+mSEC	" H2 - A19D2	: 5A
#GND	" J2 - NC	GND BUS
-10^{-4}	" K2 - A19E2	: 4A
#GND	" L2 - NC	GND BUS
-10^{-5}	" M2 - A19M2	: 3A
#GND	" N2 - NC	GND BUS
+uSEC	" P2 - A19T2	: 2A
#GND	" R2 - NC	GND BUS
-CR	" S2 - C19C2	: PA
#GND	" T2 - NC	GND BUS
-CC	" U2 - B19P2	: 11A
#GND	" V2 - NC	GND BUS

A27

$\overline{MCL}$	A27 A1 - B21 S1, C7N2, C7J2 C7R2		CL NO A
#GND	" B1 - NC		GND BUS
$\overline{STP}$	" C1 - B19K2		ST NO B
#GND	" D1 - NC		GND BUS
PB4	" E1 - A25 N2		START CA
#GND	" F1 - NC		GND BUS
PB3	" H1 - A25 L2		START NO A
#GND	" J1 - NC		GND BUS
-PB2	" K1 - B23 R2		EXEC CA
#GND	" L1 - NC		GND BUS
-PB1	" M1 - B23 P2		EXEC NO A
#GND	" N1 - NC		GND BUS
-(EX+$\overline{STO}$)	" P1 - A23 M2		SI C A, STNOA
#GND	" R1 - NC		GND BUS
-END	" S1 - A23 K2		SI NC A
#GND	" T1 - NC		GND BUS
-SI	" U1 - B23 J2		SI NO A
#GND	" V1 - NC		GND BUS

A28

EPC	A28 A1 - A21R2		MODE PB
#GND	" B1 - NC		GND BUS
$\overline{BD}$	" C1 - A25S2,D28K2, D28S2		MODE 4,5,6,7,8,9 A
#GND	" D1 - NC		GND BUS
-RD 4M	" E1 - B25E2		RD 4M CA
#GND	" F1 - NC		GND BUS
-MSEC	" H1 - A25R2		4M NC A
#GND	" J1 - NC		GND BUS
-SEC	" K1 - A25D2		4M NO A
#GND	" L1 - NC		GND BUS
-ERD	" M1 - A25 K2		RD PA
#GND	" N1 - NC		GND BUS
-1	" P1 - B25 A2		RD 1A
#GND	" R1 - NC		GND BUS
-2	" S1 - B25C2		RD 2A
#GND	" T1 - NC		GND BUS
-2$^{\frac{1}{2}}$	" U1 - B25B2		RD 3A
#GND	" V1 - NC		GND BUS

A28

2^{11}	A28 A2 - B25 T2		RD 11A
GND	" B2 - NC		GND BUS
2^{10}	" C2 - B25 R2		RD 10A
GND	" D2 - NC		GND BUS
2^{9}	" E2 - B25 S2		RD 10A
GND	" F2 - NC		GND BUS
2^{8}	" H2 - B25P2		RD 9A
GND	" J2 - NC		GND BUS
2^{7}	" K2 - B25 K2		RD 8A
GND	" L2 - NC		GND BUS
2^{6}	" M2 - B25 H2		RD 7A
GND	" N2 - NC		GND BUS
2^{5}	" P2 - B25 J2		RD 6A
GND	" R2 - NC		GND BUS
2^{4}	" S2 - B25F2		RD 5A
GND	" T2 - NC		GND BUS
2^{3}	" U2 - B25D2		RD 4A
GND	" V2 - NC		GND BUS

B1

	B1 A2 - NC	-GND	B1 A1 - GND
	" B2 - NC	-BAC00	" B1 - C19A1, A17R2 B15D1
-GND	" C2 - GND	- GND	" C1 - GND
-BAC09	" D2 - B11S2,C19S1, B18S2	-BAC01	" D1 - C19D1,A18S2, B15T1
-BAC10	" E2 - B11L2,C19P2, A18R2	-BAC02	" E1 -C19B2,A16R2, B15S1
#GND	" F2 - NC	-GND	" F1 - GND
-BAC11	" H2 - B11R2,C19T2 A18S2	-BAC03	" H1 - B9H2,C19E2, B15R1,A16S2
#GND	" J2 - NC	-BAC04	" J1 - B9E2,C19F1, B16R2,A15R2
-BIOP1	" K2 - D14 P2	-GND	" K1 - GND
#GND	" L2 - NC	-BAC05	" L1 - B9F2,C19K1, B16S2,A15S2
-BIOP2	" M2 - D14 R2	-BAC06	" M1 - C19H2,C19C1 B17R2,A14R2
#GND	" N2 - NC	-GND	" N1 - GND
-BIOP4	" P2 - D14S2	-BAC07	" P1 - C19J2,C19L2 B17S2, A14S2
#GND	" R2 - NC	- GND	" R1 - GND
-BTS5	" S2 -	-BAC08	" S1 - C19N1,C19R2 B18R2
-BTS2	" T2 - NC	-GND	" T1 - GND
-GND	" U2 - GND		" U1 - NC
-BAINIT	" V2 - NC		" V1 - NC

B3

	B3	A2 - NC		-GND	B3	A1 - GND
	"	B2 - NC		-I000	"	B1 - D5B1
-GND	"	C2 - GND		- GND	"	C1 - GND
-I009	"	D2 - D5J2, D7F2		-I001	"	D1 - D5E1
-I010	"	E2 - D5L2, D7J2		-I002	"	E1 - D5H1,D7B1
#GND	"	F2 - NC		-GND	"	F1 - GND
-I011	"	H2 - D5N2,D7L2		-I003	"	H1 - D5K1,D7E1
#GND	"	J2 - NC		I004	"	J1 - D5M1,D7H1
-$\overline{SKP}$	"	K2 - D6N2		-GND	"	K1 - GND
#GND	"	L2 - NC		-I005	"	L1-D5P1,D7K1
-$\overline{PI}$	"	M2 -D6L2		-I006	"	M1-D5S1,D7M1
#GND	"	N2 - NC		-GND	"	N1 - GND
-$\overline{RCCL}$	"	P2 - NC		-I007	"	P1 - D5U1, D7P1
#GND	"	R2 - NC		-GND	"	R1 - GND
-$\overline{BRUN}$	"	S2 - NC		-I008	"	S1 - D5F2,D7S1
	"	T2 - NC		-GND	"	T1 - GND
-GND	"	U2 - GND			"	U1 - NC
	"	V2 - NC			"	V1 - NC

B6

C1	Y	B6 A2 - D8D1	
C2	-Y	" B2 - D8F1	
C3	-X	" C2 - D8J1	
C4	X	" D2 - D8E2	
C5	V	" E2 - D8A1 (GND)	
C6	-V	" F2 - D8C1 (GND)	
C7	X-X Y-Y	" H2 - D4E2	
C8	$\overline{SPG}$	" J2 - NC	
C9	SPG	" K2 - D4H2	
C10			
C16			
C17	+5V	" U2 - +5V	
C18	GND	" V2 - GND	

B7

C1	ANAL2	B7 A2 - back panel Ch.2	
C2	AD12	" B2 - pin 8 of ADC	
C3	ANAL1	" C2 - back panel Ch.1	
C4	$\overline{INTROG}$	" D2 - A7K2	
C5	$\overline{INTC}$	" E2 - C28F1	
C6	-	" F2 - B7E2 and back panel	
C7	$\overline{SCP}$	" H2 - A7M2	
C8	HOLD	" J2 - back panel	
C9	BTS 5	" K2 - B1S2	
C10	B-BREAK	" L2 - D15H2	
C11	MADD01	" M2 - D6Y1	
C12	ADD.ACPT	" N2 - C3S2	
C13	BK REQ	" P2 - D6H2	
C14	$\overline{DODLY}$	" R2 - A7F2	
C15		" S2 - +15 v	
C16		" T2 - -15 v	
C17		" U2 - Vcc	
C18		" V2 - GND	

B9

-I	B9 A2 - C27 T2	
$\overline{BCI}$	" B2 - A9 H2	
-EBC	" C2 - A9 K2	
-TP2	" D2 - B2J P2	
-BAC4	" E2 - B1 J1	
-BAC5	" F2 - B1 L1	
-BAC03	" H2 - B1 H1	
-I^{6}	" J2 - C27 N2	
-I^{5}	" K2 - C27 P2	
-I^{7}	" L2 - C27 L2	
-I1$\overline{IOP1}$	" M2 - D14 B1	
-I^{10}	" N2 - C27 D2	
-I^{8}	" P2 - C27 J2	
-CC	" R2 - C27 A2	
-I^{9}	" S2 - C27 F2	
-I^{11}	" T2 - C27 B2	
#Vcc	" U2 - NC	
#GND	" V2 - NC	

B15

# XD1	B15 A2 - C14 A2		B15 A1 - NC
# XD2	" B2 - C14 B2		" B1 - NC
# XD3	" C2 - C14 K2		" C1 - NC
# XD4	" D2 - C14 L2		" D1 - NC
# YD1	" E2 - C15 A2		" E1 - NC
# YD2	" F2 - C15 B2		" F1 - NC
# YD3	" H2 - C15 K2		" H1 - NC
# YD4	" J2 - C15 L2		" J1 - NC
-SDA1	" K2 - NC		" K1 - NC
-SDA2	" L2 - NC		" L1 - NC
-SDA3	" M2 - NC		" M1 - NC
-SDA4	" N2 - NC		N1 - NC
-SLA1	" P2 - A13 M2		" P1 - NC
-SLA2	" R2 - A13 L2	- DA4	" R1 - B1 H1
-SLA3	" S2 - A13 K2	- DA3	" S1 - B1 E1
-SLA4	" T2 - A13 S2	- DA2	" T1 - B1 D1
# Vcc	" U2 - NC	- DA1	" U1 - B1 B1
# GND	" V2 - NC	- WE1	" V1 - D1J A1

B16

≠ XD1	B16 A2 - C14 A2	
≠ XD2	" B2 - C14 B2	
≠ XD3	" C2 - C14 K2	
≠ XD4	" D2 - C14 L2	
≠ YD1	" E2 - C15 A2	
≠ YD2	" F2 - C15 B2	
≠ YD3	" H2 - C15 K2	
≠ YD4	" J2 - C15 L2	
-SOA5	" K2 - NC	
-SOA6	" L2 - NC	
-X	" M2 - A21A2, D25V2	
-$\overline{X}$	" N2 - A21B2, D25T2	
≠ WE1	" P2 - D13 A1	
- DA5	" R2 - B1 J1	
- DA6	" S2 - B1 L1	
	" T2 - NC	
≠ Vcc	" U2 - NC	
≠ GND	" V2 - NC	

B17

≠ XD1	B17 A2 - C14 A2	
≠ XD2	" B2 - C14 B2	
≠ XD3	" C2 - C14 K2	
≠ XD4	" D2 - C14 L2	
≠ YD1	" E2 - C15 A2	
≠ YD2	" F2 - C15 B2	
≠ YD3	" H2 - C15 K2	
≠ YD4	" J2 - C15 L2	
-SOA7	" K2 - NC	
-SOA8	" L2 - NC	
-Y	" M2 - A21C2, D25R2	
-$\overline{Y}$	" N2 - A21D2, D25N2	
≠ WE1	" P2 - D13 A1	
- DA7	" R2 - B1 M1	
- DA8	" S2 - B1 P1	
	" T2 - NC	
≠ Vcc	" U2 - NC	
≠ GND	" V2 - NC	

B18

≠ XD1	B18 A2 - C14 A2	
≠ XD2	" B2 - C14 B2	
≠ XD3	" C2 - C14 K2	
≠ XD4	" D2 - C14 L2	
≠ YD1	" E2 - C15 A2	
≠ YD2	" F2 - C15 B2	
≠ YD3	" H2 - C15 K2	
≠ YD4	" J2 - C15 L2	
-SOA9	" K2 - NC	
-SOA10	" L2 - NC	
- V	" M2 - A21M2, D25L2	
- $\overline{V}$	" N2 - A21N2, D25J2	
≠ WE1	" P2 - D13 A1	
- DA9	" R2 - B1 S1	
- DA10	" S2 - B1 D2	
	" T2 - NC	
≠ Vcc	" U2 - NC	
≠ GND	" V2 - NC	

B27

			panel connections
-$\overline{V3}$	B27	A2 - A21 T2	MODE 9C
≠GND	"	B2 - NC	GND BUS
-V8	"	C2 - A21 S2	MODE 8C
≠GND	"	D2 - NC	GND BUS
-$\overline{Y8}$	"	E2 - A21 E2	MODE 7C
≠GND	"	F2 - NC	GND BUS
-Y8	"	H2 - A21 F2	MODE 6C
≠GND	"	J2 - NC	GND BUS
-$\overline{X8}$	"	K2 - A21 H2	MODE 5C
≠GND	"	L2 - NC	GND BUS
-X8	"	M2 - A21 J2	MODE 4C
≠GND	"	N2 - NC	GND BUS
-$\overline{BG}$	"	P2 - A23 B2	MODE 3A
≠GND	"	R2 - NC	GND BUS
-$\overline{INL}$	"	S2 - C7 M2	MODE 2A
≠GND	"	T2 - NC	GND BUS
+$\overline{LBG}$	"	U2 - B21 F2	MODE PA
≠GND	"	V2 - NC	GND BUS

B27

			panel connections
-PB5	B27	A1 - C7A2	LD CA
≠GND	"	B1 - NC	GND BUS
-$\overline{LDR}$	"	C1 - C7 B2	LD NOA
	"	D1 -	
	"	E1 -	
	"	F1 -	
	"	H1 -	
	"	J1 -	
	"	K1 -	
	"	L1 -	
	"	M1 -	
	"	N1 -	
	"	P1 -	
	"	R1 -	
	"	S1 -	
	"	T1 -	
	"	U1 -	
	"	V1 -	

C3

	C3	A2 - NC	-GND	C3	A1 - GND
	"	B2 - NC	-$\overline{\text{DAD00}}$	"	B1 - NC
-GND	"	C2 - GND	-GND	"	C1 - GND
-$\overline{\text{DAD09}}$	"	D2 - D3F2	-DAD01	"	D1 - NC
-$\overline{\text{DAD10}}$	"	E2 - D3J2	-$\overline{\text{DAD02}}$	"	E1 - D3B1
#GND	"	F2 - NC	-GND	"	F1 - GND
-$\overline{\text{DAD11}}$	"	H2 - D3L2	-$\overline{\text{DAD03}}$	"	H1 - D3E1
#GND	"	J2 - NC	-$\overline{\text{DAD04}}$	"	J1 - D3H1
-$\overline{\text{BRK}}$	"	K2 -	-GND	"	K1 - GND
#GND	"	L2 - NC	-$\overline{\text{DAD05}}$	"	L1 - D3K1
-DAIN	"	M2 - NC	-$\overline{\text{DAD06}}$	"	M1 - D3M1
#GND	"	N2 - NC	-GND	"	N1 - GND
-BBRK	"	P2 -	-$\overline{\text{DAD07}}$	"	P1 - D3P1
#GND	"	R2 - NC	-GND	"	R1 - GND
+BADDACC	"	S2 - NC	-$\overline{\text{DAD08}}$	"	S1 - D3S1
-$\overline{\text{MBINCR}}$	"	T2 - NC	-GND	"	T1 - GND
-GND	"	U2 - GND		"	U1 - NC
-BINIT	"	V2 -		"	V1 - NC

C5

-DAD03	C5	A2 - D8 L1	-DAD09	"	L2 - D8 V1
Open	"	B2 - NC	$\overline{\text{SPL}}$	"	M2 - A7 A2
-DAD07	"	C2 - D8 R1	-DAD10	"	N2 - D8 S2
-DAD05	"	D2 - D8 N1	-IOP2	"	P2 - D14 D1
-DAD02	"	E2 - D8 H2	-TP1	"	R2 - A23 N2
OPEN	"	F2 - NC	- S	"	S2 - A15 N2
-DAD04	"	H2 - D8 K2	-DAD08	"	T2 - D8 P2
-DAD06	"	J2 - D8 M2	#Vcc	"	U2 - NC
-DAD11	"	K2 - D8 U2	#GND	"	V2 - NC

C7

-PBS	C7	A2 - B27 A1		C7	A1 - NC
-$\overline{\text{LDM}}$	"	B2 - B27 C1		"	B1 - NC
	"	C2 - NC		"	C1 - NC
INTENS.	"	D2 - TO PDP 12 Green wire (put)		"	D1 - NC
	"	E2 - NC		"	E1 - NC
$\overline{\text{NCL}}$	"	F2 - A27 A1		"	F1 - NC
-$\overline{\text{LDMPI}}$	"	M2 - D4 D2, C16 S2		"	M1 - NC
-$\overline{\text{JSIOP1}}$	"	J2 - D9 B1		"	J1 - NC
-LDMPI	"	K2 - NC		"	K1 - NC
-$\overline{\text{INLP1}}$	"	L2 - D5 D2, C16 S1		"	L1 - NC
-$\overline{\text{INL}}$	"	M2 - B27 S2	$\overline{\text{NCL}}$	"	M1 - NC
-$\overline{\text{JSIOP4}}$	"	N2 - D9 F1	-INLPI	"	N1 - NC
-PLT	"	P2 - XY [illegible]		"	P1 - NC
-$\overline{\text{JSIOP2}}$	"	R2 - D9 D1	-PLTPI	"	R1 - NC
-$\overline{\text{PLTPI}}$	"	S2 - D3 D2, C16 T1	$\overline{\text{JIOP4}}$	"	S1 - D11 F1
$\overline{\text{JIOP1}}$	"	T2 - D11 B1 (coaxial)		"	T1 - NC
#Vcc	"	U2 - NC	$\overline{\text{EPLT}}$	"	U1 - To Scope (put)
#GND	"	V2 - NC		"	V1 - NC

C8

- VO	C8	A2 - D8 A1	- H	"	L2 - A18 M2
- $\overline{\text{VO}}$	"	B2 - D8 C1		"	M2 - NC
	"	C2 - NC		"	N2 - NC
- VMP	"	D2 - C20 J2		"	P2 - NC
- $\overline{\text{VMP}}$	"	E2 - C20 T2	# $\overline{\text{TP1}}$	"	R2 - A23 P2
	"	F2 - NC		"	S2 - NC
- VC	"	H2 - A21 U1	# $\overline{\text{CL}}$	"	T2 - B21 N1
- $\overline{\text{VC}}$	"	J2 - A21 T1	# Vcc	"	U2 - NC
	"	K2 - NC	# GND	"	V2 - NC

C6

C1	$\overline{B}_7$ (LSB)		C6	A2	- D6A1
C2	G_7 (LSB)		"	B2	-pin 23 of ADC
C3	$\overline{B}_6$		"	C2	- D6D1
C4	G_6		"	D2	- pin 18
C5	$\overline{B}_5$		"	E2	- D6F1
C6	G_6		"	F2	- pin 16
C7	$\overline{B}_4$		"	H2	- D6J1
C8	G_4		"	J2	- pin 24
C9	$\overline{B}_3$		"	K2	- DCL1
C10	G_3		"	L2	- pin 25
C11	$\overline{B}_2$		"	M2	- D6N1
C12	G_2		"	N2	- Pin 15
C13	$\overline{B}_1$		"	P2	- D6R1
C14	G_1		"	R2	- pin 3
C15	B_0 (MSB)		"	S2	- D6E2
C16	G_0 (MSB)		"	T2	- pin 5
C17	-5v		"		
C18	GND		"		

C10

- YO	C10	A2 - D8 D1			
- $\overline{\text{YO}}$	"	B2 - D8 F1			
	"	C2 - NC			
- YMP	"	D2 - C21 J2			
- $\overline{\text{YMP}}$	"	E2 - C21 T2			
	"	F2 - NC			
- YC	"	H2 - A21 H1			
- $\overline{\text{YC}}$	"	J2 - A21 F1			
	"	K2 - NC			
- H	"	L2 - A18 M2			
	"	M2 - NC			
	"	N2 - NC			
	"	P2 - NC			
# $\overline{\text{TP1}}$	"	R2 - A23 P2			
	"	S2 - NC			
# Vcc	"	U2 - NC			
# GND	"	V2 - NC			

C12

-XO	C12	A2 - D8 E2			
-$\overline{\text{XO}}$	"	B2 - D8 J1			
	"	C2 - NC			
-XMP	"	D2 - C22 J2			
-$\overline{\text{XMP}}$	"	E2 - C22 T2			
	"	F2 - NC			
-XC	"	H2 - A21 K1			
-$\overline{\text{XC}}$	"	J2 - A21 J1			
	"	K2 - NC			
- H	"	L2 - A18M2			
	"	M2 - NC			
	"	N2 - NC			
	"	P2 - NC			
#$\overline{\text{TP1}}$	"	R2 - A23 R2			
	"	S2 - NC			
#$\overline{\text{CL}}$	"	T2 - B21 T2			
#Vcc	"	U2 - NC			
#GND	"	V2 - NC			

C14 (C15)

= XD1	C14 A2 - B15 A2	= YD1	C15 A2 - B15 E2
= XD2	" B2 - B15 B2	= YD2	" B2 - B15 F2
	" C2 - NC		" C2 - NC
	" D2 - NC		" D2 - NC
	" E2 - NC		" E2 - NC
	" F2 - NC		" F2 - NC
- XL2	" H2 - B13 M2	- YL2	" H2 - B13 A2
- XL1	" J2 - B13 K2	- YL1	" J2 - B13 E2
= XD3	" K2 - B15 C2	= YD3	" K2 - B15 H2
= XD4	" L2 - B15 D2	= YD4	" L2 - B15 J2
	" M2 - NC		" M2 - NC
	" N2 - NC		" N2 - NC
	" P2 - NC		" P2 - NC
	" R2 - NC		" R2 - NC
- XL4	" S2 - B13 J2	- YL4	" S2 - B13 B2
- XL3	" T2 - B13 H2	- YL3	" T2 - B13 F2
# Vcc	" U2 - NC	# Vcc	" U2 - NC
# GND	" V2 - NC	# GND	" V2 - NC

C16

-CCLT	C16 A2 - D23 L2	C15 A1 - NC
	" B2 - NC	" B1 - NC
#$\overline{CL}$	" C2 - B21 R1	" C1 - NC
	" D2 - NC	" D1 - NC
	" E2 - NC	" E1 - NC
	" F2 - NC	" F1 - NC
	" H2 - NC	" H1 - NC
BMB02	" J2 - A1 E1	" J1 - NC
	" K2 - NC	" K1 - NC
	" L2 - NC	" L1 - NC
	" M2 - NC	" M1 - NC
-3305	" N2 - D11 N1	-3205 " N1 - D12 N1
-3105	" P2 - D14 N1	-3005 " P1 - D13 N1
-3405	" R2 - D10 N1	-3505 " R1 - D9 N1
-LDMPI	" S2 - C7 H2	-INLPI " S1 - C7 L2
PI	" T2 - D3 R2	PLTPI " T1 - C7 S2
#Vcc	" U2 - NC	BMB00 " U1 - A1 B1
#GND	" V2 - NC	BMB01 " V1 - A1 D1

C17

	C17 U2 - NC	-D0	C17 A1 - C23 K2
-AD4	" B2 - D27 E1	-AD3	" B1 - D27 K1
-AD2	" C2 - D27 P1	-AD1	" C1 - D27 G1
	" D2 - NC	-RD	" D1 - A25 T2, B19 A2
#PI	" E2 - A23 S2		" E1 - NC
-D3	" F2 - A16 M2	-D2	" F1 - A17 M2
	" H2 - NC		" H1 - NC
	" J2 - NC		" J1 - NC
	" K2 - NC		" K1 - NC
	" M2 - NC		" L1 - NC
	" N2 - NC		" M1 - NC
	" P2 - NC		" P1 - NC
-D1	" R2 - A17 M2		" R1 - NC
	" S2 - NC		" S1 - NC
	" T2 - NC		" T1 - NC
#Vcc	" U2 - NC	#Vcc	" U1 - NC
#GND	" V2 - NC	#GND	" V1 - NC

C19

-D000	C19 A2 - D5 A1	-BAC00	C19 A1 - B1 B1
-BAC02	" B2 - B1 E1	-D002	" B1 - D5 F1
-CR	" C2 - A27 S2	-$\overline{CCD}$	" C1-B19 B2 A15 A1
-D001	" D2 - D5 D1	-BAC01	" D1 - B1 D1
-BAC03	" E2 - B1 H1	-D003	" E1 - D5 J1
-D004	" F2 - D5 L1	-BAC04	" F1 - B1 J1
-BAC06	" H2 - B1 M1	-D006	" H1 - D5 R1
-BAC07	" J2 - B1 P1	-C2	" J1 - B19 B2
-D005	" K2 - D5 N1	-BAC05	" K1 - B1 L1
-BAC07	" L2 B1 P1	-D007	" L1-D5 V1
-C3	" M2 - B19 R2	-11$\overline{IOPI}$	" M1 - D14 B1
-D008	" N2 - D5 B2	-BAC08	" N1 - B1 S1
-BAC10	" P2 - B1 E2	-D010	" P1 - D5 K2
-BAC08	" R2 - B1 S1	-12$\overline{IOP4}$	" R1 - D12 S1
-BAC11	" T2 - B1 H2	-D011	" T1 - D5 M2
#Vcc	" U2 - NC	-BAC06	" U1 - B1 M1
#GND	" V2 - NC	-C1	" V1 - B19 T2
-D009	" S2 - D5 H1	-BAC09	" S1 - B1D1

C20

	C20 A2 - NC	
- $\overline{VP}$	" B2 - C28 K2	
	" C2 - NC	
	" D2 - NC	
- VP	" E2 - C28 M2	
- $\overline{VMPA}$	" F2 - C25 N2	
	" H2 - NC	
*-VMP	" J2 - C8 D2	
	" K2 - NC	
- $\overline{\bar{V}P}$	" L2 - C28 C2	
	" M2 - NC	
	" N2 - NC	
- $\bar{V}P$	" P2 - C28 E2	
- $\overline{\bar{V}MPA}$	" R2 - C25 L2	
	" S2 - NC	
*-$\bar{V}$MP	" T2 - C8 E2	
# Vcc	" U2 - NC	
# GND	" V2 - NC	

C21

	C21 A2 - NC	
- $\overline{YP}$	" B2 - D28 C1	
	" C2 - NC	
	" D2 - NC	
- YP	" E2 - D28 E1	
- $\overline{YMPA}$	" F2 - C25 H2	
	" H2 - NC	
* -YMP	" J2 - C10 D2	
	" K2 - NC	
- $\overline{\bar{Y}P}$	" L2 - D28 C2	
	" M2 - NC	
	" N2 - NC	
- $\bar{Y}P$	" P2 - D28 E2	
- $\overline{\bar{Y}MPA}$	" R2 - C25 K2	
	" S2 - NC	
* -$\bar{Y}$MP	" T2 - C10 E2	
# Vcc	" U2 - NC	
# GND	" V2 - NC	

* See C22

C22

	C22 A2 - NC	
- $\overline{XP}$	" B2 - D28 S1	
	" C2 - NC	
	" D2 - NC	
- XP	" E2 - D28 U1	
- $\overline{XMPA}$	" F2 - C25 D2	
	" H2 - NC	
*-XMP	" J2 - C12 D2	
	" K2 - NC	
- $\overline{\bar{X}P}$	" L2 - D28 K1	
	" M2 - NC	
	" N2 - NC	
- $\bar{X}P$	" P2 - D28 M1	
- $\overline{\bar{X}MPA}$	" R2 - C25 A2	
	" S2 - NC	
*-$\bar{X}$MP	" T2 - C12 E2	
# Vcc	" U2 - NC	
# GND	" V2 - NC	

C23

-$\overline{EOD}$	C23 A2 - A23 F2	
-$\overline{END2}$	" B2 - A23 J2	
-$\overline{EAD3}$	" C2 - D27 H1	
-$\overline{EAD4}$	" D2 - D27 C1	
	" E2 - NC	
	" F2 - NC	
	" H2 - NC	
	" J2 - NC	
-$\overline{OD}$	" K2 - C17 A1	
-$\overline{END1}$	" L2 - A23 D2	
-$\overline{EAD2}$	" M2 - D27M1	
-$\overline{EAD1}$	" N2 - D27 S1	
	" P2 - NC	
	" R2 - NC	
	" S2 - NC	
	" T2 - NC	
#Vcc	" U2 - NC	
#GND	" V2 - NC	

* Wire not straight to PG (C12)
to XMP, YMP, YMP wires not close

C25

- $\overline{\bar{X}MPA}$	C25 A2 - C22 R2, D28 H1	C25 N1 - NC
- $\overline{\bar{X}C}$	" B2 - A21 J1	" B1 - NC
- RF MP	" C2 - D28 M2	" C1 - NC
-$\overline{XMPA}$	" D2 - C22 F2, D28 P1	" D1 - NC
- XC	" E2 - A21 K1	" E1 - NC
- YC	" F2 - A21 H1	" F1 - NC
- $\overline{YMPA}$	" H2 - C21 F2, D28 A1	" H1 - NC
- $\overline{YC}$	" J2 - A21 F1	" J1 - NC
- $\overline{\bar{Y}MPA}$	" K2 - C21 R2, D28 A2	" K1 - NC
- $\overline{\bar{Y}MPA}$	" L2 - C20 R2, D28 A2	" L1 - NC
- $\overline{\bar{Y}C}$	" M2 - A21 T1	" M1 - NC
- $\overline{YMPA}$	" N2 - C20 F2, C28 H2	- $\overline{YCMP}$ " N1 - D28 G2
- YC	" P2 - A21 T1	" P1 - NC
	" R2 - NC	" R1 - NC
	" S2 - NC	" S1 - NC
	" T2 - NC	" T1 - NC
# Vcc	" U2 - NC	" U1 - NC
# GND	" V2 - NC	" V1 - NC

C27

			Panel connection	
-CC	C27 A2 - B9 R2		BC	11A
-Z^{11}	" B2 - B9 T2		BC	9A
#GND	" C2 - NC		GND	BCS
-Z^{10}	" D2 - B9N2		BC	8A
#GND	" E2 - NC		GND	Bus
-Z^{9}	" F2 - B9S2		BC	7A
#GND	" H2 - NC		GND	Bus
-Z^{8}	" J2 - B9P2		BC	6A
#GND	" K2 - NC		GND	BCS
-Z^{7}	" L2 - B9L2		BC	5A
#GND	" M2 - NC		GND	BCS
-Z^{6}	" N2 - B9 J2		BC	4A
#GND	" P2 - NC		GND	BCS
-Z^{5}	" R2 - B9K2		BC	3A
#GND	" S2 - NC		GND	BCS
-L	" T2 - B9 A2		BC	2A
#GND	" U2 - NC		GND	BCS
-BCD	" V2 - A9 D2		BC	9A

C27

			Panel connections
-CC	C27	A1 - B11 K2	SB 11A
-2^7	"	B1 - A11 F2	SB 9A
#GND	"	C1 - NC	GND BUS
-2^6	"	D1 - A11D2	SB 8A
#GND	"	E1 - NC	GND BUS
-2^5	"	F1 - A11 A2	SB 7A
#GND	"	H1 - NC	GND BUS
-2^4	"	J1 - A11 B2	SB 6A
#GND	"	K1 - NC	GND BUS
-2^3	"	L1 - A11 R2	SB 5A
#GND	"	M1 - NC	GND BUS
-2^2	"	N1 - A11 N2	SB 4A
#GND	"	P1 - NC	GND BUS
-2	"	R1 - A11K2	SB 3A
#GND	"	S1 - NC	GND BUS
-1	"	T1 A11 L2	SB 2A
#GND	"	U1 - NC	GND BUS
-SBO	"	V1 - A9 N2, A11 A2	SB PA

C28

	C28 A1	- GND
	" B1	- NC
	" C1	- GND
	" D1	- NC
	" E1	- GND
$\overline{INTG}$	" F1	- B7E2
	" H1	- GND
	" J1	- NC
	" K1	- GND
	" L1	- NC
	" M1	- GND
DLY	" N1	- A7B2
	" P1	- GND
INTG	" R1	- A7D2
	" S1	- GND
DPT	" T1	- A7T2
	" U1	- GND
DSPDP12	" V1	- D6C1

Panel connections are to ADC

C23

			Panel connections
-$\overline{VMPA}$	C28	N2 - C25L2	V U1
#GND	"	T2 - NC	GND BUS
-$\overline{VP}$	"	U2 - C21 N2	V Q3
#GND	"	D2 - NC	GND BUS
-$\overline{VP}$	"	E2 - C20 P2	V Q6
#GND	"	F2 - NC	GND BUS
-$\overline{VMPA}$	"	H2 - C25N2	V U1
#GND	"	J2 - NC	GND BUS
-$\overline{VP}$	"	K2 - C20 B2	V Q3
#GND	"	L2 - NC	GND BUS
-VP	"	M2 - C20 E2	V Q6
#GND	"	N2 - NC	GND BUS
DIS SPECCP	"	P2 - B4C1	DIS SPEC CA
#GND	"	R2 - NC	GND BUS
-MEM	"	S2 - A13P2	T/BMEM CA
#GND	"	T2 - NC	GND BUS
$\overline{SKP}$	"	U2 - B25 L2	ST MOD
#GND	"	V2 - NC	GND BUS

J3

#Vcc	J3 A2	- NC	-$\overline{DAD02}$	J3 A1 - D8 J2
	" B2	- NC	-$\overline{DAD02}$	" B1 - C3 E1
#GND	" C2	- NC	#GND	" C1 - GND
$\overline{PLT-P1}$	" D2	- C7 S2	-$\overline{DAD03}$	" D1 - D8 M1
-$\overline{DAD09}$	" E2	- D8 C1	-$\overline{DAD03}$	" E1 - C3 H1
-$\overline{DAD09}$	" F2	- C3 D2	-$\overline{DAD04}$	" F1 - D8L2
-$\overline{DAD10}$	" H2	- D8 T2	-$\overline{DAD04}$	" H1 - C3 J1
-$\overline{DAD10}$	" J2	- C3 E2	-$\overline{DAD05}$	" J1 - D8 P1
-$\overline{DAD11}$	" K2	- D8 V2	-$\overline{DAD05}$	" K1 - C3 L1
-$\overline{DAD11}$	" L2	- C3 H2	-$\overline{DAD06}$	" L1 - D8 N2
	" M2	- NC	-$\overline{DAD06}$	" M1 - C3 M1
	" N2	- NC	-$\overline{DAD07}$	" N1 - D8 S1
-GND	" P2	- GND	-$\overline{DAD07}$	" P1 - C3 P1
$\overline{PI}$	" R2	- D6 K2, C16 T2	-$\overline{DAD08}$	" R1 - D8 R2
I4$\overline{IOP4}$	" S2	- D10F1	-$\overline{DAD08}$	" S1 - C3 S1
$\overline{SKP}$	" T2	- D6 M2	#GND	" T1 - NC
	" U2	- NC		" U1 - NC
	" V2	- NC		" V1 - NC

D4

+Vcc	D4	A2 - NC	-$\overline{VO}$	D4	A1 - D8 B1
	"	B2 - NC	-$\overline{VO}$	"	B1 -COAX
+GND	"	C2 - NC	-Dis. Spec.	"	C1 - C28 P2
-$\overline{IOMPI}$	"	D2 - C7 H2	-$\overline{VO}$	"	D1 - D8 D2
-X$\overline{X}$Y$\overline{Y}$	"	E2 - B6 H2	-$\overline{VO}$	"	E1 - COAX
-X$\overline{X}$Y$\overline{Y}$	"	F2 - Back panel	-$\overline{VO}$	"	F1 - D8 D1
-$\overline{SPG}$	"	H2 - B6 A2	-$\overline{VO}$	"	H1 - COAX
-$\overline{SPG}$	"	J2 - Back panel	-$\overline{VO}$	"	J1 - D8 H1
	"	K2 - NC	-$\overline{VO}$	"	K1 - COAX
	"	L2 - NC	-$\overline{XO}$	"	L1 - D8 F2
	"	M2 - NC	-$\overline{XO}$	"	M1 - COAX
	"	N2 - NC	-$\overline{XO}$	"	N1 - D8 K1
GND	"	P2 - GND	-$\overline{XO}$	"	P1 - COAX
-$\overline{PI}$	"	R2 - D6 K2		"	R1 - NC
-$\overline{84IOPI}$	"	S2 - D10 B1		"	S1 - NC
-$\overline{SKP}$	"	T2 - D6 M2	+GND	"	T1 - NC
	"	U2 - NC		"	U1 - NC
	"	V2 - NC		"	V1 - NC

D5

+Vcc	D5	A2 - NC	-IOOO	D5	A1 - C19 A2
	"	B2 - NC	-IOOO	"	B1 - B3 B1
+GND	"	C2 - NC	32$\overline{IOP2}$	"	C1 - D12 D1
-$\overline{INL-PI}$	"	D2 - C7 L2	-IOO1	"	D1 - C19 D2
-IOO8	"	E2 - C19 N2	-IOO1	"	E1 - B3 D1
-IOO8	"	F2 - B3 S1	+IOO2	"	F1 - C19 B1
+IOO9	"	H2 - C19 S2	-IOO2	"	H1 - B3 E1
-IOO9	"	J2 - B3 D2	+IOO3	"	J1 - C19 E1
+IO10	"	K2 - C19 P1	-IOO3	"	K1 - B3 H1
-IO10	"	L2 - B3 E2	+IOO4	"	L1 - C19 F2
+IO11	"	M2 - C19 T1	-IOO4	"	M1 - B3 J1
-IO11	"	N2 - B3 H2	-IOO5	"	N1 - C19 K2
+GND	"	P2 - GND	-IOO5	"	P1 - B3 L1
$\overline{PI}$	"	R2 - D6 K2	+IOO6	"	R1 - C19 H1
34$\overline{IOP2}$	"	S2 - D10 D1	-IOO6	"	S1 - B3 M1
$\overline{SKP}$	"	T2 - D6 M2	+GND	"	T1 - NC
	"	U2 - NC	-IOO7	"	U1 - B3 P1
	"	V2 - NC	-IOO7	"	V1 - C19 L1

D6

$\overline{S}_7$	D6	A1 - C6A2		D6	C2 - GND
$\overline{S}_7$	"	B1 - 15R1 and C1S1		"	D2 -
DSPOP12	"	C1 - C28V1	$\overline{S}_3$	"	E2 - C6S2
$\overline{S}_6$	"	D1 - C6C2	$\overline{S}_2$	"	F2 - D15A1 and C1D1
$\overline{S}_6$	"	- D15N1 and C1P1	BK REQ	"	H2 - B7P2
$\overline{S}_5$	"	F1 - C6E2	BK REQ	"	J2 - C3K2
$\overline{S}_5$	"	H1 - D15L1 and C1M1	$\overline{PI}$	"	K2 - D4R2,D3R2,D7R2, D5R2
$\overline{S}_4$	"	J1 - C6H2	$\overline{PI}$	"	L2 - B3M2
$\overline{S}_4$	"	K1 - D15J1 and C1L1	$\overline{SKP}$	"	M2 - D4T2,D3T2,D5T2,D7T2
$\overline{S}_3$	"	L1 - C6K2	$\overline{SKP}$	"	N2 - B3K2
$\overline{S}_1$	"	M1 - D15F1 and C1J1			
$\overline{S}_2$	"	N1 - C6M2			
$\overline{S}_2$	"	P1 - D15D1 and C1H1			
$\overline{S}_1$	"	R1 - C6P2			
$\overline{S}_1$	"	S1 - D15C1 and C1E1			
	"	T1 -GND			
+ADD01	"	U1 - C3D1			
+AD001	"	V1 - B7M2			
	"	A2 - +5v.			
	"	T2 - GND			

D7

+Vcc	D7	A2 - NC	-$\overline{OAD02}$	D7	A1 - D8 J2
	"	B2 - NC	-$\overline{OAD02}$	"	B1 - B3 E1
+GND	"	C2 - NC	32$\overline{IOP1}$	"	C1 - D12 B1
$\overline{AD-PI}$	"	D2 - B25 M2	+$\overline{OAD03}$	"	D1 - D8 M1
+$\overline{OAD09}$	"	E2 - D8 U1	-$\overline{OAD0}$	"	E1 - B3 H1
-$\overline{OAD09}$	"	F2 - B3 D2	+$\overline{OAD04}$	"	F1 - D8 L2
+$\overline{OAD10}$	"	H2 - D8 T2	-$\overline{OAD04}$	"	H1 - B3 J1
-$\overline{OAD10}$	"	J2 - B3 E2	+$\overline{OAD05}$	"	J1 - D8 P1
-$\overline{OAD11}$	"	K2 - D8 V2	-$\overline{OAD05}$	"	K1 - B3 L1
-$\overline{OAD11}$	"	L2 - B3 H2	-$\overline{OAD06}$	"	L1 - D8 N2
	"	M2 - NC	+$\overline{OAD06}$	"	M1 - B3 M1
	"	N2 - NC	+$\overline{OAD07}$	"	N1 - D8 S1
-GND	"	P2 - GND	-$\overline{OAD07}$	"	P1 - B3 P1
$\overline{PI}$	"	R2 - D6 K2	+$\overline{OAD08}$	"	R1 - D8 R2
31$\overline{IOP2}$	"	S2 - D11 D1	-$\overline{OAD08}$	"	S1 - B3 S1
$\overline{SKP}$	"	T2 - D6 M2	+GND	"	T1 - NC
	"	U2 - NC		"	U1 - NC
	"	V2 - NC		"	V1 - NC

D8

-VO	D8 A1 - C8 A2, B6 E2		#Vcc	D8 A2 - NC	
-$\overline{VO}$	" B1 - D4 A1			" B2 - NC	
-$\overline{VO}$	" C1 - C8 B2, B6 F2		#GND	" C2 - NC	
-YO	" D1 - C10 A2, B6 A2		-$\overline{YO}$	" D2 - D4 D1	
-$\overline{YO}$	" E1 - D4 F1		-XO	" E2 - C12A2,B6D2	
-$\overline{YO}$	" F1 - C10 B2, B6 F1		-$\overline{XO}$	" F2 - D4L1	
-$\overline{YO}$	" H1 - D4 J1		-DADO2	" H2 - C5 E2	
-$\overline{XO}$	" J1 - C12 B2, B6 J1		-$\overline{DADO2}$	" J2 - D3A1,D7A1	
-$\overline{XO}$	" K1 - D4 N1		-DADO4	" K2 -C5 H2	
-DADO3	" L1 - C5 A2		-$\overline{DADO4}$	" L2 - D3F1, D7F1	
-$\overline{DADO3}$	" M1 - D3D1, D7D1		-DADO6	" M2 - C5J2	
-DADO5	" N1 - C5 D2		-$\overline{DADO6}$	" N2 - D3L1,D7L1	
-$\overline{DADO5}$	" P1 - D3 J1, D7 J1		-DADO8	" P2 - C5 T2	
-DADO7	" R1 - C5 C2		-$\overline{DADO8}$	" R2 - D3R1, D7R1	
-$\overline{DADO7}$	" S1 - D3 N1, D7 N1		-DAD10	" S2 - C5 N2	
#GND	" T1 - NC		-$\overline{DAD10}$	" T2 - D3H2, D7H2	
-$\overline{DADO9}$	" U1 - D3E2, D7E2		-DAD11	" V2 - C5K2	
-DADO9	" V1 - C5 L2		-$\overline{DAD11}$	" W2 - D3K2, D7K2	

D9

#Vcc	D9 A2 - NC		-35 IOP1	D9 A1 - NC			
	" B2 - NC		-35 $\overline{IOP1}$	" B1 - C7J2			
#GND	" C2 - NC		-35 IOP2	" C1 - NC			
-(0)BMB03	" D2 - A1 H1		-35 $\overline{IOP2}$	" D1 - C7R2			
-(1)BMB04	" E2 - A1 M1		-35 IOP4	" E1 - NC			
-(1)BMB05	" F2 - A1 S1		-35 $\overline{IOP4}$	" F1 - C7N2			
-(1)BMB06	" H2 - A1 E2			" H1 - NC			
-(0)BMB07	" J2 - A1 H2			" J1 - NC			
-(1)BMB08	" K2 - A1 P2			" K1 - NC			
#3Vcc	" L2 - Vcc			" L1 - D9 V2			
	" M2 - Nc			" M1 - D9 V2			
#3Vcc	" N2 - Vcc		35 $\overline{OS}$	" N1 - C16R1			
#BIOP1	" P2 - B1 K2			" P1 - NC			
#BIOP2	" R2 - B1 M2			" R1 - NC			
#BIOP4	" S2 - B1 P2			" S1 - NC			
	" T2 - NC		#GND	" T1 - NC			
+Vcc	" U2 - Vcc			" U1 - NC			
35 OS	" V2 - D9L1, D9M1			" V1 - NC			

D10

#Vcc	D10 A2 - NC		-34 IOP1	D10 A1 - NC			
	" B2 - NC		34 $\overline{IOP1}$	" B1 - D4 S2			
#GND	" C2 - NC		-34 IOP2	" C1 - NC			
-(0)BMB03	" D2 - A1 H1		-34 $\overline{IOP2}$	" D1 - D5 S2			
-(1)BMB04	" E2 - A1 M1		-34 IOP4	" E1 - NC			
-(1)BMB06	" H2 - A1 E2			" H1 - NC			
-(0)BMB07	" J2 - A1 H2			" J1 - NC			
-(1)BMB08	" K2 - A1 M2			" K1 - NC			
#3Vcc	" L2 - Vcc			" L1 - D10V2			
	" M2 - NC			" M1 - D10V2			
#3Vcc	" N2 - Vcc		34 $\overline{OS}$	" N1 - C16P2			
#BIOP1	" P2 - B1K2			" P1 - NC			
#BIOP2	" R2 - B1M2			" R1 - NC			
#BIOP4	" S2 - B1 P2			" S1 - NC			
	" T2 - NC		#GND	" T1 - Nc			
+Vcc	" U2 - Vcc			" U1 - NC			
34 OS	" V2 -D10L1,, D10M1			" V1 - NC			
-(0)BMB05	" F2 - B1N1		-$\overline{34IOP4}$	" F1 - D3S2			

D11

#Vcc	D11 A2 - NC		-33 IOP1	D11 A1 - NC			
	" B2 - NC		-33 $\overline{IOP1}$	" B1 - C7 T2			
#GND	" C2 - NC		-33 IOP2	" C1 - NC			
-(0)BMB03	" D2 - A1 H1		-33 $\overline{IOP2}$	" D1 - D7 S2			
-(1)BMB04	" E2 - A1 M1		-33 IOP4	" E1 - NC			
-(1)BMB05	" F2 - A1 S1		-33 $\overline{IOP4}$	" F1 - C7 S1			
-(0)BMB06	" H2 - A1 D2			" H1 - NC			
-(1)BMB07	" J2 - A1 K2			" J1 - NC			
-(1)BMB08	" K2 - A1 P2			" K1 - NC			
#3Vcc	" L2 - Vcc			" L1 - D11V2			
	" M2 - NC			" M1 - D11 V2			
#3Vcc	" N2 - Vcc		33 $\overline{OS}$	" N1 - C16 N2			
#BIOP1	" P2 - B1 K2			" P1 - NC			
#BIOP2	" R2 - B1 M2			" R1 - NC			
#BIOP4	" S2 - B1 P2			" S1 - NC			
	" T2 - NC		#GND	" T1 - NC			
+Vcc	" U2 - Vcc			" U1 - NC			
33 OS	" V2 - D11L1, D11M1			" V1 - NC			

D12

#Vcc	D12	A2 - NC	-J2 IOP1	D12	A1 - NC
	"	B2 - NC	-J2 $\overline{IOP1}$	"	B1 - D7C1
#GND	"	C2 - NC	-J2 IOP2	"	C1 - NC
+(0)BMB03	"	D2 - A1 H1	-J2 $\overline{IOP2}$	"	D1 - D5 C1
+(1)BMB04	"	E2 - A1 M1	-J2IOP4	"	E1 - NC
+(1)BMB05	"	F2 - A1 S1	- J2 $\overline{IOP4}$	"	F1 - C19R1
+(0)BMB06	"	H2 - A1 D2		"	H1 - NC
+(1)BMB07	"	J2 - A1 K2		"	J1 - NC
+(0)BMB08	"	K2 - A1 M2		"	K1 - NC
#JVcc	"	L2 - Vcc		"	L1 - D12 V2
	"	M2 - NC		"	M1 - D12 V2
#JVcc	"	N2 - Vcc	-J2 $\overline{OS}$	"	N1 - C16N1
#BIOP1	"	P2 - B1K2		"	P1 - NC
#BIOP2	"	R2 - B1 M2		"	R1 - NC
#BIOP4	"	S2 - B1 P2		"	S1 - NC
	"	T2 - NC	#GND	"	T1 - NC
-Vcc	"	U2 - Vcc		"	U1 - NC
J2 OS	"	V2 - D12L1,D12M1		"	V1 - NC

D13

#Vcc	D13	A2 - NC	#J0 IOP1	D13	A1 B16P2,B15V1
	"	B2 - NC	-J0 $\overline{IOP1}$	"	B1 - NC
#GND	"	C2 - NC	#J0 IOP2	"	C1 - A15P2
+(0)BMB03	"	D2 - A1 H1	-J0 $\overline{IOP2}$	"	D1 - NC
+(1)BMB04	"	E2 - A1 M1	-J0 IOP4	"	E1 - NC
+(1)BMB05	"	F2 - A1 S1	#J0 $\overline{IOP4}$	"	F1 - A13 P2
+(0)BMB06	"	H2 - A1 D2		"	H1 - NC
+(0)BMB07	"	J2 - A1 K2		"	J1 - NC
+(0)BMB08	"	K2 -A1 M2		"	K1 - NC
#JVcc	"	L2 - Vcc		"	L1 - D13 V2
	"	M2 - NC		"	M1 - D13 V2
#JVcc	"	N2 - Vcc	J0 $\overline{OS}$	"	N1 - C16 P1
#BIOP1	"	P2 - B1K1		"	P1 - NC
#BIOP2	"	R2 - B1M2		"	R1 - NC
#BIOP4	"	S2 - B1P2		"	S1 - NC
	"	T2 - NC	#GND	"	T1 - NC
-Vcc	"	U2 - Vcc		"	U1 - NC
J0OS	"	V2 - D13L1,D13M1		"	V1 - NC

D14

#Vcc	D14	A2 - NC	-J1 IOP1	D14	A1 - NC
	"	B2 - NC	-J1 $\overline{IOP1}$	"	B1 -A11M2,B9M2,C19M1
#GND	"	C2 - NC	-J1 IOP2	"	C1 - NC
+(0)BMB03	"	D2 - A1M1	-J1 $\overline{IOP2}$	"	D1 - C5P2
+(1)BMB04	"	E2 - A1 M1	-J1 IOP4	"	E1 - NC
+(1)BMB05	"	F2 - A1 S1	-J1 $\overline{IOP4}$	"	F1 - A23C2
+(0)BMB06	"	H2 - A1D2		"	H1 - NC
+(0)BMB07	"	J2 - A1 M2		"	J1 - NC
+(1)BMB08	"	K2 - A1 P2		"	K1 - NC
#JVcc	"	L2 - Vcc		"	L1 - D14V2
	"	M2 - NC		"	M1 - D14V2
#JVcc	"	N2 - Vcc	J1 $\overline{OS}$	"	N1 - C16P2
#BIOP1	"	P2 - B1K2		"	P1 - NC
#BIOP2	"	R2 - B1M2		"	R1 - NC
#BIOP4	"	S2 - B1P2		"	S1 - NC
	"	T2 - NC	#GND	"	T1 - NC
-Vcc	"	U2 - Vcc		"	U1 - NC
J1 OS	"	V2 - D14L1,D14M1		"	V1 - NC

D15

$\overline{B}_7$MSB	D15	A1 - D6F2			
B_6	"	B1 - D26V2			
$\overline{B}_5$	"	C1 - D6S1			
$\overline{B}_4$	"	D1 - D6P1			
B_3	"	E1 - D26R2			
$\overline{B}_3$	"	F1 - D6M1			
B_2	"	H1 - D26N2			
$\overline{B}_4$	"	J1 - D6K1			
B_1	"	K1 - D26L2			
$\overline{B}_5$	"	L1 - D6H1			
B_0	"	M1 - D26J2			
$\overline{B}_6$	"	N1 - D6E1			
B_{-1}	"	P1 - D26F2			
$\overline{B}_{-1}$ LSB	"	R1 - D6B1			
B_{-2}	"	S1 - D26D2			
	"	T1 - GND			
	"	U1 - NC			
	"	V1 - NC			
	"	A2 - -5V			
	"	C2 - GND			
B_{-11}	"	D2 - D26T2			
$\overline{ADDACPT}$	"	E2 - C3S2			
ADDACPT	"	F2 - A7H2			
$\overline{B\text{-}BREAK}$	"	H2 - C3P2			
B-Break	"	J2 - B7L2			
	"	K2 - NC			

D19

#Vcc	D19	A2 - NC			
	"	B2 - NC			
#GND	"	C2 - NC			
VT	"	D2 - B19J2			
	"	E2 - NC			
	"	F2 - NC			
	"	H2 - NC			
	"	J2 - NC			
	"	K2 - NC			
	"	L2 - NC			
	"	M2 - NC			
	"	N2 - NC			
	"	P2 - NC			
	"	R2 - NC			
	"	S2 - NC			
	"	T2 - NC			
	"	U2 - NC			
	"	V2 - NC			

D22

#Vcc	D22 A2 - NC	1. NA4 lamp
	" B2 - NC	2. NA3 lamp
#GND	" C2 - NC	3. NA2 lamp
NA4	" D2 - B13L2	4. NA1 lamp
	" E2 - NC	5. GND BUS WIRE
NA3	" F2 - A13J2	6. CA4 lamp
	" H2 - NC	7. CA3 lamp
NA2	" J2 - B13C2	8. CA2 lamp
	" K2 - NC	9. CA1 lamp
NA1	" L2 - B13D2	
	" M2 - NC	
CA4	" N2 - A13A2	
	" P2 - NC	
CA3	" R2 - A13H2	
	" S2 - NC	
CA2	" T2 - A13C2	
	" U2 - NC	
CA1	" V2 - A13E2	

D23

#18 Vcc	D23 A2 - NC	1. end lamp
	" B2 - NC	2. recycling lamp
#GND	" C2 - NC	3. clock lamp
(EL) END	" D2 - B23A2	4. computer lamp
	" E2 - NC	5. GND BUS WIRE
(RDLT) RE-CYC.	" F2 - A25E2	6. empty lamp
	" H2 - NC	7. empty lamp
(CLT) CLOCK	" J2 - B19D2	8. open
	" K2 - NC	9. open
CCLT (CLT) COMP	" L2 - C16A2	
	" M2 - NC	
	" N2 - NC	
	" P2 - NC	
	" R2 - NC	
	" S2 - NC	
OPEN	" T2 - NC	
	" U2 - NC	
OPEN	" V2 - NC	

D24

#18 Vcc	D24 A2 - NC	1. empty lamp
	" B2 - NC	2. DC lamp
#GND	" C2 - NC	3. S lamp
	" D2 - NC	4. SB lamp
	" E2 - NC	5. GND BUS WIRE
DC	" F2 - A14M2	6. B lamp
	" H2 - NC	7. D3 lamp
S	" J2 - A15N2	8. D2 lamp
	" K2 - NC	9. D1 lamp
SB	" L2 - A15M2	
	" M2 - NC	
B	" N2 - A16N2	
	" P2 - NC	
D3	" R2 - A16M2	
	" S2 - NC	
D2	" T2 - A17N2	
	" U2 - NC	
D1	" V2 - A17M2	

D25

#18 Vcc	D25 A2 - NC	1. C Lamp
	" B2 - NC	2. H Lamp
#GND	" C2 - NC	3. $\overline{Y}$ lamp
C	" D2 - A18N2	4. Y lamp
	" E2 - NC	5. GND BUS WIRE
H	" F2 - A18M2	6. $\overline{Y}$ lamp
	" H2 - NC	7. Y lamp
$\overline{Y}$	" J2 - B18N2	8. $\overline{X}$ lamp
	" K2 - NC	9. X lamp
Y	" L2 - B18M2	
	" M2 - NC	
$\overline{X}$	" N2 - B17N2	
	" P2 - NC	
X	" R2 - B17M2	
	" S2 - NC	
$\overline{X}$	" T2 - B16N2	
	" U2 - NC	
X	" V2 - B16M2	

D26

	D26 A2 - +5V	
	" B2 - NC	
$\overline{B}_0$MSB	" C2 - GND	
	" D2 - D15S1	
	" E2 - NC	
B_1	" F_2 -D15P1	
	" H2 - NC	
B_2	" J2 - D15M1	
	" K2 - NC	
B_3	" L2 - D15K1	
	" M2 - NC	
B_4	" N2 - D15H1	
	" P2 - NC	
B_5	" R2 - D15E1	
	" S2 - NC	
B_6	" T2 - D15D2	
	" U2 - NC	
B_7LSB	" V2 - D15B1	

Panel connections are to ADC lights

D27

			Panel connections
	D27 A1 - NC		
#GND	" B1 - NC		GND BUS
-$\overline{EAD4}$	" C1 - C23D2		AD4 Q6
#GND	" D1 - NC		GND BUS
-$\overline{AD4}$	" E1 - C17 B2		AD4 Q3
#GND	" F1 - NC		GND BUS
-$\overline{EAD3}$	" H1 - C23C2		AD3 Q6
#GND	" J1 - NC		GND BUS
-$\overline{AD3}$	" K1 - C17B1		AD3 Q3
#GND	" L1 - NC		GND BUS
-$\overline{EAD2}$	" M1 - C23M2		AD2 Q6
#GND	" N1 - NC		GND BUS
-$\overline{AD2}$	" P1 - C17C2		AD2 Q3
#GND	" R1 - NC		GND BUS
-$\overline{EAD1}$	" S1 - C23N2		AD1 Q6
#GND	" T1 - NC		GND BUS
-$\overline{AD1}$	" U1 - C17 C1		AD1 Q3
#GND	" V1 - NC		GND BUS

D28

			Panel connections
-$\overline{YMPA}$	D28 A2 - C25 K2		$\overline{Y}$ Q1
#GND	" B2 - NC		GND BUS
-$\overline{YP}$	" C2 - C21 L2		$\overline{Y}$ Q3
#GND	" D2 - NC		GND BUS
-$\overline{YP}$	" E2 - C21 P2		$\overline{Y}$ Q6
#GND	" F2 - NC		GND BUS
#$\overline{TPI}$	" H2 - A23 S2		RF Q1
#GND	" J2 - NC		GND BUS
-$\overline{BD}$	" K2 - A28C1		RF Q4
#GND	" L2 - NC		GND BUS
-RFMP	" M2 - C25 C2		RF Q6
#GND	" N2 - NC		GND BUS
#$\overline{TPI}$	" P2 - A23 S2		VD Q1
#GND	" R2 - NC		GND BUS
-$\overline{BD}$	" S2 - A28 C1		VD Q4
#GND	" T2 - NC		GND BUS
-VDMP	" U2 - C25 N1		VD Q6
#GND	" V2 - NC		GND BUS

D28

			Panel connections
-$\overline{YMPA}$	D28 A1 - C25 H2		Y Q1
#GND	" B1 - NC		GND BUS
-$\overline{YP}$	" C1 - C21 B2		Y Q3
#GND	" D1 - NC		GND BUS
-YP	" E1 - C21 E2		Y Q6
#GND	" F1 - NC		GND BUS
-$\overline{YMPA}$	" H1 - C25A2		$\overline{X}$ Q1
#GND	" J1 - NC		GND BUS
-$\overline{XP}$	" K1 - C22 L2		$\overline{X}$ Q3
#GND	" L1 - NC		GND BUS
-$\overline{XP}$	" M1 - C22P2		$\overline{X}$ Q6
#GND	" N1 - NC		GND BUS
-$\overline{XMPA}$	" P1 - C25D2		X Q1
#GND	" R1 - NC		GND BUS
-$\overline{XP}$	" S1 - C22 B2		X Q3
#GND	" T1 - NC		GND BUS
-XP	" U1 - C22E2		X Q6
#GND	" V1 - NC		GND BUS

Clear Switch

Open	NCA - NC
$\overline{MCL}$	NOA - A27A1
GND	CA - GND Bus Wire
	NCB - NC
	NOB - NC
	CB - NC
OPEN	NCC - NC
Vcc	NOC - Vcc BUS Wire
Lamps	CC - L1,L3
	NCD - NC
	NOD - NC
	CD - NC

Execute Switch

GND	NCA - GND BUS Wire
PB1	NOA - A27M1
PB2	CA -A27K1
	NCB - NC
	NO B - NC
	C B - NC
OPEN	NCC - NC
Vcc	NO C - Vcc Bus Wire
Lamps	C C - L1,L3
	NC D - NC
	NO D - NC
	C D - NC

L2 - GND

RFMP generator switch

-$\overline{TPI}$	Q1 - D28H2 Wire
#GND	Q2 - GND BUS WIRE
-$\overline{RFMP}$	Q3 - NC
-$\overline{BD}$	Q4 - D28K2 Wire
#Vcc	Q5 - Vcc BUS Wire
-RFMP	Q6 - D28 M2 Wire

VDMP generator switch

-$\overline{TPI}$	Q1 -D28P2 Wire
#GND	Q2 - GND BUS WIRE
-$\overline{VDMP}$	Q3 - NC
-$\overline{BD}$	Q4 - D28S2 Wire
#Vcc	Q5 - Vcc Bus Wire
-VDMP	Q6 - D28U2 Wire

Start Switch

GND	NCA - GND BUS Wire
PB3	NOA - A27H1 Wire
PB4	CA - A27E1 Wire
	NCB - NC
	NOB - NC
	CB - NC
OPEN	NCC - NC
Vcc	NOC - Vcc BUS Wire
Lamps	CC - L1 L3
	NCD - NC
	NOD - NC
	CD - NC

L2 - GND

Load Switch

GND	NCA - GND Bus Wire
$\overline{LDM}$	NOA - B27C1 Wire
PB5	CA - B27A1 Wire
	NC B - NC
	NOB - NC
	CB - NC
OPEN	NCC - NC
Vcc	Vcc Bus Wire
Lamps	CC - L1,L3
	NCD - NC
	NOD - NC
	CD - NC

XP generator switch

-$\overline{XMPA}$	Q1 - D28 P1 Wire
#GND	Q2 - GND BUS Wire
-$\overline{XP}$	Q3 - D28S1 Wire
#Vcc	Q5 - Vcc Bus Wire
-XP	Q6 - D28U1 Wire

$\overline{XP}$ generator switch

-$\overline{XMPA}$	Q1 - D28H1 Wire
#GND	Q2 - GND BUS WIRE
-$\overline{XP}$	Q3 - D28K1 Wire
#Vcc	Q5 - Vcc Bus Wire
-$\overline{XP}$	Q6 - D28M1 Wire

YP generator switch

-$\overline{YMPA}$	Q1 - D28A1 Wire
#GND	Q2 - GND BUS Wire
-$\overline{YP}$	Q3 - D28C1 Wire
#Vcc	Q5 - VccBus Wire
-YP	Q6 - D28E1 Wire

$\overline{YP}$ generator switch

-$\overline{YMPA}$	Q1 - D28A2 Wire
#GND	Q2 - GND BUS Wire
-$\overline{YP}$	Q3 - D28C2 Wire
#Vcc	Q5 - Vcc BUS WIRE
-$\overline{YP}$	Q6 - D28E2 Wire

ZP generator switch

-$\overline{YMPA}$	Q1 - C28M2 Wire
#GND	Q2 - GND BUS Wire
-$\overline{VP}$	Q3 - C28P2 Wire
#Vcc	Q5 - Vcc BUS Wire
-VP	Q6 - C28N2 Wire

$\overline{ZP}$ generator switch

-$\overline{YMPA}$	Q1 - C28A2 Wire
#GND	Q2 - GND BUS Wire
-$\overline{VP}$	Q3 - C28C2 Wire
#Vcc	Q5 - Vcc BUS Wire
-$\overline{VP}$	Q6 - C28E2 Wire

AD1 Switch

-EAD1	Q1 - NC
#GND	Q2 - GND BUS Wire
-$\overline{AD1}$	Q3 - D27D1 Wire
#Vcc	Q5 - Vcc BUS Wire
-$\overline{EAD1}$	Q6 - D27S1 Wire

AD2 Switch

-EAD2	Q1 - NC
#GND	Q2 - GND BUS WIRE
-$\overline{AD2}$	Q3 - D27P1 Wire
#Vcc	Q5 - Vcc BUS Wire
-$\overline{CAD2}$	Q6 - D27M1 Wire

AD3 Switch

-EAD3	Q1 - NC
#GND	Q2 - GND BUS Wire
-$\overline{AD1}$	Q3 - D27K1 Wire
#Vcc	Q5 - Vcc BUS Wire
-$\overline{EAD3}$	Q6 - D27H1 Wire

AD4 Switch

-EAD4	Q1 - NC
#GND	Q2 - GND BUS Wire
-$\overline{AD4}$	Q3 - D27E1 Wire
#Vcc	Q5 - Vcc BUS Wire
-$\overline{EAD4}$	Q6 - D27C1 Wire

DISABLE SPECTR. Switch

GND	NC A - GND BUS Wire
Vcc	NO A - Vcc BUS Wire
DISSPECTR..	C A - C28P2 Wire
	NC B - NC
	NO B - NC
	C B - NC
OPEN	NC C - NC
Vcc	NO C - Vcc BUS Wire
Lamps	C C - L1,L3
	NC D - NC
	NO D - NC
	CD - NC

L2 - GND

TOP/BOTTOM MEM Switch

GND	NC A - GND
Vcc	NO A - Vcc BUS Wire
MEM	CA - C28C2 Wire
	NC B - NC
	NO B - NC
	CB - NC
Vcc	NC C - Vcc BUS Wire
[illegible]	NO C - NC
Top Lamp	C C - L1
OPEN	NC D - NC
Vcc	NO D - Vcc BUS Wire
BOT. Lamp	CD- L3

L2 - GND

EBBCRST Switch

	1A - NC
1	2A - C27T1 Wire
2	3A - C27R1 Wire
2^4	4A - C27N1 Wire
2^3	5A - C27L1 Wire
2^4	6A - C27J1 Wire
2^5	7A - C27F1 Wire
2^6	8A - C27D1 Wire
2^7	9A - C27B1 Wire
	10A - NC
CC	11A - C27A1 Wire
	12A - NC
EBO	PA - C27V1 Wire

BCRST Switch

	1A - NC
1	2A - C27T2 Wire
2^5	3A - C27P2 Wire
2^6	4A - C27N2 Wire
2^7	5A - C27L2 - Wire
2^8	6A - C27J2 Wire
2^9	7A - C27F2 Wire
2^{10}	8A - C27D2 Wire
2^{11}	9A - C27B2 Wire
	10A - NC
CC	11A - C27A2 Wire
	12A - NC
BCO	PA - C27V2 Wire

Stop Switch

OPEN	NCA - NC
$\overline{STP}$	NOA - A27P1 Wire
GND	CA - GND BUS Wire
OPEN	NCB - NC
$\overline{STP}$	NOB - A27C1 Wire
GND	CB - GND BUS Wire
OPEN	NCC - NC
Vcc	NOC - Vcc BUS Wire
Lamps	CC - L1,L3
OPEN	NCD - NC
$\overline{STP}$	NOD - C28U2 Wire
GND	CD - GND Bus Wire

L2 - GND

SI Switch

+END	NC A - A27S1
+SI	NO A - A27U1
+EX	CA - A27P1
	NC B - NC
	NO B - NC
	C B - NC
OPEN	NC C - NC
Vcc	NO C - Vcc BUS Wire
Lamps	C C - L1, L3
	NC D - NC
	NO D - NC
	C D - NC

L2 - GND

Recycle Switch

1	1A - A28P1 Wire
2	2A - A28S1 Wire
2^2	3A - A28U1 Wire
2^3	4A - A28U2 Wire
2^4	5A - A28S2 wire
2^5	6A - A28P2 Wire
2^6	7A - A28M2 Wire
2^7	8A - A28K2 Wire
2^8	9A - A28H2 Wire
2^9	10A - A28E2 Wire
2^{10}	11A - A28C2 Wire
2^{11}	12A - A28A2 Wire
ERD	PA - A28M1 Wire

Clock Switch

	1A - NC
μSec	2A - A27P2 Wire
10^{-5}	3A - A27M2 Wire
10^{-4}	4A - A27K2 Wire
m Sec	5A - A27H2 Wire
10^{-2}	6A - A27E2 Wire
10^{-1}	7A - A27C2 Wire
SEC	8A - A27A2 Wire
	9A - NC
	10A - NC
CC	11A - A27U2 Wire
	12A - NC
CR	PA - A27S2 Wire

MODE Switch

OPEN	1A - NC	OPEN	1B- NC
$-\overline{INL}$	2A - B27S2 Wire	Vcc	2B - Vcc Bus Wire
$-\overline{BC}$	3A - B27P2 Wire	Vcc	3B - Vcc BUS Wire
$-\overline{BD}$	4A - A28C1 Wire	GND	4B - GND BUS Wire
$-\overline{BD}$	5A - A28C1 - Wire	GND	5B - GND BUS Wire
$-\overline{BD}$	7A- "	GND	6B - "
$-\overline{BD}$	6A - "	GND	7B - "
$-\overline{BD}$	8A - "	GND	8B "
$-\overline{BD}$	9A A28C1 Wire	GND	9B - GND BUS Wire
$-\overline{LBC}$	PA - B27U2 Wire	EPc	PB - A28A1 Wire

	1C - NC
	2C - NC
	3C - NC
XB	4C - B27M2 Wire
$\overline{XB}$	5C - B27K2 Wire
YB	6C - B27H2 Wire
$\overline{YB}$	7C - B27E2 Wire
YB	8C - B27C2 Wire
$\overline{YB}$	9C - B27A2 Wire
GND	Pc - GND BUS Wire

CHAPTER IV

SOFTWARE

I. INTRODUCTION

The spectrometer is controlled by an expandable executive routine known as GOLEM 2. The layout of this program in the 8 fields (8k) of core in our PDP 12 is as follows:

Field	Contents
0	Fourier Transform
1	Alfanumeric display
2	Real average
3	Imaginary average
4	Spectrometer control routines
5	Phase correction
6	Real input
7	Imaginary input

A list of commands follows in the next section and immediately after this is a listing of the program.

Additional commands can be added to GOLEM 2 very simply:

(a) write subroutine for command execution somewhere in free core space. Exit from subroutine to BURST in Segment 4.

(b) assign two letter code and add at the end of INDX and with suffix AD at the end of TABLE

(c) make table entry the name of first location for sub-routine.

The operation of GOLEM 2 is self-explanatory from the listing (with detailed comments). The only instructions not included in the PDP 12 list are some I/O commands (6xxx). These are the instructions which service the peripherals (pulse programmer, plotter); they are coded and explained under device selection codes in the hardware section of this thesis. Further details may be understood by appealing to the detailed schematics.

The command pointer is an * . After execution of any command the executive routine is reentered and this displays the contents of the data buffer until a new command is received from the teletype. Typing rubout at any stage will cause an immediate reinitialization of the command buffer as indicated by an* . GOLEM2 may be restarted at any time by putting the PDP12 in LINK mode, setting the left switches to $(10200)_8$ and pressing start left switches. Alternatively if it has been destroyed in core, the load and go option of DIAL may be used to fetch it from magnetic tape.

An additional program used in spectrometer control is PPMOD: this creates, files and loads new pulse programs. This is not detailed here--an updated version and description is maintained by Mr. S. Kaplan.

I am grateful to Dr. W.E. Good Jr. for his assistance in writing the programs.

II. GOLEM2 COMMANDS

A. LISTING

COMMAND	DESCRIPTION
DL	Call "Dial"
RS	Run spectrometer, display input
RA	Run with averaging, display average
RA,$\alpha_1\alpha_2\alpha_3\alpha_4$	Run with averaging $(\alpha_1\alpha_2\alpha_3\alpha_4)_8$ times
CA	Continue - averaging
CA,$\alpha_1\alpha_2\alpha_3\alpha_4$	Average another $(\alpha_1\alpha_2\alpha_3\alpha_4)_8$ times
DI	Display input
DA	Display average
PD	Plot data
CL	Clear data buffers
FT	Fourier transform average
IT	Inverse transform average
SD,$\alpha_1\alpha_2\alpha_3\alpha_4$	Save average as no. $(\alpha_3\alpha_4)_8$ on tape 1
CD,$\alpha_1\alpha_2\alpha_3\alpha_4$	Call data no. $(\alpha_3\alpha_4)_8$ from tape 1 into average buffer
ST	Stop; this exits from all other commands
MX	Phase mix average; angle determined by POT 7.
AD	Add constant to average up to cursor; const ≡ POT 3.
SM,$\alpha_1\alpha_2\alpha_3\alpha_4$	Smooth average $(\alpha_3\alpha_4)_8$ times
RUBOUT	Return command pointer (*)

DISPLAY OPTIONS

SENSE SWITCH	POTENTIOMETERS
0 - expanded display	0-move, 1-horizontal expand, 2-vertical expand
1 - data buffer, real or imag.	
2 - display every second point	
3 - alfanumeric + cursor	5-coarse cursor 6 - fine cursor

B. DESCRIPTION OF COMMANDS

We present only a brief description of some of the commands. The operation will be referenced to the discussion of the pulse programmer operation in the hardware section.

DL: Brings the PDP12 linctape operating system "DIAL MS" into core.

RS: Runs the spectrometer when the pulse programmer is in CC (Computer Control) mode. The end of a RD is sensed by the computer (6342) and it then initializes by clearing flags and counters in the pulse programmer and initializes a new burst through $\overline{\text{CCBG}}$ to the MS generator (6314). Now, while data is being received via data break into fields 6 and 7 the computer waits in a loop . The RD request causes a PI which returns GOLEM2 to the spectrometer service routine.

RA: Data from fields 6 and 7 is stable averaged into fields 2 and 3. The remainder of the operation is the same

as for RS. Averaging is performed at the end of the RD for all 1024 complex points and takes ~ 250 msec so is not suited to ultra rapid data acquisition. This may easily be streamlined. The stable average algorithm is due to Hewlett-Packard. If $\bar{S}_N$ is the average after N passes and S_n the input at pass n then:

$$\bar{S}_N = \frac{1}{N} \sum_{n=1}^{N} S_n \tag{1}$$

This may be written

$$\bar{S}_N = \frac{N-1}{(N-1)N} \sum_{n=1}^{N-1} S_n + \frac{1}{N} S_{N-1}$$

$$\bar{S}_N = \frac{N-1}{N} \bar{S}_{N-1} + \frac{1}{N} S_{N-1}$$

or finally

$$\bar{S}_N = \bar{S}_{N-1} + \frac{S_{N-1} - \bar{S}_{N-1}}{N} \tag{2}$$

This expression is exact. It may now be made operationally very convenient for a computer by introducing the approximation

$$\bar{S}_N = \bar{S}_{N-1} + \frac{S_{N-1} - \bar{S}_{N-1}}{2^k} \tag{3}$$

where k is an integer satisfying

$$2^{k-1} < N < 2^k + 1 \tag{4}$$

This is an excellent approximation and easily implemented in

the program: the current average is subtracted from incoming data, the result is shifted by k and added to the current average to give the next average.

CA: continues averaging if RA,$\alpha_1\alpha_2\alpha_3\alpha_4$ was not sufficient. May be done after some intermediate commands (FT) as well.

DI: displays input buffer (fields 6 and 7)

DA: displays average buffer (fields 2 and 3)

PD: data is plotted on the Hewlett-Packard plotter (see hardware section) from exactly what is viewed on the PDP12 screen. This therefore benefits from all the display options described above. Plotting is very efficient, in that the plotter runs at a speed compatible with the distance between points, by generating signals to the PDP12 when each point is plotted. This is sensed (6344) by the computer, which clears the flag (6354) and plots the next point. The plotter is driven by X-Y signals from the PDP12 scope display and the scope intensify pulse. The plotter can be enabled and disabled (6331 and 6334) to prevent jitter during normal unplotted display of GOLEM 2.

FT: performs a fast Fourier transform (FFT) on 1024 complex 12 bit words in the average buffer (fields 2 and 3). The transform is placed into the average buffer.

Transformation is accomplished in approximately 5 seconds. The size of the transform may be decreased by changing N and NU on the first page of the subroutine. The sine table is used as a general lookup table for both the FFT and the phase mixing routine.

IT: Same as FT but performs inverse transform.

SD: data in the field under display (2,3,6, or 7) is stored on magnetic tape UNIT 1. If the data number requested is $(00XY)_8$ then the data will take up blocks $(00XY + 4)_8 \cdot 10_8$ on magnetic tape. This uses up only one half of the storage space--the remainder can be used to store pulse programs.

MX: this performs a phase correction of data in the average buffer. The correction is on line with the display, and the angle α (-90° to $+90^\circ$) is determined by potentiometer 7. The routine performs the operation

$$(\text{real})_{\text{corr}} = \cos\alpha \cdot \text{real} + \sin\alpha \cdot \text{imag}$$

$$(\text{imag})_{\text{corr}} = -\sin\alpha \cdot \text{real} + \cos\alpha \cdot \text{imag}$$

AD: a constant determined by potentiometer 3 is added to the data. If we are not in alfanumeric display option (sense switch 3) then all the data in the displayed field are affected. If the alfanumeric option is activated then only points up to and including the cursor are affected. The display may be restabilized

by typing ST .

SM: a three point quadratic (0.25 N-1 + 0.5 N + 0.25 N+1) smoothing of data in the average buffer is performed. It can be shown easily that smoothing with this algorithm in one domain, say time, is equivalent to filtering in the other (frequency) with a transfer function:

$$g(\omega) = \frac{1}{2} (1 + \cos \omega \Delta t) \qquad (5)$$

where Δt is the time domain sampling period. For this to be effective, the input should be band-limited by a filter with cutoff frequency equal to the Nyquist frequency

$$\omega_F = \frac{\pi}{\Delta t} \qquad (6)$$

since (5) does not eliminate noise folded over into this band. For repeated smoothings, $(\alpha_1 \alpha_2 \alpha_3 \alpha_4)_8$ large, it is easily shown that the smoothing approaches Gaussian. (Gaussian filtering in the other domain). Smoothing is frequency domain accomplishes what one normally calls "apodization" of the time domain signal by a function of the form of (5).

DISPLAY: the alfanumeric option (switch 3) will produce a cursor by brightening one of the displayed data points.

The cursor position is controlled by coarse and fine potentiometers (5 and 6). The coordinates of this point will appear at the top right hand corner of the screen. The top number is the (decimal) location of the selected point in the displayed buffer (0-1023). The lower one is the contents of that location as scaled for the screen display (vertical coordinate).

III. PROGRAM LISTING

A computer printout of the source program follows.

```
GOLEM2,I  LN=1


        SEGMNT 4
                        /
        *1              /FLAGS POINTERS COUNTERS AND
REGISTERS
                        /
BFLAG,  0               /BUFFFER
AFLAG,  0               /AVERAGE
RFLAG,  0               /RUN
PFLAG,  0               /PLOT
X,      0               /DATA
Y,      0               /DATA
EFLAG,  0               /EXPAND
CPOINT, 0               /COMMAND
TPOINT, 0               /TABLE
IPOINT, 0               /INDEX
ACOUNT, 0               /AVERAGE
DIV,    0               /DIVISION
MXFLAG, 0               /MIX
ANFLAG, 0               /ALFANUMERIC
                        /
        SEGMNT 0
                        /
        *40             /FOR PROGRAM INTERRUPT (PI)
                        /
        0
        IOB
        6031            /WAS IT TELETYPE (TTY)?
        JMP .+3         /NO - THEN ASSUME IT WAS RECYCLE
DELAY (RD)
        LIF 4           /YES
        JMP TTY
        LIF 4
        JMP CHKAVE      /AND CONTINUE
                        /
        SEGMNT 4
                        /
        *20
                        /
ENTER,  LDA I
        252
        IOB
        6046            /WRITE *
        SET I ACOUNT
        0               /SET AVERAGE COUNTER
        SET I BFLAG
        1               /AVERAGE BUFFER
        SET I AFLAG
        0               /AVERAGE FLAG OFF
        SET I RFLAG
        0               /RUN FLAG OFF
        SET I PFLAG
        0               /PLOT FLAG OFF
        SET I MXFLAG
        0               /MIX FLAG OFF
        SET I ANFLAG
        0               /ALFANUMERIC FLAG OFF
        JMP BUFF
```

```
GOLEM2,2  LN=71


                        /
        *100
                        /
BUFF,   LDA
        BFLAG
        AZE
        JMP .+7         /AVERAGE BUFFER
        SNS I 1         /INPUT BUFFER
        JMP .+3
        LDF 6           /REAL INPUT
        JMP .+10
        LDF 7           /IMAG INPUT
        JMP .+6
        SNS I 1
        JMP .+3
        LDF 2           /REAL AVERAGE
        JMP .+2
        LDF 3           /IMAG AVERAGE
CHKALF, SAM 5           /ALFANUMERIC
        ADA I
        1000            /MAKE POSITIVE
        BCL I
        7               /TO PREVENT JITTER - COARSE
        STC SAMREG      /FOR ALFNUM AND ADDITION ROUTINES
        SAM 6           /FINE CURSOR ADJUSTMENT
        SCR 4
        ADA
        SAMREG
        STC SAMREG
COORD,  SET I X
        0
        SET I Y
        3777
        SET I EFLAG
        0               /EXPAND FLAG OFF
        SNS I 0         /MOVE AND EXPAND?
        JMP MOVE        /YES
DISPLY, JMP FPLOT       /GO CHECK PLOT FLAG
        SNS 0
        JMP .+12        /NORMAL DISPLAY
        SAM 2           /VERTICAL SCALING
        COM
        SCR 7
        BCL I
        7774
        ADA I
        SCR
        STC VERT
        JMP .+4
        LDA I
        SCR 3           /NORMAL VERTICAL SCALE
        STC VERT
        LDA I Y
VERT,   0               /SCALE
        DIS X           /DISPLAY
        SNS 3           /ALFANUMERIC?
        JMP NOALF       /NO
```

```
GOLEM2,3  LN=162


         LDA
         Y
         BCL I
         2000
         SAE I
SAMREG,  0
         JMP NOALF+3
         LDA
         VERT
         STC VERT1
         LDA Y
VERT1,   0
         DIS X
         DIS X
         DIS X
         DIS X
         DIS X
         DIS X
         DIS X
         DIS X
         DIS X
         DIS X
                        /
ALFNUM,  LDA
         SAMREG
ADDRESS
         LIF 1
         JMP 20
- DECIMAL CONVERSION OF
         LDA I
         340
         LIF 1
         JMP 200
(DECIMAL)
         LDA Y
CONTENTS
         LIF 1
         JMP 20
         LDA I
         300
         LIF 1
         JMP 200
         JMP NOALF+3
                        /
NOALF,   LDA I
         1777
         STC SAMREG
         XSK I X
         NOP
         SNS 2
         JMP .+3
         XSK I Y
POINT
         NOP
         LDA
         EFLAG
         AZE
```

/SCALE

/TO BRIGHTEN

/PREPARE TO DISPLAY ALFANUMERIC

/GO TO SUBROUTINE OCTDEC FOR OCTAL
ADDRESS

/YCOORDINATE

/GO TO DISCHR FOR ADDRESS DISPLAY

/PREPARE TO DISPLAY ALFANUMERIC

/GO TO OCTDEC

/YCOORDINATE

/GO TO DISCHR

/FOR SNS3=0 - SAMREG HAS 1777

/INCREMENT X

/CONCENTRATED DISPLAY?

/NO

/YES - DISPLAY EVERY SECOND DATA

/EXPAND?

```
GOLEM2,4  LN=246


        JMP EXPAND      /YES
        LDA
        X
        ROL 2
        APO I           /DISPLAY REACHED END OF PDP SCOPE?
        JMP DISPLY      /NO
        LDA             /YES
        PFLAG
        AZE I           /DID WE JUST PLOT?
        JMP .+6         /NO
        IOB
        6344
        JMP .-2         /YES - SO WAIT FOR LAST POINT TO BE
PLOTTED
        IOB
        6357            /CLEAR DEVICE FLAGS
        SET I PFLAG
        0               /PLOT FLAG OFF
        JMP TTY         /GO CHECK TTY

                        /
FPLOT,  LDA             /SUBROUTINE TO CHECK IF POINT
SHOULD BE PLOTTED. IF SO  IT WAITS UNTIL PLOTTER READY
        0
        STC SUBPLT      /FOR EXIT
        LDA
        PFLAG
        AZE I   /PLOT FLAG ON?
        JMP 0           /NO - GO DISPLAY
        IOB
        6344
        JMP .-2         /YES - WAIT FOR COMPLETE PLOT PULSE
        IOB
        6357            /CLEAR DEVICE FLAGS
        IOB
        6331            /REENABLE PLOTTER
        JMP SUBPLT      /EXIT
                        /
SUBPLT, 0
                        /
MOVE,   SAM 0
        BCL I
        7000
        ROL 1
        XSK I Y
        NOP
        ADM
        Y
        SET I EFLAG
        1               /TURN ON EXPAND FLAG
        JMP 0           /EXIT
                        /
EXPAND, SAM 1
        BCL I
        7000
        SCR 3
        ADM
```

GOLEM2,5 LN=335

```
        X
        JMP 0           /EXIT
                        /
TTY,    SET I CPOINT
        COMM            /COMMAND BUFFER
        IOB
        6031            /TTY READ FLAG ON?
        SKP             /NO
        JMP READ-3      /YES
                        /
CHKMIX, LDA
        MXFLAG
        AZE I           /IN PHASE MIXING LOOP?
        JMP .+3         /NO - CONTINUE
        LIF 0           /YES GO TO MIX ROUTINE
        JMP 201
                        /
CHKADD, LDA
        ANFLAG
        AZE I           /IN ADDITION LOOP?
        JMP .+2         /NO - CONTINUE
        JMP DOADD       /YES - GO ADD
RD,     IOB
        6342            /END OF RD?
        JMP BUFF        /NO
        LDA             /YES
        RFLAG
        AZE I           /RUN FLAG ON?
        JMP BUFF        /NO
                        /
BURST,  PDP             /YES
        PMODE
        CLA
        6042            /CLEAR TTY WRITE FLAG TO PREVENT PI
        ION
        LINC
        LMODE
        IOB
        6357            /CLEAR DEVICE FLAGS
        IOB
        6312            /CLEAR SAMPLE  COUNTER
        NOP
        NOP
        NOP
        IOB
        6314            /INITIALIZE BURST
        NOP
        JMP .-1         /WAIT FOR PI (FROM RD)
                        /
CHKAVE, LDA
        AFLAG
        AZE             /AVERAGE FLAG ON?
        JMP STAVE       /YES
        JMP BUFF
                        /
STAVE,  LDA
        AFLAG
```

```
GOLEM2,6  LN=426


         SAE I
         2                  /ARE WE ON FIRST AVERAGE PASS OF RA
COMMAND?
         JMP .+4            /NO - AVERAGE
         SET I AFLAG        /
         1                  /YES - DO NOT AVERAGE. FOR CASE RD
NOT >> T1
         JMP BUFF
         LDA
         ACOUNT             /AVERAGE COUNTER
         SAE
         NAVE               /REACHED PRESET COUNT?
         JMP .+6            /NO
         SET I AFLAG        /YES
         0                  /AVERAGE FLAG OFF
         SET I RFLAG
         0                  /RUN FLAG OFF
         JMP BUFF
                            /
AGO,     XSK I ACOUNT       /INCREMENT AVERAGE COUNTER
         NOP
         LDA
         ACOUNT
         JMP INCR           /GO SEE IF AVERAGED ANOTHER 2000
TIMES
         STC ACOUNT         /IF SO STORE MODIFIED AVERAGE COUNT
(+2000)
         SET I DIV
         0                  /POWER OF TWO FOR AVERAGE DIVISION
         JMP POWER
                            /
INCR,    STC STORE          /STORE AVERAGE COUNT
         LDA
         0
         STC SUBINC         /FOR EXIT
         LDA
         STORE
         BCL I
         6000
         AZE                /IS AVERAGE COUNT MULTIPLE OF 2000?
         JMP .+6            /NO
         LDA                /YES
         STORE
         ADA I
         2000               /TRANSFER TO NEXT 2000
         JMP SUBINC         /EXIT
         LDA
         STORE              /NO MODIFICATION OF AVERAGE COUNT
         JMP SUBINC         /EXIT
STORE,   0
SUBINC,  0
                            /
POWER,   LDA
         ACOUNT
         SCR 1
         BCL I
         4000               /IN CASE AVERAGE COUNT WAS >3777
```

```
GOLEM2,7  LN=512


OTHERWISE SCALE NEVER REACHES 0
        AZE I           /FOUND POWER OF TWO FOR AVERAGE
COUNT?
        JMP .+4         /YES
        XSK I DIV       /NO - INCREMENT POWER OF TWO
        NOP
        JMP POWER+2     /AND GO SCALE AGAIN
        LDA
        DIV
        ADA I
        SCR
        STC SHFT        /FOR DIVISION
        SET I X
        1777            /DATA COUNTER
        SET I Y
        3777            /DATA POINTER
        SET I EFLAG
        0               /EFLAG USED AS BUFFER INDICATOR
        LDA I           /SET UP DATA FIELD COMMANDS FOR
AVERAGING
        LDF 2
        STA
        D1
        STA
        D3
        LDA I
        LDF 6
        STA
        D2
                        /
AVE,    CLR             /START AVERAGING
D1,     0               /AVERAGE BUFFER
        LDA I Y
        STC SHFT-2
D2,     0               /INPUT BUFFER
        LDA Y
        STC SHFT-3
        PDP             / DO TWOS COMPLEMENT ARITHMETIC
SINCE DIGITIZER INPUT IS IN THIS FORM
        PMODE
        TAD AVB
        CIA
        TAD INB         /IN-AVE ==> AC
        JMP .+3
INB,    0
AVB,    0
        LINC
        LMODE
SHFT,   0               /DIVIDE - SCALE BY K WHERE
2POWER(K-1)<C(ACOUNT)<2POWER(K)+1
        PDP
        PMODE
        TAD AVB         /(IN-AVE)/K + AVE ==> AC
        LINC
        LMODE
D3,     0               /AVERAGE BUFFER
        STA Y   /(IN-AVE)/K + AVE ==> AVE
```

```
GOLEM2,10  LN=577


        XSK I X          /DONE 2000 POINTS?
        JMP AVE          /NO
        LDA              /YES
        EFLAG
        AZE              /JUST DONE IMAGINARY DATA?
        JMP BUFF         /YES
        SET I EFLAG      /NO
        1                /PUT BUFFER INDICATOR ON IMAG
        LDA I            /SET BUFFERS TO IMAG
        LDF 3
        STA
        D1
        STA
        D3
        LDA I
        LDF 7
        STA
        D2
        SET I X
        1777             /RESET DATA COUNTER
        SET I Y
        3777             /RESET DATA POINTER
        JMP AVE          /GO AVERAGE IMAG DATA
                         /

        CLR
        10B
        6044             /DUMMY WRITE TO SET TTY WRITE FLAG
                         /
READ,   LDA I
        0707
        STA
        COMM+1
        STA
        COMM+2           /PUT 7777 IN NUMBER PART OF COMMAND
BUFFER SO WE SMOOTH OR AVERAGE 8000 TIMES IF NO PRESET COUNT IS
SPECIFIED
        JMP RTT          /GO READ TTY
        JMP CHKRUB       /SEE IF RUB
        JMP WRT          /NO - ECHO
        STH CPOINT       /SAVE FIRST HALF
        JMP RTT          /GET NEXT HALF
        JMP CHKRUB
        JMP WRT
        STH I 10         /SAVE IT
        SHD I 10         /INCREMENT HALF WORD
        NOP
        LDA
        CPOINT
        SAE I
        COMM+2           /ON LETTER (XX) OR NUMBER (AAAA)
PART OF COMMAND?
        SKP              /LETTER
        JMP READ+6       /NUMBER
                         /
CHAR,    JMP RTT         /GET NEXT CHARACTER
        JMP CHKRUB       /SEE IF RUB
        SAE I
```

GOLEM2,11 LN=665

```
         254                /COMMA?
         JMP .+3            /NO
         JMP WRT            /YES
         JMP READ           /ECHO AND GO GET NEXT  CHARACTER
         SAE I
         215                /CR?
         JMP CHAR           /NO - GO TRY AGAIN FOR LEGAL
CHARACTER (RUB,COMMA,CR)
         JMP WRT            /YES - ECHO
         LDA I
         212
         JMP WRT            /WRITE LF
         LDA I
         252
         JMP WRT            /WRITE *
         SET I CPOINT
         COMM               /RESET COMMAND POINTER
         JMP CNTRL
                            /
RTT,     PDP                /READ TTY
         PMODE
         6031
         JMP .-1            /WAIT FOR TTY READ FLAG
         6036               /CLEAR FLAG AND READ
         LINC
         LMODE
         JMP 0              /EXIT
                            /
WRT,     PDP                /WRITE ON TTY
         PMODE
         6041
         JMP .-1            /WAIT FOR TTY WRITE FLAG
         6046               /CLEAR FLAG AND WRITE
         LINC
         LMODE
         JMP 0              /EXIT
                            /
CHKRUB,  SAE I
         377                /RUB OUT?
         JMP 0              /NO
         JMP RUB            /YES
                            /
RUB,     SET I CPOINT       /RUB OUT COMMAND
         COMM               /RESET COMMAND POINTER
         LDA I
         215
         JMP WRT            /WRITE CR
         LDA I
         212
         JMP WRT            /WRITE LF
         LDA I
         252
         JMP WRT            /WRITE *
         JMP READ           /RETURN
                            /
CNTRL,   SET I TPOINT
         TABLE-1
```

```
GOLEM2,12  LN=755


        SET I IPOINT
        INDX-1
CMPAR,  XSK I TPOINT    /ADVANCE IN TABLE
        XSK I IPOINT    /ADVANCE IN INDEX
        LDA
        IPOINT
        SAE I
        COUNT           /COMMAND NOT IN INDEX?
        SKP
        JMP READ        /NO
        LDA CPOINT
        SAE IPOINT      /FOUND COMMAND IN INDEX?
        JMP CMPAR       /NO
        LDA TPOINT      /YES
        ADA I
        JMP
        STC EXEC
                        /
EXEC,   0               /GO EXECUTE COMMAND
                        /
COMM,   0
        0
        0
        0
        0
        0
        0
        0
        0
        0
        0
        0
        0
        0
        0
        0
        0
        0
        0
        0
        0
        0
        0
        0
                        /
INDX,   2324            /ST - STOP
        2223            /RS - RUN SPECTROMETER
        2201            /RA - RUN WITH AVERAGING
        0301            /CA - CONTINUE AVERAGING
        0411            /DI - DISPLAY INPUT
        0401            /DA - DISPLAY AVERAGE
        2004            /PD - PLOT DATA
        0314            /CL - CLEAR BUFFERS
        0624            /FT - FOURIER TRANSFORM AVERAGE
        1124            /IT - INVERSE TRANSFORM AVERAGE
        2304            /SD - SAVE DATA ON TAPE
        0304            /CD - CALL DATA FROM TAPE
        1520            /MP - MAKE PULSE PROGRAM
```

```
GOLEM2,13  LN=1046


        1420            /LP - LOAD PULSE PROGRAM
        1530            /MX - PHASE MIX AVERAGE
        0104            /AD - ADD CONSTANT TO DATA
        0414            /DL - CALL DIAL
        2315            /SM - SMOOTH DATA
                        /
COUNT,  0               /INDICATES END OF INDEX
                        /
TABLE,  STAD            /COMMAND EXECUTE ADDRESSES
        RSAD
        RAAD
        CAAD
        DIAD
        DAAD
        PDAD
        CLAD
        FTAD
        ITAD
        SDAD
        CDAD
        MPAD
        LPAD
        MXAD
        ADAD
        DLAD
        SMAD
                        /
STAD,   SET I AFLAG     /STOP
        0
        SET I RFLAG
        0
        SET I PFLAG
        0
        SET I MXFLAG
        0
        SET I ANFLAG
        0
        JMP BUFF
                        /
RSAD,   SET I BFLAG     /RUN SPECTROMETER
        0
        SET I AFLAG
        0
        SET I PFLAG
        0
        SET I RFLAG
        1
        SET I MXFLAG
        0
        SET I ANFLAG
        0
        JMP BURST
                        /
RAAD,   SET I PFLAG     /RUN WITH AVERAGING
        0
        SET I BFLAG
        1
```

```
GOLEM2,14  LN=1137


         SET I AFLAG
         2
         SET I RFLAG
         1
         SET I MXFLAG
         0
         SET I ANFLAG
         0
         SET I ACOUNT
         0                  /RESET AVERAGE COUNTER
         JMP ACOMM
         JMP BURST          /RETURN
ACOMM,   NOP
         SET I CPOINT       /NOW TAKE NUMBER PART OF COMMAND
BUFFER (COMM+1 AND COMM+2) REPACK AS A SINGLE NUMBER AND STORE
IN NAVE
         COMM+1
         LDH CPOINT         /GET FIRST DIGIT FROM NUMBER PART
OF RA COMMAND
         BCL I
         7770
         ROL 11
         STC TEMM1
         LDH I CPOINT       /SECOND DIGIT
         BCL I
         7770
         ROL 6
         STC TEMM2
         LDH I CPOINT       /THIRD DIGIT
         BCL I
         7770
         ROL 3
         STC TEMM3
         LDH I CPOINT       /FOURTH DIGIT
         BCL I
         7770
         ADD TEMM1          /PACK FOUR DIGITS
         ADD TEMM2
         ADD TEMM3
         STC NAVE           /STORE IN PRESET AVERAGE COUNT
REGISTER
         SET I CPOINT
         COMM
         JMP 0              /RETURN
                            /
NAVE,    0
TEMM1,   0
TEMM2,   0
TEMM3,   0
                            /
CAAD,    SET I PFLAG        /CONTINUE AVERAGING
         0
         SET I BFLAG
         1
         SET I AFLAG
         2
         SET I RFLAG
```

```
GOLEM2,15  LN=1224


          1
          SET I MXFLAG
          0
          SET I ANFLAG
          0
          JMP ACOMM          /GO READ NUMBER OF REQUESTED
AVERAGE PASSES
          JMP BURST          /GO AVERAGE
DIAD,     SET I BFLAG        /DISPLAY INPUT
          0
          JMP BUFF
                             /
DAAD,     SET I BFLAG        /DISPLAY AVERAGE
          1
          JMP BUFF
                             /
PDAD,     SET I AFLAG        /PLOT DATA
          0
          SET I RFLAG
          0
          SET I PFLAG
          1
          SET I MXFLAG
          0
          SET I ANFLAG
          0
          IOB
          6331               /ENABLE PLOTTER
          CLR
          DIS PFLAG          /DUMMY PLOT OF POINT (0,0) TO GIVE
PLOT COORDINATES ORIGIN AND TO SEND OUT FIRST COMPLETE PLOT
PULSE
          JMP BUFF
                             /
CLAD,     LDF 2              /CLEAR DATA BUFFERS
          SET I Y
          3777
SCL,      CLR
          STA Y
          XSK I Y
          JMP SCL
          LDA
          CLAD
          SAE I
          LDF 3              /CLEARED AVERAGE BUFFER?
          JMP .+5            /NO
          LDA I              /YES
          LDF 6
          STC CLAD           /SWITCH TO INPUT BUFFER
          JMP CLAD
          SAE I
          LDF 7              /CLEARED ALL?
          JMP .+5            /NO
          LDA I
          LDF 2
          STC CLAD           /RESET CLAD
          JMP BUFF           /YES
```

```
GOLEM2,16  LN=1312


         ADA I
         1                  /INCREMENT DATA FIELD
         STC CLAD
         JMP CLAD
                            /
FTAD,    SET I AFLAG        /FOURIER TRANSFORM AVERAGE
         0
         SET I RFLAG
         0
         SET I BFLAG
         1
         SET I MXFLAG
         0
         SET I ANFLAG
         0
         LDF 2              /SET DATA FIELD FOR FT
         LIF 0
         JMP 20
                            /
ITAD,    SET I AFLAG        /INVERSE TRANSFORM AVERAGE
         0
         SET I RFLAG
         0
         SET I BFLAG
         1
         SET I MXFLAG
         0
         SET I ANFLAG
         0
         LDF 2              /SET DATA FIELD FOR IT
         LIF 0
         JMP 30
                            /
/
SDAD,    SET I AFLAG        /SAVE DATA ON TAPE
         0
         SET I RFLAG
         0
         SET I MXFLAG
         0
         SET I ANFLAG
         0
         JMP PACK           /GO GET DATA NUMBER
         ROL 3              /X10
         ADA I
         3004
         STC STAP
         715                /WRITE
STAP,    0                  /4 BLOCKS FROM CURRENT DATA FIELD
ONTO TAPE STARTING AT BLOCK NUMBER (10 X DATA NUMBER) + 4
         JMP BUFF
                            /
CDAD,    SET I AFLAG        /CALL DATA FROM TAPE
         0
         SET I RFLAG
         0
         SET I MXFLAG
```

```
GOLEM2,17  LN=1402


        0
        SET I ANFLAG
        0
        JMP PACK        /GO GET DATA NUMBER
        ROL 3           /X10
        ADA I
        3004
        STC CTAP
        711             /READ
CTAP,   0               /4 BLOCKS FROM TAPE ADDRESS (10 X
DATA NUMBER)+4 INTO CURRENT DATA FIELD
        JMP BUFF
                        /
PACK,   SET I CPOINT
        COMM+2          /PACKS THIRD AND FOURTH DIGITS OF
NUMBER PART OF SD CD MP LP SM COMMANDS
        LDH CPOINT      /GET THIRD DIGIT
        BCL I
        7770
        ROL 3
        STC TEMM1
        LDH I CPOINT    /GET FOURTH DIGIT
        BCL I
        7770
        ADD TEMM1       /PACK
        JMP 0           /EXIT
                        /
MPAD,   JMP BUFF
LPAD,   JMP BUFF
                        /
ADAD,   SET I AFLAG     /FOR ADDING CONSTANT TO DATA IN AVE
BUFFER
        0
        SET I RFLAG
        0
        SET I MXFLAG
        0
        SET I ANFLAG
        1
        JMP SMSTRT      /GO TRANSFER DATA TO INPUT BUFFER
DOADD,  SET I Y
        3777
        SAM 3           /ADDITION CONSTANT
        BCL I
        1               /TO PREVENT JITTER
        SAE
        ADDREG          /CONSTANT SAME AS BEFORE?
        JMP .+2         /NO - GO ADD
        JMP 100         /YES - RETURN TO CONTROL AND DISPLAY
        STC ADDREG      /STORE NEW CONSTANT
ADSTRT, SNS 1           /REAL OR IMAGINARY DATA?
        JMP .+3
        LDF 7           /IMAG
        SKP
        LDF 6           /REAL
        LDA I Y
        ADA I
```

```
GOLEM2,20  LN=1470


ADDREG, 0                  /ADD CONSTANT
        SNS 1              /REAL OR IMAGINARY DATA?
        JMP .+3
        LDF 3              /IMAG
        SKP
        LDF 2              /REAL
        STA Y              /STORE NEW VALUE
        LDA
        Y
        BCL I
        2000               /STRIP OFF DATA FIELD INDEX
        SAE
        SAMREG             /ADDED TO ALL REQUESTED POINTS?
                           /SAMREG HAS REQUESTED ALFANUMERIC
POINT FOR SNS3=1 AND HAS 1777 FOR SNS3=0
        JMP ADSTRT         /NO - GO DO NEXT POINT
        JMP DOADD          /YES - GO CHECK FOR CHANGE OF
CONSTANT
                           /
MXAD,   SET I MXFLAG
        1
        SET I ANFLAG
        0
        JMP SMAD+14        /AVERAGE BUFFER ==> INPUT BUFFER
        CLR
        LIF 0
        JMP 200            /GO MIX
                           /
DLAD,   SET I EFLAG        /CALL DIAL
        2015
        LDF 2
        LDA I
        701                /SET UP TAPE INSTRUCTION
        STA I EFLAG
        LDA I
        7300
        STA I EFLAG
        LIF 2
        LDF 3
        JMP 16
                           /
SMAD,   SET I AFLAG
        0
        SET I RFLAG
        0
        SET I MXFLAG
        0
        SET I ANFLAG
        0
        JMP PACK           /GET REQUESTED NUMBER OF SMOOTHINGS
        STC NAVE
        LDA
        ACOUNT
        STC TMCONT         /PROTECT CURRENT NUMBER OF AVERAGE
PASSES
        SET I ACOUNT
        0                  /FOR SMOOTHING COUNT
```

```
GOLEM2,21  LN=1556


SMSTRT, SET I X
        3777
SMD1,   LDF 2           /MAY BE LDF 3
        LDA X
SMD2,   LDF 6           /MAY BE LDF 7
        STA X           /AVERAGE BUFFER ==> INPUT BUFFER
        XSK I X         /TRANSFERRED 2000 POINTS?
        JMP SMD1        /NO
        LDA             /YES
        SMD1
        SAE I
        LDF 3           /TRANSFERRED IMAG DATA?
        SKP
        JMP .+10        /YES
        LDA I           /NO - SET UP FOR IMAG
        LDF 3
        STC SMD1
        LDA I
        LDF 7
        STC SMD2
        JMP SMSTRT
        LDA I           /RESET TO REAL
        LDF 2
        STC SMD1
        LDA I
        LDF 6
        STC SMD2
        LDA
        MXFLAG
        AZE I           /WAS THIS DATA TRANSFER FOR MIXING?
        JMP .+2         /NO - CONTINUE
        JMP MXAD+5      /YES - RETURN TO MIXING ROUTINE
        LDA
        ANFLAG
        AZE I           /WAS THIS DATA TRANSFER FOR
ADDITION?
        JMP .+2         /NO - CONTINUE
        JMP DOADD       /YES - RETURN TO ADDITION ROUTINE
SMOOTH, SET I X
        3777
        JMP SMD3        /SMOOTH NEXT POINT
SDONE,  LDA             /DONE 2000 POINTS
        SMD4
        SAE I
        LDF 3           /SMOOTHED IMAG DATA?
        JMP SMIMAG      /NO - GO DO IMAG
        LDA I           /YES - RESET FOR REAL
        LDF 2
        STC SMD4
        LDA I
        LDF 6
        STC SMD3
        XSK I ACOUNT    /INCREMENT SMOOTHING COUNTER
        NOP
        LDA
        ACOUNT
        SAE
```

```
GOLEM2,22  LN=1646

         NAVE              /SMOOTHED PRESET COUNT?
         JMP SMSTRT        /NO - GO SMOOTH AGAIN
         LDA
         TMCONT
         STC ACOUNT        /RESTORE AVERAGE COUNTER
         SET I PFLAG
         0
         SET I RFLAG
         0
         SET I AFLAG
         0
         SET I BFLAG
         1
         JMP BUFF          /RETURN
SMIMAG,  LDA I             /SET FOR IMAGINARY
         LDF 3
         STC SMD4
         LDA I
         LDF 7
         STC SMD3
         JMP SMOOTH
SMD3,    LDF 6             /MAY BE LDF 7
         LDA X
         SCR 2
         STC SMTEM1        /0.25C(X-1)
         LDA I X
         SCR 1
         STC SMTEM2        /0.5C(X)
         LDA I X
         SCR 2             /0.25C(X+1)
         PDP               /FOR TWOS COMPLEMENT
         PMODE
         TAD SMTEM1
         TAD SMTEM2        /0.25C(X-1) + 0.5C(X) + 0.25C(X+1)
FOR 0<X<1777
         JMP .+4
SMTEM1,  0
SMTEM2,  0
SMTEM3,  0
         LINC
         LMODE
SMD4,    LDF 2             /MAY BE LDF 3
         STC SMTEM3
         LDA
         X
         SAE I
         2000              /DONE 2000 POINTS?
         JMP .+2           /NO
         JMP .+5           /YES - STORE LAST POINT AND RETURN
         ADA I
         -1
         STC X
         JMP .+10
         LDA I
         3777
         STC X
         LDA
```

```
GOLEM2,23  LN=1736


        SMTEM3
        STA X
        JMP SDONE
        LDA
        SMTEM3
        STA X           /SMOOTHED POINT ==> AVERAGE BUFFER
        JMP SMOOTH+2
TMCONT, 0
                        /
                        /
                        /
                        /
        SEGMNT 0
                        /
        *20
        PDP
        PMODE
        JMS I DOFFT
        JMS I SQRT
        LINC
        LMODE
        LIF 4
        JMP 100         /RETURN TO BUFF
                        /
        *30
        PDP
        PMODE
        JMS I DOIFFT
        JMS I SQRT
        LINC
        LMODE
        LIF 4
        JMP 100         /RETURN TO BUFF
                        /
                        /
PMODE
*50
/FFTS,COMPLEX
/PAGE ZERO
/TABLE PARAMETERS
N, 2000 /NUMBER OF POINTS
NU, 12 /LOG(BASE 2) N
L,0
S,      0       /GIVE SPACING BETWEEN NODES PAIRS IN LTH
ARRAY
F,      0       /USED FOR SCALING NODE POSITION TO GET
NUMBERS IN NODES
NOVER4, 0       /STORAGE FOR N/4
MAXNU,  BIGSNU  /LARGEST TABLE SIZE (POWER OF 2)
MNOVR2, 0 /STORAGE FOR -N/2
/INDEXING VARIABLES
QR,     0       /POINTER TO REAL PART OF X(Q)
QI,     0       /POINTER TO IMAG PART OF X(Q)
PR,     0       /POINTER TO REAL PART OF X(P)
PI,     0       /POINTER TO IMAG PART OF X(P)
Q,      0       /NUMERICAL INDEX Q(=0,...N-1)
P,      0       /NUMERICAL INDEX P(=0,...N-1)
```

```
GOLEM2,24  LN=2025


K,      0       /NUMBER IN THE NODE BEING OPERATED ON
/LOOP DELIMITERS
C,      0       /INTERRUPTS COMPUTATION OF LTH ARRAY EVERY
S PASSES
/DATA VARIABLES
ADD2,   0       /USED BY SUBROUTINE ADDR AS DATA (ADDEND)
TEMPR,  0       /TEMPORARY STORAGE REGISTER FOR REAL PARTS
SINE,   0       /TEMP STORAGE FOR SIN(2*PI*K/N)
COSINE, 0       /TEMP STORAGE FOR COS(2*PI*K/N)
GR,     0       /REL PART OF PRODUCT 8WK)*X(P)
GI,     0       /IMAG PART OF (WK)*X(P)
/SUBROUTINE CALL LIST
ADDER,  ADDR    /ADD C(AC) TO C(ADD2) AND SCALE RIGHT
SORT,   SORTX   /BIT INVERTED BUFFER SORTED
INVERT, INVRT   /WORD IN AC OF NU BITS IS BIT INVERTED
MULT,MULTI
GETRIG, TRIGET  /FETCH SIN AND COS OF 2*PI*C(AC)/N
DOFFT,  FFT     /DO FOURIER TRANSFORM ON DATA IN BUFFER
DOIFFT, IFFT    /DO INVERSE OF THE BUFFER
/DATA TABLES
SINLOC, SINTAB  /TABLE OF SIN(2*PI*I/N) FOR I=0,....,N-1
XRLOC,  XRTAB   /INPUT BUFFER AND TABLE OF ARRAYS (REAL
DATA)
XLOCDF, XITAB-XRTAB     /DIFFERENCE IN ADDRESSES OF REAL
AND IMAG TABLES
/PSEUDO FLOATING POINT FORMAT FLAGS
SCALE,  0       /PSEUDO EXPONENT OF FOURIER COEFFICIENTS
SHFLAG, 1       /IF =1, ADD WITH SHIFT,IF=0,ADD WITHOUT
SHIFT
SHFCHK, 0       /INDICATES IF ALL X IN AN ITERATION ARE
LESS THAN .5
/DATA FOR SIN TABLE LOOK UP
SHIFT1, 0       /NUMBER OF SHIFTS ,NEGATIVE
SHIFT2, SHF     /SHIFT COUNTER
*400
FFT, 0
CLA IAC CLL
DCA L
DCA SCALE
IAC
        DCA SHFLAG
        DCA SHFCHK
        TAD N
        CLL RTR
        DCA NOVER4
        TAD NU
        CIA
        TAD MAXNU
CMA
DCA SHIFT1
TAD SHIFT1
DCA I SHIFT2
NOP
        TAD N
        CLL RAR
        DCA S
                TAD S
```

```
GOLEM2,25  LN=2111


        CIA
DCA MNOVR2
        CMA
        TAD S
        TAD XRLOC
        DCA QR
        TAD NU
        CIA
        IAC
        DCA F
LOOP1,  TAD QR
        TAD S
DCA PR
        TAD QR
TAD XLOCDF
DCA QI
TAD PR
TAD XLOCDF
DCA PI
TAD I QI
DCA ADD2
TAD I PI
JMS I ADDER
DCA TEMPR
TAD I QI
DCA ADD2
TAD I PI
CIA
JMS I ADDER
DCA I PI
TAD TEMPR
DCA I QI
TAD I QR
DCA ADD2
TAD I PR
JMS I ADDER
DCA TEMPR
TAD I QR
DCA ADD2
TAD I PR
CIA
JMS I ADDER
DCA I PR
TAD TEMPR
DCA I QR
TAD XRLOC
CIA
TAD QR
SPA SNA CLA
JMP CHKPT
CMA
TAD QR
DCA QR
JMP LOOP1
/PAGE 3
CHKPT, TAD L
CIA
```

```
GOLEM2,26  LN=2202


TAD NU
SNA CLA
JMP I FFT
TAD SHFCHK
DCA SHFLAG
TAD SHFCHK
SNA CLA
ISZ SCALE
DCA SHFCHK
ISZ L
TAD S
CLL RAR
DCA S
ISZ F
NOP
CMA
TAD N
TAD XRLOC
DCA PR
SETC, CLA IAC
DCA C
BUILD, TAD PR
TAD XLOCDF
DCA PI
TAD XRLOC
CIA
TAD PR
DCA P
TAD F
CIA
LINC
LMODE
BSE I
SCR I
STC .+2
ADD P
0
PDP
PMODE
/PAGE 4
JMS I INVERT
TAD MN0VR2
JMS I GETRIG
ADJSGN, NOP
DCA SINE
TAD I PR
JMS I MULT
COSINE
DCA ADD2
TAD I PI
JMS I MULT
SINE
TAD ADD2
DCA GR
/FOR IMAGINARY
TAD I PI
JMS I MULT
```

GOLEM2,27 LN=2273

```
COSINE
DCA ADD2
TAD I PR
JMS I MULT
SINE
CIA
TAD ADD2
DCA GI
TAD S
CIA
TAD PR
DCA QR
TAD QR
TAD XLOCDF
DCA QI
TAD I QR
DCA ADD2
TAD GR
CIA
JMS I ADDER
DCA I PR
TAD I QI
DCA ADD2
TAD GI
CIA
JMS I ADDER
DCA I PI
TAD I QR
DCA ADD2
TAD GR
JMS I ADDER
DCA I QR
TAD I QI
DCA ADD2
TAD GI
/PAGE 5
JMS I ADDER
DCA I QI
CMA
TAD P
DCA P
CMA
TAD PR
DCA PR
TAD C
CIA
TAD S
SZA CLA
JMP CNOTS
TAD P
CMA
TAD S
SNA CLA
JMP I RECHK
TAD S
CIA
TAD PR
```

```
GOLEM2,30  LN=2364


DCA PR
JMP I RESETC
CNOTS, ISZ C
JMP I RBUILD
RBUILD, BUILD
RESETC, SETC
RECHK, CHKPT
/PAGE 6
SORTX,0
CMA
TAD N
DCA Q
REVERS, TAD Q
JMS I INVERT
DCA P
TAD P
CIA
TAD Q
SPA SNA CLA
JMP SWAPED
TAD P
TAD XRLOC
DCA PR
TAD Q
TAD XRL0C
DCA QR
TAD PR
TAD XLOCDF
DCA PI
TAD QR
TAD XLOCDF
DCA QI
TAD I PR
DCA TEMPR
TAD I QR
DCA I PR
TAD TEMPR
DCA I QR
TAD I PI
DCA TEMPR
TAD I QI
DCA I PI
TAD TEMPR
DCA I QI
SWAPED, TAD Q
SNA CLA
JMP I SORTX
CMA
TAD Q
DCA Q
JMP REVERS
/PAGE 7, INVERSE TRANSFORM
IFFT,0
CLA CLL
TAD CCIA
DCA I SGNADJ
JMS I DOFFT
```

```
GOLEM2,31  LN=2455


TAD CNOP
DCA I SGNADJ
JMP I IFFT
SGNADJ, ADJSGN
CCIA, CIA
CNOP, NOP
*1000
MULTI,0
        CLL
SPA
TAD M1
        DCA TEM1        /PUT AWAY MULTIPLIER
TAD I MULTI
        DCA TEM2        /SAVE IT
        TAD I TEM2      /GET MULTIPLICAND
SPA
TAD M1
ISZ MULTI
        LINC
LMODE
SCR 1
        MUL     /MULTIPLY
        TEM1+4000       /AS A FRACTION
        LZE     /IS RESULT NEGATIVE?
        COM     /YES,MAKE IT POS
        SCR 12  /SHIFT IT INTO MQ
        QAC     /BRING IT BACK WITH ANOTHER BIT
        QLZ     /DOES NEXT BIT=1?
        ADD ONE /YES, ROUND UP
PDP
PMODE
SZL
CIA
JMP I MULTI
TEM1,   0
TEM2,   0
ONE,    1
M1, -1
/PAGE 9
INVRT, 0
DCA WORD
DCA WORDP
TAD NU
CIA
DCA FLIPCT
FLIP, TAD WORD
CLL RAR
DCA WORD
TAD WORDP
RAL
DCA WORDP
ISZ FLIPCT
JMP FLIP
TAD WORDP
JMP I INVRT
WORD,0
WORDP,0
```

```
GOLEM2,32  LN=2546


FLIPCT,0
/PAGE 10
TRIGET,0
DCA K
TAD K
CLL CIA
TAD NOVER4
DCA NO4MIK
SZL
JMP QUAD1
QUAD2, TAD NO4MIK
CIA
JMS SHIFT
TAD I INDEX
CIA
DCA COSINE
TAD NO4MIK
TAD NOVER4
JMP SINRET
QUAD1, TAD NO4MIK
JMS SHIFT
TAD I INDEX
DCA COSINE
TAD K
SINRET, JMS SHIFT
TAD I INDEX
JMP I TRIGET
SHIFT,0
SKP
CLL RAL
ISZ SHF
JMP .-2
TAD SINLOC
DCA INDEX
TAD SHIFT1
DCA SHF
JMP I SHIFT
SHF,0
NO4MIK,0
INDEX,0
/PAGE 11
ADDR,0
DCA ADD1
TAD SHFLAG
SNA CLA
JMP ADDWOS
TAD ADD1
LINC
LMODE
SCR 1
STC ADD1
ADD ADD2
SCR 1
STC ADD2
QAC
PDP
PMODE
```

```
GOLEM2,33  LN=2637


RTL
CMA CML
SMA SNL CLA
IAC
ADDWOS, TAD ADD1
TAD ADD2
DCA XSUM
TAD XSUM
SPA
CIA
RAL
SMA CLA
JMP NOTNOR
IAC
DCA SHFCHK
NOTNOR, TAD XSUM
JMP I ADDR
ADD1, 0
XSUM,0
SINTAB, 0000
        0015
        0031
        0046
        0062
        0077
        0113
        0130
        0144
        0161
        0176
        0212
        0227
        0243
        0260
        0274
        0311
        0325
        0342
        0356
        0373
        0407
        0424
        0440
        0455
        0471
        0505
        0522
        0536
        0553
        0567
        0603
        0620
        0634
        0650
        0664
        0701
        0715
```

```
GOLEM2,34  LN=2730

          0731
          0745
          0762
          0776
          1012
          1026
          1042
          1056
          1072
          1106
          1123
          1137
          1153
          1166
          1202
          1216
          1232
          1246
          1262
          1276
          1312
          1325
          1341
          1355
          1370
          1404
          1420
          1433
          1447
          1462
          1476
          1511
          1525
          1540
          1554
          1567
          1602
          1616
          1631
          1644
          1657
          1672
          1705
          1720
          1734
          1747
          1761
          1774
          2007
          2022
          2035
          2050
          2062
          2075
          2110
          2122
          2135
```

```
GOLEM2,35  LN=3021

        2147
        2162
        2174
        2207
        2221
        2233
        2246
        2260
        2272
        2304
        2316
        2330
        2342
        2354
        2366
        2400
        2411
        2423
        2435
        2447
        2460
        2472
        2503
        2515
        2526
        2537
        2551
        2562
        2573
        2604
        2615
        2626
        2637
        2650
        2661
        2672
        2703
        2713
        2724
        2734
        2745
        2755
        2766
        2776
        3007
        3017
        3027
        3037
        3047
        3057
        3067
        3077
        3107
        3117
        3126
        3136
        3145
```

GOLEM2,36 LN=3112

3155
3164
3174
3203
3212
3222
3231
3240
3247
3256
3265
3274
3302
3311
3320
3326
3335
3343
3351
3360
3366
3374
3402
3410
3416
3424
3432
3440
3445
3453
3460
3466
3473
3501
3506
3513
3520
3525
3532
3537
3544
3551
3556
3562
3567
3573
3600
3604
3610
3614
3621
3625
3631
3635
3640
3644
3650

```
GOLEM2,37  LN=3203


        3653
        3657
        3662
        3666
        3671
        3674
        3700
        3703
        3706
        3711
        3713
        3716
        3721
        3724
        3726
        3731
        3733
        3735
        3740
        3742
        3744
        3746
        3750
        3752
        3754
        3755
        3757
        3761
        3762
        3764
        3765
        3766
        3767
        3770
        3771
        3772
        3773
        3774
        3775
        3776
        3776
        3777
        3777
        3777
        3777
        3777
        3777
XRTAB=4000
        XITAB=6000
        BIGSNU=12
                        /
                        /
                        /
        LMODE
                        /
        SEGMNT 0
```

```
GOLEM2,40  LN=3274


                        /
        *200
                        /
PHMIX,  STC MXANGL      /FIRST ANGLE=0
FND,    SET I 2
        3777            /FOR DATA
        CLR
        SAM 7           /READ NEW ANGLE
        SCR 1           /SCALE FOR SIN TABLE
        BCL I
        1               /TO PREVENT JITTER
        SAE
        MXANGL          /ANGLE SAME AS BEFORE?
        JMP .+3         /NO - GO MIX
        LIF 4           /YES RETURN TO CONTROL FOR DISPLAY
        JMP 100
        STA
        MXANGL          /STORE NEW ANGLE
        PDP PMODE
        SPA             /IS IT NEGATIVE?
        CLL CML CMA     /YES - CHANGE SIGN AND SET LINK
        LINC
        LMODE
        STA
        NWANGL          /POSITIVE ANGLE
        ADA I
        SINTAB          /MAKE POINTER
        STC PNTR        /SAVE
        LDA PNTR        /GET VALUE FOR SIN
        LZE             /WAS ARGUMENT NEGATIVE?
        COM             /YES - MAKE SIN NEGATIVE
        STC SIN         /SAVE
        CLR             /CLEAR LINK
        ADD NWANGL
        COM             /FOR COS
        ADA I
        SINTAB+400
        STC PNTR
        LDA PNTR        /GET VALUE FOR COS
        STC COS         /SAVE
PMIX,   LDF 7           /IMAG DATA
        LDA I 2         /GET IMAGINARY COEFFICIENT
        APO             /NEGATIVE?
        ADD MM1         /YES - ONES COMPLEMENT
        STA I
IM,     0
        LDF 6           /REAL DATA
        LDA 2           /GET REAL COEFFICIENT
        APO             /NEGATIVE?
        ADD MM1                 /YES - ONES COMPLEMENT
        STA I
RE,     0
        MUL
        SIN+4000        /AS FRACTION TIMES SIN
        COM             /CHANGE SIGN
        STC SAVMX
        ADD RE          /GET REAL COEFFICIENT AGAIN
```

```
GOLEM2,41  LN=3365


        MUL
        COS+4000        /X COS
        STC RE          /SAVE FIRST PART
        ADD IM          /GET IMAGINARY COEFFICIENT
        MUL
        SIN+4000        /X SIN
        ADD RE          /ADD FIRST PART
        APO             /NEGATIVE?
        ADD ONE1        /YES - TWOS COMPLEMENT
        LDF 2
        STA 2           /STORE PHASE CORRECTED VALUE
        CLR
        ADD IM          /GET IMAGINARY COEFFICIENT AGAIN
        MUL
        COS+4000        /X COS
        ADA I
SAVMX,  0               /ADD OTHER RESULT
        APO             /NEGATIVE?
        ADD ONE1        /YES - TWOS COMPLEMENT
        LDF 3
        STA 2           /STORE
        XSK 2           /LAST POINT?
        JMP PMIX        /NO - GO DO NEXT ONE
        JMP FND         /YES - CHECK FOR ANGLE CHANGE
                        /
PNTR=3
SIN,    0
COS,    0
MM1,    -1
ONE1,   1
MXANGL, 0
NWANGL, 0
                        /
                        /
                        /
        SEGMNT 1
                        /
        *20             /HERE WE HVE OCTAL-DECIMAL
CONVERSION AND CHARACTER DISPLAY
                        /
OCTDEC, PDP
        PMODE
        DCA DWORD
        DCA DECREG      /IN DECREG-DECREG+4 ARE STORED SIGN
AND 4 BCD DIGITS
        DCA DECREG+1
        DCA DECREG+2
        DCA DECREG+3
        DCA DECREG+4
        TAD DWORD
        SPA             /CHECK FOR SIGN
        JMP NWRD        /NEGATIVE
        CLA CLL
        TAD TENS
        DCA DECREG      /POSITIVE - SO PUT 12 (BLANK) IN
DECREG
        JMP VWRD
```

```
GOLEM2,42  LN=3453


NWRD,    CLA CLL
         TAD NEG
         DCA DECREG       /SO PUT 13 (-) IN DECREG
         TAD DWORD
         CIA
         DCA DWORD        /AND MAKE POSITIVE
VWRD,    TAD DWORD
IREG1,   TAD THOSC        /-1000 DECIMAL
         SPA              /FOUND THOUS?
         JMP VVWRD        /YES
         ISZ DECREG+1
         JMP IREG1        /NO - SUBTRACT ANOTHER THOUS
VVWRD,   TAD THOS         /+1000 DECIMAL
IREG2,   TAD HUNDC        /-100 DECIMAL
         SPA              /FOUND HUNDR?
         JMP VVVWRD       /YES
         ISZ DECREG+2
         JMP IREG2        /NO - SUBTRACT ANOTHER HUNDR
VVVWRD,  TAD HUND         /+100 DECIMAL
IREG3,   TAD TENSC        /-10 DECIMAL
         SPA              /FOUND TENS?
         JMP FWRD         /YES
         ISZ DECREG+3
         JMP IREG3        /NO - SUBTRACT ANOTHER TEN
FWRD,    TAD TENS         /+10 DECIMAL
         DCA DECREG+4     /UNITS
ODEND,   LINC
         LMODE
         LIF 4
         JMP 0            /RETURN
THOS,    1750             /1000
HUND,    144              /100
TENS,    12               /10
THOSC,   6030             /-1000
HUNDC,   7634             /-100
TENSC,   7766             /-10
NEG,     13               /-
DWORD,   0
DECREG,  0
         0
         0
         0
         0
         0
         0
         0
         0
         0
                          /
         *1
XC,      620              /XCOORDINATE FOR CHARACTER DISPLAY
YC,      0                /YCOORDINATE
ALFPNT,  0                /POINTER TO INPUT CHAR BUFFER
NUMREG,  0                /POINTER TO CHARACTER PATTERN TABLE
                          /
         *200
DISCHR,  STC 2            /VERTICAL COORD
```

```
G0LEM2,43  LN=3544


        SET I ALFPNT
        DECREG-1
        LDA
        0
        STC SUBCHR
        JMP DISDIG
                        /
NUMTAB, 4136            /CHARACTER PATTERN TABLE - 0
        3641
        2101            /1
        0177
        4523            /2
        2151
        4122            /3
        2651
        2414            /4
        0477
        5172            /5
        0651
        1506            /6
        4225
        4443            /7
        6050
        5126            /8
        2651
        5122            /9
        3651
        0000            /BLANK
        0000
        0404            /-
        0404
DISDIG, LDA I ALFPNT
        ROL 1           /X2
        ADA I
        NUMTAB          /=CHARACTER DISPLAY PATTERN
        STC NUMREG
        LDA
        YC
        DSC NUMREG      /DISPLAY FIRST HALF CHARACTER
        DSC I NUMREG    /DISPLAY SECOND HALF
        LDA I
        4
        ADM
        XC              /TO MAKE SPACE BETWEEN CHARACTERS
        LDA
        ALFPNT
        SAE I
        DECREG+4        /DISPLAYED 5 CHARACTERS?
        JMP DISDIG      /NO - DISPLAY NEXT
        SET I XC
        620             /YES - RESET XCOORDINATE
        LDA
        SUBCHR
        STC 0
        LIF 4
        JMP 0
SUBCHR, 0
```

CHAPTER V

TIME-REVERSAL EXPERIMENTS IN DIPOLAR-COUPLED SPIN SYSTEMS

CHAPTER V

TIME-REVERSAL EXPERIMENTS IN DIPOLAR-COUPLED SPIN SYSTEMS

PHYSICAL REVIEW B VOLUME 3, NUMBER 3 1 FEBRUARY 1971

Time-Reversal Experiments in Dipolar-Coupled Spin Systems*

W-K. Rhim, A. Pines, and J. S. Waugh
Department of Chemistry and Research Laboratory of Electronics, Massachusetts Institute of Technology, Cambridge, Massachusetts 02139
(Received 3 September 1970)

By applying a suitable sequence of strong rf fields, a system of dipolar-coupled nuclear spins can be made to behave as though the sign of the dipolar Hamiltonian had been reversed. The system then appears to develop backward in time, and states of nonequilibrium magnetization can be recovered in systems which would superficially appear to have decayed to equilibrium. This behavior is consistent with dynamical and thermodynamical principles, but shows that the spin-temperature hypothesis must be employed with caution. The theory of the time-reversal phenomenon is discussed, including the practical limitations on the accuracy with which it can be achieved. Various echo experiments in the laboratory and in the rotating frame are reported. The application of repeated time reversals to the problem of high-resolution NMR in solids is discussed.

I. INTRODUCTION

One's first impression on seeing a spin echo tends to be of having witnessed a spontaneous fluctuation of an apparently disordered system into an ordered (magnetized) state. Actually, of course, the system was by no means as disordered as it seemed to be: It had to be prepared from a magnetized state in a special way, such that its microscopic dynamical equations guaranteed a return to the magnetized state; and the name "echo" of course expresses just this fact. The importance of a dynamical, as opposed to thermodynamical, interpretation is particularly transparent in the case of the Hahn echo.[1-3] There the spin Hamiltonian is *inhomogeneous*, i.e., it represents a sum over uncoupled spins or isochromats interacting with fixed local fields. One is not dealing with a "many-body" system at all, and the formation of an echo is easily understood by superposing the quantum-

mechanical (or classical) motion of individually precessing magnetic moments. The same is true of quadrupole echoes,[4,5] though a purely classical picture is not quite so convenient there, and also of photon echoes,[6] whose interpretation follows the same lines as the Hahn echo if a fictitious spin[7] is suitably introduced.

One feels intuitively that the situation ought to be different in the case of *interacting* particles, such as the nuclear spins in a rigid solid. There "spin diffusion" prevents one's using pictures based on isochromats moving in local fields. Moreover, there is no known way to integrate the microscopic dynamical equations even approximately over times much longer than T_2, the time which characterizes the decay of transverse magnetization from an initially coherent state. Under these circumstances recourse is made to the "spin-temperature" hypothesis,[8-10] which asserts that the system approaches a state which is adequately described as one of internal equilibrium (sometimes called semi-equilibrium, to emphasize that the spin system can be considered isolated from the surrounding lattice only for a certain time T_1, usually much greater than T_2).

A particularly simple internal equilibrium state is obtained by first polarizing the system for a long time in a very strong external field $H_0 \gg H_{\rm loc}$, where $\gamma H_{\rm loc} \sim T_2^{-1}$. The state of the system is then assumed to belong to a canonical ensemble characterized by the lattice temperature T_l:

$$\sigma_\epsilon(0) = (1/Z)\, e^{-\mathcal{H}_\epsilon/kT_l} , \qquad (1)$$

$$\mathcal{H}_\epsilon = -\gamma H_0 I_\epsilon + O(\gamma H_{\rm loc}) .$$

We shall henceforth speak in terms of the reduced density matrix

$$\rho_\epsilon(0) = 1 + \gamma H_0 I_\epsilon / kT_l \qquad (2)$$

appropriate to the high-temperature approximation and to the removal of $Z \sim (2I+1)^N$. A 90° pulse of resonant rf field is now applied to bring the magnetization along the y direction:

$$\rho_y(0) = 1 + \gamma H_0 I_y / kT_l . \qquad (3)$$

The magnetization $\gamma \langle I_y \rangle$ now precesses about $\vec{H}_0$ {because $[\rho_y(0), \mathcal{H}_\epsilon] \neq 0$} and decays to zero {because $[\rho_y(0), \mathcal{H}_{\rm int}] \neq 0$}, where $\mathcal{H}_{\rm int}$ is the Hamiltonian of the spin-spin interactions. If the system approaches internal equilibrium, it is then to be described by

$$\rho(\infty) = 1 - \mathcal{H}_\epsilon / kT_s . \qquad (4)$$

Since Zeeman energy must be conserved under the time-independent Hamiltonian acting during the decay,

$$E(\infty) = E(0) = \mathrm{Tr}[\rho_y(0)\, \mathcal{H}_\epsilon] = 0 , \qquad (5)$$

one must set the spin temperature $T_s = \infty$ in (4). Thus $\rho(\infty) = 1$. It is now clear that no echo phenomena can be evoked by applying any external fields: The Hamiltonian representing their interactions with the system commutes trivially with $\rho(\infty)$.

To be sure, some echo phenomena are known in solids.[11,12] However, these echoes can be evoked only by interrupting the development of $\rho_y(0)$ *before* the system has had an opportunity to approach the postulated equilibrium state, and they are weaker the longer that decay is permitted to proceed before interruption.

In this paper, we shall describe a form of echo[13] which can be made to occur even after $\rho_y(0)$ has been allowed to develop for a time much greater than T_2. Its occurrence shows that the spin-temperature hypothesis in the simple form employed above is not correct. Of course, no violation of the second law of thermodynamics is implied, and the spin-temperature hypothesis retains its utility in describing *most* NMR experiments in solids. We shall return to this point later.

Briefly, the experiments depend on the fact that the time development of the system is dynamically reversible in a microscopic sense, whereas it may behave irreversibly on a thermodynamic scale. The apparent conflict between these manifestations is sometimes called Loschmidt's paradox.[14] We shall find it useful to introduce the concept of a "Loschmidt demon" who is able to reverse the dynamical behavior of a system, thereby retracing a path which *seemed* to be irreversible. The Loschmidt demon differs from the familiar Maxwell demon in that he accomplishes the reversal by changing the sign of the system Hamiltonian rather than by exercising control over microscopic dynamical variables. Since the state of the system obeys the Schrödinger equation

$$\psi(t) = e^{-i\mathcal{H}t}\psi(0) ,$$

such a sign reversal is clearly equivalent to a reversal of the time coordinate.

In Sec. II, we show how this is done, and dispel any doubts about its conflict with thermodynamic principles. In Sec. III, we give the results of several experiments. The theory is expanded in Sec. IV, and Sec. V describes an important extension and application of this phenomenon.

II. SIMPLE TREATMENT

A. Theory

The spin Hamiltonian in which we will be mainly interested is the dipole-dipole coupling $\mathcal{H}_d$ in a rigid lattice of like spins $\vec{I}_i$, or, more precisely, the truncated form of this interaction $\mathcal{H}_d^0$ appropriate to the reference frame R which rotates at the spectrometer frequency ω about a very strong Zeeman field $H_0 = \omega_0/\gamma$ in the z direction. We have

$$\mathcal{H}_d^0 = \sum_{i<j}\sum b_{ij}(\vec{I}_i \cdot \vec{I}_j - 3I_{zi}I_{zj}) ,$$
$$b_{ij} = \gamma^2\hbar r_{ij}^{-3} P_2(\cos\theta_{ij}) . \tag{6}$$

The Loschmidt demon will convert $\mathcal{H}_d^0$ into $k\mathcal{H}_d^0$, with k a negative number, so that the system retraces its previous normal dipolar development and departs from what appears to be a state of equilibrium, as mentioned in Sec. I. This conversion cannot be made in a literal sense, but its effects can be simulated through the agency of suitable external forces.[15] Suppose a strong rf field $(2\omega_1/\gamma)\cos\omega t$ is applied in the x direction with $|\omega_0 - \omega| \ll \omega_0$. The Hamiltonian in the rotating frame now includes in addition to (6), the Zeeman effect due to the field

$$[\omega_1 \vec{I} + (\omega_0 - \omega)\vec{k}]/\gamma .$$

As Redfield has shown,[16] it is convenient to view the system from the vantage point of the doubly (tilted) rotating frame (DTR), defined by the transformations

$$\rho_{DTR} = DTR\rho_{LAB}(DTR)^{-1} ,$$
$$R = e^{-i\omega t I_z} ,$$
$$T = e^{i\xi I_y} ; \quad \tan\xi = \omega_1/(\omega_0 - \omega) , \tag{7}$$
$$D = e^{-i\omega_e t I_z} ; \quad \omega_e = [\omega_1^2 + (\omega_0 - \omega)^2]^{1/2} .$$

In this frame the density matrix obeys the Liouville equation

$$\frac{\partial}{\partial t}\rho_{DTR} = -i[\mathcal{H}_{DTR}, \rho_{DTR}] , \tag{8}$$

with

$$\mathcal{H}_{DTR} = \mathcal{H}_d^0 P_2(\cos\xi) + \mathcal{H}_{ns} , \tag{9}$$

$$\mathcal{H}_{ns} = \tfrac{1}{2}\sin\xi\cos\xi\sum_{i<j}\sum b_{ij} \times [(I_{+i}I_{zj} + I_{zi}I_{+j})\ e^{-i\omega_e t} + \text{c. c.}]$$
$$- \tfrac{1}{4}\sin^2\xi\sum_{i<j}\sum b_{ij}(I_{+i}I_{+j}e^{-2i\omega_e t} + \text{c. c.}) . \tag{10}$$

When ω_e is large ($\omega_e T_2 \gg 1$), the oscillatory part $\mathcal{H}_{ns}$ can be removed for purposes of calculating the secular development of the system, just as one truncates the ordinary rotating frame Hamiltonian $\mathcal{H}_R$ to obtain (6) when $\omega_0 T_2 \gg 1$. We will discuss this step more fully later. Assuming it to be valid, we see that (9) has the desired form $k\mathcal{H}_d^0$, with k adjustable between 1 and $-\frac{1}{2}$ at the experimenter's discretion.

Remember, however, that this result refers to observations made in the DTR frame, and does not by itself embody a means of reversing the time development of ρ_R in the rotating frame. In fact, the full effect on ρ_R of applying a burst of effective field ω_e/γ for a time t_B is more complicated:

$$\rho_R(t_1 + t_B) = T^{-1}D^{-1}\exp[-it_B\mathcal{H}_d^0 P_2(\cos\xi)]DT\,\rho_R(t_1)$$
$$\times T^{-1}D^{-1}\exp[it_B\mathcal{H}_d^0 P_2(\cos\xi)]DT . \tag{11}$$

It can be simplified by modifying the experiment in the following two ways:

(a) Make the duration of the burst by a resonant number of periods of the precession about $\vec{\omega}_e$: $\omega_e t_B = 2n\pi$, then $D = D^{-1}$ in (11).

(b) Immediately precede the curst by a resonant rf pulse chosen to rotate any magnetization present through an angle ξ about the y axis of the rotating frame (i.e., the rf carrier in the pulse is in phase quadrature to that in the burst), and terminate it by a similar pulse rotation through $-\xi$. The effects of these pulses can be represented by $e^{\mp i\xi I_y} = T^{\mp 1}$ acting on ρ_R which annihilate the transformations T, T^{-1} in (11).

The effect of this treatment is then simply

$$\rho_R(t_1 + t_B) = \exp[-it_B\mathcal{H}_d^0 P_2(\cos\xi)]\rho_R(t_1)$$
$$\times\exp[it_B\mathcal{H}_d^0 P_2(\cos\xi)] , \tag{12}$$

and the Loschmidt demon has been realized if we choose ξ such that $P_2(\cos\xi) < 0$. Just this procedure for interconversion between reference frames has been employed by Jeener *et al.*[17] but not for the same purpose. If it is to be used for time reversal over reasonably long times it suffers from a severe practical limitation: Any appreciable inhomogeneity in the applied field, especially the rf field, will result in failure to satisfy condition (a) above in all parts of the sample. The result is a quick destruction of the coherence of the inverse time development and failure of the experiment. This difficulty can be circumvented by adding the further condition:

(c) Periodically reverse the direction of $\vec{\omega}_e$ (i.e., the rf carrier phase and the offset from resonance, $\omega_0 - \omega$). By this means the dephasing of isochromats caused by field inhomogeneity is prevented from accumulating. (There are theoretical benefits to be gained by this procedure even if the fields are homogeneous, as we will see later.) The reversal should be made as often as possible, but at integral multiples of the period expressed in (10). For the general case, a reversal could be made every $2\pi/\omega_e$ sec. For the special case of exact resonance ($\xi = \frac{1}{2}\pi$), the first term of (10) vanishes, and the reversal can be made twice as often if desired, i.e., the burst consists of a train of contiguous phase-alternated 180° pulses. From now on we restrict ourselves to the exact resonance case ($\xi = \frac{1}{2}\pi$), as this was the one adopted for the majority of our experiments.

In summary, the free dipolar time development of the spin system which occurred at a time t can be reversed by applying for a time $2t$ a special

sequence consisting of a pair of 90° pulses along the $+y$ and $-y$ axes of the rotating frame, enclosing an even number of contiguous n_τ pulses which alternate between the $+x$ and $-x$ axes: Calling this sequence $B(t_B)$ we have the equivalence

$$e^{+i\mathcal{H}_d^0 t_B/2} \rightarrow B(t_B) .$$

$B(t_B)$ is depicted in Fig. 1(a). All this evidently holds for any interaction with the same transformation properties as $\mathcal{H}_d^0$. We now present a simple pictoral representation of these equations and apply it to a well-known experiment. [13]

B. Simple Picture

The normal inhomogeneous spin echo[1,2] is very conveniently described in terms of the evolution of spin isochromats which precess at different frequencies about an external inhomogeneous magnetic field. The behavior of dipolar-coupled spins, on the other hand, is normally not amenable to such a simple "hand-waving" description. However, even for these systems, the simple picture of inhomogeneously perturbed noninteracting spins is sometimes valuable, and if employed carefully, allows a simple understanding of many experiments as well as facilitating further extensions and predictions. [18,19]

We describe here the use of such a model which is appropriate for some of our experiments and

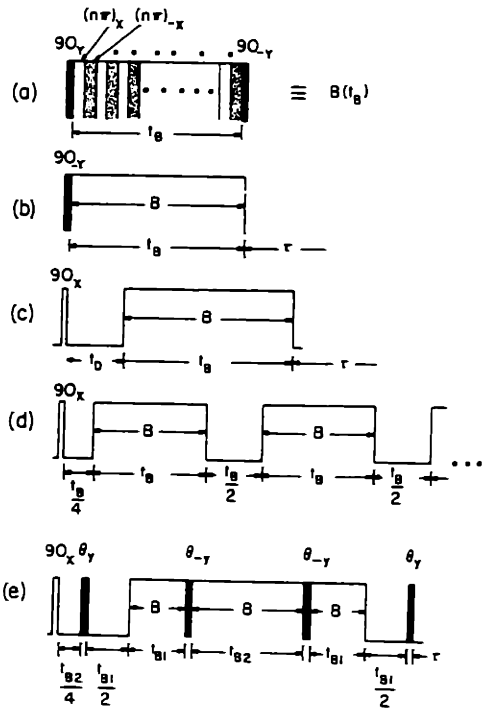

FIG. 1. Pulse sequences used for various experiments. $B(t_B)$ in (a) is the time-reversing sequence referred to in the text, and is depicted as B in the other pulse sequences. θ_μ or $(\theta)_\mu$ means a $\theta°$ pulse along the μ axis of the rotating frame.

utilizes Eqs. (7)–(9) with $\xi = 90°$ as a guideline for its construction. The discussion takes place in the reference frame rotating at frequency ω_0 about the z axis. With no rf applied we adopt the well-known picture of spin isochromats in an inhomogeneous field in the z direction. There is a distribution between fast to slow isochromats (labeled 1 and 2 in Fig. 2) which precess, respectively, clockwise and anticlockwise about the z axis. During an rf burst along the x axis we use a similar picture with the following differences: The inhomogeneous field is now along the x axis and the sense of precession of the isochromats about this axis is opposite to that about z. Further, the rate of precession is reduced by a factor of 2. 90° pulses are treated as usual, whereas the system is invariant to 180° pulses. These stipulations incorporate pictorially the main features of Eqs. (7)–(9): (i) The rf burst converts the effective Hamiltonian from $\mathcal{H}_d^0$ in the rotating frame to $-\frac{1}{2}\mathcal{H}_d^0$ in the tilted rotating frame [taking account of (iii)]. (ii) 90° y pulses transform the density matrix to and from the above frames. (iii) Our time scale during the burst is limited to integral cycle times of the rf field.

Figure 2 demonstrates the application of this simple picture to the echo experiment described previously[13] and referred to again in Sec. III. We see that most of the qualitative features of the experiment are incorporated neatly in this description, but we emphasize that this should not be taken too seriously and serves only as a useful pictorial accessory when used in conjunction with the appropriate equations. The reader will no doubt appreciate the trivial extension to multiple echoes described briefly in Secs. III and V.

C. Remarks on Statistical Mechanics

For an echo of magnitude M_0 to occur at time $t = 0$ in an isolated system of energy E_0, the representative point of the system must lie in some region $\mathcal{S}(0)$ of the phase space. This region is much smaller than the total constant-energy surface $\mathcal{E}_0$, expressing the fact that the magnetized state is one of low entropy. Every possible representative point in $\mathcal{S}(0)$ arrived there from a sequence of earlier locations, completely determined by the system Hamiltonian through the microscopic equations of motion. That is, a knowledge of $\mathcal{H}$ specifies a sequence of mappings of $\mathcal{S}(0)$ onto the precursor regions $\mathcal{S}(-t)$. The problem confronting an experimenter who wishes to produce an echo at time $t = 0$ is how to prepare a system which is known to be in $\mathcal{S}(-t_0)$.

This is a more subtle task than to prepare the system in $\mathcal{S}(0)$. The latter can be accomplished, for example, by bringing the spins to equilibrium with a lattice in a strong field and then applying a

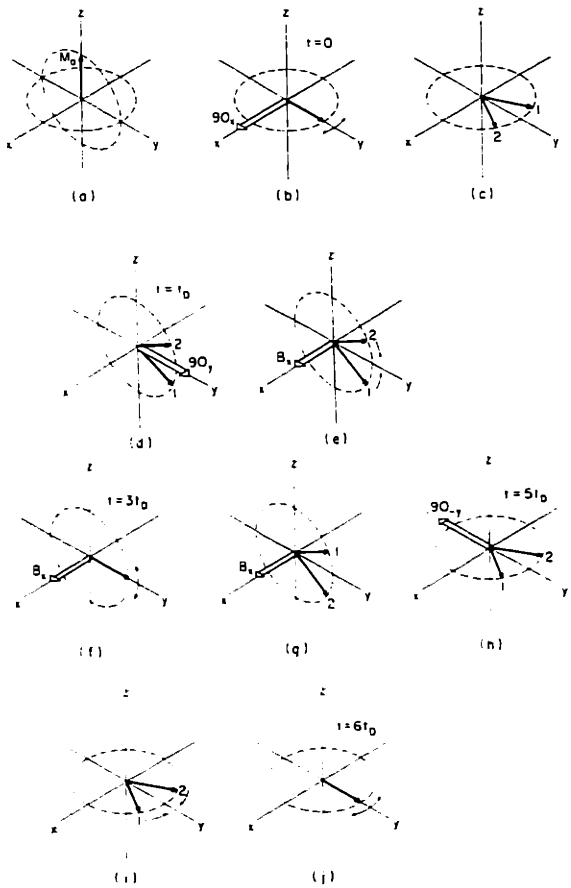

FIG. 2. Rotating-reference-frame description of the spin echo in Fig. 4, using the simple picture in Sec. II. The spin system in equilibrium (a) is irradiated at time $t=0$ with a 90° pulse along the x direction (90_x) nutating the magnetization into the x-y plane (b). The magnetization decays with "fast" spins precessing clockwise and "slow" spins anticlockwise about the z axis, and we see a normal free induction decay (c). At time $t=t_D$ a 90_y pulse brings the dephased spins into the y-z plane (d) and a rf burst is applied along the x axis. According to our picture the spins now precess about the x axis with "slow" and "fast" spins having interchanged their sense of precession (e), and refocus at time $t=3t_D$ (f). This produces the rotary echo described in Sec. III. The spins now dephase about the x axis (g) and at $t=5t_D$ the rf burst is terminated with a 90_{-y} pulse which returns the dephased spins to the x-y plane (h). We now have situation (c) except that the "fast" and "slow" spins are interchanged in position (i) and the spins rephase leading to a spontaneous echo (j) observed in Fig. 4. Note that the time-reversing rf sequence in (d) through (h) is analogous, for the case of homogeneous dipolar-coupling, to the 180° refocusing pulse employed for the normal inhomogeneous spin echo.

90° pulse: It requires only the ability to establish specified values of the macroscopic variables M and E, since $\mathcal{S}(0)$ includes by definition all dynamical states consistent with these values. $\mathcal{S}(-t_0)$, on the other hand, cannot be specified by macroscopic variables alone but requires a knowledge of *all* the dynamical variables and how they change over a time t_0 under the influence of the equations of motion. The necessary knowledge and ability of selection characterize the Maxwell demon, who violates the second law of thermodynamics in playing his role.

The Loschmidt demon needs no such microscopic control. Beginning with a system prepared in $\mathcal{S}(0)$ as described above, he changes the sign of the Hamiltonian function of the system. After a time t_0, $\mathcal{H}$ is returned to its normal form. The change is to be accomplished by external means which make no reference to the dynamical state of the system. An analogy is useful here to a gas of molecules interacting according to a potential $U(r)$:

$$\mathcal{H}=\sum_{i=1}^{N}\frac{1}{2m_i}\,\vec{p}_i\cdot\vec{p}_i+\sum\sum_{i<j}U_{ij}(r_{ij})\ .$$

A second kind of Maxwell demon exploits the apparent possibility of recalling the previous history of the gas by reversing the signs of all $\vec{p}_i$ at some instant. It might seem that such a reversal would require a knowledge of the dynamical state at that instant (although Hahn has pointed out in discussion a case of two dimensions in which it apparently does not). Note also that the sign of $\mathcal{H}$ is not changed. The Loschmidt demon, as we define him, might instead change the signs of all the m_j and U_{ij}. Such an action certainly requires no knowledge of the dynamical state. It implies a degree of control over the *nature* of the system which may be difficult to credit in the case of gas dynamics but which clearly can be exercised, as we have seen, in certain restricted spin systems. The question of the class of Hamiltonians for which a Loschmidt demon is in principle realizable is an interesting but unsolved one.

How does the spin-temperature hypothesis fit into this discussion? In its strong form it would claim that a distribution $\rho(0)$ uniformly occupying $\mathcal{S}(0)$ at the beginning of a Bloch decay would come to fill the much larger region $\mathcal{E}_0$ uniformly after several times T_2. However, Liouville's theorem tells us that the total volume of $\mathcal{S}(t)$ is conserved. The fact is that $\mathcal{S}(t)$ may come to fill $\mathcal{E}_0$ in a coarse-grained sense only. $\mathcal{S}(0)$ is relatively compact, but $\mathcal{S}(t>T_2)$ is complicated and has a large surface-to-volume ratio, as it were, especially if forces are present between the particles of the system.[14] Thus, *for many purposes* the distribution may be treated as though it filled $\mathcal{E}_0$ uniformly. However one must be on guard against performing manipulations which inadvertently exploit the dynamical history of the system to bring $\mathcal{S}(t)$ into a condition characterized by "nonequilibrium" values of the macroscopic observables. It is worth noting that some of the experiments of Jeener *et al.*,[17] which

seemed to verify the spin-temperature hypothesis, might well have done the contrary, had their experimental conditions been adjusted somewhat differently.

Finally, we remind the reader that our experiments on solids do not actually involve a reversal in sign of $\mathcal{H}$: During the rf burst the representative point *appears* to move under a Hamiltonian $-\frac{1}{2}\mathcal{H}_d^0$ from the viewpoint of a phase space which is accelerated with respect to the "ordinary" one, the net effect upon conclusion of the time-reversing sequence being to bring the system into $S(-t_0)$. The language one uses to describe the motion of the system depends, as always, on the representation in which the motion is viewed.

III. EXPERIMENTS

In this section we describe some experiments based on the properties of the time-reversing sequence described in Sec. II. All experiments were performed at the exact ^{19}F resonance frequency of 54 MHz on a single crystal of CaF_2 oriented approximately along the (110) direction. The peak H_1 field was ~100 G and our pulses had rise and fall times of ~150 nsec. The apparatus is to be described in more detail elsewhere.[20]

A trivial experiment is one in which $B(t_B)$ is applied to the spin system initially in equilibrium with the lattice in a field H_0. $B(t_B)$ reverses the (nonexistent) time development of the z component of the magnetization, leaving the system in its original state.

A more interesting case is the reversal of the time development of the x, y components. Assume, therefore, that we apply the pulse sequence of Fig. 1(b) with $n = 1$, consisting of a time-reversing sequence preceded by a 90_{-y} pulse. (Note that this pulse is immediately negated by the leading 90_y pulse of the time-reversing sequence. In practice we simply omit both from the experiment.) During the burst the system undergoes a reversed dipolar development with Hamiltonian $-\frac{1}{2}\mathcal{H}_d^0$ corresponding to a normal rotary free induction decay at resonance, treated for example by Goldburg and Lee.[21] At time t_B the system reverts to normal dipolar development and should return to the initial state at $\tau = \frac{1}{2}t_B$ as indicated by the appearance of an echo. This sequence is formed by stages (f)–(j) of Fig. 2. The result of the experiment is shown in Fig. 3. The open circles depict the magnetization along the y axis during the burst and were obtained by observing the signal immediately following the receiver dead time of about 2 μsec without the final 90_{-y} pulse, while the number of $(x, -x)$ pulse pairs was varied. The oscillations were introduced deliberately for this part of the data by misadjusting the pulse widths during the burst and having x pulses of nutation angle $\pi - \alpha$ and $-x$ pulses of nutation angle $\pi + \alpha$ with $\alpha \simeq 25°$. This introduces a slow accumulative precession of frequency $\omega_1\alpha/\pi$ which leads to the observed oscillations, and the free induction decay envelope can be extracted simply by inspection as indicated in the figure. This is necessary because any slower oscillations due to small misadjustments, which are almost unavoidable, would make extraction of the envelope a much less certain proposition. The full circles show the observed echo whose maximum comes at $\frac{3}{2}t_B$, as expected. The shape of the rotary free induction decay is the same as that of the normal free induction decay except stretched by a factor of 2, as observed previously.[21–23]

In the experiment of Fig. 4 (which is the one described by the simple picture of Fig. 2), we first apply a 90_x pulse after which we see a normal free induction decay. The time-reversing sequence with $n = 1$ is then applied as in Fig. 1(c) such that $t_B = 4t_D$, and at time $\tau = t_D$ we see the expected echo. Figure 5 shows the initial decay (full circles) and also the magnetization during the burst (open circles) with the data collected as before by misadjusting the π pulse widths and omitting the final 90_{-y} pulse. The envelope shows a rotary spin echo (which is of course entirely different in character from the inhomogeneous rotary spin echo observed by Solomon[24]). The width is stretched by a factor of 2 and we see that the

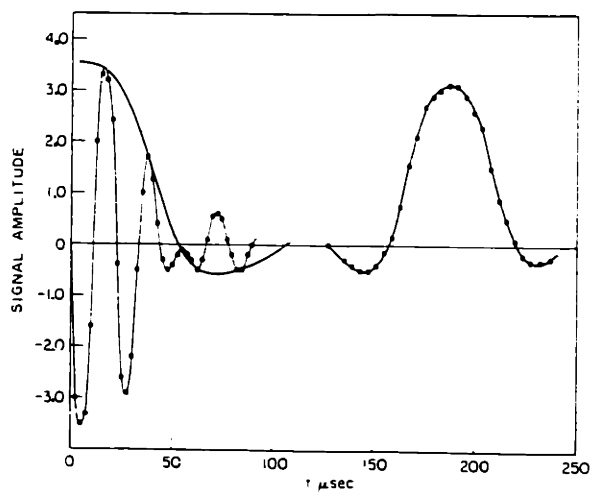

FIG. 3. Transient magnetization of ^{19}F nuclei in CaF_2 observed along the y axis of the rotating frame using the pulse sequence of Fig. 1(b). The closed circles depict the echo obtained in this experiment with a rf burst of ~120 μsec. In order to see the evolution of the magnetization during the burst the final 90_{-y} pulse was omitted and the number of pairs of $(x, -x)$ pulses was varied, leading to the data recorded as open circles. The oscillations were introduced deliberately for this part of the experiment as explained in the text, and the envelope is drawn by inspection. Note the characteristic beat structure in the rotary free induction decay.

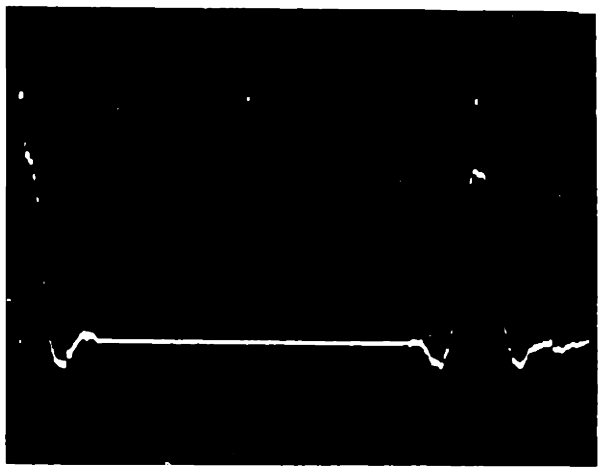

FIG. 4. Oscilloscope trace of the ^{19}F transient magnetization in CaF_2 using the pulse sequence of Fig. 1(c). Following the initial free induction decay a time-reversing burst (B) is applied at the noise-free section of the trace and an echo then appears, $t_D = 88\ \mu$sec, $t_B = 350\ \mu$sec. This is the experiment described by the simple picture of Fig. 2.

shape and beat structure are again preserved by our phase-alternation technique.

In this experiment, we have obtained substantial echoes for burst lengths of up to 650 μsec, meaning a recovery of the magnetization after about 1 msec from the first 90° pulse. The reasons for decay of the echo amplitude are discussed later and are probably dominated by machine instabilities and errors. Figure 6 demonstrates that the same effect may be obtained by using a train of narrow phase-alternated 90_x pulses in the time-reversing sequence instead of the contiguous $n\pi$ pulses, since the secular part of the Hamiltonian is the same for both. A nice feature of this experiment is the direct observation of the rotary echo during the pulse train. The efficiency of this pulse train for longer bursts, however, is lower than that of 1(a) if compared using the same average rf power. This point is brought up again in Sec. V.

$t_B = 2t_D$ corresponds to the peak of the rotary echo and Fig. 7 shows the signal observed in an experiment where the burst is terminated soon after this point without the final 90_{-y} pulse. We see a large recovery of the magnetization with $t_D = 133\ \mu$sec, which is substantially larger than T_2. (The negative signal is due to a peak negative value in the oscillation caused by a pulse width misadjustment or by change of the nutation angle due to rf power droop during the burst.)

Figure 8 shows that if we apply an additional time-reversing sequence at $\tau = 2t_D$ another echo appears, and this may of course be extended to multiple echoes in a manner analogous to that of Carr and Purcell.[25] The efficiency with which these echoes are summoned suggests that such echo trains might form the basis of a powerful approach to the problem of line narrowing in solids. This is treated briefly in Sec. V.

As a final demonstration of a simple application of the time-reversing sequence, let us look at the experiment of Fig. 9 which employs the pulse sequence in Fig. 1(e) with $\theta = 60°$. The first 90_y pulse following the free induction decay produces the well-known "solid

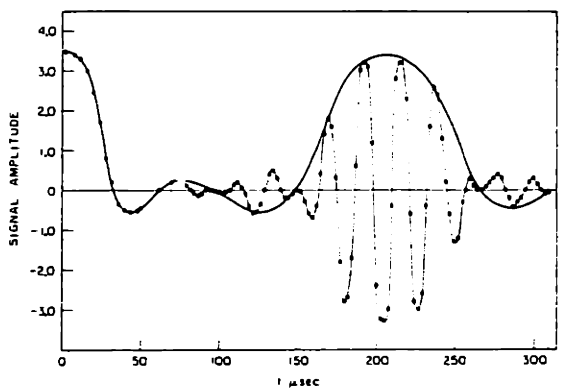

FIG. 5. Experiment designed to show the evolution of the magnetization during the rf burst in an experiment like that of Fig. 4. This is done as in Fig. 3 by omitting the final 90_{-y} pulse from the pulse train which follows the free induction decay (closed circles) and plotting the magnetization immediately following the burst vs burst length (open circles). The oscillations were again introduced deliberately as explained in the text. The envelope shows the "rotary echo" and note again the intact beat structure characteristic of the ^{19}F signal in CaF_2.

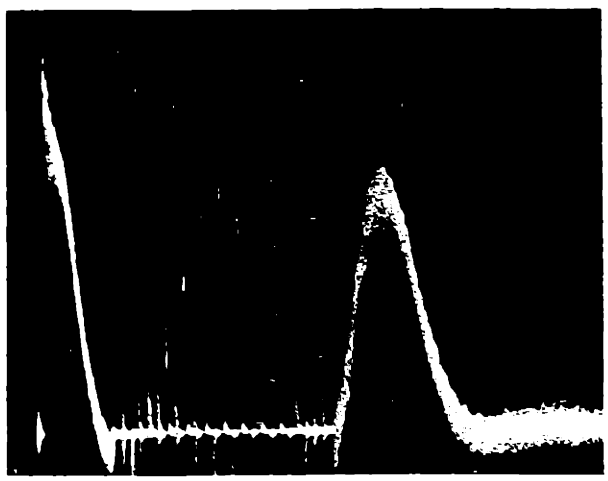

FIG. 6. Pulsed version of the experiment in Figs. 4 and 5. In this experiment, the time-reversing sequence (B) in pulse sequence 1(c) was modified by replacing the contiguous $(n\pi)_x$ and $(n\pi)_{-x}$ pulses with a train of alternate 90_x and 90_{-x} pulses spaced 5 μsec apart. In addition to the free induction decay and echo, observed as in Fig. 4, we see the "rotary echo" of Fig. 5 during the "windows" in the pulse train.

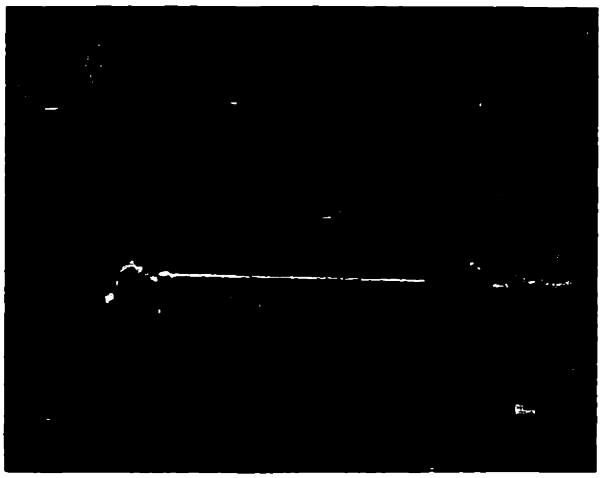

FIG. 7. Oscilloscope trace of magnetization in an experiment like that of Fig. 4. In this case, the time-reversing sequence terminated near the peak of the rotary echo of Fig. 5 and we see a normal free induction decay. The parameters are $t_D = 133$ μsec, $t_B = 345$ μsec. The fact that the second signal has a negative value is explained in the text.

echo."[11] By sequentially using the properties of the time-reversing sequence we see that the first half of the burst brings the system back to its initial state, and the second half produces a rotary free induction decay and corresponding "rotary solid echo." Thus on terminating the burst we see a negative time development solid echo and the final 90° pulse brings the system back again to the initial state. In this way the effects of any number of pulses may be reversed. This experiment vividly demonstrates the more efficient nature of our echoes as compared to the solid echoes. This matter is referred to again in Secs. IV and V. For $\theta = 45°$, we obtain an analogous reversal of Jeener and Broeckaert's pulse sequence[19] showing that their postulated dipolar state is not an adequate description of the system for this type of experiment.

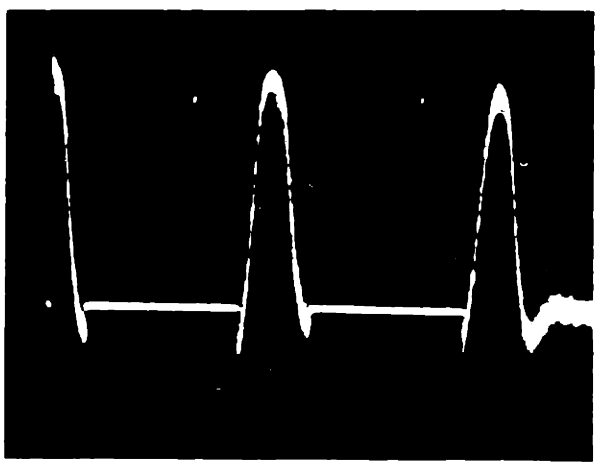

FIG. 8. Double-echo version of the experiment in Fig. 4 using pulse sequence 1(d) with $t_B = 180$ μsec. This shows that an extension of our echoes analogous to that of Carr and Purcell is possible.

IV. NONIDEALITIES

A. General Framework

The ideal treatment in Sec. II was based on the assumption that the effect of a time-reversing sequence could be represented by replacing $\mathcal{H}_d^0$ with $-\frac{1}{2}\mathcal{H}_d^0$ as the effective Hamiltonian during the burst (for the case $\xi = \frac{1}{2}\pi$). Here we investigate the validity of this assumption and discuss the effect and extent of various nonidealities encountered in practice.

We begin by writing the time development during the burst as

$$\rho_R(t_B) = U_B(t_B)\,\rho_R(0)\,U_B^\dagger(t_B)\,, \qquad (13)$$
$$U_B(t_B) = \exp[-it_B(-\tfrac{1}{2}\mathcal{H}_d^0 + \lambda V)]\,,$$

where V is some correction to $\mathcal{H}_{DTR}$ whose matrix elements are of order T_2^{-1}, and λ is a small parameter. No generality is lost at this stage by insisting that V be time independent; it may depend parametrically on t_B but in most cases to be discussed it will not have even that indirect time dependence. The nature and origin of λV will be discussed later; at present we simply investigate the consequences of (13).

It is easily shown that[26]

$$U_B(t_B) = e^{i\mathcal{H}_1^0 t_B/2}\; T\exp[-i\lambda \textstyle\int_0^{t_B} V(t)\,dt]\,, \qquad (14)$$

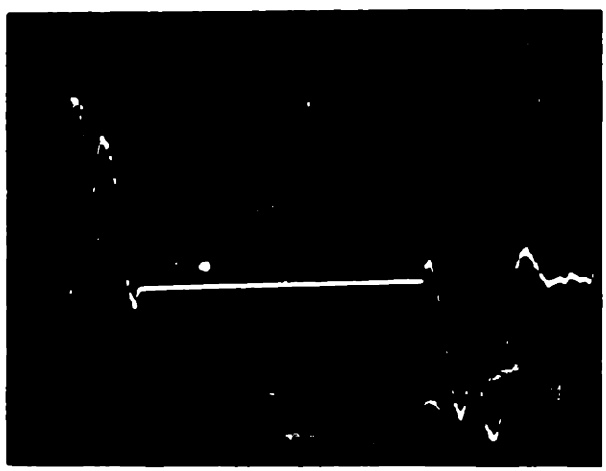

FIG. 9. Time reversal of a two-pulse experiment, using the pulse sequence in Fig. 1(e) with $\theta = 90°$. The first two pulses bring about a free induction decay and "solid echo." The following rf burst reverses this total sequence and then propagates it further backwards in time leading to the ensuing "mirror image" of the "solid-echo" experiment when the burst is terminated. The negative value of the "mirror image" is explained in the text. For this experiment $2t_{B1} + t_{B2} = 342$ μsec, corresponding to the noise-free portion of the trace.

where T is a time-ordering operator and

$$V(t) = e^{-i\mathcal{H}_d^0 t/2}\, V\, e^{i\mathcal{H}_d^0 t/2} . \tag{15}$$

For the condition

$$\lambda t_B \ll T_2 \tag{16}$$

we may expand the exponential in (14) to first order:

$$U_B(t_B) \approx e^{i\mathcal{H}_d^0 t_B/2} \exp[-i\lambda \int_0^{t_B} V(t)\,dt] . \tag{17}$$

Now we consider the general situation in which the burst is preceded and followed by unperturbed dipolar developments of duration t_1 and t_2. The total propagator is

$$U(t_1+t_2+t_B) = e^{-it_2\mathcal{H}_d^0} U_B(t_B)\, e^{-it_1\mathcal{H}_d^0} . \tag{18}$$

Combining this with (17) and rearranging a little we find

$$U(t_1+t_2+t_B) = U(\tfrac{1}{2}t_B+\tau) = e^{-i\tau\mathcal{H}_d^0} e^{-i\lambda t_B \bar{V}} , \tag{19}$$

where $\tau = t_1 + t_2 - \frac{1}{2}t_B$ and $\bar{V}$ is given by

$$\bar{V} = (1/t_B) \int_{-2t_1}^{t_B-2t_1} V(t)\,dt . \tag{20}$$

If the initial magnetization of the system was along the μ axis in the rotating frame, $\langle I_\mu(0)\rangle$, then its final value is

$$\langle I_\mu(\tfrac{1}{2}t_B+\tau)\rangle = \mathrm{Tr}(e^{-i\tau\mathcal{H}_d^0} e^{-i\lambda t_B\bar{V}} I_\mu e^{i\lambda t_B\bar{V}} e^{i\tau\mathcal{H}_d^0} I_\mu). \tag{21}$$

We now introduce the notation

$$\{|a^n \cdot b^m|\} = \mathrm{Tr}([a[a\ldots[a, I_\mu]]\ldots][b[b\ldots[b, I_\mu]]\ldots]), \tag{22}$$

where a and b appear n and m times, and

$$\{|a^n \cdot 1|\} = \{|1 \cdot a^n|\} = \{|a^n|\} , \tag{23}$$

where the last is the bracket introduced by Waugh and Wang.[27] Using this and expanding (21) in τ and λt_B we obtain

$$\langle I_\mu(\tfrac{1}{2}t_B+\tau)\rangle = \sum_{n=0}^{\infty} M_n \frac{\tau^n}{n!} , \tag{24}$$

where M_n are the moments of the echo, given by

$$M_n = \sum_{k=0}^{n} i^{n-k} \frac{(\lambda t_B)^k}{k!} \{|\mathcal{H}_d^{0n} \cdot \bar{V}^k|\} . \tag{25}$$

B. Lifetime of Echo

The time $\tau = 0$ corresponds to the expected position of the echo maximum from the discussion in Sec. II. Substituting $\tau = 0$ in (24) and (25) we obtain

$$\langle I_\mu(\tfrac{1}{2}t_B)\rangle = \sum_{k=0}^{\infty} (-1)^k \frac{(\lambda t_B)^{2k}}{(2k)!} \{|\bar{V}^{2k}|\} , \tag{26}$$

the odd powers all vanishing, as is well known.[28]

Assuming now that $\|\bar{V}\| \sim T_2^{-1}$ and remembering condition (16) we see that (26) expresses a recovery of the magnetization with an attenuation of order $\frac{1}{2}(\lambda t_B/T_2)^2$. Thus we expect the magnetization to recover to an appreciable extent for burst lengths that satisfy condition (16) for fixed T_2 and λ. In order to estimate this, we now inquire into the sources and nature of V and the size of λ. The first place it occurs to us to look is at the truncation of $\mathcal{H}_{DTR}$ carried out in Sec. II. Since $\mathcal{H}_{DTR}$ of (9) is periodic and the burst contains an integral number of cycles, its effects can be replaced by those of an average Hamiltonian[29]

$$\bar{\mathcal{H}}_{DTR} = \sum_{n=0}^{\infty} \bar{\mathcal{H}}_{DTR}^{(n)} \tag{27}$$

whose terms are defined by a Magnus expansion over a single cycle of $\mathcal{H}_{ns}(t)$. For Eq. (10) we have the cycle time $t_c = 2\pi/\omega_e$, and thus

$$\bar{\mathcal{H}}_{DTR}^{(0)} = -\tfrac{1}{2}\mathcal{H}_d^0 . \tag{28}$$

Cutting off (27) at this point corresponds to the well-known procedure of "truncation." The next term does not vanish: At this point remember we have not used quite the Hamiltonian of Eq. (9) since we have periodically reversed the direction of H_1. Under these conditions it is easily verified that

$$\bar{\mathcal{H}}_{DTR}^{(1)} = 0 , \tag{29}$$

thus leaving $\bar{\mathcal{H}}_{DTR}^{(2)}$ as the leading correction term. An estimate of this factor shows that it is of the order of $\frac{1}{6}(t_c/2\pi T_2)^2$ smaller than $\mathcal{H}_d^0$. Thus for this case we identify λV with $\mathcal{H}_{ns}^{(2)}$ and λ is of order $\frac{1}{6}(t_c/2\pi T_2)^2$, which for our experimental condition is about 10^{-4}. Condition (16) is thus satisfied for t_B of many msec, and taking only the nonsecular terms into account we might expect the echo to live this long. In fact, we have obtained in the echo experiment of Sec. III a more than 98% recovery of the magnetization for t_B up to 350 μsec and a 75% recovery for t_B of 500 μsec. So some other mechanism could be contributing to the destruction of the echo.

We now turn to some other errors which stem from practical sources. The treatment up till now has assumed that the time-reversing sequence contains a series of continguous ideal $(n\pi)_x$ and $(n\pi)_{-x}$ pulses. Evidently, this cannot be realized in practice because of the finite rise and fall times of the pulses which lead to "windows" in the continuous rf irradiation, since the carrier phase of the two pulses differs by π. Thus the time-reversing sequence is better represented in practice by the pulse sequence in Fig. 10.

Another source of error is the fact that the pulses may not be exactly of nutation angle $n\pi$, as this is exceedingly difficult to adjust. Accordingly, in Fig. 10 we have indicated this by writing the angles as $n\pi+\epsilon$ and $n\pi+\epsilon'$, where ϵ and ϵ' are small error angles. We assume $|\epsilon - \epsilon'| \ll |\epsilon|$ for reasons that will become clear later. We find on calculating the average Hamiltonian $\bar{\mathcal{H}}_{DTR}^{(0)}$ in this case and taking only the first order in ϵ and δ, where $1-\delta$

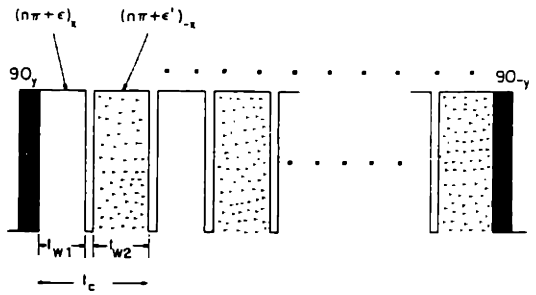

FIG. 10. Nonideal time-reversing sequence discussed in Sec. IV.

$= (t_{w_1} + t_{w_2})/t_c$:

$$\bar{\mathcal{H}}^{(0)}_{\mathrm{DTR}} = -\tfrac{1}{2}\mathcal{H}^0_d + \tfrac{3}{2}\left(\delta + \frac{\epsilon}{n\pi}\right)\sum_{i<j}\sum b_{ij}(I_{xi}I_{xj} - I_{yi}I_{yj}). \tag{30}$$

We see that $\bar{\mathcal{H}}^{(0)}_{\mathrm{DTR}}$ is of the form $-\frac{1}{2}\mathcal{H}^0_d + \lambda V$, where $\lambda \sim \delta + \epsilon/n\pi$ and $\|V\| \sim \|\mathcal{H}^0_d\|$. For $n = 1$ we have with our apparatus $\delta \sim 0.1$. With $\epsilon \simeq 0$ this would lead to very short lived echoes since $\lambda \sim \delta$. However, we see from (30) that by advertently adjusting the pulse widths away from $n\pi$ such that $\delta + \epsilon/n\pi \sim 0$, this factor can be eliminated to a certain extent. The adjustment is quite critical and requires $\epsilon < 0$ as we have indeed observed. A factor limiting this adjustment is the H_1 inhomogeneity which normally amounts to several percent. Practically, this means that ϵ is not constant over the sample and thus the adjustment $\delta + \epsilon/n\pi \sim 0$ cannot be made simultaneously over the whole sample. The H_1 inhomogeneity probably makes a significant contribution to the destruction of the echo for long bursts.

The effect of ϵ and δ becomes less serious as n is made larger since $\epsilon/n\pi$ and δ both decrease, but for large n this may be offset by a harmful increase in phase-switching cycle time.

Other machine errors not treated explicitly here probably make some additional contribution to the destruction of the echo. These include misadjustment of phases, power droop in the pulse transmitter, phase transients,[20] etc.

C. Shape of Echo

We now return to Eq. (24) and investigate $\langle I_\mu(\frac{3}{2}t_B + \tau)\rangle$ for $\tau \neq 0$, the shape of the echo about its expected maximum. An examination of (25) shows that the first term in the expansion is just the corresponding normal FID moment. The higher terms make a small contribution if condition (16) is fulfilled and lead only to a slight distortion of the echo line shape as compared to the free induction decay. This suggests a useful new means for obtaining moments of the free induction decay when the initial transient is obscured by receiver dead time; we simply produce an echo with λ small enough so that (16) is fulfilled to the desired accuracy with some particular dead time t_d [we need $t_B > 2t_d$ for pulse sequence 1(b), and $t_B > 4t_d$ for 1(c)]. This method has one important advantage over solid echoes.[11,12] In the latter, assuming a dead time t_d, the terms contributing to the distortion of the echo line shape have some inherent fixed value dependent on powers of t_d. In our case, we have the same distortion in powers of λt_B, not t_B, and this can be made arbitrarily small at least for the t_d of practical interest. Using pulse sequence 1(b) we have measured some echo line shapes for different burst lengths. These are compared with the free induction decay in Fig. 11 with no adjustable parameters except for normalization of the echo with $t_B = 110$ μsec. The agreement is very good within experimental error. For $t_B = 110$ μsec, the onset of some distortion is clearly visible. Comparison with the first part of the free induction decay is of course not possible, but the theory and other experimental evidence indicate no reason why this should not be good too. For $t_d < 10$ μsec, we need $t_B \simeq 20$ μsec and this should give us a very accurate representation of the line shape even for moderate H_1 fields. In any case, the reduction in peak echo amplitude is an indication of the amount of distortion to expect (notwithstanding the remarks below) as we have indeed found in practice.

An interesting feature of Eqs. (24) and (25) as we have seen, is the fact that the first correction term to the peak echo amplitude is in $(\lambda t_B)^2$, whereas those to the higher moments are in (λt_B). This means that distortion of the line shape should occur more rapidly than destruction of the peak echo amplitude might indicate. This is indeed evident in our experiments where for large t_B the echoes acquire a

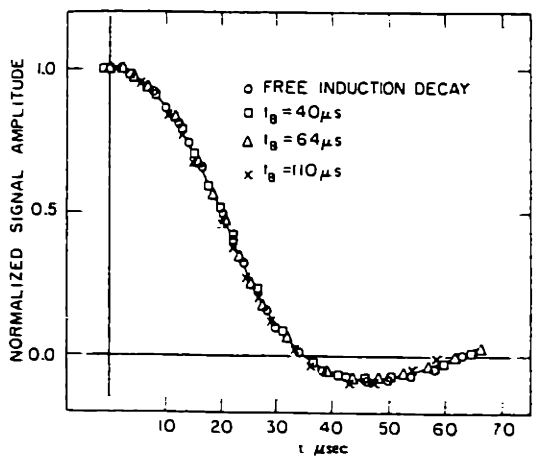

FIG. 11. Comparison of the echo line shapes of the experiment in Fig. 3 for various burst lengths. Only the right-hand portion of each echo is depicted, except for burst length 0 (free induction decay) where part of the signal is obscured by receiver dead time. No parameters are involved except the normalization of data for $t_B = 110$ μsec, where the peak echo amplitude had decreased.

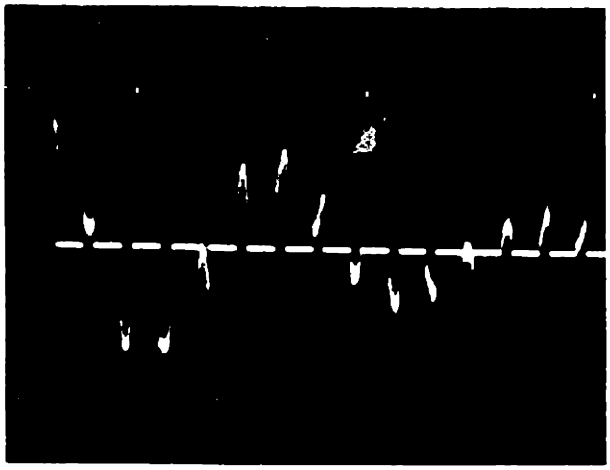

FIG. 12. Multiple-burst line-narrowing sequence [Fig. 1(d)] applied to the ^{19}F nuclei of CaF_2 with the magnet set slightly off-resonance. The cycle time $\frac{3}{2}t_B$ for this experiment was 136 μsec, and we observe a prolonged decay with a scaled off-resonance beat. This multiple-echo phenomenon has also been used to observe chemical shifts in solids in an analogous way.

progressively narrow shape corresponding to a larger destruction of magnetization for $\tau \neq 0$ than for the echo peak.

V. APPLICATION TO LINE NARROWING

A. Multiple Bursts

We have discussed at length elsewhere[29] the possibility of removing the effects of dipolar broadening by repeated application of a suitably chosen cycle of rf perturbations. These cycles have the property that the effective dipolar Hamiltonian in some suitable reference frame, while large, varies during the cycle in such a way that its net effect over a full cycle vanishes to some approximation. The present echo experiments clearly have the same property over a cycle of duration $\frac{1}{2}t_B$: The system behaves as though $\bar{\mathcal{H}}_R = \mathcal{H}_d^0$ except during the bursts where $\bar{\mathcal{H}}_R = -\frac{1}{2}\mathcal{H}_d^0$ to first order. Thus for a cycle of duration $\frac{1}{2}t_B$ the effective dipolar Hamiltonian is 0 and if the cycle is repeated indefinitely as in Fig. 1(e), the envelope of the magnetization sampled at integral cycle times should generate a very long decay corresponding to an effective line narrowing.

Consider the more interesting case in which the Hamiltonian contains chemical shifts in addition to the dipolar interaction and is given by (31). Removal of the large dipolar broadening is then a necessity if we wish to observe the fine structure associated with the chemical shifts. We have

$$\mathcal{H}_R = \mathcal{H}_d^0 + \mathcal{H}_c \ . \tag{31}$$

During the burst the effective Hamiltonian is given by

$$\bar{\mathcal{H}}_R^{(B)} = -\tfrac{1}{2}\mathcal{H}_d^0 + \bar{\mathcal{H}}_c^{(B)} + \lambda V \ ,$$

where superscript B denotes the presence of the burst and λV is a correction to the average Hamiltonian. It is easily verified that the total first correction term vanishes, including the dipolar-chemical-shift cross term, so that λV can be associated with the second correction term and λ is of order $\frac{1}{6}(t_c/2\pi T_2)^2$.

The average Hamiltonian for the total $\frac{3}{2}t_B$ cycle is

$$\bar{\mathcal{H}}_R^{(0)} = \tfrac{1}{3}(\mathcal{H}_c + 2\bar{\mathcal{H}}_c^{(B)}) + \tfrac{2}{3}\lambda V \ . \tag{32}$$

The higher correction terms depend on the symmetry of the circle. For the symmetric cycle in the pulse sequence of Fig. 1(e), we find for the total first correction term

$$\bar{\mathcal{H}}_R^{(1)} = 0, \tag{33}$$

again including the dipolar-chemical-shift cross term. The higher-order pure-dipolar correction terms evidently vanish and thus all correction terms are attenuated at least by λ or Δ, where the latter is the magnitude of the largest chemical shift. The only nonvanishing second-order term, for example, is found to be attenuated by $\sim\lambda\Delta$ from the magnitude of the usual corresponding pure-dipolar term. The normal requirement of our previous pulse experiments, namely, that we have the cycle time $t_c \lesssim T_2$, is therefore not so stringent in this experiment, and much larger cycle times should be tolerable if λ and Δ are small, as we have indeed observed. This is a good example of the exploitation of the properties of subcycles (in this case during the burst) in an effort to increase the efficiency of the full cycle.[29]

Figure 12 shows a preliminary example of the application of this pulse sequence to the ^{19}F nuclei of CaF_2 with a cycle time of 136 μsec and using 360^c x and $-x$ pulses ($n = 2$). A prolonged decay with an off-resonance beat scaled by $\frac{1}{3}$ ($\bar{\mathcal{H}}_c^{(B)} = 0$), is observed: With this cycle time our previous pulse experiments fail completely.

To summarize, we mention briefly several apparent advantages of this new method as compared to some previous line-narrowing techniques. The experiment is essentially continuous wave, except for the 90_y pulses, with the magnetization sampling windows forming part of the sequence. We therefore require less power[29] than in our pulsed experiments and do not have to contend to such an extent with the adverse effects of finite pulse width. Further, the experiment does not require the additional video pulses necessary in "magic angle" experiments.[23,29] An additional advantage is the vanishing of the first-order cross correction term between dipolar and chemical-shift interactions, and the attenuation in magnitude of the higher-order correction terms. Most important we see that while t_B may be of order T_2 or more, the line-narrowing

efficiency is determined from (32) essentially by the subcycle time inside the burst, which can be made extremely small since no observation of the magnetization is necessary during this time.

Last, we mention that an analogous experiment employing only 90° rf pulses can be done if the $n\pi$ pulses in the time-reversing sequence are replaced by a train of 90° pulses along the $\pm x$ directions, but that this would not benefit from all the advantages mentioned above.

B. Symmetric Cycles

We recall from above that the total first-order correction term, including the dipolar-chemical-shift cross term, vanished both for the multiple-burst full cycle and the burst subcycle This is a special case of a more general principle which applies to any symmetric cycle. Adopting the notation in Eq. (15) of Ref. 29, a symmetric cycle is one for which

$$\bar{\mathcal{H}}(t) = \bar{\mathcal{H}}(t_c - t), \tag{34}$$

where t_c is the pertinent cycle time. It is easily shown for such cycles that the first-order correction term vanishes,

$$\bar{\mathcal{H}}^{(1)} = 0. \tag{35}$$

We see that our cycle and subcycle do indeed have the requisite symmetry, leading to (35). Using (34), other sequences with this property will doubtless occur to the reader, and a general approach to elimination of the first correction term is simply symmetrization of the cycle within the constraints imposed by the requirements of the average Hamiltonian itself. A trivial example is our 4-pulse sequence.[30] Preparing the system with a 90° pulse along the y axis, it is

$$P_y - (\tau - P_x - \tau - P_{-y} - 2\tau - P_y - \tau - P_{-x} - \tau)_n .$$

It is easily verified that (34) holds over a cycle with $t_c = 6\tau$, and thus (35) is fulfilled. This sequence is simpler than a 6-pulse modification recently proposed by Mansfield,[31]

$$P_y - (\tau - P_{-x} P_y - \tau - P_{-y} - 2\tau - P_y - \tau - P_{-y} P_x - \tau)_n ,$$

and a 3-dimensional sequence proposed by Silberszyc.[32]

ACKNOWLEDGMENTS

Special thanks are due Dr. M. Mehring who constructed the rf transmitter used in these experiments and from whose advice and assistance we benefited greatly. We also acknowledge the assistance of M. G. Gibby who constructed a major part of the pulse spectrometer, the technical aid of S. Kaplan and J. D. Read, and some stimulating discussions with J. D. Ellett, Jr., R. G. Griffin, and J. M. Deutch. We thank Professor E. L. Hahn for illuminating discussions of Loschmidt's paradox.

---

*Work supported by the National Science Foundation and the National Institutes of Health.

[1]E. L. Hahn, Phys. Rev. 80, 580 (1950).
[2]H. Y. Carr and E. M. Purcell, Phys. Rev. 88, 415 (1952).
[3]S. R. Hartmann and E. L. Hahn, Phys. Rev. 128, 2042 (1962).
[4]I. Solomon, Phys. Rev. 110, 61 (1958).
[5]M. Bloom, E. L. Hahn, and B. Herzog, Phys. Rev. 97, 1699 (1955).
[6]I. D. Abella, N. A. Kurnit, and S. R. Hartmann, Phys. Rev. 141, 391 (1966).
[7]R. P. Feynman, F. L. Vernon, Jr., and R. W. Hellwarth, J. Appl. Phys. 28, 49 (1957).
[8]J. Jeener, *Advances in Magnetic Resonance* (Academic, New York, 1968), Vol III.
[9]M. Goldman, *Spin Temperature and Nuclear Magnetic Resonance in Solids* (Oxford U. P., London, England, 1970).
[10]A. G. Redfield, Science 164, 1015 (1969).
[11]J. G. Powles and P. Mansfield, Phys. Letters 2, 58 (1962); J. G. Powles and J. H. Strange, Proc. Phys. Soc. (London) 82, 6 (1963).
[12]E. D. Ostroff and J. S. Waugh, Phys. Rev. Letters 16, 1097 (1966).
[13]W-K. Rhim, A. Pines, and J. S. Waugh, Phys. Rev. Letters 25, 218 (1970).
[14]R. C. Tolman, *The Principles of Statistical Mechanics* (Clarendon, London, England, 1962), p. 152 ff.; G. E. Uhlenbeck and G. W. Ford, *Lectures on Statistical Mechanics* (Am. Math. Soc., Providence, R. I., 1963), Chap. 1.
[15]W-K. Rhim, Ph. D. thesis, University of North Carolina, 1969 (unpublished); H. Schneider and H. Schmiedel, Phys. Letters 30A, 298 (1969); W-K. Rhim and H. Kessemeier (unpublished).
[16]A. G. Redfield, Phys. Rev. 98, 1787 (1955).
[17]J. Jeener, R. DuBois, and P. Broekaert, Phys. Rev. 139, A1959 (1965).
[18]A. G. Anderson and S. R. Hartmann, Phys. Rev. 128, 2023 (1962).
[19]J. Jeener and P. Broekaert, Phys. Rev. 157, 232 (1967).
[20]J. D. Ellett *et al.*, *Advances in Magnetic Resonance* (Academic, New York, 1971), Vol. V.
[21]W. I. Goldburg and M. Lee, Phys. Rev. Letters 11, 255 (1963).
[22]D. Barnaal and I. J. Lowe, Phys. Rev. Letters 11, 258 (1963).
[23]M. Lee and W. I. Goldburg, Phys. Rev. 140, A1261 (1965).
[24]I. Solomon, Phys. Rev. Letters 2, 301 (1959).
[25]H. Y. Carr and E. M. Purcell, Phys. Rev. 94, 630 (1954).
[26]R. M. Wilcox, J. Math. Phys. 8, 962 (1967).
[27]J. S. Waugh and C. H. Wang, Phys. Rev. 162, 209 (1967).
[28]A. Abragam, *The Principles of Nuclear Magnetism* (Clarendon, London, England, 1961), p. 110 ff.
[29]U. Haeberlen and J. S. Waugh, Phys. Rev. 175, 453 (1968).
[30]J. S. Waugh, L. M. Huber, and U. Haeberlen, Phys.

Rev. Letters 20, 180 (1968).
[31]P. Mansfield, Phys. Letters 32A, 485 (1970)..
[32]W. Silberszyc (unpublished).

BIOGRAPHICAL SKETCH

Alexander Pines, first child of Michael and Neima Pines, was born in Tel-Aviv, Israel on June 22, 1945. He graduated from the Hebrew University of Jerusalem in 1967 and began doctoral studies in Physical Chemistry at the Massachusetts Institute of Technology in September, 1968. He has served as a teaching assistant and has held a Dalton Predoctoral Fellowship while at M.I.T. In August, 1967 he married Ayala Malach and on July 3, 1970 their son, Itai was born. The author has been elected to the Society of Sigma Xi and to Phi Lambda Upsilon, and is a member of the American Physical Society and the American Chemical Society. He has co-authored more than 25 scientific papers.